Self-assembly of ABA triblock methacrylate copolymers

Xinmo Zhang

Department of Materials

Imperial College London

Submitted in partial fulfilment of the requirements

for the degree of *Doctor of Philosophy*

Declaration of Originality

I declare that the work presented in this PhD thesis is of my own, unless stated or appropriately referenced. Any contributions are clearly stated.

Copyright Declaration

The copyright of this thesis rests with the author. Unless otherwise indicated, its contents are licensed under a Creative Commons Attribution-Non Commercial-No Derivatives 4.0 International Licence (CC BY-NC-ND).

Under this licence, you may copy and redistribute the material in any medium or format on the condition that; you credit the author, do not use it for commercial purposes and do not distribute modified versions of the work.

When reusing or sharing this work, ensure you make the licence terms clear to others by naming the licence and linking to the licence text.

Please seek permission from the copyright holder for uses of this work that are not included in this licence or permitted under UK Copyright Law.

ABSTRACT

Polymersomes are nano polymeric structures that have gained tremendous interest since they can be used as versatile carriers in biomedical applications. This thesis aims to synthesise triblock methacrylate copolymers with different chemistry and composition, to investigate the composition effect on the properties of fabricated polymersomes. Specifically, three different families of amphiphilic block copolymers have been successfully synthesised via Group Transfer Polymerisation, and the corresponding polymersomes have been formed by self-assembly of the copolymers and the properties of polymersomes have been investigated.

i) In the first study, five triblock copolymers with different compositions have been synthesised using hydrophilic monomer tri(ethylene glycol) methyl ether methacrylate (TEGMA) and hydrophobic, pH-responsive monomer 2-(diethylamino) ethyl methacrylate (DEAEMA);

ii) In the second study, six triblock copolymers with different compositions have been synthesised, the hydrophilic blocks are formed by monomer tri(ethylene glycol)ethyl ether methacrylate (TEGEMA) and hydrophobic blocks are statistically formed by monomer 2-(diethylamino ethyl methacrylate) (DEAEMA) and n-butyl methacrylate (BuMA).

iii) In the third study, six triblock copolymers with different compositions have been synthesised, hydrophilic blocks have been synthesised from monomer penta(ethylene glycol) methyl ether methacrylate (PEGMA), hydrophobic blocks have been synthesised using 2-(diethylamino ethyl methacrylate) (DEAEMA) and n-butyl methacrylate (BuMA), the two hydrophobic monomers have been mixed statistically.

In conclusion, the composition of the block copolymers is proven to affect the properties of polymersomes, in: i) thermoresponsiveness; ii) pH-responsiveness; iii) size; iii) membrane thickness; iv) encapsulation efficiency and release of molecules.

ACKNOWLEDGEMENTS

Firstly, I would like to express my gratitude to my supervisor, Dr Theoni K. Georgiou, for her generous help throughout my PhD. She guided this work, shared her expertise in polymer chemistry and experimental skills, also, she gave the whole research group a positive environment to study.

Also, I would like to thank my second supervisor Dr Fang Xie for her instructions on my Early Stage Assessment and Dr Stefano Angioletti-Uberti for my Late Stage Review.

I would like to thank Dr Mahmoud Ardakani and Dr Catriona M. McGilvery for their help with the TEM.

I would like to express my gratitude to Dr Claudia Contini, who has excellent skills in operating TEM and helped me with many images with great quality. Also, she is a great teacher who guided me on the experiments performed in the lab in White City campus.

I would like to thank Department of Materials at Imperial College, as I have had a pleasant time studying and working here.

I also would like to thank Imperial College London as it funds me during the pandemic of Covid-19 to support my PhD studies.

I would like to thank all the members in Theoni's group. Firstly, a special thanks to Dr Anna Constantinou and Dr Dean Carroll, who have helped me from the first day I joined the group, until the time I finished writing up this thesis. They have answered a number of questions from me and helped me with all the equipment in and outside our lab with great patience. Also, I would like to thank Dr Birsen Somuncuoglu as my colleague and friend for the days we spent together in the lab or in the gelato shop, no matter happy or stressful, together we can always find something interesting to laugh at or talk about.

I would like to thank my colleagues Bailin Feng, William Lee, Qian Li and Shuchen Wang for the enjoyable time we spent together in and outside the lab. I would like to

thank Shengyang Chen and Zheng Xie for the help to my studies and the time we spent in the office and in ethos. I would also like to thank Joana, Thanos, Haffsah, Anna Li Volsi, Maria as we had worked together happily in Georgiou's group.

Moreover, a big thank you to my friends. Thank you Yuan Zhong, Yuxin Qi, Zhiyao Xu, and Chunbing Huang, thank you as you have supported me and brought me a lot of joy in London, especially during Covid-19 pandemic.

Last but not least, I would like to thank my selfless parents. Their mental and financial help is the backbone that supports me to finish this long journey. I am very lucky to be your child and I keep thinking if I could ever do better as a parent. I share my life, both good things and bad things with you and you have always been loving and supportive. Thank you both so much.

PhD is never an easy journey. It takes time, energy, interest, patience and luck. I have experienced moments with joy and happiness, as well as frustration and results with non-sense. I would like to finish this acknowledgement by quoting an article which was written 2000 years ago by Xun Kuang, who is a very famous philosopher in China:

"A wise man says: Learning should never cease. Blue comes from the indigo plant but is bluer than the plant itself. Ice is made of water but is colder than water ever is. If a wiseman studies widely and examines himself every day, his wisdom will become clear and his conduct will become without any fault.

I once tried spending the whole day in thought, but I found it of less value than a moment of study. I once tried standing on tiptoe and gazing into the far distance, but I found I could see much farther by climbing to a higher place. If I climb to a higher place and wave to people, it is not as though my arms were any longer, and yet people can see you from much farther away. If I shout down the wind, it is not as though my voice was any louder than usual, and yet people can hear me much more clearly. Those who make use of carriages or horses may not run any faster than others, and yet they are able to travel a thousand miles. Those who make use of boats may not know how to swim, and yet they manage to get across rivers. A wise man is by birth not different from any

others, it is just he is good at making use of things.

Pile up earth to make a mountain, the wind and the rain will rise up from it; Pile up water to make a deep pool, then dragons will appear. Pile up good deeds to create virtue, and godlike understanding will come of itself; there the mind of the sage will find completion. But, unless I pile up little steps, I can never journey a thousand miles; unless I collect tiny streams, I can never make a river or a sea. The finest thoroughbread cannot jump for 10 steps at one time, but the sorriest nag can go a 10 days' journey. Achievement consists of never giving up."

PUBLICATIONS AND PRESENTATIONS

The work contained within this PhD thesis has given rise to the following publications and presentations:

1. Zhang, X., Contini, C., Constantinou, A. P., Doutch, J. J., & Georgiou, T. K. (2021). How does the hydrophobic content of methacrylate ABA triblock copolymers affect polymersome formation?. *Journal of Polymer Science*.

2. Oral presentation: "Novel self-assembled polymersomes for biological applications", 2nd year pizza lunch for the biomaterials theme, Department of Materials, Imperial College London, London, UK, June 2017.

3. Poster presentation: "Self-assembly of ABA triblock copolymer: effect of block ratio" MacroGroup UK Young Researchers meeting – University of Kent, Canterbury, UK, July 2019.

4. Poster presentation: "Novel Self-assembled polymeric structures for biological applications", London Polymer Group 4th Annual Meeting, Kings College London, London, UK, November 2018.

TABLE OF CONTENTS

Declaration of Originality **2**

Copyright Declaration **3**

ABSTRACT **4**

ACKNOWLEDGEMENTS **5**

PUBLICATIONS AND PRESENTATIONS **8**

LIST OF FIGURES **13**

LIST OF TABLES **19**

LIST OF ABBREVIATIONS **22**

CHAPTER 1 INTRODUCTION AND LITERATURE REVIEW **26**

1.1 Cell Membrane and Liposomes 26

1.2 Introduction of Polymersomes and Micelles 30

1.2.1 Polymersomes 30

1.2.2 Micelles 32

1.3 Block Copolymers 33

1.3.1 Selection of Monomers 33

1.3.2 Polymerisation Techniques 36

1.3.3 Characterisation of Copolymers 41

1.3.4 Conformation of Blocks 46

1.3.5 Self-Assembly of Amphiphilic Block Copolymers 48

1.4 Fabrication of Polymersomes 49

1.4.1 Solvent Free Approach 50

1.4.2 Solvent Displacement Approach 53

1.5 Applications of Polymersomes 54

1.5.1 Drug Loading and Release 55

1.5.2 Other Applications 61

CHAPTER 2 AIM OF THIS THESIS 74

CHAPTER 3 EXPERIMENTAL 78

3.1 Synthesis and Characterisation of Polymers 78

3.1.1 Materials and Equipment 78

3.1.2 Methods of Polymer Synthesis 80

3.1.3 Methods of Polymer Characterisation 83

3.2 Fabrication and Characterisation of Polymersomes 85

3.2.1 Fabrication of Polymersomes 85

3.2.2 Characterisation of Polymersomes 85

CHAPTER 4 POLYMERSOMES BASED ON TRIBLOCK COPOLYMER TEGMA-*b*-DEAEMA-*b*-TEGMA 90

4.1 Chemistry of Block Copolymers 90

4.1.1 Polymer Synthesis 91

4.1.2 Molar Mass and Composition.....93

4.2 Properties in Aqueous Solution.....98

4.3 Size Distribution in Polymer Solutions 98

4.3.1 DLS.....99

4.3.2 TEM.....106

4.4 Encapsulation and Release Study 117

4.5 Conclusions 119

CHAPTER 5 POLYMERSOMES BASED ON TRIBLOCK COPOLYMER TEGEMA-*b*-(DEAEMA-*co*-BUMA)-*b*-TEGEMA 123

5.1 Chemistry of Block Copolymers 123

5.1.1 Polymer Synthesis 124

5.1.2 Molar Mass and Composition.....125

5.2 Properties in Aqueous Solution.....130

5.3 Size Distribution in Polymer Solutions 131

5.3.1 DLS.....131

5.3.2 TEM.....135

5.4 Conclusions 137

CHAPTER 6 POLYMERSOMES BASED ON TRIBLOCK COPOLYMER PEGMA-*b*-(DEAEMA-*co*-BUMA)-*b*-PEGMA 140

6.1 Chemistry of Block Copolymers 140

6.1.1 Polymer Synthesis 141

6.1.2 Molar Mass and Composition 142

6.2 Properties in Aqueous Solution 147

6.2.1 Effective pK_as 147

6.2.2 Cloud Point 148

6.3 Size Distribution in Polymer Solutions 149

6.3.1 DLS 149

6.3.2 TEM 156

6.4 Encapsulation and Release of Dyes 160

6.5 SANS 163

6.6 Conclusions 164

CHAPTER 7 CONCLUSIONS AND FUTURE WORK 168

7.1 Conclusions 168

7.2 Future Work 169

APPENDIX 171

LIST OF FIGURES

Figure 1.1 A simplified illustration of cell membrane.

Page 27

Figure 1.2 Schematic representation of the cross section of a liposome in aqueous environment. The hydrophilic heads are represented with blue circles and hydrophobic tails are represented with red lines.

Page 28

Figure 1.3 Schematic representation of a polymersome formed by amphiphilic ABA block copolymers in aqueous solution, with blue and red represent the hydrophilic and hydrophobic components of the polymer, respectively.

Page 30

Figure 1.4 Schematic representation of a spherical micelle formed by amphiphilic ABA block copolymers in aqueous solution, and two configurations of ABA triblock copolymer chains that constitute micelles. Blue and red colours represent the hydrophilic and hydrophobic components of the polymer, respectively.

Page 32

Figure 1.5 Mechanics of "associative" pathway of GTP.

Page 39

Figure 1.6 Mechanics of "dissociative" pathway of GTP.

Page 49

Figure 1.7 Schematic representation of a commercially available GPC apparatus. From the top to the bottom, the apparatus includes: a solvent reservoir, a waste reservoir, a pump, a sample plate, a precolumn, a separation column (main column) and a detector. On the left of the figure shows a calibration curve, a chromatogram

and a schematic of the cross section of the separation column.[75]

Page 44

Figure 1.8 Molecular conformations of the polymersome membrane formed by AB, BAB and ABA copolymers.[19]

Page 47

Figure 1.9 Illustration of the formation of polymersomes via film rehydration method. With red and blue the hydrophobic and hydrophilic chains of the polymer are illustrated, respectively.[1]

Page 52

Figure 1.10 Illustration of the formation of polymersomes via direct injection method. With red and blue the hydrophobic and hydrophilic chains of the polymer are illustrated, respectively.[1]

Page 53

Figure 4.1 Chemical structures, names, abbreviations and related properties of the monomers used for the polymerisation of the polymer series AP.

Page 91

Figure 4.2 Illustration of the sequential GTP reaction for the synthesis of TEGMA-*b*-DEAEMA-*b*-TEGMA triblock copolymers. TEGMA and DEAEMA are the two monomers, TBABB, MTS, THF are the catalyst, monofunctional initiator and solvent used in the reaction, respectively.

Page 92

Figure 4.3 Schematic representation of the triblock copolymers. Blue circles represent hydrophilic TEGMA units, red circles represent hydrophobic DEAEMA units, the theoretical compositions of the polymers are listed.

Page 93

Figure 4.4 GPC chromatograms of ABA triblock polymer $TEGMA_{14}$-*b*-$DEAEMA_{15}$-*b*-$TEGMA_{14}$ and its linear precursors: $TEGMA_{14}$ in black solid line, $TEGMA_{14}$-*b*-$DEAEMA_{15}$ in red solid line and triblock polymer $TEGMA_{14}$-*b*-$DEAEMA_{15}$-*b*-$TEGMA_{14}$ in blue solid line.

Page 94

Figure 4.5 The ^{1}H NMR spectra of Polymer AP4 and its precursors. From top to bottom: $TEGMA_{12}$-*b*-$DEAEMA_{19}$-*b*-$TEGMA_{12}$, $TEGMA_{12}$-*b*-$DEAEMA_{19}$, and $TEGMA_{12}$ homopolymer. On the left, the chemical structure of TEGMA units is in light blue, the structure of DEAEMA units is in red.

Page 98

Figure 4.6 TEM images of structures formed by APs. The solutions were prepared via film rehydration in DI water with a polymer concentration of 10 mg mL^{-1}, and the pH of solution was adjusted to 6. Uranyl acetate was used as a negative staining agent.

Page 107

Figure 4.7 TEM images of structures formed by APs. The solutions were prepared via film rehydration in DI water with a polymer concentration of 10 mg mL^{-1}, and the pH of solution was adjusted to 7. Uranyl acetate was used as a negative staining agent.

Page 109

Figure 4.8 TEM images of structures formed by APs. The solutions were prepared via film rehydration in PBS with a polymer concentration of 10 mg mL^{-1}. Uranyl acetate was used as a negative staining agent.

Page 113

Figure 4.9 (a) TEM images of the TEGMA-*b*-DEAEMA-*b*-TEGMA polymersomes formed by film rehydration and (b) image analysis used to determine the difference in membrane thickness changing from P1 to P5. (c) The measured membrane thickness (blue) is plotted versus the theoretical coil-like conformation (red) of TEGMA-*b*-

DEAEMA-*b*-TEGMA copolymers. Scale bars are 50 nm and 10 nm in panel a and b respectively. The figure has been adapted from “Zhang, Xinmo, et al. "How does the hydrophobic content of methacrylate ABA triblock copolymers affect polymersome formation?." *Journal of Polymer Science* (2021).”

Page 117

Figure 4.10 Cumulative release of sodium fluorescein versus time by polymersomes. The figure has been adapted from “Zhang, Xinmo, et al. "How does the hydrophobic content of methacrylate ABA triblock copolymers affect polymersome formation?." *Journal of Polymer Science* (2021).”

Page 118

Figure 5.1 Chemical structures, names, abbreviations and related properties of the monomers used for the polymerisation of polymer series CP.

Page 124

Figure 5.2 Illustration of the sequential GTP reaction for the synthesis of TEGEMA-*b*-(DEAEMA-*co*-BuMA)-*b*-TEGEMA triblock copolymers. TEGEMA, DEAEMA and BuMA are the three monomers; TBABB, MTS, THF are the catalyst, monofunctional initiator and solvent used in the reaction, respectively.

Page 125

Figure 5.3 Schematic representation of CP triblock copolymers. Blue coloured circles represent hydrophilic TEGEMA units, red and green coloured circles represent hydrophobic DEAEMA and BuMA units, respectively. The theoretical compositions of polymers are listed.

Page 126

Figure 5.4 GPC chromatograms of ABA triblock polymer $TEGEMA_{15}$-*b*-($DEAEMA_5$-*co*-$BuMA_6$)-*b*-$TEGEMA_{15}$ and its linear precursors: $TEGEMA_{15}$ in black solid line, $TEGEMA_{15}$-*b*-($DEAEMA_5$-*co*-$BuMA_6$) in red solid line and the triblock copolymer

TEGEMA$_{15}$-*b*-(DEAEMA$_5$-*co*-BuMA$_6$)-*b*-TEGEMA$_{15}$ in blue solid line.

Page 126

Figure 5.5 The ^{1}H NMR spectra of polymer CP5 and its precursors. From top to bottom: TEGEMA$_7$-*b*-(DEAEMA$_{15}$-*co*-BuMA$_{19}$)-*b*-TEGEMA$_7$, TEGEMA$_7$-*b*-(DEAEMA$_{15}$-*co*-BuMA$_{19}$), and TEGEMA homopolymer. On the left, the chemical structure of TEGEMA units is in light blue, the structure of DEAEMA units is in red and the structure of BuMA units is in green.

Page 128

Figure 5.6 TEM images of structures formed by CPs. The solutions were prepared via film rehydration in water/ethanol = 50/50 (vol%) with a polymer concentration of 10 mg mL^{-1}. Uranyl acetate was used as a negative staining agent.

Page 135

Figure 5.7 TEM images of structures formed by CPs. The solutions were prepared via film rehydration in water/ethanol = 30/70 (vol%) with a polymer concentration of 10 mg mL^{-1}. Uranyl acetate was used as a negative staining agent.

Page 136

Figure 6.1 Chemical structures, names, abbreviations and related properties of the monomers used for the polymerisation of polymer series DP.

Page 140

Figure 6.2 Illustration of the sequential GTP reaction for the synthesis of PEGMA-*b*-(DEAEMA-*co*-BuMA)-*b*-PEGMA triblock copolymers. PEGMA, DEAEMA and BuMA are the three monomers; TBABB, MTS, THF are the catalyst, monofunctional initiator and solvent used in this reaction.

Page 142

Figure 6.3 A schematic representation of DP triblock copolymers. Blue coloured

circles represent hydrophilic PEGMA units, red circles represent hydrophobic DEAEMA units, green circles represent hydrophobic BuMA units, respectively, and the theoretical composition of the polymers are listed.

Page 143

Figure 6.4 GPC chromatograms of ABA triblock polymer $PEGMA_{10}$-*b*-($DEAEMA_7$-*co*-$BuMA_9$)-*b*-$PEGMA_{10}$ and its linear precursors. $PEGMA_{10}$ in black solid line, $PEGMA_{10}$-*b*-($DEAEMA_7$-*co*-$BuMA_9$) in red solid line and the polymer in blue solid line.

Page 144

Figure 6.5 The ^1H NMR spectra of Polymer DP5 and its precursors. From top to bottom shows triblock copolymer $PEGMA_6$-*b*-($DEAEMA_{14}$-*co*-$BuMA_{19}$)-*b*-$PEGMA_6$, diblock precursor $PEGMA_6$-*b*-($DEAEMA_{14}$-*co*-$BuMA_{19}$), and PEGMA homopolymer. On the left, the chemical structure of PEGMA units is in light blue, the structure of DEAEMA units is in red and the structure of BuMA units is in green.

Page 146

Figure 6.6 Effective pK_as of the six copolymers. Data points from right to left represent DP1, DP2, DP3, DP4, DP5 and DP6, respectively.

Page 147

Figure 6.7 TEM images of structures formed by DPs. The solutions were prepared via film rehydration in PBS with a polymer concentration of 10 mg mL^{-1}. Uranyl acetate was used as a negative staining agent.

Page 156

Figure 6.8 Time dependent cumulative release of sodium fluorescein by polymersomes.

Page 162

LIST OF TABLES

Table 1.1 A List of typical monomers used to form polymersomes.

Page 34

Table 1.2 Examples of polymersomes fabricated from AB, BAB and ABA copolymers.

Page 48

Table 1.3 Examples of polymersomes that have been fabricated in applications of encapsulation and release of molecules.

Page 60

Table 4.1 Theoretical polymer structure, experimental number-average MM (M_n), the molar mass that corresponds to the maximum of the peak (M_p) MM distribution ($Đ$) and weight ratios of ABA units of APs.

Page 95

Table 4.2 Hydrophilic weight ratio of APs before and after protonation.

Page 100

Table 4.3 Summary of DLS results of APs at pH = 6 with different stirring time.

Page 103

Table 4.4 Summary of DLS results of APs at pH = 7 with different stirring time.

Page 104

Table 4.5 Summary of DLS results of APs in PBS (bulk hydration).

Page 105

Table 4.6 Summary of DLS results of APs in PBS (film rehydration)

Page 106

Table 4.7 Theoretical polymer structures, pK_a values, theoretical and experimental membrane thickness of polymersomes

Page 116

Table 5.1 Theoretical polymer structure, molar mass ($MM^{theor.}$), experimental number-average MM (M_n), the MM that corresponds to the maximum of the peak (M_p), MM distribution ($Đ$), experimental weight percentage of each block of the polymers and their precursors of CPs.

Page 129

Table 5.2 Solubility of CPs in 3 solvents at 25°C by visual observation, polymer concentration is 10 mg mL^{-1}. Partially dissolved means polymer pieces are present in the solution, dissolved means the solution is transparent, with no polymers visible.

Page 130

Table 5.3 Polymer structures, theoretical and experimental hydrodynamic diameters, polydispersity indices (PDI) of polymer solutions between two fabrication methods.

Page 133

Table 5.4 Polymer structures, theoretical and experimental hydrodynamic diameters, polydispersity indices (PDI) of polymer solutions between two solutions.

Page 134

Table 6.1 Theoretical polymer structure, molar mass ($MM^{theoretical}$), experimental number-average MM (M_n), the MM that corresponds to the maximum of the peak (M_p), MM distribution ($Đ$), composition of the polymers and their precursors of DPs.

Page 145

Table 6.2 Theoretical polymer structures, cloud point and precipitation temperature of DPs.

Page 148

Table 6.3 Summary of DLS results of DPs with different fabrication methods (bulk hydration and film rehydration). Polymers are dissolved in DI water (10 mg mL^{-1}).

Page 152

Table 6.4 Summary of DLS results of DPs in different solvents (DI water and PBS). The polymer concentration is 10 mg mL^{-1}.

Page 153

Table 6.5 Summary of DLS results of DPs in different stirring time (from 1 day to 1 week, and at 1 month), the polymers were dissolved in PBS, the concentration is 10 mg mL^{-1}.

Page 154

Table 6.6 Diameters of large vesicles measured by ImageJ.

Page 160

Table 6.7 Summary of SANS results. The concentration of the polymer solutions is 10 mg mL^{-1} and the polymers were dissolved in PBS.

Page 164

LIST OF ABBREVIATIONS

MM: Molar mass

MMD: Molar mass distribution

FDA: Food and Drug Administration

PEG: Polyethylene glycol

DP: Degree of polymerisation

PS: Polystyrene

PEGMA: Penta(ethylene glycol) methyl ether methacrylate

PCL: Polycaprolactone

PMOXA: Poly(2-methyloxazonline)

PDMS: Poly(dimethylsiloxane)

PBD: Poly(butadiene)

PPS: Poly(phenylene sulphide)

PEE: Poly(ethyl ethylene)

PAA: Polyacrylic acid

PLA: Poly(lactic acid)

GTP: Group transfer polymerisation

RAFT: Reversible addition-fragmentation chain transfer polymerisation

ATRP: Atom transfer reversible polymerisation

ROP: Ring opening polymerisation

CROP: Cationic ring opening polymerisation

AROP: Anionic ring opening polymerisation

GPC: Gel permeation chromatography

SEC: Size exclusion chromatography

NMR: Nuclear magnetic resonance

DLS: Dynamic light scattering

TEM: Transmission electron microscopy

TBABB: Tetrabutylammonium bibenzoate

MTS: Trimethylsilyl dimethylketene acetal

CTA: Chain transfer agent

PISA: Polymerisation-induced self-assembly

MPC 2-(methacryloyloxy) ethyl phosphorylcholine

DPA 2-(diisopropylamino)ethyl methacrylate

EE Encapsulation efficiency

DLC Drug loading cotent

DTX: Docetaxel

PTEMBPEC: Poly(2,4,6-trimethoxybenzylidenepentaerythritolcarbonate

DOX·HCl: Doxorubicin hydrochloride

PTX: Pacilitaxel

PNIPAM: Poly(*N*-isopropylacrylamide)

PLGA: Poly(lactic-co-glycolic acid)

PTMC: Poly(trimethylene carbonate)

PGA: Poly($_{L}$-glutamic acid)

PTTMA: Poly(2,4,6-trimethoxybenzylidene-1,1,1-tris(hydroxymethyl)ethane methacrylate)

PLeu: Poly($_{L}$-leucine)

NGF: Nerve growth factor and brain-derived neurotrophic factor

NMDAR: N-Methyl-$_{D}$-aspartate receptor

PIAT: Poly($_{L}$-isocyanoalanine(2-thiophen-3-yl-ethyl) amide)

CALB: *Candida antarctica* lipase B

HRP: Horseradish peroxidase

GOX: Glucose oxidase

PSBA: Poly(styrene boronic acid)

GFP: Green fluorescent protein

GGP: Giant glycosylated polymersomes

NMDAR: N-Methyl-$_{D}$-aspartate receptor

DEAEMA: 2-(Diethylamino) ethyl methacrylate

BuMA: n-Butyl methacrylate

TEGMA: Tri(ethylene glycol) methyl ether methacrylate

TEGEMA: Tri(ethylene glycol) ethyl ether methacrylate

UV-Vis: Ultraviolet−Visible

RT: Room temperature

SANS: Small angle neutron scattering

To my parents, Haifeng and Zihu

CHAPTER 1 INTRODUCTION AND LITERATURE REVIEW

1.1 Cell Membrane and Liposomes

Understanding the cell structure and its functionalisation is vital to life sciences. Compartmentalisation is regarded as one of the fundamental features of cells to create life, since it protects and separates organelles with distinct functions, and provides them undisturbed environment for essential biological processes.[1,2] Both eukaryotic and prokaryotic cells, after the incredibly long period of evolution, have developed the effective cellular compartmentalisation, resulting in the organisational complexity. Incontrovertibly, the most important role in compartmentalisation is the cell membranes.

Cell membranes have not been correctly distinguished from the cell walls for hundreds of years. With the development of microscopy, as well as the studies on osmosis and permeability, cell membranes have finally been recognised in the late 19th century.[3] Since then, the study on cell membrane has been carried out over 100 years, one of the reasons is the continuous enthusiasm paid by the researchers on cell-mimicking, not only for a deeper understanding of the natural biological processes, but also for any improvements of artificial biological applications.

Ernest Overton firstly suggested that cell membranes could be made of cholesterol and phospholipids in the late 1800s.[4,5] Afterwards, Gorter and Grendel proposed the lipid bilayer hypothesis in 1925,[6] supposing that the polar groups are directing inside and outside of a bilayer of lipoids. Based on which, in last century, scientists have created numerous models to explain the structure of the cell membranes. In 1970s, fluid mosaic model was established by Singer and Nicolson,[7] and it became the most acceptable model for understanding the structure of cell membranes. Also, the model has been perfected and added details with developing techniques as well as new findings. **Figure 1.1** is a schematic illustration of the cell membrane based on fluid mosaic model. In this

model, cell membranes have a matrix of fluid or elastic bilayer phospholipid, in which the polar groups protrude from the membrane into the aqueous phase, while the nonpolar groups stay in the hydrophobic interior. Proteins are partially covered, dispersed, or embedded in the membrane matrix. Moreover, some small carbohydrates and cholesterol are bound to the cell membrane.[8] This model has explained and suggested possible mechanisms for various membrane functions and membrane-mediated phenomena, and it has raised tremendous interest on the amphiphilic lipid bilayer membranes.

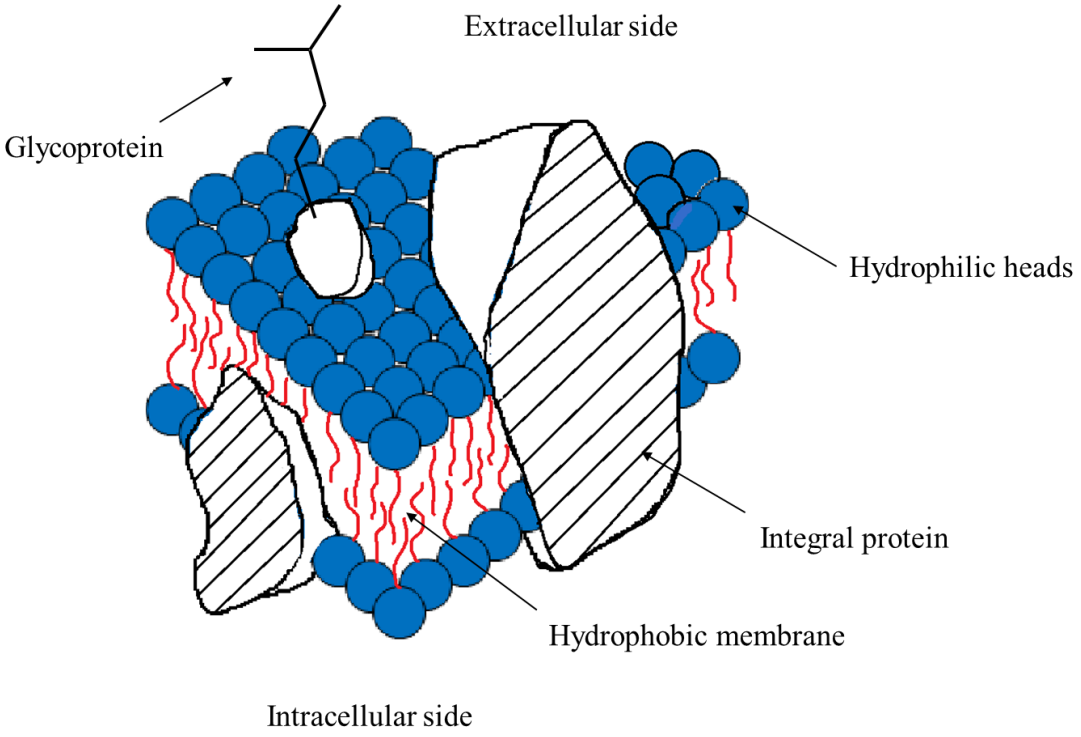


Figure 1.1 A simplified illustration of cell membrane.

In 1960s, a new structure was observed and described firstly by Bangham and Horne and it was named liposome.[9,10] The name derives from two Greek words: lipos and soma, corresponding to "body of fat". It was so named because its composition is primarily, and mostly of phospholipids. A liposome is a hollow spherical vesicle, composing of at least one lipid bilayer. The membrane of liposome is a simplified version of a cell membrane without its ornaments. A schematic of a liposome formed by phospholipids in an aqueous solution is shown in **Figure 1.2**.

Liposomes are mostly made of phospholipids, especially phosphatidylcholine, but other lipids have also been reported, for instance, egg phosphatidylethanolamine.[10] The lipids are amphiphilic, and they are usually described as composing of a hydrophilic head and a hydrophobic tail. Since liposomes are artificial cell mimics, their membranes have many similarities with cell membranes. The structure of a liposome contains a core filled with aqueous solution, a (or several) bilayer amphiphilic membrane(s). In the membrane, the hydrophilic heads protruding to the outer aqueous environment and interior aqueous core, hydrophobic tails prone to stay inside the membrane, to have minimum contact with water. This arrangement of amphiphilic molecules attributes to hydrophobic effect, which is the tendency of nonpolar substances to aggregate in an aqueous solution and exclude water molecules. In the light of the structure of liposomes, it is explicit that the liposomes can be used as carriers for both hydrophilic and hydrophobic small molecules. In a liposome, the hydrophilic molecules can be encapsulated inside the lumen, while hydrophobic molecules can spread or embed inside the membrane, and this feature facilitates the application of liposomes in drug delivery.

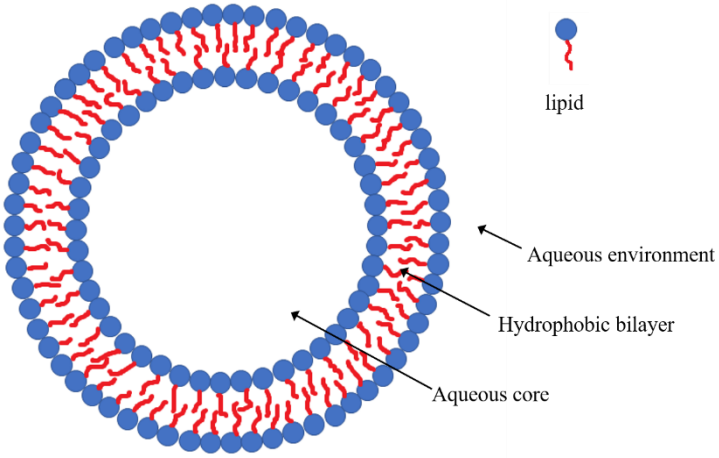


Figure 1.2 Schematic representation of the cross section of a liposome in aqueous environment. The hydrophilic heads are represented with blue circles and hydrophobic tails are represented with red lines.

In fact, the application of liposomes in drug delivery have been well studied and the

related industrial possibilities have been explored for a few decades, a number of liposome- or liposome-like-based pharmaceutical products have been approved by the US FDA (Food and Drug Administration), such as DOXIL, Daunosomes, Ableet, Amphotech, AmbiSome and recently added Vyxoes®.[11,12,13] Undeniably, liposomes have been proven effective in the reduction of side effects of encapsulated drugs and passively accumulating in areas of high vasculature when the particle size is below 200 nm.[14]

However, at the same time, liposomes also have shortcomings that are non-negligible. Subject to the chemical and biological nature of lipids, physical and chemical instability and drug leakage over time can be problematic.[15,16] Lack of control over the rate of drug release has also been reported, as well as the insufficient loading of drugs.[17] Hence, despite lipids being highly biocompatible, researchers have been motivated to find alternatives that are more versatile, easily obtainable and behave in many aspects like lipids: amphiphilic polymers.[18,19,20] Amphiphilic diblock polymers are similar to lipids in terms of function and morphology, since both of them have a polar end (hydrophilic or charged head in lipids) covalently bound to a hydrophobic tail.[1] This similarity in structure results in the similar mechanism for both lipids and amphiphilic diblock polymers to form vesicles in aqueous solution, which is the hydrophobic effect. The hollow vesicles formed by self-assembly of amphiphilic diblock polymers are named polymersomes.

1.2 Introduction of Polymersomes and Micelles

1.2.1 Polymersomes

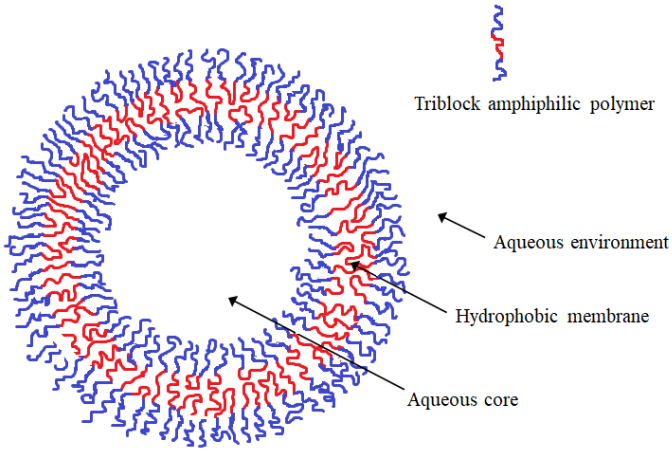


Figure 1.3 Schematic representation of a polymersome formed by amphiphilic ABA block copolymers in aqueous solution, with blue and red represent the hydrophilic and hydrophobic components of the polymer, respectively.

The concept of polymersome has been firstly introduced by Disher et al. in 1999 as "tough vesicles made from diblock copolymers" or "polymer-based liposomes".[21] To be specific, polymersomes are hollow spherical nano-structures which are formed by self-assembly of amphiphilic block polymers in aqueous solutions. Since then, continuous research interest has been undertaken. Polymersomes can be formed not just by diblock copolymers but also by triblock, tetrablock and multiblock copolymers and their characteristics have been further compared and distinguished from liposomes from the following aspects:

a) Size. Phospholipids that form liposomes usually have a MM of 100 – 1000 g mol^{-1} whereas the amphiphilic block polymers that form polymersomes have a MM over 1000 g mol^{-1}.[1] The remarkable difference in MM of the vesicular subunits have an impact on the size of the vesicles, especially in the hydrophobic membrane. For liposomes, the membrane thickness is between 3-5 nm whereas polymersomes usually

have a membrane of 5-50 nm.[22,23,24,25] In addition, the thickness of the membrane is found to be related to the hydrophobic content in polymersomes, which is understandable since hydrophobic units mainly contribute to the membrane (this is discussed in detail in **Chapter 4**). In terms of diameter, liposomes and polymersomes both can be in the range of 10 nm to over 1000 nm depending on the chemistry and fabrication method.[26]

b) Permeability and stability. Liposomes have been applied to biomedical drug delivery for years, however, they have been described as problematically leaky, and it is related to the structure of the lipids-formed liposome membrane. The relatively low MM of lipids contributes to the high lateral fluidity of the membrane, further resulting in the high permeability of liposomes. In contrast, the membrane formed by polymersomes is rigid, having lower lateral fluidity and more capable of retaining the cargo inside the membrane or the aqueous core.[1]

c) Chemical versatility. Liposomes are all formed from lipids, natural or synthetic.[1] The problem is that the lipids are already highly specialised, leaving only a limited range of candidate selection and chemical modification. One successful example is, to avoid detection by the immune system in the body, PEG (polyethylene glycol) was coated outside the liposome membrane, allowing for longer circulatory life for the drug delivery system.[27,28] These liposomes were named “stealth liposomes”. On the other hand, the chemical modification is also possible for hydrophobic tails in lipids; however, it often requires several synthetic steps.[29] For polymersomes, on contrary, a large pool of hydrophilic and hydrophobic monomers is available, their overall MM, dispersity and block ratio can be easily controlled using suitable polymerisation techniques, also the architecture of copolymers can be varied from AB, ABA, ABC, ABCA and other structures.[19] Hence, the permeability, stability, biocompatibility, and physical properties can be tailored to fit in various applications.

1.2.2 Micelles

Micelles are also a type of nano structures that formed on account of the amphiphilic nature of molecules.[30] Polymeric micelles, as the name indicates, are micelles that formed by amphiphilic polymers. A micelle has a core-shell structure with a hydrophobic core and a hydrophilic shell, notably, unlike polymersomes, micelles don't have an empty core, the centre of the structure is occupied by hydrophobic moieties of the polymers.[31] Thus, the size of micelles (several tens nm) is usually smaller than that of polymersomes. **Figure 1.4** is a schematic representation of a micelle made from triblock ABA copolymers. As shown in the figure, the polymer chain has two ways to constitute the micelle structure, they can either present in an extended "I" shape or a more collapsed "U" shape.

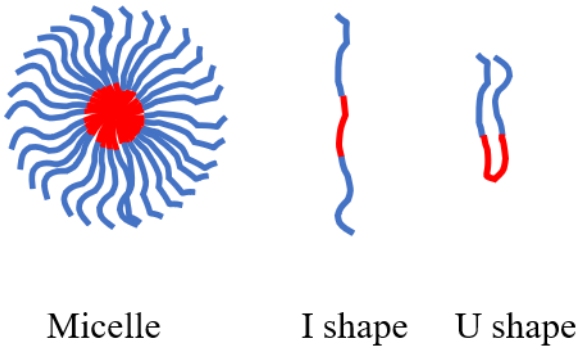


Figure 1.4 Schematic representation of a spherical micelle formed by amphiphilic ABA block copolymers in aqueous solution, and two configurations of ABA triblock copolymer chains that constitute micelles. Blue and red colours represent the hydrophilic and hydrophobic components of the polymer, respectively.

When amphiphilic polymers are dissolved in aqueous solutions, micelles and polymersomes can both be present in the solutions.[32]

1.3 Block Copolymers

Compared to liposomes, the most promising feature of polymersome is the flexibility of the chemistry. The properties of a polymersome can be simply adjusted by tuning the chemistry of block copolymers. To synthesise block copolymers, selection of monomers, polymerisation technique and polymer composition are all important. Over 20 years of research, a large pool of monomer candidates are available and their overall MM and DP can be controlled using various polymerisation techniques. In addition, based on the developing understanding of polymersome, the shape, size, fluidity, permeability, stability, biocompatibility and responsiveness are all tailorable by tuning the chemistry of copolymers and/or polymerisation techniques. [23,33]

1.3.1 Selection of Monomers

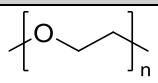
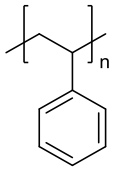
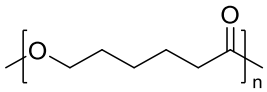
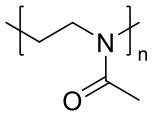
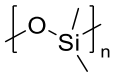
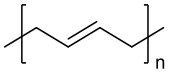
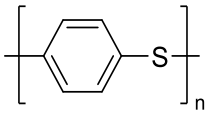
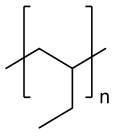
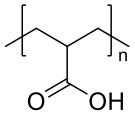
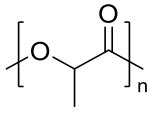
Monomer selection is the basis of the synthesis of a copolymer, and the copolymer is the basis of a polymersome. Block copolymers comprise at least two blocks, and each block is synthesised from a specific monomer or a combination of several different monomers. The copolymer that forms polymersome should be amphiphilic, it should be consisted of both hydrophilic and hydrophobic blocks. These blocks are prepared from hydrophilic and hydrophobic monomers.

A list of commonly used monomers to form polymersomes are shown in **Table 1.1**. As elucidated before, these monomers have distinct chemical groups, and their hydrophilicity (or hydrophobicity) is also different. In addition, depending on their chemical versatility, the polymerisation technique also varies, and the fabricated polymersomes have significantly different application (further discussed in **1.5**).

Block copolymers can be classified in two groups: degradable and non-degradable, the degradability of a copolymer is directly related to the monomer used for polymerisation. Normally, non-degradable copolymers include monomers that have conjugated or aromatic hydrocarbon blocks, such as poly(ethyl ethylene) (PEE),[21] poly(butadiene)

(PBD),[34] polystyrene (PS),[34,35,36,37,38] poly(dimethylsiloxane) (PDMS).[39,40,41] These mentioned monomers are commonly used to fabricate the hydrophobic component of polymersomes.

Table 1.1 A List of typical monomers used to form polymersomes.

Name	Abbreviation	Block Chemical Structure
Poly(ethylene glycol)	PEG	
Polystyrene	PS	
Polycaprolactone	PCL	
Poly(2-methyloxazonline)	PMOXA	
Poly(dimethylsiloxane)	PDMS	
Poly(butadiene)	PBD	
Poly(phenylene sulphide)	PPS	
Poly(ethyl ethylene)	PEE	
Polyacrylic acid	PAA	
Poly(lactic acid)	PLA	

On the contrary, poly(lactic acid) (PLA),[42,43,44] polycaprolactone (PCL),[45] and poly(2-methyloxazonline) (PMOXA)[46] are regarded as degradable, because they undergo hydrolytic cleavage of the ester or carbonate linkages in the main chains in aqueous media, and these polymers are water-soluble. The rate of hydrolysis depends on the hydrophobicity, the MM of the block, the pH and the presence of enzymes. Interestingly, in these degradable monomer candidates, PEG, PMOXA are applied as hydrophilic monomers whereas PCL and PLA are used as hydrophobic.

In terms of the hydrophilic component, two monomers have been the most popular: PMOXA and PEG. Specifically, PEG is often selected as a hydrophilic monomer for its resistance in surface layers to blood protein adsorption, moreover, it has been approved by FDA for its safety *in vivo*. PMOXA is also found to be protein repellent, which is helpful for medical applications to avoid the inappropriate response of the immune system.[47] This protein repellence is linked to PEGylated liposomes (stealth liposomes, introduced in **1.2**), which show better blood circulation properties than non-PEGylated ones.[48] Moreover, since the hydrophilic blocks of the polymersomes are in contact with the body fluids, its non-ionic nature is much preferable in comparison with charged polymersomes. It also attributes to the immune response of the body, since the charged polymersomes have a higher chance to stimulate the immune system.[49]

In biomedical applications, one crucial criterion is if the polymersomes (or fragments of the polymersomes) can be cleared from the blood stream after a short period. It is notable that the degradable polymers should be subject to certain MM, since polymers with larger MM prone to accumulate in human body. In light of literature,[50] elimination of polymer from body is typically through kidney clearance, the threshold of MM for renal filtration is usually 30,000 to 50,000 g mol^{-1}. On the contrary, nondegradable polymers can be excreted from the body, unless they are too large, if so, they can stay in the body for extended period of time.[51]

Current research has investigated polypeptide-based polymersomes, the advantages of which include very low toxicity, easier functionalisation and complete

biocompatibility.[52,53,54]

1.3.2 Polymerisation Techniques

To have precise control over the properties of polymersomes, well-defined copolymers i.e., polymers with defined MM, structure, composition and narrow MM distribution are needed. These polymers can be formed by living polymerisations.[55] Living polymerisation is a form of chain growth polymerisation, where the chain termination and chain transfer reactions are absent. In living polymerisations, the rate of the chain initiation is much faster than the rate of propagation,[56] resulting in a more constant rate in chain growth and more homogeneous chain length (low dispersity index) in comparison with traditional chain polymerisations like free radical polymerisation. Hence, living polymerisations have become popular for the synthesis of block copolymers as the lack of chain termination allows the blocks to be synthesised in stages, by the sequential addition of different monomers. Moreover, the polymerisation process leads to predetermined relatively accurate MM and control over end-groups, these features are all desirable for materials design. Group transfer polymerisation (GTP) belongs to living anionic polymerisations.

Reversible addition-fragmentation chain transfer polymerisation (RAFT) and atom transfer reversible polymerisation (ATRP) are controlled free radical polymerisation methods that have control over the kinetics, hence, they have some of the advantages of the living methods, such as control of the structure to produce block copolymers, narrow molar mass distribution (MMD) and better control over the MM and composition.[56]

In addition, ring opening polymerisation (ROP) has also been used to synthesise block copolymers for the fabrication of polymersomes.[57]

1.3.2.1 GTP

Group transfer polymerisation (GTP) was first discovered by Webster in 1983.[58] This method is applied to *α,β*-unsaturated carbonyl monomers (can be *α,β*-unsaturated esters, ketones, nitriles, and carboxamides) and the initiator is usually a silyl ketene acetal.[58,59] In addition, a metal-free nucleophile catalyst is needed to start the reaction.

GTP is a living anionic polymerisation method and thus has the advantages of a living polymerisation, such as the controlled MM, the narrow MMD. Sequentially, GTP has been extensively used to produce polymers with complex structures, for instance, star and graft copolymers, polymeric networks (covalently cross-linked gels), etc.[59]

Compared with other living polymerisation techniques, GTP has unique advantages. Firstly, the conventional living anionic polymerisation usually performs at 0 °C, while GTP can take place at room temperature, which means less cooling energy is required. In addition, it can be performed at higher concentrations; thus, less solvent is required. These two examples both indicate that GTP is an energy-saving, cost-effective method.[60] Secondly, GTP is easy to scale up and thus is why it has been used at an industrial level for the last 40 years.[61] Thirdly, GTP is time-effective. Specifically, at each addition, the monomer is consumed within 15 mins and thus the next monomer can be added, while some of the controlled radical polymerisation techniques take 30 mins to 8 days for the addition of each block.[60,62]

On the other hand, GTP also has limitations compared with other living/controlled polymerisation techniques. Since GTP is an anionic living polymerisation, any compounds contain labile protons (hydroxyl and carboxyl groups) are not suitable for GTP. However, it is possible to protect these group prior to GTP and deprotect them after GTP, but it immensely increases the complexity of the whole polymerisation process and it is not applicable to all the chemicals.[59] The main disadvantage of GTP is that it can only be used to polymerise acrylates and methacrylates. Furthermore, polymers synthesised from acrylates have an upper limit of MM, which is 10 kg mol^{-1}, due to the relatively short living time of the polymer chains.[59,63] Methacrylates based

polymers with GTP can reach 100 kg mol^{-1} depending on the choice of the monomer, even though it used to be believed that only polymers with MM around 30 kg mol^{-1} can be reached.

The basic chemical mechanism for the polymerisation reaction is Michael addition while two mechanical pathways of GTP have been reported in literature.[59,63] **Figure 1.4** and **Figure 1.5** show the chemical mechanism of the two pathways, which are named "associative" and "dissociative", respectively.

Associative pathway is where the name "group transfer polymerisation" comes from. In **Figure 1.4**, the catalyst (presented as a circle) first reacts with the initiator methyl trimethylsilyl dimethylketene acetal (MTS), forming an intermediate. Then the intermediate complex becomes "activated", and reacts with the monomers. The trimethyl silyl group thus transfers from the initiator to the end of the polymer chain.

The mechanics of dissociative pathway is shown in **Figure 1.5**. The catalyst presented is tetrabutylammonium bibenzoate (TBABB). In this mechanism, the initiator and the catalyst react with each other and, unlike the associative pathway, the trimethyl silyl group transfers to the catalyst, the initiator is activated and reacts with monomers, forming the polymer chain.[63]

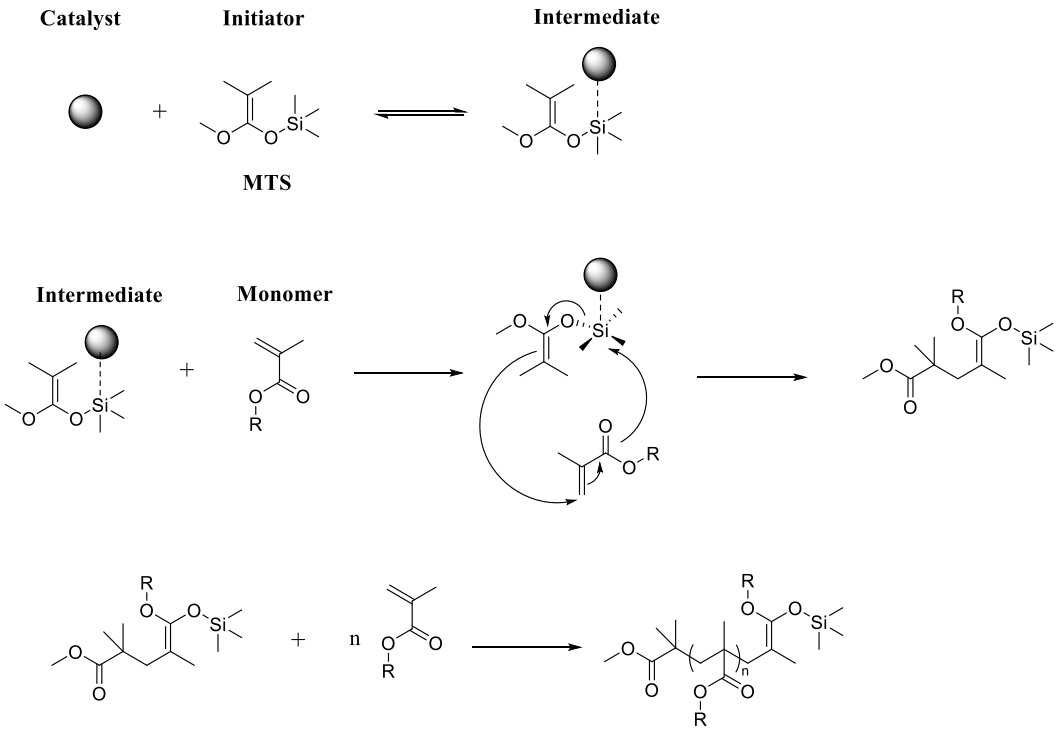


Figure 1.5 Mechanics of "associative" pathway of GTP.

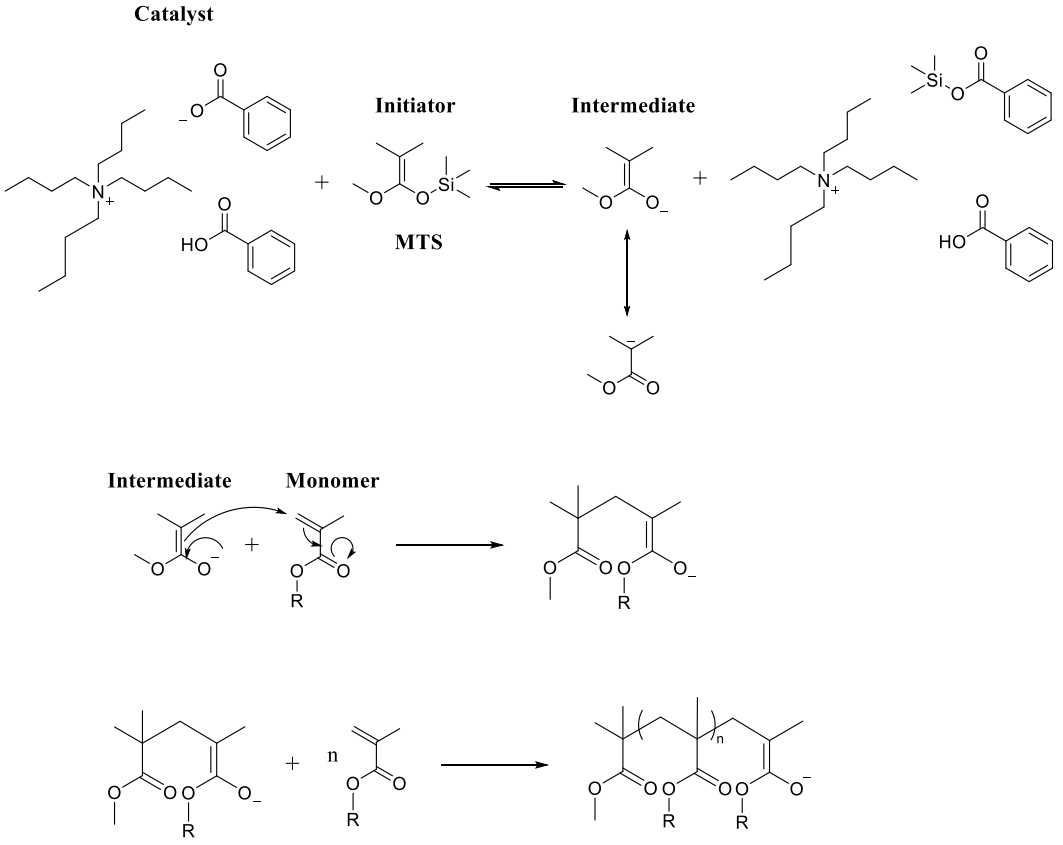


Figure 1.6 Mechanics of "dissociative" pathway of GTP.

1.3.2.2 RAFT

Reversible addition-fragmentation chain transfer polymerisation (RAFT) was first reported in 1998.[64] Since then, it has been extensively applied in polymer chemistry for the synthesis of block copolymers. Unlike the anionic living polymerisations, RAFT belongs to the controlled radical polymerisation methods where the free radical polymerisation kinetics are controlled, specifically, a chain transfer agent (CTA) is used to control the polymerisation kinetics and consequently the MM and the dispersity of each polymer block. One of the biggest advantages of RAFT is the capability to various functional groups, wide temperature ranges and solvents including water.[65] However, RAFT also has limitations. The CTA should be fine-tuned to the specific monomer types which means it must be compatible with all the monomers.[66] Some of the amphiphilic block copolymers synthesised via RAFT and used to form polymersomes are: poly(styrene)-*b*-poly(*N*-isopropylacrylamide-*co*-spironaphthoxazine methacryloyl) (PS-*b*-P(NIPAAm-*co*-SPO),[36] polystyrene-*b*-poly(vinyl benzyl chloride) (PS-b-PVBC) and PS-*b*-PVBC-*b*-PS.[37]

1.3.2.3 ATRP

Atom transfer reversible polymerisation (ATRP) is also a controlled radical polymerisation technique that has been commonly used to synthesise block copolymers. A catalyst (transition metal complex, usually copper based), an initiator (alkyl halides) and a ligand (amine based most commonly) are used to form carbon-carbon bonds between vinyl monomers, leading to the chain propagation. The typically used monomers in ATRP are molecules with substitutes that can stabilise the propagating radicals, such as styrenes, (meth)arylates, (meth)acrylamides.[67] One of the advantages of ATRP is the polymerisation reactions are quite robust, they are highly tolerant of various functional groups like allyl, amino, hydroxyl, vinyl groups in both monomer and the initiator.[68] However, the most significant drawback is the high concentration of catalyst used in the reaction. As previously mentioned, the catalyst is usually copper

based, and its removal can be problematic and commercially expensive.[2] Some common examples of copolymers formed using ATRP are: dextran-*b*-polystyrene (dex-*b*-PS),[69] and poly(polyethylene glycol)-S-S-polylactide (pPEGMA-S-S-PLA).[70]

1.3.2.4 ROP

Ring opening polymerisation (ROP) is one of the chain-growth polymerisation techniques, it has been widely used in the synthesis of polymers composed of cyclic monomers. These polymers contain the hydrolytically cleavable ester and carbonate links in the backbone of the polymer chain,[71] thus they have been recognised as degradable and triggered extensive research interest.[2] For the reaction of ROP, the end of a polymer chain attacks cyclic monomers to increase the chain length, and the reactive centre can be radical, anionic or cationic although cationic ring opening polymerisation (CROP) and anionic ring opening polymerisation (AROP) are the two main approaches of ROP. They are differentiated based on the chemistry of monomers, CROP is used mainly for oxazoline, epoxide and carbonate polymerisation whereas AROP is used for lactone and lactide polymerisation.[2] Poly(ethylene oxide)-*b*-poly(2-(3-ethylheptyl)-2-oxazoline) (PEO-*b*-PEHOx) is one example of block copolymers synthesised via ROP.[57]

1.3.3 Characterisation of Copolymers

Once the block copolymers are synthesised, some major characterisation techniques have been applied to verify if the copolymers are qualified for the further applications. The properties include the MM, MMD, degree of polymerisation (DP, block length) and hydrophilic-hydrophobic weight ratios and other significant features.

1.3.3.1 GPC

Gel permeation chromatography (GPC) is the most basic and important tool for the polymer synthesis and characterisation. It is a type of size exclusion chromatography (SEC), separates the chemicals based on size, and usually applies in organic solvent. The term of GPC can be traced back to 1960s and it has been commercialised right after.[72] Now the GPC systems and consumables are available from multiple manufacturers. The most important information that GPC gives is the MM and the MMD of the polymer sample. MM can be specified by definition: M_n (number average MM), M_w (weight average MM), M_z (size average MM) or M_v (viscosity average MM), where M_v and MMD can be directly obtained by GPC, all the rest can be determined based on GPC along with other data. The equations for M_n, M_w, M_z, M_v and MMD are listed below, where M_i is the MM of polymer with i monomer units in the chain, N_i is the number of polymers with i polymer units, α is a constant that depends on the polymer/solvent pair used in the viscosity experiments.

$$M_n = \frac{\sum_{i=1}^{i=\infty} M_i N_i}{\sum_{i=1}^{i=\infty} N_i} \qquad \textbf{Equation 1.1}$$

$$M_w = \frac{\sum_{i=1}^{i=\infty} M_i^2 N_i}{\sum_{i=1}^{i=\infty} M_i N_i} \qquad \textbf{Equation 1.2}$$

$$M_z = \frac{\sum_{i=1}^{i=\infty} M_i^3 N_i}{\sum_{i=1}^{i=\infty} M_i^2 N_i} \qquad \textbf{Equation 1.3}$$

$$M_v = \left[\frac{\sum_{i=1}^{i=\infty} M_i^{1+a} N_i}{\sum_{i=1}^{i=\infty} M_i N_i}\right]^{\frac{1}{a}} \qquad \textbf{Equation 1.4}$$

$$MMD = \frac{M_w}{M_n} \qquad \textbf{Equation 1.5}$$

In addition, the DP is defined as:

$$DP = \frac{MM\ of\ polymer}{MM\ of\ repeated\ unit} \qquad \textbf{Equation 1.6}$$

Figure 1.6 has shown a simplified model of a commercially available GPC apparatus.

The separation column is the core of GPC, as can be seen on the left, inside the column placed packed porous polymer beads (blue circles with green dots). The separation of different polymer samples is determined by the size of the pores. When the samples (green dots for low MM sample and red dots for high MM sample) pass the column, the low MM sample tend to be delayed in the small pores whereas the high MM sample travels fast through the bigger gaps of the gel beads that the column is packed with. Thus, the different travel rates separate the molecules with different MMs, and; the high MM sample elutes faster than the low MM sample. In the chromatogram, the signal of high MM sample is firstly detected (shown in red).

Moreover, A calibration curve is needed before the analysis of the samples, it is usually plotted by several data points, and the data points correspond to standard well-defined polymers (the MMs of the polymers are known). With the assist of the calibration curve, the MM of the samples can be determined.[73] In addition, GPC also helps to monitor and prove the sequential addition of a multi-step polymerisation, for instance, when polymerising a triblock copolymer, after the completion of the reaction of each step, a sample can be collected and analysed by GPC, showing a homopolymer, a diblock copolymer and a triblock copolymer, then the successful sequential polymerisation can be confirmed.

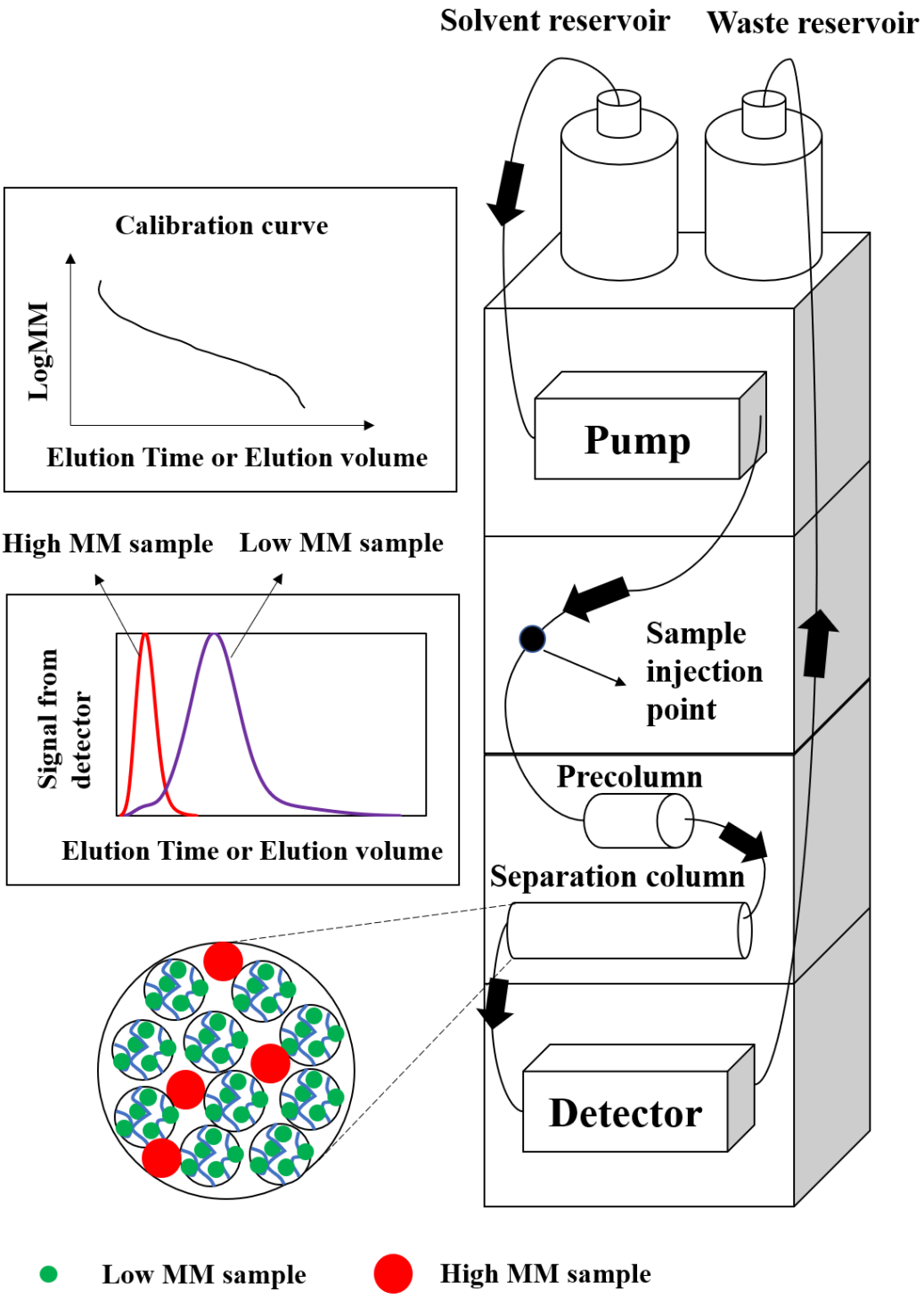


Figure 1.7 Schematic representation of a commercially available GPC apparatus. From the top to the bottom, the apparatus includes: a solvent reservoir, a waste reservoir, a pump, a sample plate, a precolumn, a separation column (main column) and a detector. On the left of the figure shows a calibration curve, a chromatogram and a schematic of the cross section of the separation column.[75]

1.3.3.2 NMR Spectroscopy

Nuclear magnetic resonance (NMR) spectroscopy observes the local magnetic fields around atomic nuclei.[73] The NMR signal is produced by the excitation of nuclei sample with radio waves into nuclear magnetic resonance, and this signal is detected by radio receivers. The resonance frequency is affected by the intramolecular magnetic field, thus, the electronic structure of a molecule (including individual functional groups and their position in the molecule) can be speculated. In organic chemistry, NMR spectroscopy is usually used as a definitive tool to identify organic compounds. In polymer chemistry, the most common application of NMR is to confirm the chemistry of the polymers and obtain the experimental polymer composition (the degree of polymerisation), by analysing the chemical shift of the specific peaks on the spectra, along with the integration. The most common types of NMR are ^{1}H and ^{13}C NMR spectroscopy.

1.3.3.3 DLS

Dynamic light scattering (DLS) is a technique related to the scattering of light by particles.[73,75] This technique is mostly used to determine the size and size distribution of small particles in solution, to be specific, in polymer chemistry, the most common application is the characterisation of the size and size distribution of polymeric particles in aqueous solution. The direct result DLS gives is the hydrodynamic diameter (D_h). D_h of a molecule is defined as the diameter of a perfect solid sphere that would exhibit the same hydrodynamic friction as the molecule of interest. Thus, the D_h value reflects primarily the hydrodynamic friction but is usually also a good estimation of the size of the molecule. Generally, the more globular the shape of a molecule is, the better the D_h value reflects the actual diameter.

The mechanism of this technique is based on the light scattering and the Brownian motion of small particles: a beam of light is scattered in all directions when it hits small particles, the scattering intensity fluctuates over time as the particles in suspension

undergo Brownian motion, and within this intensity fluctuation, information is collected and the size and size distribution can be calculated via different models. The viscosity of the solvent, the temperature and the size of the particles can all affect the results, so the setting of the parameters are significant while carrying out the measurement.[73]

1.3.4 Conformation of Blocks

The first polymersome was made from a diblock hydrophilic-hydrophobic copolymer.[21] Since then, polymersomes with different block copolymer conformations have been studied: AB, ABA, BAB, ABABA, ABC, and ABCA,[19] where A, C stand for distinct hydrophilic blocks and B stands for hydrophobic block. AB block copolymers have similar structures with lipids, and the molecular conformation of the fabricated polymersomes is also similar to liposomes, where the hydrophilic moieties pointing to the aqueous environment or the aqueous lumen, while the hydrophobic blocks stay inside to get a minimum contact with water. For BAB copolymers, the two hydrophobic ends stack to form a hydrophobic membrane while the hydrophilic middle block forms a loop (U shape) to stabilise the whole structure in water. In these two cases, both conformations only have one configuration of blocks to fabricate vesicles in aqueous media. On the other hand, the hydrophilic-hydrophobic-hydrophilic copolymers, such as ABA and ABC, have two models of forming polymersomes: 1. the hydrophobic block can bend into a loop (U shape) so the hydrophilic chains are on the same side; 2. The hydrophobic block stretched in the middle while hydrophilic chains are pointing to the different sides (I shape). Similar conformations can be also found in pentablock copolymers (ABABA).[76] **Figure 1.7** is an illustration of the possible molecular conformations of the membrane formed by AB, BAB and ABA copolymers.

Even though AB and ABA block copolymers are most frequently used for fabrication of polymersomes, other compositions, especially more complex ones, have also been discovered. In 2009, Bae and colleagues reported a AB_2 type 3-miktoarm star

copolymer, which has PEG as the A arm and poly(L-lactic acid) (PLLA) as the two B arms.[77] In 2010, Kumar and colleagues synthesised a branched $(PEG)_3$-PLA copolymer to form polymersomes.[78] Moreover, in 2013, a comb-like graft copolymer P(NVK-*co*-VBC)-*comb*-P(DMAEMA-*co*-AAc) was synthesised and the fabricated polymersomes were studied.[79]

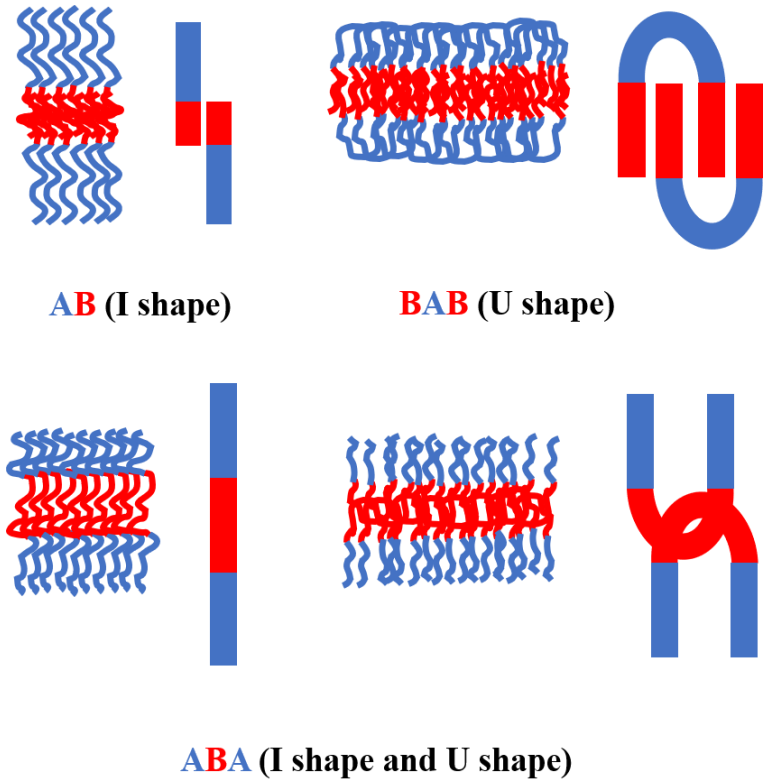


Figure 1.8 Molecular conformations of the polymersome membrane formed by AB, BAB and ABA copolymers.[19]

Table 1.2 is a summary of commonly fabricated AB, ABA or BAB polymersomes. The chemistry of the blocks can be referred to **Table 1.1**.

Table 1.2 Examples of polymersomes fabricated from AB, BAB and ABA copolymers.

Polymer composition	Architecture	Polymersome fabrication method	Reference
PEG-*b*-PEE	AB	Electroformation	21
PEG-*b*-PS	AB	Phase inversion	80
PEG-*b*-PLA	AB	Film rehydration	43, 81, 82
PEG-*b*-PCL	AB	Film rehydration	83
PLA-*b*-PEG-*b*-PLA	BAB	Double emulsion (w/o/w)	44
PMOXA-*b*-PDMS-*b*-PMOXA	ABA	Film rehydration	46, 84
PEG-*b*-PPS-*b*-PEG	ABA	Film rehydration	85

1.3.5 Self-Assembly of Amphiphilic Block Copolymers

As previously mentioned, amphiphilic block copolymers have a tendency to self-assemble in aqueous solution. It is notable that polymersome, which is the focus of this thesis, is not the only possible structure formed. Researchers have put massive interest in studying the self-assembly principles, theories, structures and properties of the assemblies for a few decades.[86] Various structures have been observed in aqueous solution, including spherical micelles, cylindrical micelles, lamellae and vesicles. A parameter, p, is introduced and it determines the morphology of the aggregates. The equation of p is $p = v/a_o l_c$, where v is the volume of the hydrophobic moiety, a_o is the contact area of the head group, l_c is the length of the hydrophobic moiety. When $p < 1/3$, spheres are formed; when $1/3 < p < 1/2$, cylinders are formed; when $1/2 < p < 1$, flexible lamellae or vesicles are formed; when $p = 1$, planar lamellae is formed. If $p > 1$, inverted structures can be observed.[86]

Another parameter f, which is a phospholipid-like ratio of hydrophilic to total mass, introduced by Discher and Ahmed,[23] indicates that the formation of the polymersome

should fulfil $f \approx 35\% \pm 10\%$. If $f > 45\%$, micelles can be expected to form; whereas $f < 25\%$ can be expected to form inverted microstructure. However, the authors also admitted that the sensitivities of the above rules for chain chemistry and MM had not been exhaustively probed. In the same book chapter, the authors also suggested that the hydrophobic membrane thickness was in relation with the MM, which is understandable, the higher MM structurally leads to the thicker membrane.

Also, different fabrication methods have an impact on the morphologies of the amphiphiles. Following the introduction of two main approaches (solvent displacement and solvent free) of forming polymersomes, when solvent displacement approach is conducted, it has often been observed that the amphiphiles transit from spherical micelles to cylindrical micelles and finally to vesicles, as a consequence of the increase in interfacial tension.[87,88] On the other hand, when solvent free approach is applied, the water concentration directly affects the formation of polymeric structures.[19] When increasing the water content, lamellar phases (connected membrane) are firstly observed, and then vesicular gels, and finally vesicles. In addition, the MM of the copolymer also has an impact on the morphology during dissolution, it has been observed that the low MM copolymer tends to assemble into an inverted hexagonal structure whereas high MM copolymer dissolves directly to the lamellar phase.

The average dimension of polymersomes is also strongly affected by the fabrication method. For the same block copolymer, it has been observed that the phase inversion and electroformation method produce micrometre-sized vesicles while the film rehydration (with vigorous stirring) and sonication, or extrusion usually have nanometre-sized vesicles.[19,89]

1.4 Fabrication of Polymersomes

Polymersomes are fabricated from self-assembly of amphiphilic block copolymers. Various methods and techniques have been applied to the process in order to modify the size, size distribution, shape and other characteristics of targeted polymersomes.

Despite the number of techniques reported, they can all be classified in two approaches: solvent free approach and solvent displacement approach. The difference between two approaches is whether organic solvent participate in the step of polymersome formation, if organic solvent participates, it's solvent displacement approach; if not, solvent free approach. Hence, for most common polymersome fabrication methods, bulk hydration, film rehydration, electroformation, PISA (polymerisation-induced self-assembly) belong to solvent free approach, while direct injection, emulsion phase transfer and method related to micro-fluidics are solvent displacement approaches.

1.4.1 Solvent Free Approach

Bulk hydration, or bulk swelling method, is the simplest method to fabricate polymersomes.[90] The polymers are directly dissolved in aqueous solutions, the whole process does not require the involvement of any organic solvent. However, long and vigorous agitation is needed to fully hydrate the polymer sample, leading to the defects in structure of the polymersomes and it has a broad size distribution.[91]

Film rehydration has been also recognised straightforward and simple method to form polymersomes,[92,93] and most of the solvent free methods are variations of film rehydration. A sample of amphiphilic polymer is fully dissolved in organic solvent, and the solution is usually placed on a solid surface. After complete evaporation of the organic solvent, remaining polymers spontaneously form a thin film on the surface. Upon the addition (usually dropwise) of an aqueous solution, water molecules permeate through the defects on the polymer film, leading to bulging and eventual separation of the polymersomes from the polymer thin film.[45] The process is illustrated in **Figure 1.8**. This technique is an easy, fast, energy saving method, however, it gives a relatively broad distribution of vesicle sizes. If the desired polymersomes need a narrow size distribution, filters with set pore diameters are usually applied and the polymersomes-containing solution is extruded through the filter.[94]

The mechanism of electroformation method is identical to film rehydration method, the

difference is the introduction of alternating current in the rehydration process. The aim to apply electric current is to facilitate the bulging and release of the polymersomes, resulting in a narrow size distribution. This method was firstly reported in 1986 on liposomes,[95] later applied in the formation of polymersomes in 1999.[21]

Recently, a method named polymerisation-induced self-assembly (PISA) has been extensively used.[96,97,98] The method has been popular among research groups since polymersomes can be formed *in situ* during polymerisation, that is to say, no more post polymerisation processing is needed to fabricate polymersomes, time and energy can be saved. PISA is based on the solubility differences in water between the monomer and polymer: hydrophilic monomers are firstly polymerised on a water-miscible initiator, since the introduction of hydrophobic monomers, the whole polymer chain extends and becomes more hydrophobic. At some critical degree of polymerisation, the polymer chains entropically self-assemble into nano polymeric structures. The interesting fact is that; different structures (such as small spheres, worn-like micelles, polymersomes) can be obtained by adjusting the amphiphile concentration or the degree of polymerisation of the polymer chain. PISA is most commonly applied with RAFT polymerisation.[1,99,100,101]

In addition, pH-switch is a method suitable for the fabrication of pH-responsive polymersomes. In 2005, Du et al. synthesised a diblock copolymer PMPC-*b*-PDPA (poly[2-(methacryloyloxy) ethyl phosphorylcholine]-*block*-poly[2-(diisopropylamino)ethyl methacrylate]) via ATRP, from monomers 2-(methacryloyloxy)ethyl phosphorylcholine (MPC) and 2-(diisopropylamino)ethyl methacrylate (DPA).[102] Since DPA has tertiary amino groups that can be protonated in aqueous solutions, the hydrophilicity of the polymer can be easily tuned, which means the formation of corresponding polymersomes can be manipulated by pH adjustment. Thus, the diblock copolymer was firstly dissolved in an acidic solution (pH < 6), due to the protonation of tertiary amino groups, at this pH the copolymer is very hydrophilic and no formation of vesicles are detected in the solution. However, by simply increasing the pH value above 7, the deprotonation of tertiary amino groups will increase the

hydrophobicity of PDPA block, resulting in the formation of polymersomes and the results were confirmed by DLS and TEM.[90] Hence, pH-switch is a simple and effective method for the fabrication of pH-responsive polymersomes.

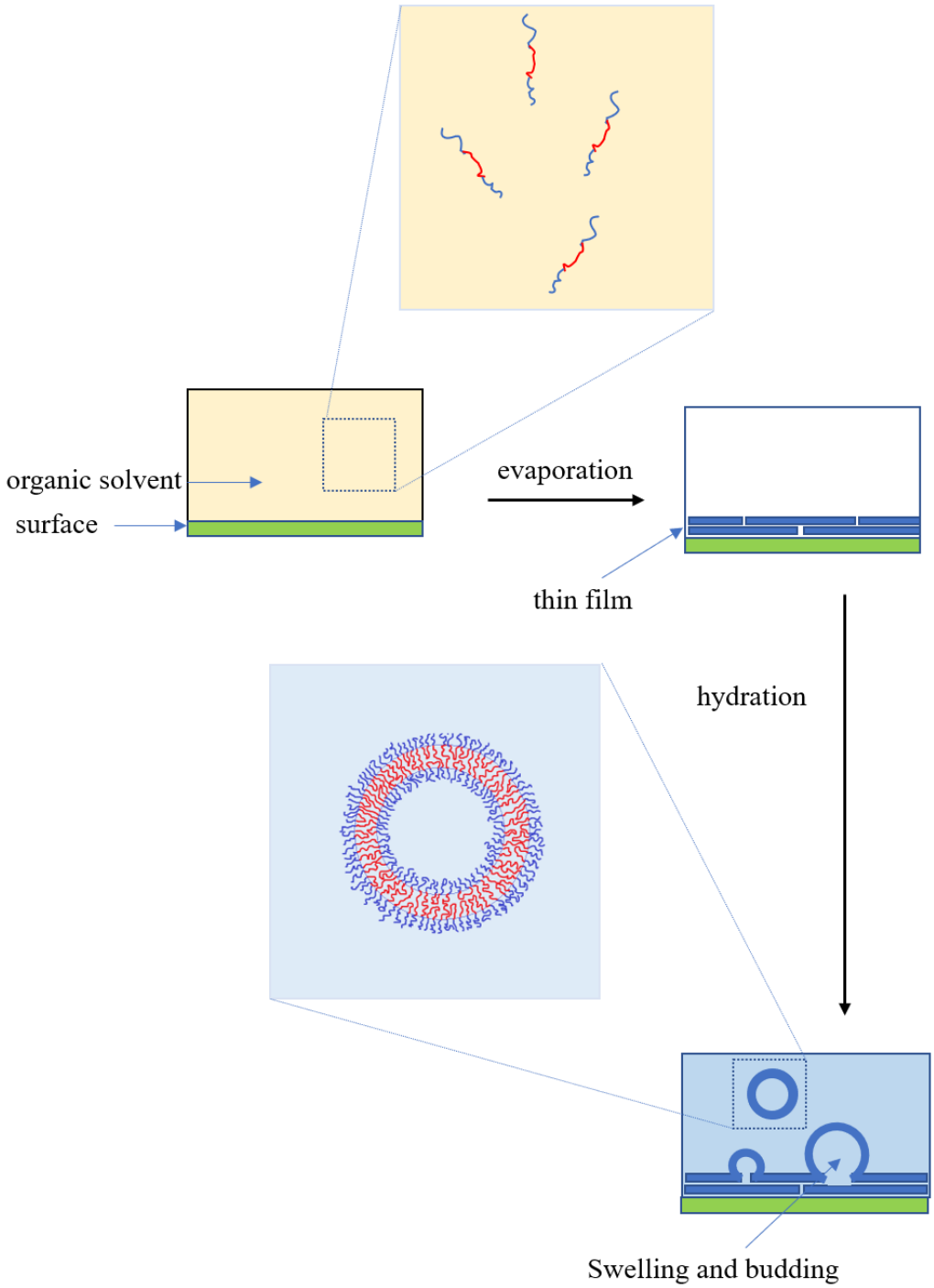


Figure 1.9 Illustration of the formation of polymersomes via film rehydration method. With red and blue the hydrophobic and hydrophilic chains of the polymer are illustrated, respectively.[1]

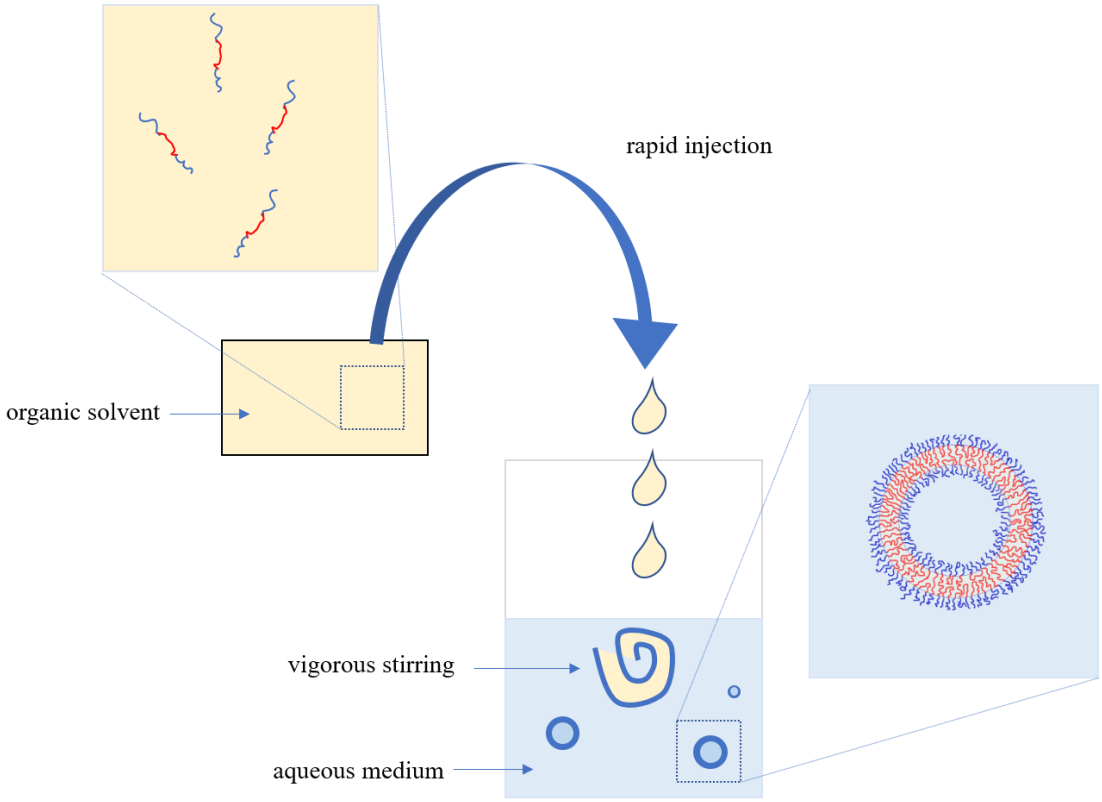


Figure 1.10 Illustration of the formation of polymersomes via direct injection method. With red and blue the hydrophobic and hydrophilic chains of the polymer are illustrated, respectively.[1]

1.4.2 Solvent Displacement Approach

All methods belonging to solvent displacement approach have organic solvent and aqueous solution together in the step of the formation of polymersomes. Generally, the co-existence of organic and aqueous solutions is to promote the self-assembly of amphiphilic polymers.[1] However, the introduction of organic solvent may be problematic: the molecules of organic solvent can be trapped in the hydrophobic bilayer of the polymersomes or contact with sensitive materials (protein, DNA and other small molecules), leading to limitations in applications since the organic solvent is possible to be toxic, or inactive the sensitive molecules.[103]

Direct injection is the most common method in solvent displacement approach. An organic solvent is selected to dissolve the block copolymers completely, then the

polymer-solvent solution is injected to an aqueous solution (under vigorous stirring). Upon addition, since the hydrophobic block is insoluble in aqueous media, the increase of the interfacial tension between the block and water molecules accelerates the formation of polymersomes. Also, the process can work reversibly, which means water can be injected to the polymer-solvent solution to trigger self-assembly.[104] Similar to film rehydration, direct injection produced vesicles with a rather broad size distribution, however, the sizes of vesicles can be homogenised by extrusion through filters.

To have a better control of the size distribution of vesicles, emulsion phase transfer method has been developed.[105,106,107] The amphiphilic polymers are firstly dissolved in an organic solution, while the addition of a small volume of aqueous media, a w/o (water-in-oil) emulsion is prepared via vigorous agitation. Secondly, in another vessel, an oil-in-water biphasic system is prepared, with a layer of amphiphilic polymer sitting on the oil/water interface. Thirdly, the emulsion is poured into the system and get contact with the interface of oil and water. Due to the density difference, the oil-coated water droplets sink to the water phase and get another coating with the existing layer of amphiphilic polymers,[2] resulting in a water-in-oil-in-water (w/o/w) double emulsion. Polymersomes are formed in the process, and their final sizes is controlled by the initial inner water droplet.

An up-to-date method derived from emulsion phase transfer is related to microfluidics.[108,109,110] This method has an excellent control of the polymersome size and size distribution. The basic mechanism of the method is similar to emulsion phase transfer: the two methods both create a w/o/w double emulsion and the vesicles are formed in this process. The method requires specialised equipment including two junctions, and the flow rates can be tuned at each junction, leading to the precise control of the vesicle size.

1.5 Applications of Polymersomes

Polymersomes, from the day they have been discovered, has been compared extensively

with liposomes. Polymersomes are expected to overcome the shortages of liposome and improve in performance of liposomes, for instance, polymersomes have been proved to circulate as long or longer than stealth liposomes.[23]

Thus, similar with liposomes, the most straight-forward application of polymersomes is the encapsulation and delivery of therapeutic molecules for biomedical applications. Due to the amphiphilic nature of polymersomes, the encapsulation of both hydrophilic and hydrophobic molecules is possible, since the hydrophilic molecules can be encapsulated in the aqueous lumen whereas hydrophobic molecules can stay in the hydrophobic membrane. In addition, amphiphilic molecules can also be loaded in polymersomes. Encapsulation efficiency (EE) and drug loading content (DLC) are two important parameters to describe the capability of polymersomes in encapsulation of drugs. They are defined as following:

$$Encapsulation\ efficiency\ (EE)\ (100\%) = \frac{weight\ of\ loaded\ drug}{weight\ of\ drug\ in\ feed} \times 100\% \qquad \textbf{Equation 1.7}$$

$$Drug\ loading\ content\ (DLC)\ (100\%) = \frac{weight\ of\ loaded\ drug}{weight\ of\ polymer} \times 100\% \qquad \textbf{Equation 1.8}$$

Besides, other applications of polymersomes have also been discovered, polymersomes can be used as nano-reactor, due to the cell-mimicking nature, and these applications are introduced in **1.5.2**.

1.5.1 Drug Loading and Release

A chemotherapeutic drug, Docetaxel (DTX) is a semi-synthetic analogue of paclitaxel prepared from a non-cytotoxic precursor extract of the European yew tree. It has been used to treat several types of malignancy, such as breast, lung, ovarian, prostate, head and neck cancers.[111] However, the drug has a low solubility in water. To have a longer systemic circulation time and a reduction of side effects, a polymeric carrier is desirable.

Polymersomes fabricated from a diblock copolymer OA-PEG_{1000} via solvent displacement approach has been reported,[111] and the encapsulation efficiency and loading capacity percentages were estimated as 22.2% and 0.43% respectively. The fabricated polymersomes have an average size of 221.3 ± 8.06 nm (by DLS) and the authors have demonstrated that the DTX loaded polymersomes are well qualified as a promising anticancer *Nanodrug*.

In 2010, pH sensitive degradable diblock copolymer poly(ethylene glycol)-*b*-poly(2,4,6-trimethoxybenzylidenepentaerythritolcarbonate) (PEG-*b*-PTMBPEC) was synthesised, and both micelles and polymersomes were fabricated. The drugs capsulated in the polymeric structure were doxorubicin hydrochloride (DOX·HCl) and pacilitaxel (PTX).[112] The release study revealed that the release can be drastically accelerated at mildly acidic pH when compared with physiological pH. The authors have claimed that the polymersomes were the first reported degradable stimuli-sensitive polymersomes. In addition, the degradation, drug encapsulation and pH-triggered drug release behaviours of micelles and polymersomes were compared, showing that polymersomes have a more rapid response to mildly acidic pH, even if they were fabricated from similar diblock copolymers. This work has inspired extensive research interest on stimuli-responsive polymersomes (especially pH-responsive ones). In 2012, diblock copolymers PEG-*b*-PLA and poly(*N*-isopropylacrylamide)-*b*-poly(lactic-*co*-glycolic acid) (PNIPAM-*b*-PLGA) were synthesised.[82] Specially designed polymersomes, of which membranes contain above two distinct diblock copolymers and photothermal gold nanoparticles, were fabricated from W/O/W double-emulsion (emulsion phase transfer method). The authors claimed that the polymersomes release the encapsulants if the temperature increases above the lower critical solution temperature (LCST) of the thermoresponsive amphiphiles (thermosensitive PNIPAM blocks), indicating the thermoresponsiveness of the polymersomes. On the other hand, the polymersomes also release the encapsulants upon laser illumination (attributes to the embedded gold nanoparticles in polymersome membrane), which proves the photoresponsiveness of the polymersomes. A very recent study also shows the

encapsulation of anticancer drugs and presents a co-delivery by designed polymersomes. The polymersomes were fabricated by triblock copolymer methoxyl poly(ethylene glycol)-*b*-poly(*N*-isopropylacrylamide)-*b*-poly[2-(diethylamino)ethyl methacrylate-*co*-2-hydroxy-4-(methacryloyloxy)benzophenone] (mPEG-*b*-PNIPAM-*b*-P(DEAEMA-*co*-BMA)). Interestingly, the polymersome shows multi stimuli-responsiveness, which are pH responsiveness and thermoresponsiveness.[113] The loaded anticancer drugs are hydrophilic-hydrophobic drug pair DOX·HCl and PTX. The authors have proved the separate control on the release of the two drugs, triggered by the change of pH and temperature, since the two drugs are capsulated in different domain of polymersome. A list of different experimental conditions has been set (varied pH and temperature), and the cumulative release of drugs have been compared. One notable fact is, the pH-responsiveness of the polymersome comes from PDEAEMA, the thermo-responsiveness comes from PNIPAM and mPEG was employed to enhance the biocompatibility and achieve the stealth property.

DOX is usually used as a model hydrophilic anticancer drug, to monitor localisation of the drug within lipid bilayers and polymersome delivery system.[114] By intercalating into DNA strands, the cancer cell growth can be inhibited.[113] In the application of drug delivery, the responsiveness of polymersomes to a stimulus has drown much attention and has been well studied in the last decades. In 2013, Lecommandoux and colleagues synthesised poly(trimethylene carbonate)-*b*-poly($_{L}$-glutamic acid) (PTMC-*b*-PGA) copolymer by ROP.[115] The USPIOs (γ-Fe_2O_3) loaded polymersomes were fabricated by the nanoprecipitation method (solvent assisted dispersion), further loaded with DOX. The polymersomes responded to an implied magnetic field, which induces a very local hyperthermia effect at the level of polymersome membrane, resulting in drug release. pH-sensitive degradable polymersomes were fabricated from triblock copolymer poly(ethylene glycol)-*b*-poly(2,4,6-trimethoxybenzylidene-1,1,1-tris(hydroxymethyl)ethane methacrylate)-*b*-poly(acrylic acid) (PEG-*b*-PTTMA-*b*-PAA), and encapsulated with DOX·HCl. The authors verified the successful releasing of DOX·HCl in a controlled and pH-dependent manner. The polymersomes showed an

extremely high encapsulation efficiency of 88.8% and a drug loading contents of 15.9 wt.%. In another study, diblock copolymers PEG-*b*-PLA (both blocks are biocompatible) were synthesised and self-assembled in micelles and polymersomes based on the different hydrophilic volume fraction.[81] Under varied conditions, the encapsulation efficiency was up to 98.63 ± 0.12%, and the highest loading content was 11.04 ± 1.594%. The authors have proved the qualified properties of DOX-loaded polymersomes, their promising *in vitro* stability and release characteristics in comparison with DOX-loaded micelles. Moreover, folate-targeted, redox-responsive polymersomes fabricated from diblock copolymer poly(polyethylene glycol)-S-S-polylactide with disulfide linkage were discovered, and loaded with DOX, to compare the delivery characteristics with commercially available DOXIL nano formulation. The authors have demonstrated the superior colloidal stability, low protein adsorption, and hemocompatibility of the polymersomes. Importantly, the polymersomes showed excellent performance in tumour suppression as compared to free drug and commercially available DOXIL formulation in EAT tumour bearing Swiss albino mice. At the same time, no significant toxicity showed in the drug delivery process to heart, kidneys, liver, spleen and lungs.[42] Another work present by Zhong et al. shows chimaeric polymersomes based on poly(ethylene glycol)-*b*-poly(L-leucine)-*b*-poly(L-glutamic acid) (PEG-*b*-PLeu-*b*-PLG), and the polymersomes presented efficient loading and intracellular release of DOX·HCl.[52] The polymersomes were pH-dependent, thus, the *in vitro* release of DOX·HCl was highly dependent on pH, which were about 24.0% and 75.7% at pH 7.4 and pH 5.0, respectively. This phenomenon was explained by the authors as the configuration change of Pleu block, leading to the enhanced drug diffusion.

Fluorescent dyes have been used as a model drug in *in vitro* studies due to their sensitive fluorescence. A zwitterionic triblock copolymer poly(*N*-[3-(dimethylamine) propyl] methacrylamide)-*b*- poly(dimethylsiloxane)-*b*- poly(*N*-[3-(dimethylamine) propyl] methacrylamide) (ZPDMAPM-*b*-PDMS-*b*-ZPDMAPM) was synthesised and corresponding polymersomes were fabricated.[116] Efficient encapsulation and release of

curcumin, a fluorescent dye, have been achieved by the polymersomes, the results are given in **Table 1.3**. The authors further prepared a hydrogel based on the polymersomes and this formulation paves a new direction in therapeutic contact lens applications. Carboxyfluorescein was used as a model compound and it was encapsulated in polymersomes made from diblock copolymer PDMS-*b*-PMOXA.[39] The authors have addressed the average diameter of the polymersomes, which is 150 nm, and the encapsulation efficiency and loading content are shown in **Table 1.3**, respectively.

Proteins have also been capsulated in polymersomes. In 2018, Rangel-Yagui and colleagues fabricated polymersomes via film rehydration method, from the diblock copolymer poly(ethylene glycol)-*b*-poly(lactic acid) (PEG-*b*-PLA).[43] ASNase and BSA are two types of proteins, in this work, they were encapsulated in the polymersomes and the encapsulation efficiency was calculated as up to 25% for ASNase and 21% for BSA. Interestingly, the authors have fabricated 3 types of polymersomes based on the same chemistry with different degree of polymerisation of each block, to investigate the impact of MM and hydrophilicity of polymersomes on molecule encapsulation, and the results have proven that the larger the polymersomes are, the higher encapsulation efficiency they will achieve, since larger polymersomes enclose larger aqueous volumes (the protein molecules are hydrophilic). As for the two different protein molecules, the authors claimed that the encapsulation depended mainly on the concentration of the protein molecules in solution, not related to protein size and/or MM. Similarly, in another work of the same year,[46] PMOXA-*b*-PDMS-*b*-PMOXA was synthesised and fabricated into polymersomes, which were further loaded with neurotrophins (nerve growth factor and brain-derived neurotrophic factor, NGF), a large protein CD109, and a fluorescent drug curcumin. In addition, the polymersomes were also decorated with rhodamine, N-Methyl-$_{D}$-aspartate receptor (NMDAR) agonists and antagonists, for the neuron targeting. This paper revealed the successful incorporation of biologically active trophic factor plus hydrophilic agents into polymersomes, and the characteristics of the polymersomes have been demonstrated in selected central and peripheral tissue models.

Table 1.3 A summary of polymersomes in drug encapsulation study.

Chemistry of Polymersome	Molecule Encapsulated	Encapsulation Efficiency and Loading Content	Size of polymersome (nm)	Reference
OA-*b*-PEG_{1000}	Docetaxel, anticancer drug	EE 22.2%, DLC 0.43%	221.3 ± 8.06	111
mPEG-*b*-PNIPAM-*b*-P(DEAEMA-*co*-BMA)	DOX·HCl and PTX as a pair	Dependent on the experimental conditions	140 at pH 6, 80 at pH 8	113
PEG-*b*-PTTMA-*b*-PAA	DOX·HCl	EE up to 88.8%, DLC up to 15.9 wt.%	63.9 – 112.1	117
PEG-*b*-PLA	DOX·HCl	EE up to 98.63 ± 0.12%, DLC up to 11.04 ± 1.594%	120	81
ZPDMAPM-*b*-PDMS-*b*-ZPDMAPM	curcumin	EE 63.4%, DLC 4.2%	265 ± 5	116
PDMS-*b*-PMOXA	carboxyfluorescein	EE up to 92.2%, DLC is 1.5 ± 0.2 nmol CF per mg of polymersome	150	39
$(PEGMA)_n$-S-S-PLA	DOX	EE 76.55 ± 4.53%, DLC is 20.33 ± 1.20%	110	42
PEG-*b*-PLeu-*b*-PLG	DOX·HCl	Only release data is available	54.4 – 71.6	52
PEG-*b*-PLA	ASNase and BSA	EE up to 25% for ASNase and 21% for BSA	94 – 226	43
PMOXA-*b*-PDMS-*b*-PMOXA	Neurotrophins (NGF), CD109, curcumin	Curcumin: EE up to 82.3%, DLC 2.4 %; CD109: EE 4.3 %,	10 – 140	46

		DLC 20.72%; NGF: EE 100% and DLC 4.4 %.		
PTMC-*b*-PGA	DOX	EE 28%, DLC 5.6%	140 – 194	115
PEG-*b*-PTMBPEC	DOX·HCl and PTX	DOX·HCl: EE 19.5-26.2%, DLC 2.14-7.85%; PTX: EE 30.0-37.7%, DLC 3.0-7.5%	100 – 200	112
A combination of PEG-*b*-PLA and PNIPAM-*b*-PLGA	Dye molecules	N/A	N/A	82

In **Table 1.3**, the molecules that were encapsulated inside polymersomes can be classified into 3 categories: anticancer drugs, dyes, and proteins. DOX·HCl has been a popular candidate for the encapsulation of polymersomes, and the highest EE (98.63%) was achieved by polymersomes made from PEG-*b*-PLA;[43] the highest DLC (20.33%) was achieved by polymersomes made from $(PEGMA)_n$-S-S-PLA.[55] The biggest polymersomes in the table were made from copolymer ZPDMAPM-*b*-PDMS-*b*-ZPDMAPM, with diameters around 265 nm,[116] while the smallest polymersomes have diameters around 54 nm and were made from PEG-*b*-PLeu-*b*-PLG.[41] The EE and DLC data varies drastically depending on the chemistry of polymersomes, size of polymersomes, experimental conditions (pH, temperature, etc.) and the molecules encapsulated. Thus, for a specific drug delivery system, all those aspects need to be carefully considered.

1.5.2 Other Applications

In 2007, Hest and colleagues designed polymersomes (fabricated from PS-*b*-PIAT) that can be used as nanoreactors for cascade reactions, based on their multi-

compartmentalisation nature.[118] The polymersomes have membranes that are sufficiently porous, to allow diffusion of small molecules while larger molecules, such as enzymes, are kept securely inside.[119] Three types of enzymes, *Candida antarctica* lipase B (CALB), horseradish peroxidase (HRP), and glucose oxidase (GOX) were selected and loaded, creating a unique three-enzyme-polymersome system. The successful one-pot multistep reactions, and the possibility of using the enzyme-incorporated polymersomes have been proven by enzyme-activity assays, since the external CALB first converted the substrate GAc_4 into glucose, which was then used by GOX and HRP to generate $ABTS^{\cdot+}$. This study also demonstrated that the encapsulation of enzymes could maintain the enzyme activity for a much longer time in contrast to the same enzyme in bulk solution. This work is the first reported encapsulation of enzymes in the hydrophobic membrane of polymersomes, and it provided a new type of nanoreactors that are made from polymersomes. These reactors have superior properties than liposome reactors, for instance, they are less dynamic and more stable. Similarly, in 2009, Hest et al. reported another nanoreactor that shows stimuli-responsiveness,[80] and this nanoreactor (a novel polymersome) was fabricated by two copolymers: PEG-*b*-PS and poly(ethylene glycol)-*b*-poly(styrene boronic acid) (PEG-*b*-PSBA). Due to the difference in polarity, the nonpolar PS block and the polar PSBA block would have phase separation upon bilayer formation when the two polymers were mixed to form the polymersome. The authors designated PEG-*b*-PS as the matrix-forming block copolymer and PEG-*b*-PSBA as a stimuli-responsive block copolymer. If an optimal amount of PEG-*b*-PSBA was used, it could be assumed that the PSBA domains would disperse throughout the PS matrix. Upon the applied stimuli (in this work, change of pH and the concentration of sugar molecules in aqueous medium) the solubility of the PSBA block would change, whereas the PS matrix would still maintain the integrity of membrane structure. This smart design of membrane structure enables controllable permeability of polymersomes, leading to more possible applications on stimuli-responsive nanoreactors.

The membranes of polymersomes, at first, are mimics of cell membranes. Accordingly,

the polymersomes, along with the biomacromolecules encapsulated inside can be considered artificial cells. One of the applications has been reported in 2011.[84] A traditional ABA triblock copolymer PMOXA-*b*-PDMS-*b*-PMOXA, along with a diblock copolymer poly[styrene-*b*-poly(L-isocyanoalanine(2-thiophen-3-yl-ethyl) amide)], (PS-*b*-PIAT) have been synthesised and multicompartmentalised polymersomes are formed using the polymers. To be specific, the authors created a polymersome-in-polymersome system, where the PMOXA-*b*-PDMS-*b*-PMOXA polymersomes are designated outer vesicles and PS-*b*-PIAT polymersomes are inner vesicles. In this system, green fluorescent proteins (GFPs) were kept inside the inner vesicles, whereas cyanine-5 conjugated immunoglobulin G proteins (Cy5-IgG) were encapsulated outside the inner vesicles, but inside the outer vesicles. These two types of molecules were kept in the separate vesicular compartments; hence, the function of the molecules can be non-interfering, the system provides a suitable prototype for creating more advanced cell mimics.

In 2019, PDMS-glyco-polymersomes were fabricated,[41] and the ability of the polymersomes to interact with bio-receptors was confirmed on both the nanoscale and microscale. The giant glycosylated polymersomes (GGPs) are designed as a synthetic cell mimic, since they have been decorated with different ligands. Interestingly, the glucose-decorated GGPs have shown distinct behaviour upon addition of certain bacteria, in comparison with galactose-decorated GGPs, which shows the possibility of modulating the response of synthetic cell mimics towards bio-entities, through a considered choice of carbohydrate functionality.

REFERENCE

1. Rideau, E., Dimova, R., Schwille, P., Wurm, F. R., & Landfester, K. (2018). Liposomes and polymersomes: a comparative review towards cell mimicking. *Chemical society reviews*, *47*(23), 8572-8610.

2. Lefley, J., Waldron, C., & Becer, C. R. (2020). Macromolecular design and preparation of polymersomes. *Polymer Chemistry*, *11*(45), 7124-7136.

3. Lombard, J. (2014). Once upon a time the cell membranes: 175 years of cell boundary research. *Biology direct*, *9*(1), 1-35.

4. Overton, E. (1899). Uber die allgemeinen osmotischen eigenschaften der zelle. *Naturforsch. Ges. Zurich*, *44*, 87-136.

5. Branton, D., & Deamer, D. W. (1972). Membrane structure. In *Membrane Structure* (pp. 1-70). Springer, Vienna.

6. Gorter, E., & Grendel, F. J. E. M. (1925). On bimolecular layers of lipoids on the chromocytes of the blood. *The Journal of experimental medicine*, *41*(4), 439.

7. Singer, S. J., & Nicolson, G. L. (1972). The fluid mosaic model of the structure of cell membranes. *Science*, *175*(4023), 720-731.

8. Bangham, A. D., & Horne, R. W. (1962). Action of saponin on biological cell membranes. *Nature*, *196*(4858), 952-953.

9. Bangham, A. D., & Horne, R. W. (1964). Negative staining of phospholipids and their structural modification by surface-active agents as observed in the electron microscope. *Journal of molecular biology*, *8*(5), 660-IN10.

10. Cevc, G. (2012). Rational design of new product candidates: the next generation of highly deformable bilayer vesicles for noninvasive, targeted therapy. *Journal of controlled release*, *160*(2), 135-146.

11. Lasic, D. D., & Papahadjopoulos, D. (Eds.). (1998). *Medical applications of liposomes*. Elsevier.

12. Stuart, D. D., & Allen, T. M. (2000). A new liposomal formulation for antisense oligodeoxynucleotides with small size, high incorporation efficiency and good stability. *Biochimica et Biophysica Acta (BBA)-Biomembranes*, *1463*(2), 219-229.

13. Krauss, A. C., Gao, X., Li, L., Manning, M. L., Patel, P., Fu, W., ... & Pazdur, R. (2019). FDA approval summary:(daunorubicin and cytarabine) liposome for injection for the treatment of adults with high-risk acute myeloid leukemia. *Clinical Cancer Research*, *25*(9), 2685-2690.

14. Aibani, N., Khan, T. N., & Callan, B. (2020). Liposome mimicking polymersomes; A comparative study of the merits of polymersomes in terms of formulation and stability. *International journal of pharmaceutics: X*, *2*, 100040.

15. He, H., Lu, Y., Qi, J., Zhu, Q., Chen, Z., & Wu, W. (2019). Adapting liposomes for oral drug delivery. *Acta pharmaceutica sinica B*, *9*(1), 36-48.

16. Qin, G., Li, Z., Xia, R., Li, F., O'Neill, B. E., Goodwin, J. T., ... & Li, K. C. (2011). Partially polymerized liposomes: stable against leakage yet capable of instantaneous release for remote controlled drug delivery. *Nanotechnology*, *22*(15), 155605.

17. Barenholz, Y. (2001). Liposome application: problems and prospects. *Current opinion in colloid & interface science*, *6*(1), 66-77.

18. Jesorka, A., & Orwar, O. (2008). Liposomes: technologies and analytical applications. *Annu. Rev. Anal. Chem.*, *1*, 801-832.

19. LoPresti, C., Lomas, H., Massignani, M., Smart, T., & Battaglia, G. (2009). Polymersomes: nature inspired nanometer sized compartments. *Journal of Materials Chemistry*, *19*(22), 3576-3590.

20. Winzen, S., Bernhardt, M., Schaeffel, D., Koch, A., Kappl, M., Koynov, K., ... & Kroeger, A. (2013). Submicron hybrid vesicles consisting of polymer–lipid and polymer–cholesterol blends. *Soft Matter*, *9*(25), 5883-5890.

21. Discher, B. M., Won, Y. Y., Ege, D. S., Lee, J. C., Bates, F. S., Discher, D. E., & Hammer, D. A. (1999). Polymersomes: tough vesicles made from diblock copolymers. *Science*, *284*(5417), 1143-1146.

22. Chandrawati, R., & Caruso, F. (2012). Biomimetic liposome-and polymersome-based multicompartmentalized assemblies. *Langmuir*, *28*(39), 13798-13807.

23. Discher, D. E., & Ahmed, F. (2006). Polymersomes. *Annu. Rev. Biomed. Eng.*, *8*, 323-341.

24. Otrin, L., Marušič, N., Bednarz, C., Vidakovic-Koch, T., Lieberwirth, I., Landfester, K., & Sundmacher, K. (2017). Toward artificial mitochondrion: mimicking oxidative phosphorylation in polymer and hybrid membranes. *Nano letters*, *17*(11), 6816-6821.

25. Schulz, M., & Binder, W. H. (2015). Mixed hybrid lipid/polymer vesicles as a novel membrane platform. *Macromolecular rapid communications*, *36*(23), 2031-2041.

26. Kita-Tokarczyk, K., Grumelard, J., Haefele, T., & Meier, W. (2005). Block copolymer vesicles—using concepts from polymer chemistry to mimic biomembranes. *Polymer*, *46*(11), 3540-3563.

27. Blume, G., & Cevc, G. (1990). Liposomes for the sustained drug release in vivo. *Biochimica et Biophysica Acta (BBA)-Biomembranes*, *1029*(1), 91-97.

28. Klibanov, A. L., Maruyama, K., Torchilin, V. P., & Huang, L. (1990). Amphipathic polyethyleneglycols effectively prolong the circulation time of liposomes. *FEBS letters*, *268*(1), 235-237.

29. Bayer, A. M., Alam, S., Mattern-Schain, S. I., & Best, M. D. (2014). Triggered liposomal release through a synthetic phosphatidylcholine analogue bearing a

photocleavable moiety embedded within the sn-2 acyl chain. *Chemistry–A European Journal*, *20*(12), 3350-3357.

30. Owen, S. C., Chan, D. P., & Shoichet, M. S. (2012). Polymeric micelle stability. *Nano today*, *7*(1), 53-65.

31. Miyata, K., Christie, R. J., & Kataoka, K. (2011). Polymeric micelles for nano-scale drug delivery. *Reactive and Functional Polymers*, *71*(3), 227-234.

32. Erfani-Moghadam, V., Nomani, A., Zamani, M., Yazdani, Y., Najafi, F., & Sadeghizadeh, M. (2014). A novel diblock of copolymer of (monomethoxy poly [ethylene glycol]-oleate) with a small hydrophobic fraction to make stable micelles/polymersomes for curcumin delivery to cancer cells. *International journal of nanomedicine*, *9*, 5541.

33. Winzen, S., Bernhardt, M., Schaeffel, D., Koch, A., Kappl, M., Koynov, K., ... & Kroeger, A. (2013). Submicron hybrid vesicles consisting of polymer–lipid and polymer–cholesterol blends. *Soft Matter*, *9*(25), 5883-5890.

34. Liang, H., Zhou, Q., Long, Y., Wei, W., Feng, S., Liang, G., & Zhu, F. (2018). Synthesis and self-assembly of a novel amphiphilic diblock copolymer consisting of isotactic polystyrene and 1, 4-trans-polybutadiene-graft-poly (ethylene oxide). *RSC advances*, *8*(23), 12752-12759.

35. So, S., & Lodge, T. P. (2015). Interfacial tension-hindered phase transfer of polystyrene-b-poly (ethylene oxide) polymersomes from a hydrophobic ionic liquid to water. *Langmuir*, *31*(1), 594-601.

36. Kim, M. R., & Cheong, I. W. (2016). Stimuli-triggered Formation of Polymersomes from W/O/W Multiple Double Emulsion Droplets Containing Poly (styrene)-block-poly (N-isopropylacrylamide-co-spironaphthoxazine methacryloyl). *Langmuir*, *32*(36), 9223-9228.

37. Jonikaite-Svegzdiene, J., Kudresova, A., Paukstis, S., Skapas, M., & Makuska, R. (2017). Synthesis and self-assembly of polystyrene-based diblock and triblock coil–brush copolymers. *Polymer Chemistry*, *8*(36), 5621-5632.

38. Houga, C., Giermanska, J., Lecommandoux, S., Borsali, R., Taton, D., Gnanou, Y., & Le Meins, J. F. (2009). Micelles and polymersomes obtained by self-assembly of dextran and polystyrene based block copolymers. *Biomacromolecules*, *10*(1), 32-40.

39. Kiene, K., Schenk, S. H., Porta, F., Ernst, A., Witzigmann, D., Grossen, P., & Huwyler, J. (2017). PDMS-b-PMOXA polymersomes for hepatocyte targeting and assessment of toxicity. *European Journal of Pharmaceutics and Biopharmaceutics*, *119*, 322-332.

40. Porta, F., Ehrsam, D., Lengerke, C., & Meyer zu Schwabedissen, H. E. (2018). Synthesis and characterization of PDMS–PMOXA-based polymersomes sensitive to MMP-9 for application in breast cancer. *Molecular pharmaceutics*, *15*(11), 4884-4897.

41. Martin, L., Gurnani, P., Zhang, J., Hartlieb, M., Cameron, N. R., Eissa, A. M., & Perrier, S. (2019). Polydimethylsiloxane-based giant glycosylated polymersomes with tunable bacterial affinity. *Biomacromolecules*, *20*(3), 1297-1307.

42. Nehate, C., Moothedathu Raynold, A. A., Haridas, V., & Koul, V. (2018). Comparative Assessment of Active Targeted Redox Sensitive Polymersomes Based on pPEGMA-SS-PLA Diblock Copolymer with Marketed Nanoformulation. *Biomacromolecules*, *19*(7), 2549-2566.

43. Apolinário, A. C., Magoń, M. S., Pessoa Jr, A., & Rangel-Yagui, C. D. O. (2018). Challenges for the self-assembly of poly (ethylene glycol)–poly (lactic acid)(PEG-PLA) into polymersomes: beyond the theoretical paradigms. *Nanomaterials*, *8*(6), 373.

44. Danafar, H., Rostamizadeh, K., Davaran, S., & Hamidi, M. (2014). PLA-PEG-PLA copolymer-based polymersomes as nanocarriers for delivery of hydrophilic and hydrophobic drugs: preparation and evaluation with atorvastatin and lisinopril. *Drug development and industrial pharmacy*, *40*(10), 1411-1420.

45. Lefley, J., Waldron, C., & Becer, C. R. (2020). Macromolecular design and preparation of polymersomes. *Polymer Chemistry*, *11*(45), 7124-7136.

46. Moquin, A., Ji, J., Neibert, K., Winnik, F. M., & Maysinger, D. (2018). Encapsulation and delivery of neutrophic proteins and hydrophobic agents using PMOXA–PDMS–PMOXA triblock polymersomes. *ACS omega*, *3*(10), 13882-13893.

47. Konradi, R., Pidhatika, B., Mühlebach, A., & Textor, M. (2008). Poly-2-methyl-2-oxazoline: a peptide-like polymer for protein-repellent surfaces. *Langmuir*, *24*(3), 613-616.

48. Immordino, M. L., Dosio, F., & Cattel, L. (2006). Stealth liposomes: review of the basic science, rationale, and clinical applications, existing and potential. *International journal of nanomedicine*, *1*(3), 297.

49. Zhang, X. Y., & Zhang, P. Y. (2017). Polymersomes in nanomedicine-A review. *Current Nanoscience*, *13*(2), 124-129.

50. Fox, M. E., Szoka, F. C., & Fréchet, J. M. (2009). Soluble polymer carriers for the treatment of cancer: the importance of molecular architecture. *Accounts of chemical research*, *42*(8), 1141-1151.

51. Duncan, R., & Kopeček, J. (1984). Soluble synthetic polymers as potential drug carriers. *Polymers in medicine*, 51-101.

52. Chen, P., Deng, C., Meng, F., Zhang, J., Cheng, R., & Zhong, Z. (2015). Chimaeric polymersomes based on poly (ethylene glycol)-b-poly (l-leucine)-b-poly (l-glutamic acid) for efficient delivery of doxorubicin hydrochloride into drug-resistant cancer cells. *Journal of controlled release: official journal of the Controlled Release Society*, *213*, e87-e88.

53. Vlakh, E., Ananyan, A., Zashikhina, N., Hubina, A., Pogodaev, A., Volokitina,

M., ... & Tennikova, T. (2016). Preparation, characterization, and biological evaluation of poly (glutamic acid)-b-polyphenylalanine polymersomes. *Polymers*, *8*(6), 212.

54. Liarou, E., Varlas, S., Skoulas, D., Tsimblouli, C., Sereti, E., Dimas, K., & Iatrou, H. (2018). Smart polymersomes and hydrogels from polypeptide-based polymer systems through α-amino acid N-carboxyanhydride ring-opening polymerization. From chemistry to biomedical applications. *Progress in Polymer Science*, *83*, 28-78.

55. Webster, O. W. (1991). Living polymerization methods. *Science*, *251*(4996), 887-893.

56. Braunecker, W. A., & Matyjaszewski, K. (2007). Controlled/living radical polymerization: Features, developments, and perspectives. *Progress in Polymer Science*, *32*(1), 93-146.

57. Daubian, D., Gaitzsch, J., & Meier, W. (2020). Synthesis and complex self-assembly of amphiphilic block copolymers with a branched hydrophobic poly (2-oxazoline) into multicompartment micelles, pseudo-vesicles and yolk/shell nanoparticles. *Polymer Chemistry*, *11*(6), 1237-1248.

58. Webster, O. W., Hertler, W. R., Sogah, D. Y., Farnham, W. B., & RajanBabu, T. V. (1983). Group-transfer polymerization. 1. A new concept for addition polymerization with organosilicon initiators. *Journal of the American Chemical Society*, *105*(17), 5706-5708.

59. Rikkou-Kalourkoti, M., Webster, O. W., & Patrickios, C. S. (2002). Group Transfer Polymerization. *Encyclopedia of Polymer Science and Technology*.

60. Carroll, D. R., Constantinou, A. P., Stingelin, N., & Georgiou, T. K. (2018). Scalable syntheses of well-defined pentadecablock bipolymer and quintopolymer. *Polymer Chemistry*, *9*(25), 3450-3454.

61. Muir, A. V. (1997). Industrial Applications of Living Polymerization. *Macromolecular Design of Polymeric Materials*, *40*, 123.

62. Ward, M. A., & Georgiou, T. K. (2012). Thermoresponsive triblock copolymers based on methacrylate monomers: effect of molecular weight and composition. *Soft Matter*, *8*(9), 2737-2745.

63. Webster, O. W. (2003). Group transfer polymerization: a critical review of its mechanism and comparison with other methods for controlled polymerization of acrylic monomers. *New Synthetic Methods*, 1-34.

64. YK, C. J. C., & Ercole, F. (1998). Living free-radical polymerization by reversible addition− fragmentation chain transfer: the RAFT process. *Macromolecules*, *31*, 5559-5562.

65. McCormick, C. L., & Lowe, A. B. (2004). Aqueous RAFT polymerization: recent developments in synthesis of functional water-soluble (co) polymers with controlled structures. *Accounts of chemical research*, *37*(5), 312-325.

66. Perrier, S., & Takolpuckdee, P. (2005). Macromolecular design via reversible addition–fragmentation chain transfer (RAFT)/xanthates (MADIX) polymerization. *Journal of Polymer Science Part A: Polymer Chemistry*, *43*(22), 5347-5393.

67. Patten, T. E., & Matyjaszewski, K. (1998). Atom transfer radical polymerization and the synthesis of polymeric materials. *Advanced Materials*, *10*(12), 901-915.

68. Cowie, J. M. G., & Arrighi, V. (2007). *Polymers: chemistry and physics of modern materials*. CRC press.

69. Houga, C., Giermanska, J., Lecommandoux, S., Borsali, R., Taton, D., Gnanou, Y., & Le Meins, J. F. (2009). Micelles and polymersomes obtained by self-assembly of dextran and polystyrene based block copolymers. *Biomacromolecules*, *10*(1), 32-40.

70. Nehate, C., Moothedathu Raynold, A. A., Haridas, V., & Koul, V. (2018). Comparative Assessment of Active Targeted Redox Sensitive Polymersomes Based on pPEGMA-SS-PLA Diblock Copolymer with Marketed Nanoformulation. *Biomacromolecules*, *19*(7), 2549-2566.

71. Jérôme, C., & Lecomte, P. (2008). Recent advances in the synthesis of aliphatic polyesters by ring-opening polymerization. *Advanced drug delivery reviews*, *60*(9), 1056-1076.

72. Moore, J. C. (1964). Gel permeation chromatography. I. A new method for molecular weight distribution of high polymers. *Journal of Polymer Science Part A: General Papers*, *2*(2), 835-843.

73. Young, R. J., & Lovell, P. A. (2011). *Introduction to polymers*. CRC press.

74. Stetefeld, J., McKenna, S. A., & Patel, T. R. (2016). Dynamic light scattering: a practical guide and applications in biomedical sciences. *Biophysical reviews*, *8*(4), 409-427.

75. Constantinou, A. (2019). *Thermoresponsive gels: how do the structural parameters affect the gelation properties?* (PhD). Imperial College London.".

76. Sommerdijk, N. A., Holder, S. J., Hiorns, R. C., Jones, R. G., & Nolte, R. J. (2000). Self-assembled structures from an amphiphilic multiblock copolymer containing rigid semiconductor segments. *Macromolecules*, *33*(22), 8289-8294.

77. Yin, H., Kang, S. W., & Bae, Y. H. (2009). Polymersome formation from AB_2 type 3-miktoarm star copolymers. *Macromolecules*, *42*(19), 7456-7464.

78. Ayen, W. Y., Chintankumar, B., Jain, J. P., & Kumar, N. (2011). Effect of PEG chain length and hydrophilic weight fraction on polymersomes prepared from branched (PEG) 3-PLA co-polymers. *Polymers for Advanced Technologies*, *22*(1), 158-165.

79. Chang, H. Y., Lin, Y. L., Sheng, Y. J., & Tsao, H. K. (2013). Structural characteristics and fusion pathways of onion-like multilayered polymersome formed by

amphiphilic comb-like graft copolymers. *Macromolecules*, *46*(14), 5644-5656.

80. Kim, K. T., Cornelissen, J. J., Nolte, R. J., & van Hest, J. C. (2009). A Polymersome nanoreactor with controllable permeability induced by stimuli-responsive block copolymers. *Advanced materials*, *21*(27), 2787-2791.

81. Alibolandi, M., Ramezani, M., Abnous, K., Sadeghi, F., & Hadizadeh, F. (2015). Comparative evaluation of polymersome versus micelle structures as vehicles for the controlled release of drugs. *Journal of Nanoparticle Research*, *17*(2), 1-16.

82. Amstad, E., Kim, S. H., & Weitz, D. A. (2012). Photo-and thermoresponsive polymersomes for triggered release. *Angewandte Chemie International Edition*, *51*(50), 12499-12503.

83. Ansari Asl, A., & Rahmani, S. (2019). Synthesis, characterization and self-assembly investigation of novel PEG-g-PCL copolymers by combination of ROP and ‘‘click’’chemistry method as a sustained release formulation for hydrophobic drug. *International Journal of Polymeric Materials and Polymeric Biomaterials*, *68*(9), 540-550.

84. Fu, Z., Ochsner, M. A., de Hoog, H. P. M., Tomczak, N., & Nallani, M. (2011). Multicompartmentalized polymersomes for selective encapsulation of biomacromolecules. *Chemical Communications*, *47*(10), 2862-2864.

85. Onaca, O., Enea, R., Hughes, D. W., & Meier, W. (2009). Stimuli-responsive polymersomes as nanocarriers for drug and gene delivery. *Macromolecular bioscience*, *9*(2), 129-139.

86. Mai, Y., & Eisenberg, A. (2012). Self-assembly of block copolymers. *Chemical Society Reviews*, *41*(18), 5969-5985.

87. Shen, H., & Eisenberg, A. (1999). Morphological phase diagram for a ternary system of block copolymer PS310-b-PAA52/dioxane/H2O. *The Journal of Physical Chemistry B*, *103*(44), 9473-9487.

88. Discher, D. E., & Eisenberg, A. (2002). Polymer vesicles. *Science*, *297*(5583), 967-973.

89. Gregoriadis, G. (1984). Liposome technology. Volume I: Preparation of liposomes.

90. Zhu, Y., Yang, B., Chen, S., & Du, J. (2017). Polymer vesicles: Mechanism, preparation, application, and responsive behavior. *Progress in Polymer Science*, *64*, 1-22.

91. Du, J., & O'Reilly, R. K. (2009). Advances and challenges in smart and functional polymer vesicles. *Soft Matter*, *5*(19), 3544-3561.

92. Fetsch, C., Gaitzsch, J., Messager, L., Battaglia, G., & Luxenhofer, R. (2016). Self-Assembly of amphiphilic block copolypeptoids–Micelles, worms and polymersomes. *Scientific reports*, *6*(1), 1-13.

93. Rideau, E., Wurm, F. R., & Landfester, K. (2018). Giant polymersomes from non-assisted film hydration of phosphate-based block copolymers. *Polymer Chemistry*, *9*(44), 5385-5394.

94. Bartenstein, J. E., Robertson, J., Battaglia, G., & Briscoe, W. H. (2016). Stability of polymersomes prepared by size exclusion chromatography and extrusion. *Colloids and Surfaces A: Physicochemical and Engineering Aspects*, *506*, 739-746.

95. Angelova, M. I., & Dimitrov, D. S. (1986). Liposome electroformation. *Faraday discussions of the Chemical Society*, *81*, 303-311.

96. Warren, N. J., & Armes, S. P. (2014). Polymerization-induced self-assembly of block copolymer nano-objects via RAFT aqueous dispersion polymerization. *Journal of the American Chemical Society*, *136*(29), 10174-10185.

97. Gonzato, C., Semsarilar, M., Jones, E. R., Li, F., Krooshof, G. J., Wyman, P., ... & Armes, S. P. (2014). Rational synthesis of low-polydispersity block copolymer vesicles in concentrated solution via polymerization-induced self-assembly. *Journal of the American Chemical Society*, *136*(31), 11100-11106.

98. Albertsen, A. N., Szymański, J. K., & Pérez-Mercader, J. (2017). Emergent properties of giant vesicles formed by a polymerization-induced self-assembly (PISA) reaction. *Scientific reports*, *7*(1), 1-8.

99. Warren, N. J., Mykhaylyk, O. O., Mahmood, D., Ryan, A. J., & Armes, S. P. (2014). RAFT aqueous dispersion polymerization yields poly (ethylene glycol)-based diblock copolymer nano-objects with predictable single phase morphologies. *Journal of the American Chemical Society*, *136*(3), 1023-1033.

100. Blanazs, A., Madsen, J., Battaglia, G., Ryan, A. J., & Armes, S. P. (2011). Mechanistic insights for block copolymer morphologies: how do worms form vesicles?. *Journal of the American Chemical Society*, *133*(41), 16581-16587.

101. Wan, W. M., Hong, C. Y., & Pan, C. Y. (2009). One-pot synthesis of nanomaterials via RAFT polymerization induced self-assembly and morphology transition. *Chemical Communications*, (39), 5883-5885.

102. Du, J., Tang, Y., Lewis, A. L., & Armes, S. P. (2005). pH-sensitive vesicles based on a biocompatible zwitterionic diblock copolymer. *Journal of the American Chemical Society*, *127*(51), 17982-17983.

103. Akbarzadeh, A., Rezaei-Sadabady, R., Davaran, S., Joo, S. W., Zarghami, N., Hanifehpour, Y., ... & Nejati-Koshki, K. (2013). Liposome: classification, preparation, and applications. *Nanoscale research letters*, *8*(1), 1-9.

104. Pijpers, I. A., Meng, F., van Hest, J. C., & Abdelmohsen, L. K. (2020). Investigating the self-assembly and shape transformation of poly (ethylene glycol)-b-poly (d, l-lactide) (PEG-PDLLA) polymersomes by tailoring solvent-polymer interactions. *Polymer Chemistry*, *11*(2), 275-280.

105. Walde, P., Cosentino, K., Engel, H., & Stano, P. (2010). Giant vesicles: preparations and applications. *ChemBioChem*, *11*(7), 848-865.

106. Pautot, S., Frisken, B. J., & Weitz, D. A. (2003). Engineering asymmetric vesicles. *Proceedings of the National Academy of Sciences*, *100*(19), 10718-10721.

107. Tsumoto, K., Hayashi, Y., Tabata, J., & Tomita, M. (2018). A reverse-phase method revisited: Rapid high-yield preparation of giant unilamellar vesicles (GUVs) using emulsification followed by centrifugation. *Colloids and Surfaces A: Physicochemical and Engineering Aspects*, *546*, 74-82.

108. Utada, A. S., Lorenceau, E., Link, D. R., Kaplan, P. D., Stone, H. A., & Weitz, D. A. (2005). Monodisperse double emulsions generated from a microcapillary device. *Science*, *308*(5721), 537-541.

109. Ahn, J., Ko, J., Lee, S., Yu, J., Kim, Y., & Jeon, N. L. (2018). Microfluidics in nanoparticle drug delivery; From synthesis to pre-clinical screening. *Advanced drug delivery reviews*, *128*, 29-53.

110. Roces, C. B., Christensen, D., & Perrie, Y. (2020). Translating the fabrication of protein-loaded poly (lactic-co-glycolic acid) nanoparticles from bench to scale-independent production using microfluidics. *Drug delivery and translational research*, 1-12.

111. Haghshenas, V., Sariri, R., Naderi Sohi, A., & Nazari, H. (2020). Encapsulation of Docetaxel into Diblock Polymeric Polymersome as a Nanodrug. *ChemistrySelect*, *5*(29), 8924-8928.

112. Chen, W., Meng, F., Cheng, R., & Zhong, Z. (2010). pH-Sensitive degradable polymersomes for triggered release of anticancer drugs: a comparative study with micelles. *Journal of controlled release*, *142*(1), 40-46.

113. Zhou, D., Fei, Z., Jin, L., Zhou, P., Li, C., Liu, X., & Zhao, C. (2021). Dual-responsive polymersomes as anticancer drug carriers for the co-delivery of doxorubicin and paclitaxel. *Journal of Materials Chemistry B*, *9*(3), 801-808.

114. Karukstis, K. K., Thompson, E. H., Whiles, J. A., & Rosenfeld, R. J. (1998). Deciphering the fluorescence signature of daunomycin and doxorubicin. *Biophysical chemistry*, *73*(3), 249-263.

115. Oliveira, H., Pérez-Andrés, E., Thevenot, J., Sandre, O., Berra, E., & Lecommandoux, S. (2013). Magnetic field triggered drug release from polymersomes for cancer therapeutics. *Journal of Controlled Release*, *169*(3), 165-170.

116. Banerjee, S. L., Samanta, S., Sarkar, S., & Singha, N. K. (2020). A self-healable and antifouling hydrogel based on PDMS centered ABA tri-block copolymer polymersomes: a potential material for therapeutic contact lenses. *Journal of Materials Chemistry B*, *8*(2), 226-243.

117. Du, Y., Chen, W., Zheng, M., Meng, F., & Zhong, Z. (2012). pH-sensitive

degradable chimaeric polymersomes for the intracellular release of doxorubicin hydrochloride. *Biomaterials*, *33*(29), 7291-7299.

118. Vriezema, D. M., Garcia, P. M., Sancho Oltra, N., Hatzakis, N. S., Kuiper, S. M., Nolte, R. J., ... & Van Hest, J. C. (2007). Positional assembly of enzymes in polymersome nanoreactors for cascade reactions. *Angewandte chemie*, *119*(39), 7522-7526.

119. Vriezema, D. M., Hoogboom, J., Velonia, K., Takazawa, K., Christianen, P. C., Maan, J. C., ... & Nolte, R. J. (2003). Vesicles and polymerized vesicles from thiophene-containing rod–coil block copolymers. *Angewandte Chemie International Edition*, *42*(7), 772-776.

CHAPTER 2 AIM OF THIS THESIS

The first aim of thesis is to investigate how the composition of the amphiphilic block copolymer (hydrophilic/hydrophobic ratio of the amphiphilic block copolymer) affects the formation and the properties of polymersomes.

It has been summarised in **Chapter 1** that the fabrication of polymersomes is based on the self-assembly of amphiphilic block copolymers in aqueous media, and it is determined by the factors that contribute to the free energy in this process.[1] As previously mentioned in **1.3.5**, self-assembly of amphiphilic block copolymers is strongly dependent on the weight fraction of the hydrophilic blocks. Various polymeric nano-structures have been observed, including spherical micelles, rods, cylindrical micelles, lamellae and polymersomes.[2] To understand how hydrophilic-hydrophobic ratio of polymers affect the final morphologies and properties of the obtained structures, researchers defined several parameters to describe and predict the different morphologies which can be possibly formed, the most frequently used are *p* (packing parameter) and *f* (ratio of hydrophilic to total mass).[3] However, this theory cannot be applied to all cases, mainly due to the following aspects: 1. For the packing parameter, not all commonly used copolymers have a convinced *p*, which brings difficulties in applying the parameter and predicting the morphologies; 2. Most of the study on this topic focuses on the self-assembled structures fabricated by AB diblock copolymers,[4] not many focus on ABA triblock copolymers; 3. Some of the previous work considered the composition effect on the formation of polymersomes, whereas the MM of the polymers was not kept the same. For example, by keeping the A block the same and varying the length of the B block. However, the MM does have an impact on the self-assembly of the amphiphilic copolymers;[1] In light of the above discussion, in this thesis, the first and the main aim is to investigate the composition effect of ABA amphiphilic block copolymers on the formation of polymersomes as well as the properties of polymersomes, while maintaining the same monomer chemistry and similar MM of the triblock copolymers. In this case, well-defined block copolymers are needed and GTP

was used since it is a living polymerisation method that is ideal to produce methacrylate polymers with relatively low MMD.

The second aim of this thesis is to fabricate pH-responsive polymersomes and investigate the properties of polymersomes at different pH.

As mentioned in **Chapter 1**, stimuli-responsive polymersomes have triggered tremendous interest, as they may result in significantly enhanced therapeutic efficacy and minimal side effects.[5] Among all stimuli, acidic pH as an internal stimulus is intriguing, because tumour, inflammatory tissues and intracellular compartments such as endosomes and lysosomes of cells all have mildly acidic pH. The existing tumoral pH variation has been recognised as an excellent trigger for the selective release of anticancer drugs in tumour tissues and within tumour cells. Ideally, the drug should be released in early or secondary endosomes by pH-controlled hydrolysis (pH drop from physiological 7.4 – 7.5 to 6 in endosomes or 4 – 5 in lysosomes).[6] Thus, polymersomes made from pH-responsive amphiphilic block copolymers are promising candidates for biomedical applications. Moreover, pH-responsive block copolymers have been investigated but normally the pH responsiveness is in the hydrophilic block,[7] whereas in this thesis, we decided to have it in the hydrophobic block. Hence, DEAEMA was selected as a pH-responsive hydrophobic monomer for all polymers in this work.

The third aim of this thesis is to optimise the composition of the amphiphilic block copolymers in order to fabricate polymersomes with sizes in the range of 150 – 200 nm.

As mentioned in **Chapter 1**, polymersomes are designed to be used for biomedical applications *in vivo*, size control is important. Since liposomes have proven useful in reducing the side effects of encapsulated drugs and passively accumulating in areas of high vasculature when the particle size is below 200 nm,[8] polymersomes with the same size range are particularly of interest. It has been found that polymersomes with very small sizes (< 10 nm) are excreted rapidly through renal filtration, whereas large polymersomes (> 200 nm) are at risk of being caught immediately by cells of the mononuclear phagocyte system and end up in the liver and spleen.[9] In addition, organs

and tissues with discontinuous endothelium can have pores of 40 – 60 and up to 150 nm.[10] Particles with a size below that range will be excreted or trapped within the tissue resulting in clearance from the circulation. Thus, polymersomes with a range between 150 and 200 nm are desirable.

REFERENCE

1. Feng, A., & Yuan, J. (2014). Smart Nanocontainers: Progress on Novel Stimuli-Responsive Polymer Vesicles. *Macromolecular rapid communications*, *35*(8), 767-779.

2. Mai, Y., & Eisenberg, A. (2012). Self-assembly of block copolymers. *Chemical Society Reviews*, *41*(18), 5969-5985.

3. Discher, D. E., & Ahmed, F. (2006). Polymersomes. *Annu. Rev. Biomed. Eng.*, *8*, 323-341.

4. Apolinário, A. C., Magoń, M. S., Pessoa Jr, A., & Rangel-Yagui, C. D. O. (2018). Challenges for the self-assembly of poly (ethylene glycol)–poly (lactic acid) (PEG-PLA) into polymersomes: beyond the theoretical paradigms. *Nanomaterials*, *8*(6), 373.

5. Chen, W., Meng, F., Cheng, R., & Zhong, Z. (2010). pH-Sensitive degradable polymersomes for triggered release of anticancer drugs: a comparative study with micelles. *Journal of controlled release*, *142*(1), 40-46.

6. Ulbrich, K., & Šubr, V. (2004). Polymeric anticancer drugs with pH-controlled activation. *Advanced drug delivery reviews*, *56*(7), 1023-1050.

7. Rakhmatullina, E., & Meier, W. (2008). Solid-supported block copolymer membranes through interfacial adsorption of charged block copolymer vesicles. *Langmuir*, 24(12), 6254-6261.

8. Aibani, N., Khan, T. N., & Callan, B. (2020). Liposome mimicking polymersomes; A comparative study of the merits of polymersomes in terms of formulation and stability. *International journal of pharmaceutics: X*, *2*, 100040.

9. Bleul, R., Thiermann, R., & Maskos, M. (2015). Techniques to control polymersome size. *Macromolecules*, *48*(20), 7396-7409.

10. Drummond, D. C., Meyer, O., Hong, K., Kirpotin, D. B., & Papahadjopoulos, D. (1999). Optimizing liposomes for delivery of chemotherapeutic agents to solid tumors. *Pharmacological reviews*, *51*(4), 691-744.

CHAPTER 3 EXPERIMENTAL

3.1 Synthesis and Characterisation of Polymers

3.1.1 Materials and Equipment

Materials

All the polymers investigated in this thesis were synthesised in the lab using commercially available monomers, initiators and solvents. The catalyst (TBABB) was synthesised in the lab using chemicals that were commercially available. The monomers were purchased from Sigma Aldrich Co Ltd., Irvine, United Kingdom (UK) and Tokyo Chemical Industry UK Ltd. Monomers purchased from Sigma Aldrich Co Ltd., Irvine, UK are TEGMA (MM = 232.27 g mol^{-1}, 94%), PEGMA (MM = 300 g mol^{-1}, 95%) and BuMA (MM = 142.20 g mol^{-1}, 99%). Monomers purchased from Tokyo Chemical Industry UK Ltd. are DEAEMA (MM = 185.27 g mol^{-1}, 98.5%) and TEGEMA (MM = 246.30 g mol^{-1}, 95%). The initiator in the polymerisation reaction was purchased from Sigma Aldrich Co Ltd., Irvine, UK: MTS (95%); the solvent used in polymerisation reaction was purchased from Sigma Aldrich Co Ltd., Irvine, UK: THF (HPLC grade, not stabilised, ≥ 99.9%); The solvent used in polymer precipitation was from Fisher Scientific UK Ltd., Loughborough, UK. The compounds used in catalyst (TBABB) synthesis were tetrabutylammonium hydroxide (40% in water) and benzoic acid, and they were purchased from Acros Organics (the UK distributor is Fisher Scientific UK Ltd., Loughborough, UK). Other chemicals that purchased from Sigma Aldrich Co Ltd., Irvine, UK and used for polymer synthesis and characterisation were: calcium hydride (CaH_2, ≥ 90%), basic aluminium oxide ($Al_2O_3 \cdot KOH$), the free radical inhibitor 2,2-diphenyl-1-picrylhydrazyl hydrate (DPPH), sodium hydroxide pellets (NaOH, 97%), concentrated hydrochloric acid (HCl, ACS reagent, 37%), hydrochloric acid solution (1M), triethylamine (Et_3N, HPLC grade, used as a co-solvent in GPC), deuterated chloroform ($CDCl_3$, 99.8%, used as a solvent to dissolve chemicals for NMR). In addition, polytetrafluoroethylene (PTFE) syringe filters (0.45 μm in pore size, 13 mm in diameter) were purchased from WR International Ltd., Lutterworth, UK.

PTFE syringe filters (0.45 μm in pore size, 25 mm in diameter) and Nylon syringe filters (0.45 μm in pore size, 25 mm in diameter) were purchased from Fisher Scientific UK Ltd., Loughborough, UK. Poly(methyl methacrylate) (PMMA) standard samples (MM equal to 2000, 4000, 8000, 20000, 50000, 100000 g mol^{-1}.) for GPC calibration were purchased from Fluka, Sigma Aldrich Co Ltd., Irvine, UK.

Equipment

The synthesis and characterisation of polymers and derived polymeric structures were carried out at Department of Materials and Department of Chemistry at Imperial College London. All the equipment were the property of the TKG research group or belong to Department of Materials and Department of Chemistry.

Gel Permeation Chromatography (GPC) was used in the characterisation of polymers and the instrument was purchased from Agilent technologies UK Ltd., Shropshire, UK. The instrument was equipped with an Agilent SECurtiy GPC system, which included: 1)

a MIXED-D column (PL1110-6504, PLgel 5 μm, 300 x 7.5 mm, Agilent technologies UK Ltd, thermostated at 30°C) 2) an Agilent guard column (PL1110-1520, PLgel Mixed, dimensions [mm]: 50 × 7.5, particle size [μm]: 5), 3) an Agilent 1250 refractive index (RI) detector and 4) a "1260 Iso" isocratic pump. The mobile phase (THF with 5 vol% Et_3N) was pumped with a flow rate of 1 mL min^{-1}.

Proton Nuclear Magnetic Resonance (^{1}H NMR) Spectroscopy was used to confirm the chemical composition of the precursors during the polymerisation and the polymers. The experiments were performed using a 400 MHz Avance Bruker NMR spectrometer (Bruker, UK Ltd., Coventry, UK).

Dynamic Light Scattering (DLS) measurements were carried out using a Zetasizer Nano ZSP (Malvern Instruments Ltd., Malvern, UK).

Transmission Electron Microscopy (TEM) was used to determine the morphology and

size distributions of polymersomes and other polymeric structures. JEOL STEM/TEM 2100Plus and JEOL JEM-2100F TEM (JEOL UK Ltd., Hertfordshire, UK) were used to obtain the images.

A solvent purification system was used to purify the organic solvent (THF) used in the polymerisation and characterisation of polymers. The system was equipped with an activated alumina column (Pure SolvTM Micro 100 Liter solvent purification system, purchased from Sigma Aldrich).

A portable HI98103 pH checker (from Hanna instruments) was used for the pH adjustment and potentiometric titrations.

For cloud point measurements, two methods were applied and compared with each other; for the visual tests, an IKA RCT stirrer hotplate and an IKA ETS-D5 temperature controller were used; for the transmittance test, a Cary 3500 Compact Peltier UV-Vis System (purchased from Agilent technologies UK Ltd., Shropshire, UK) was used.

For small angle neutron scattering (SANS) measurements, time-of-flight SANS instrument ZOOM was used at the ISIS pulsed neutron source at the Rutherford Appleton Laboratory (Didcot, UK).

3.1.2 Methods of Polymer Synthesis

Monomer Purification

The purchased low MM monomers (TEGMA, TEGEMA, DEAEMA, BuMA) were purified before polymerisation via a four-step procedure: 1) The monomers were passed through two 5 cm basic alumina columns in sequence to remove the free-radical inhibitor monomethyl ether hydroquinone (MEHQ) in the bottles of the monomers, 2) DPPH (a different free-radical inhibitor) was added after passing through the columns to prevent undesirable polymerisations in the flasks, 3) Calcium hydride (CaH_2) was added to the flask and followed by at least 3-hour stirring. CaH_2 worked as a drying agent to remove any humidity in the monomer flasks, 4) The monomer flasks were kept

in a refrigerator for at least 3 days before the distillation. The reduced pressure distillation was performed one day before polymerisation and it was to obtain the pure monomers in Schlenk's tubes without CaH_2, $Ca(OH)_2$ (production of CaH_2 and humidity in the flask) and inhibitor DPPH. The obtained monomers in Schlenk's tubes were usually kept in the refrigerator for one night before the polymerisation due to the time arrangement of experiments, but it has been verified that freshly distilled monomers have better performance. The monomers were directly taken from the Schlenk's tubes during polymerisation. For relatively high MM monomer (in this thesis: PEGMA), it was purified differently following a four-step procedure: 1) PEGMA was diluted at a concentration of 50 vol% with THF (freshly obtained from the solvent purification system), 2) diluted PEGMA was passed through two 5 cm basic alumina columns in sequence to remove MEHQ, 3) CaH_2 was added to the monomer flask and stirred for 3 hours, 4) The monomer flask was kept in the refrigerator for at least 7 days before the polymerisation and no distillation was needed. The different procedures in dealing with low MM monomers and PEGMA were based on the capacity of distillation. For PEGMA, the MM was 300 g mol^{-1}, which was not possible for the reduced pressure distillation in the lab, based on which, DPPH was not added to the PEGMA solution. It was also the reason for the monomer flask to stay longer in the refrigerator, since no distillation might result in more humidity in the monomer solution. The monomer itself was viscous, in order to add the monomer via a glass syringe during polymerisation, it was diluted with THF at a concentration of 50 vol%. PTFE 0.45 μm filters were installed between the syringe and the needle to remove any CaH_2 and $Ca(OH)_2$ before the injection to the reaction flask.

Initiator Purification

The initiator used in the polymerisation was MTS. It was purified via reduced pressure distillation on the same day or one day before polymerisation. The MTS was also collected in a Schlenk's tube.

Synthesis of catalyst

The synthesis of catalyst (TBABB) followed the procedure reported by Dicker *et al*.[1] 80 mL of tetrabutyl ammonium solution (40% in water) and 10 g of benzoic acid were added to a 250 mL round bottom flask with constant stirring until the mixture was homogeneous. Then the mixture was transferred to a separation funnel, followed by the addition of 75 mL of $CHCl_3$. Two phases (aqueous and organic) were presented in the funnel and the aqueous phase was extracted after 3 times of changing the organic phase. The organic phase was kept each time after extraction in the same beaker, at the end, another 10 g of benzoic acid was added to the beaker, $MgSO_4$ was also added as a desiccant. The excess $MgSO_4$ and $MgSO_4 \cdot 7H_2O$ were removed by filtration. Then the solvent ($CHCl_3$) was removed by rotary evaporation, after which the obtained product was in a white solid form. Then the solid was dissolved in 100 mL warm THF, and recrystallised in 70 mL dried diethyl ether. Finally, the product was dried in a vacuum oven at 50 °C for at least 3 days.

Group Transfer Polymerisation

All polymers synthesised in this PhD thesis were products of group transfer polymerisation (GTP). The general procedure was identical for all ABA triblock polymers, only the addition sequence and steps varied slightly depending on the specific composition of polymers. One example is shown below to demonstrate the general procedure of GTP: To synthesise triblock copolymer $TEGMA_{16}$-*b*-$DEAEMA_{10}$-*b*-$TEGMA_{16}$, all the glassware was kept in an oven (120°C) over night before use to remove any residual humidity including a round bottom 250 mL flask (reaction flask) hydrophobized with dichlorodimethylsilane for 4 hours prior to placing in the oven. On the polymerisation day, the reaction flask was taken out of the heat oven and instantly loaded with TBABB (catalyst, ~10 mg), then the flask was sealed with a rubber septum and purged with argon gas to maintain a dry environment. Freshly purified THF was

obtained from the solvent purification system and instantly injected into the flask, followed by injection of 0.35 mL MTS (0.3 mg, 1.7 mmol). The reaction started after adding 6 mL TEGMA (6.2 g, 26.7 mmol), the temperature in the solution was monitored by a thermo couple, an increase was observed because the polymerisation reaction was exothermic. When the temperature decreased and close to the room temperature, the reaction paused (usually took ~15 mins). Then 2 samples were taken from the flask for the GPC and ^{1}H NMR analysis. The second monomer, 3.36 mL of DEAEMA (3.1 g, 16.7 mmol) was injected to restart the reaction. When the second block finished, following the same procedure 6 mL of TEGMA (6.2 g, 26.7 mmol) were added. In the end, 1 mL of methanol was added to quench the reaction when all 3 blocks had been synthesised. Then the polymers were recovered by precipitation in hexane and dried at room temperature in a vacuum oven for a week.

3.1.3 Methods of Polymer Characterisation

Gel Permeation Chromatography (GPC)

A calibration curve of PMMA was the basis of characterising the MM and dispersity of polymers. 6 standard samples of PMMA were purchased, the MM of which were 2, 4, 8, 20, 50 and 100 kg mol^{-1}, respectively. Before use, the PMMA samples were filtered through 0.45 μm PTFE filters to remove any aggregates. The calibration curve was plotted by linear fitting of the data points. The mobile phase for all the polymers synthesised in this thesis in the GPC was THF + 5% Et_3N (vol%). The key data obtained from GPC was the average number molar mass and the dispersity.

Proton Nuclear Magnetic Resonance (^{1}H NMR) Spectroscopy

All polymers and their precursors were characterised by ^{1}H NMR as a supplementary to GPC. The key information ^{1}H NMR gave was the chemical composition of the polymers, it determined the experimental degree of polymerisation of the blocks. The values described how close the actual polymer composition was compared to the

theoretical. Deuterated chloroform ($CDCl_3$) was used as the solvent to dissolve polymer samples. From the ^1H NMR spectrum, different monomer units have distinctive peaks, by analysing those peaks, the completion of polymerisation reaction and the experimental degree of polymerisation of each block can be obtained.

Potentiometric Titration

1 M hydrochloride acid was added dropwise to pre-prepared polymer solutions (polymers dissolved in deionised (DI) water or PBS, 10 mg mL^{-1}), the pH decrease was monitored by a pH meter and the pH was adjusted to 2. Then 0.25 M NaOH solution (NaOH in DI water) was added dropwise to increase the pH to 12. The pH change was recorded after each addition. The effective pK_a of a polymer was the pH at which half of the ionisable DEAEMA units were protonated, it can be calculated based on the data recorded.

Cloud Point Measurements

Visual tests: Polymer solutions (polymers dissolved in DI water or PBS, 10 mg mL^{-1}) were prepared in small glass vials and heated up in a water bath, from 25 ℃ to 80 ℃, every 1 ℃, using an IKA RCT basic stirrer hot plate. The temperature was controlled by an IKA ETS-D5 temperature controller. When the temperature reached the set temperature, the state of solution was recorded after 2 min to ensure the solution has reached the desire temperature. The cloud point was recorded as temperature at which the solutions became cloudy.[3] The solution may have different phases: transparent, slightly cloudy, cloudy, gel and precipitation.

Ultraviolet−Visible (UV−Vis) Spectroscopy: Polymer solutions (polymers dissolved in DI water or PBS, 10 mg mL^{-1}) were prepared and injected into the glass cuvettes, then the cuvette was placed in the sample holder in an Agilent Cary UV-Vis Compact Peltier UV-Vis spectrometer with a temperature probe. The polymer solution then was heated up at a rate of 1 ℃ min^{-1} and data was collected every 1 ℃ at 550 nm. The temperature

was recorded as cloud point at which the transmittance was 50%.

3.2 Fabrication and Characterisation of Polymersomes

3.2.1 Fabrication of Polymersomes

Film Rehydration

Film rehydration was the method used for the fabrication of polymersomes. To a round bottom 50 mL flask the polymers were placed, followed by the addition of THF. For 0.1 g polymers, 5 mL THF should be added to get an instant and complete dissolution. Then the organic solution was rotary evaporated under vacuum and slightly heated by a 40 ℃ water bath for 20 mins, after which the flask was transferred to a vacuum oven and stayed overnight to remove any residual THF. DI water or PBS was injected to the flask dropwise to re-hydrated the polymers depending on different research purposes. A stir bar was placed and the solution was kept stirring for at least one day before further analysis.

pH Adjustment

The solubility of polymers in aqueous solution varies with the MM, composition and monomer chemistry. For example, TEGEMA-*b*-(DEAEMA-*co*-BuMA)-*b*-TEGEMA polymers have very low solubility in water at room temperature. After film rehydration, the polymers had been stirred for weeks; however, they were still not fully dissolved. To enhance the solubility, one way was to protonate the amino groups in DEAEMA blocks. The pH of the polymer solution was adjusted to 6 or 7 based on different research purposes.

3.2.2 Characterisation of Polymersomes

Dynamic Light Scattering (DLS)

In aqueous solution, amphiphilic block copolymers tend to self-assemble into various structures, dynamic light scattering gives an investigation on size and size distribution of those structures. The polymer solutions (polymers dissolved in DI water or PBS, 10 mg mL^{-1}) were prepared and injected in the cuvettes without filtration, this is for a comprehensive understanding on the particle size distribution of the polymeric particles.

Each polymer solution was analysed three times at RT (usually around 25 ℃), and the scattered light collected at a backscatter angle of 173° was reported after each measurement. The hydrodynamic diameters (d_hS) reported were the mean values corresponding to the maximum of the peak by intensity and by number.

Transmission Electron Microscopy (TEM)

Sample preparation: Due to the low contrast of the polymers in background (carbon film on the copper grids), polymer loaded grids were negatively stained before TEM, which means the background of the grids (not the polymersomes) was stained in order to increase the contrast under microscope. In this study, the staining agent was uranyl acetate (UA) solution (uranyl acetate in DI water, 0.02 g mL^{-1}). UA scatters electrons strongly and absorbs to biological matter well, meanwhile, polymersomes or the other polymeric structures have low electron-scattering power. After negative staining, a distinctive border was created between the specimen (polymeric structures) and the carbon copper grids. The UA was used as a saturated solution and was prepared with the following procedure: 0.2 g UA powder was added to a centrifuge tube filled with 10 mL DI water. The mixture was shaken vigorously for 1 min, then left still for 10 min, and repeated the shaking process twice. The centrifuge tube was then covered with aluminium foil and parafilm (UA is light sensitive) and kept in the refrigerator at least for one day before use.

Two types of grids were used for TEM in this thesis: holey carbon copper grids and carbon copper grids. They both had a thin carbon film placed on top of copper grids, whereas holey carbon grids had many holes, in order to increase the contrast. One fact

to note was, even with two types of grids, they showed no difference on the morphology of the polymersomes and the other polymeric structures, so the images and results were consistent.

The polymer solution was dropped on top of a grid and stayed for 1 min, then the grid was blotted by a filter paper. Then the grid was allowed to dry completely. The UA solution was taken out of the fridge and allowed to reach RT. 1.5 – 2 mL solution was filtered with a 0.45 μm Nylon filter and syringed to a 2 mL Eppendorf tube, then the solution was filtered again and injected to a second Eppendorf tube to remove any big UA chunks. 30 μL of solution was taken by a pipette and dropped on the top of the grid. After 30 s, the grid was blotted by a filter paper, and it was allowed to dry completely before tested by TEM.

Encapsulation and Release Study

In the study of encapsulation and release of molecules by polymersomes, sodium fluorescein was used as a model drug. The polymer thin film was prepared as described in film rehydration method above. Then it was rehydrated with a 0.08 mg mL^{-1} sodium fluorescein solution in PBS. The concentration of the polymer solution was 10 mg mL^{-1}. After constantly stirring for one day, the polymersomes were formed and the sodium fluorescein was partially encapsulated in the polymersomes. Then, 2.6 mL of solution was syringed into a pre-hydrated 3000 MWCO dialysis tube. The dialysis tube was placed in a beaker with 578 mL of PBS. The sample was left to dialysed over 24 hours to remove the excess sodium fluorescein. After that, the dialysis tube was transferred to a 50 mL glass vial with 40 mL PBS. A sample of was taken out at regular intervals and the concentration of fluorescein was determined using UV-Vis.[2]

Small Angle Neutron Scattering (SANS)

A polymersome solution prepared with the film rehydration method in deuterated PBS (the concentration is 10 mg mL^{-1}) was analysed with SANS (after a week of

preparation). The experiment was performed at the time-of-flight SANS instrument ZOOM at the ISIS pulsed neutron source at the Rutherford Appleton Laboratory (Didcot, UK), the source-to-sample (L_1) and sample-to-detector (L_2) distances were set as $L_1 = L_2 = 4$ m and wavelengths were 1.5 – 16.5 Å. The data were reduced using MantidPlot, and the resulted SANS curves were fitted using the SasView (version 5) software. The fitting took into account the presence of both micelles (sphere model) and the presence of polymersomes (vesicles model).[2]

Contributions:

- Dr Anna Constantinou and Miss Qian Li assisted with the GTP.
- Dr Anna Constantinou provided the catalyst TBABB.
- Dr Claudia Contini assisted with TEM.
- Dr James Doutch assisted with SANS.
- Miss Maria Mikropoulou assisted with the DLS and cloud point measurements in **Chapter 5**.
- Miss Shuchen Wang assisted with the ^{1}H NMR for two polymers in **Chapter 6**.

REFERENCE

1. Dicker, I. B., Cohen, G. M., Farnham, W. B., Hertler, W. R., Laganis, E. D., & Sogah, D. Y. (1990). Oxyanions catalyze group-transfer polymerization to give living polymers. *Macromolecules*, *23*(18), 4034-4041.

2. Zhang, X., Contini, C., Constantinou, A. P., Doutch, J. J., & Georgiou, T. K. (2021). How does the hydrophobic content of methacrylate ABA triblock copolymers affect polymersome formation?. *Journal of Polymer Science*.

3. Constantinou, A. P., Sam-Soon, N. F., Carroll, D. R., & Georgiou, T. K. (2018). Thermoresponsive Tetrablock Terpolymers: Effect of Architecture and Composition on Gelling Behavior. *Macromolecules*, *51*(18), 7019-7031.

CHAPTER 4 POLYMERSOMES BASED ON TRIBLOCK COPOLYMER TEGMA-*b*-DEAEMA-*b*-TEGMA

Note to the readers: This chapter, excluding the discussion of pH-responsiveness of polymersomes, has already been published and can be found in: "**https://doi.org/10.1002/pol.20210371**, Zhang, X., Contini, C., Constantinou, A. P., Doutch, J. J., & Georgiou, T. K. (2021). How does the hydrophobic content of methacrylate ABA triblock copolymers affect polymersome formation? *Journal of Polymer Science*."

4.1 Chemistry of Block Copolymers

To design a series of amphiphilic block copolymers to form polymersomes, polymer composition is crucial. It has been reported that the hydrophilic fraction of the amphiphilic copolymers can affect the morphologies of polymeric structures, micelles, lamellar structures and polymersomes are all possible structure formed by self-assembly of amphiphilic block copolymers.[1] In the case of polymersomes, the hydrophilic/hydrophobic ratio can affect the size, membrane thickness and encapsulation efficiency of the polymersomes.[2]

In our research group, methacrylate-based stimuli-responsive polymers are of special interest,[3,4,5] because they can be synthesised using living chain growth polymerisations that allow the well control of the MM, composition and architectures, as well as easy functionalisation.[6] This enables systematic investigations on how the polymer structural characteristics affect their self-assembly and properties. For polymersome fabrication, to our knowledge, most pure methacrylate-based polymersomes are made from diblock copolymers.[7,8,9,10,11,12] In fact, only one study has been reported on ABA methacrylate-based vesicles and the polymer contains a non-ionic hydrophobic B block and pH responsive hydrophilic A block.[13] Hence, in this study, a series of ABA triblock methacrylate-based copolymers has been synthesised, with a hydrophilic non-ionic hydrophilic A block and an ionic pH-responsive hydrophobic B block. Specifically,

triethylene glycol methyl ether methacrylate (TEGMA) has been chosen as the hydrophilic A block and 2-(diethylamino) ethyl methacrylate (DEAEMA) has been chosen as the hydrophobic B block. The chemical structure of the series of polymers can be presented as $TEGMA_x$-*b*-$DEAEMA_y$-*b*-$TEGMA_x$. This series of polymers have not been reported so far. To investigate the composition effect on polymersome fabrication, five polymers have been synthesised. They have been named as AP1, AP2, AP3, AP4 and AP5, respectively, following an ascending trend of hydrophilicity. Their hydrophilic weight ratios to the total MM are designed 30%, 40%, 50%, 60% and 70%, respectively. While studying the composition effect, it is important to keep the MM of the polymers similar, to reduce the MM effect on the results. Hence, the MM is designed as 9000 g mol^{-1} (in consideration of the addition of MTS, the initiator, the final theoretical MM is 9100 g mol^{-1}), which means the five polymers are synthesised with the same monomers, designed with the same MM, the only variation factor is the composition. The following figure shows the chemical structures, names and abbreviations of the monomers used for this polymer series.

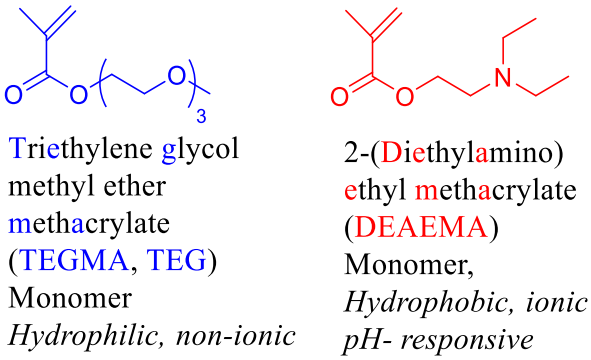


Figure 4.1 Chemical structures, names, abbreviations and related properties of the monomers used for the polymerisation of the polymer series AP.

4.1.1 Polymer Synthesis

The polymer series (five polymers) were synthesised using GTP. Due to the similarity

in architecture, the protocol for all five polymers was identical except for the amount of chemicals added. Details of the protocol can be found in **Chapter 3**; **Figure 4.2** is an illustration of the synthetic route. As all five polymers are ABA triblock copolymers, monomers (TEGMA and DEAEMA) were sequentially injected into the reaction flask after the addition of the catalyst (TBABB), the solvent (anhydrous THF) and the monofunctional initiator (MTS). 15 mins were taken between two monomer additions to reach the completion of the reaction.

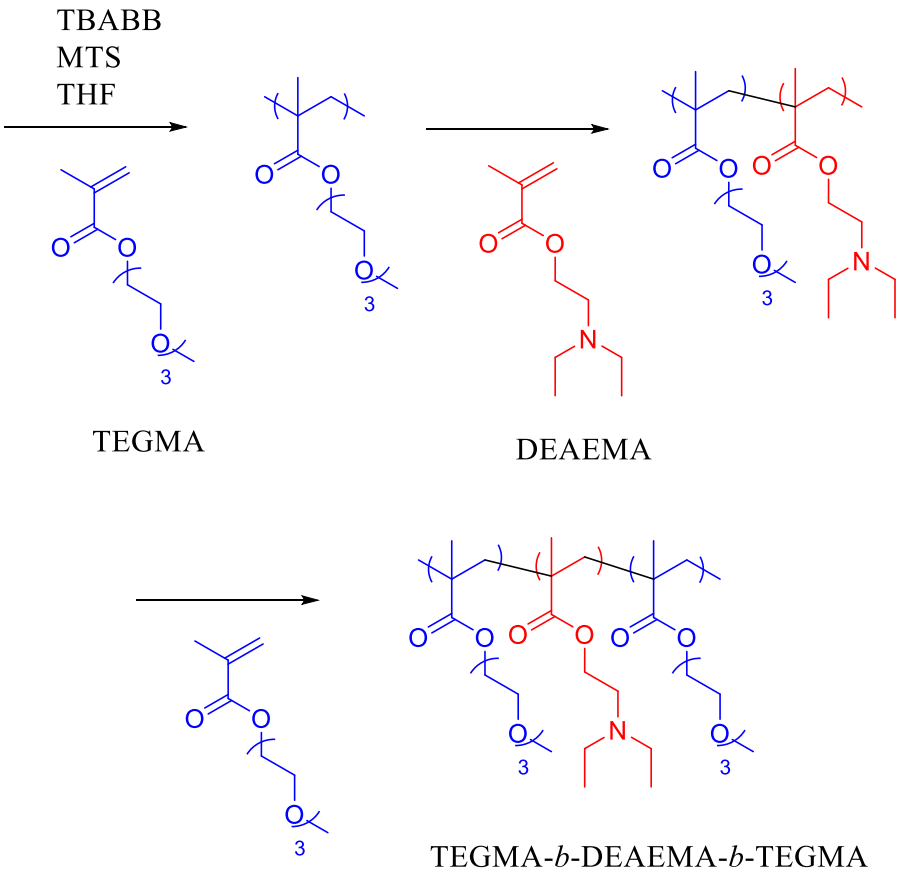


Figure 4.2 Illustration of the sequential GTP reaction for the synthesis of TEGMA-*b*-DEAEMA-*b*-TEGMA triblock copolymers. TEGMA and DEAEMA are the two monomers, TBABB, MTS, THF are the catalyst, monofunctional initiator and solvent used in the reaction, respectively.

Composition has an effect on the softness of the polymers, it has been found that from

AP1 to AP5, the softness of polymers increases with the increase of hydrophilicity. The colour of all the polymers was transparent.

4.1.2 Molar Mass and Composition

Figure 4.3 is the schematic representation of polymer composition. The blue coloured circles stand for hydrophilic units and red coloured circles stand for the hydrophobic. The theoretical MM of all polymers was kept the same, so the study was particularly focused on the composition effect. Also, the compositions listed below were theoretical, the experimental data is shown in **Table 4.1**.

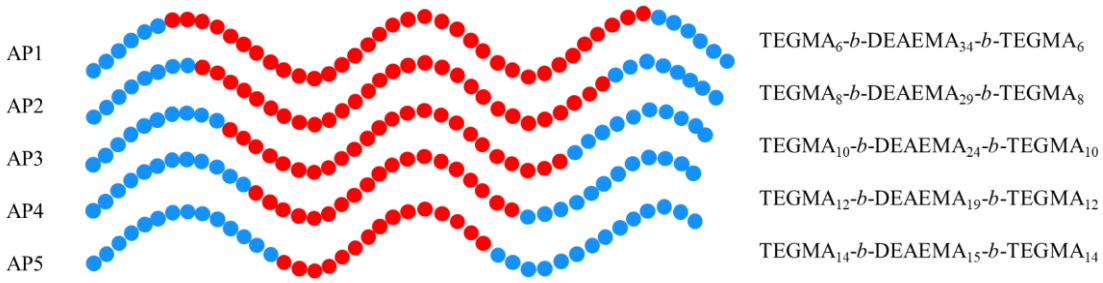


Figure 4.3 Schematic representation of the triblock copolymers. Blue circles represent hydrophilic TEGMA units, red circles represent hydrophobic DEAEMA units, the theoretical compositions of the polymers are listed.

GPC and ^{1}H NMR have been used to investigate the MM and the composition of the synthesised polymers. During the polymerisation, for each ABA copolymer, 6 samples were taken from the reaction flask, 3 of them were for GPC and the other 3 were for ^{1}H NMR. These samples were the TEGMA homopolymer precursor, the diblock precursor TEGMA-*b*-DEAEMA and the final triblock copolymer TEGMA-*b*-DEAEMA-*b*-TEGMA. GPC chromatograms of AP5 and its precursors are shown in **Figure 4.4**, where the black solid line represents the triblock copolymer, red solid line represents the diblock precursor during polymerisation and the black solid line represents homopolymer.

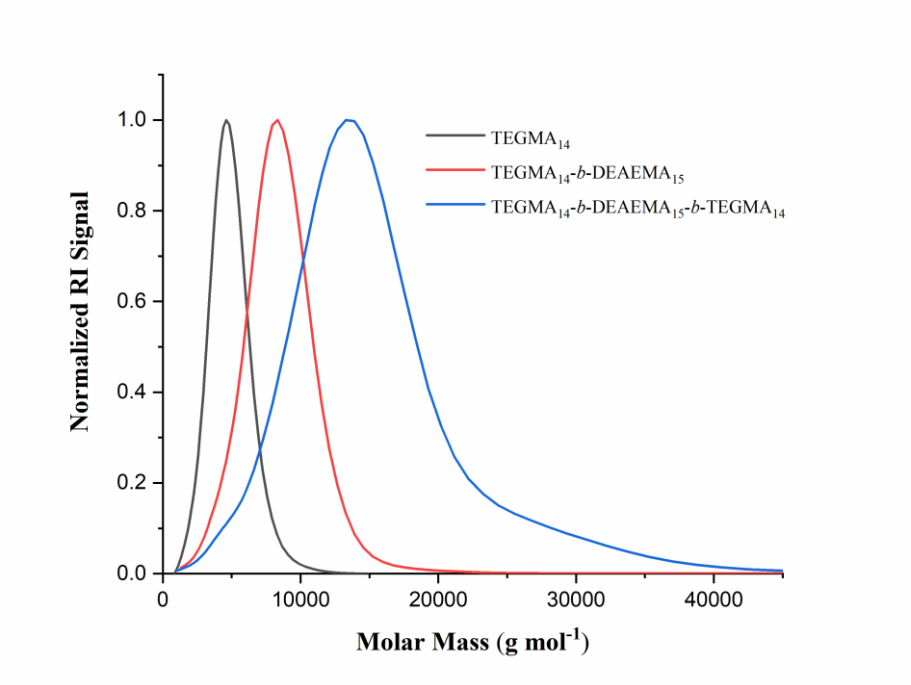


Figure 4.4 GPC chromatograms of ABA triblock polymer $TEGMA_{14}$-*b*-$DEAEMA_{15}$-*b*-$TEGMA_{14}$ and its linear precursors: $TEGMA_{14}$ in black solid line, $TEGMA_{14}$-*b*-$DEAEMA_{15}$ in red solid line and triblock polymer $TEGMA_{14}$-*b*-$DEAEMA_{15}$-*b*-$TEGMA_{14}$ in blue solid line.

In **Figure 4.4**, the peaks move to higher MM values from the homopolymer, to the diblock precursor and to the final product triblock copolymer, indicating the successful sequential polymerisation. The peak corresponding to monomer has not shown in the figure, confirming the complete consumption of the monomers. In some GPC chromatograms of other polymers (can be found in **Figure A1, Appendix**), the curves corresponding to triblock copolymer may show a small peak at low MM values, this is due to the termination of some reactive chains during the polymerisation. This is also observed in other GTP studies containing PEG based methacrylate monomers.[14,15,16] These peaks though are very small and negligible, thus, the synthesis is considered successful.

Table 4.1 Theoretical polymer structure, experimental number-average MM (M_n), the molar mass that corresponds to the maximum of the peak (M_p) MM distribution ($Đ$) and weight ratios of ABA units of APs.

No.	Theoretical Polymer Structure [a]	$MM^{theor.}$ (g mol^{-1})	M_n [c] (g mol^{-1})	M_p [c] (g mol^{-1})	$Đ$ [c]	TEGMA-*b*-DEAEMA-*b*-TEGMA (w/w%)	
						Theoretical	Experimental
AP1	$TEGMA_6$	1450	2210	2770	1.18	100-0-0	100-0-0
	$TEGMA_6$-*b*-$DEAEMA_{34}$	7750	11200	13800	1.17	18-82-0	19-81-0
	$TEGMA_6$-*b*-$DEAEMA_{34}$-$TEGMA_6$	9100	13800	16900	1.20	15-70-15	16-70-14
AP2	$TEGMA_8$	1900	2600	3260	1.18	100-0-0	100-0-0
	$TEGMA_8$-*b*-$DEAEMA_{29}$	7300	9530	11400	1.15	25-75-0	24-76-0
	$TEGMA_8$-*b*-$DEAEMA_{29}$-*b*-$TEGMA_8$	9100	11900	14700	1.19	20-60-20	20-62-18
AP3	$TEGMA_{10}$	2350	3350	4140	1.18	100-0-0	100-0-0
	$TEGMA_{10}$-*b*-$DEAEMA_{24}$	6850	8980	11700	1.21	33-67-0	34-66-0
	$TEGMA_{10}$-*b*-$DEAEMA_{24}$-*b*-$TEGMA_{10}$	9100	12200	16500	1.26	25-50-25	26-50-24
AP4	$TEGMA_{12}$	2800	3850	4820	1.15	100-0-0	100-0-0
	$TEGMA_{12}$-*b*-$DEAEMA_{19}$	6400	8890	11800	1.18	43-57-0	42-58-0
	$TEGMA_{12}$-*b*-$DEAEMA_{19}$-*b*-$TEGMA_{12}$	9100	13300	18500	1.31	30-40-30	31-40-29
AP5	$TEGMA_{14}$	3250	3830	4620	1.15	100-0-0	100-0-0
	$TEGMA_{14}$-*b*-$DEAEMA_{15}$	5950	6620	8250	1.16	54-46-0	56-44-0
	$TEGMA_{14}$-*b*-$DEAEMA_{15}$-*b*-$TEGMA_{14}$	9100	10500	13800	1.23	35-30-35	40-32-27

[a] TEGMA, DEAEMA stand for tri(ethylene glycol)methyl ether methacrylate, 2-(diethylamino) ethyl methacrylate, respectively.

[b] The theoretical MM values have been calculated by adding the product of the molar mass of each repeated unit by the degree of polymerisation. 100 g mol^{-1} corresponds to the part of the

initiator that stays on the polymer chain after the completion of the polymerisation, thus it is added to the result.

c The values of the number-average molar mass (M_n), the molar mass that corresponds to the maximum of the peak (M_p), and the dispersity indices ($Đ$) are based on a linear calibration using well-defined poly(methyl methacrylate) standard samples of molar mass equal to 2000, 4000, 8000, 20000, 50000, 100000 g mol^{-1}.

Theoretical polymer structures, experimental number average MM (M_n), MM distribution ($Đ$), and weight ratios of each block in the triblock copolymers are listed in **Table 4.1**. The series of ABA triblock copolymers are named AP, and the five polymers are named AP1 to AP5, respectively. To minimise the difference in MM, two polymerisations were taken to obtain the final five polymers to make sure their MMs are close enough to each other.

The target MM for the series of polymers is 9100 g mol^{-1}, in which 9000 g mol^{-1} is the total monomer mass and 100 g mol^{-1} is the MM of the initiator MTS. The reason for which experimental MM values are higher than the theoretical is, during the polymerisation, humidity deactivate some of the initiator molecules or the reactive polymer chains (or both), resulting in increased length of the other chains, which results in the increased MM on average. The higher the experimental MM is, the more deactivation happened during the polymerisation. In general, if on the same day, the later the polymer is synthesised, the more chances of deactivation happened during the reaction. Due to the increased number of times syringe needles pierced the rubber septa, the risks for the flasks to be exposed in air have increased over a day.

The MM distribution (denoted as dispersity index, $Đ$) is also a decisive parameter to determine whether the polymer is suitable for the project. $Đ$ measures the distribution of MM in a given polymer sample, indicates the degree of "non-uniformity" of the MM distribution. Ideally, if no deactivation happened, $Đ$ equals 1. In other studies published by our research group, $Đ$ was usually in a range of 1.07 to 1.27, attributed to the "living"

nature of the method.[14,15,16] In **Table 4.1**, as for AP4, the *Đ* is 1.31, slightly higher than the commonly reported values, however, the value is also subject to the reactivity of the monomers. The monomer TEGMA used in this project is less reactive than the frequently used monomers, such as MMA, BuMA, and DMAEMA, resulting in relatively higher *Đ*. In addition, it is well documented that all PEG based methacrylate monomers contain some dimethacrylate impurities as well as hydroxyl derivative (instead of methoxy side group), so often some termination and higher MM are observed for these samples.[14,15,16]

In **Table 4.1**, M_n and *Đ* values were obtained directly from GPC, while the weight percentages of the blocks in polymers were calculated from the ^{1}H NMR results (**Figure A2.1** – **A2.5**, **Appendix**). **Figure 4.5** is one example, from the top to the bottom, the three ^{1}H NMR spectra represent TEGMA homopolymer, the TEGMA-*b*-DEAEMA diblock precursor and the TEGMA-*b*-DEAEMA-*b*-TEGMA triblock copolymer, respectively. On the left, the chemical structures of the corresponding samples are listed, where light blue stands for TEGMA blocks and red stands for DEAEMA blocks. From the spectra, no monomer peak has been observed, confirming the complete consumption of the monomers. From the bottom to the top, the change of peaks clearly proved the sequential addition of the blocks. The experimental polymer structures and experimental polymer compositions (listed in **Table 4.1** in weight ratios of the blocks) can be calculated by integration of the peaks.

The results show the experimental polymer structures (AP1 to AP5) are close enough to the theoretical, those five polymers are good candidates for the study of the composition effect.

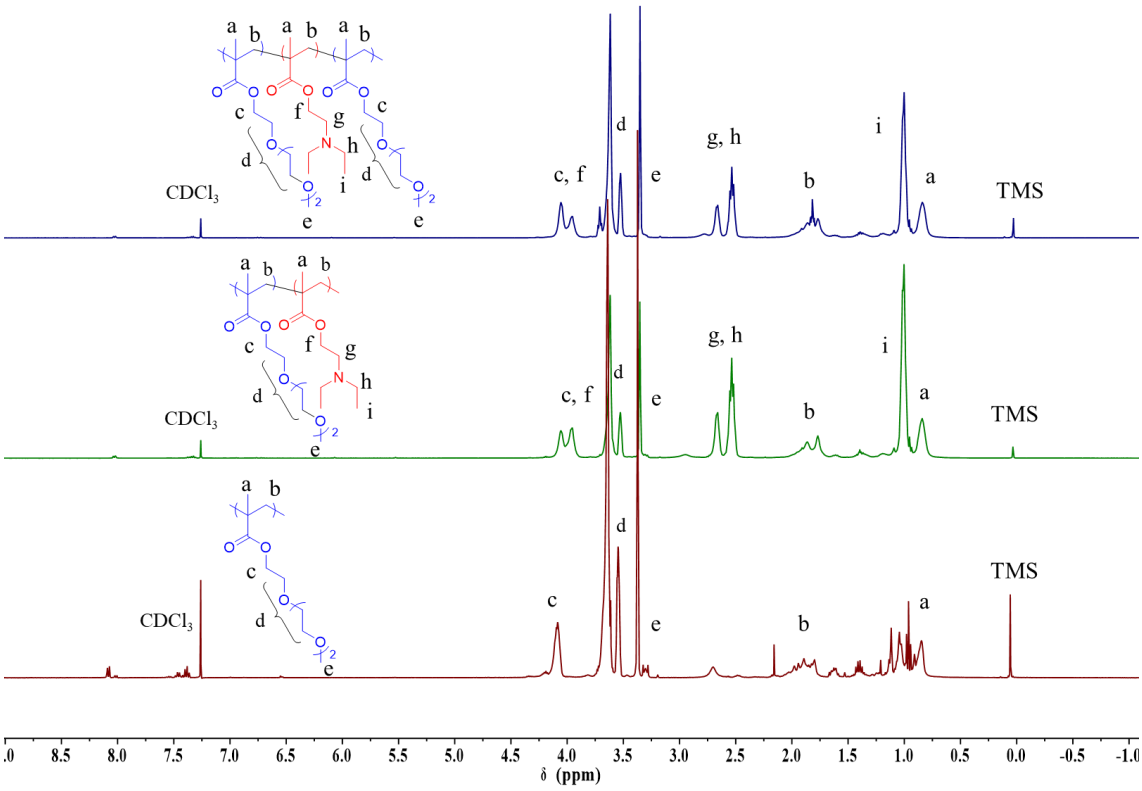


Figure 4.5 The ^{1}H NMR spectra of Polymer AP4 and its precursors. From top to bottom: $TEGMA_{12}$-*b*-$DEAEMA_{19}$-*b*-$TEGMA_{12}$, $TEGMA_{12}$-*b*-$DEAEMA_{19}$, and $TEGMA_{12}$ homopolymer. On the left, the chemical structure of TEGMA units is in light blue, the structure of DEAEMA units is in red.

4.2 Properties in Aqueous Solution

The pK_a for all polymers with experimental error is 7.2 ± 0.1. In theory, the pK_a decreases as the weight of the hydrophobic block DEAEMA increases,[19] however, subject to the sensitivity of the method, a clear trend was not observed, although the results agree with the former findings for the pK_a of other DEAEMA containing polymers in our research group.[20]

4.3 Size Distribution in Polymer Solutions

In order to form polymersomes with amphiphilic block copolymers in water or in PBS

(for biomedical applications), solvent free approaches (bulk hydration and film rehydration) are the simplest and most energy-saving techniques. According to literature,[14] film rehydration is more preferable since the method produces more large polymersomes than the small micelles as well as it provides a narrower size distribution of particles. This conclusion has been verified in dynamic light scattering (DLS) experiments.

4.3.1 DLS

The theoretical diameter of micelles formed by block copolymers can be calculated via following equation:[6]

$$d_h\,(nm) = [DP_B + 2 \times DP_A] \times 0.254 \qquad \textbf{Equation 4.1}$$

Where A and B stand for hydrophilic and hydrophobic units, respectively. DP_A and DP_B stand for degree of polymerisation of the hydrophilic and the hydrophobic blocks. 0.254 nm is the projected length of a methacrylate unit. In this model, it was assumed that spherical micelles are formed. For APs, the theoretical micelles size was calculated via above equation, and it was expected be around 10 nm.

4.3.1.1 Three Variables of Experiments

Hydrodynamic diameter is an important parameter to describe the size of polymeric structures in aqueous solution. DLS experiments give the hydrodynamic diameters of nano-particles in the aqueous solution.

For DLS experiments of APs, three factors are considered to have an impact on the formation of polymersome, leading to the change of polymersome size and size distribution:

pH of the solution All five APs have more or less DEAEMA units in their structures, based on which the polymers are pH-responsive. DEAEMA contains amino groups that

can be protonated. The protonation of amino groups increases the solubility of the units and the polymers, it solves the problem that AP1 does not fully dissolve in DI water. In this work, 15 solutions in 3 different pH values were tested: pH = 6, pH = 7 and original pH. Moreover, while adjusting the pH, the hydrophilicity of polymers has been changed. The DEAEMA units are regarded as "hydrophobic" originally, but after protonation they show good hydrophilicity. If the weight ratio of TEGMA units in a polymer is considered "hydrophilic weight ratio" while weight of DEAEMA units without protonation is considered "hydrophobic weight", the protonated DEAEMA is considered "hydrophilic weight ratio", the overall "hydrophilic weight ratio" of polymers at pH = 6, pH = 7 and original pH is listed in **Table 4.2**. The weight percentage data is calculated from the titration experiments. It is clear that at pH = 6, the polymers turn extremely hydrophilic. According to literature,[18] polymers do not tend to form large polymer vesicles with this high hydrophilicity, and this phenomenon is observed in **Table 4.3**. At pH = 7, it is expected a better formation of large polymer vesicles, it is also observed in **Table 4.4**.

Table 4.2 Hydrophilic weight ratio of APs before and after protonation.

Polymer	AP1	AP2	AP3	AP4	AP5
Original	30	40	50	60	70
pH = 6, protonated	93	95	95	96	96
pH = 7, protonated	73	77	80	83	88

Stirring time The solutions have been kept constant stirring once made, it is to assist and accelerate the formation of polymersomes. To investigate the influence of stirring time on polymersome formation, the solutions were running through DLS experiments with three different stirring times, which are 3 days, 1 week and 1 month.

Solvent In this work, polymersomes are characterised in aqueous solutions. DI water is the most straight forward solution to investigate while PBS is a non-toxic widely-used solution in biomedical research because it has the same ionic strength as the body liquids. Thus, unlike water, PBS prevents cells rupturing or shrivelling up due to osmosis. Hence, DI water and PBS were the two solvents used in this study.

4.3.1.2 Results and Discussion

pH = 6, dissolved in DI water

As mentioned above, five polymers were dissolved in DI water and the pH of the solutions was adjusted to 6, the solution of AP1 became clear due to the pH adjustment.

The average diameter (by intensity), maximum diameter (by intensity) and maximum diameter (by number) are listed in **Table 4.3**. The corresponding DLS graphs are shown in **Figure A4.1 – A4.3**, **Appendix**.

Several conclusions have been summarised as following:

1. The sizes of vesicles or other structures do not show a linear relation with the hydrophilicity of the polymers, however, AP1, AP3 and AP5 do form larger vesicles than AP2 and AP4.
2. AP2 and AP4 have two peaks (by intensity) while AP1, AP3 and AP5 only show one peak.
3. The difference between max peaks (by intensity) and max peaks (by number) indicates structures with various diameters are present in the solution.
4. In general, the particles formed in the solution have diameters less than 220 nm.

pH = 7, dissolved in DI water

Similarly, the data of diameter of polymer vesicles at pH = 7 is listed in **Table 4.4**. One notable fact is, at pH = 7, AP1 is partially dissolved as the solution is still a bit cloudy, it leads to broad multiple peaks and it explains the highest PDI of AP1 among five

polymers. The corresponding DLS graphs are shown in **Figure A4.4 – A4.6**, **Appendix**.

The conclusions are:

1. In general, the sizes of particles formed at pH = 7 are larger than sizes of pH = 6.
2. AP1 forms very large polymersomes. After one month's stirring, the average size (by intensity) exceeds 600 nm.
3. The average size of particles fluctuates with time, but it shows no huge difference between 1 day, 1 week and 1 month's stirring.
4. Based on the discussion in **Chapter 2**, AP3 is the best candidate among all APs for polymersome formation at pH = 7, since the average size of polymersomes AP3 formed is always below 200 nm and only 1 peak was observed during the whole time (by intensity), proving that AP3 has a relatively homogeneous formation of polymersomes.

Table 4.3 Summary of DLS results of APs at pH = 6 with different stirring time

pH	Stirring Time	No.	Polymer Structure	Max Peak (by intensity)		Max Peak (nm) (by number) (± 1 nm)	PDI
				Peak 1 (nm) (± 1 nm)	Peak 2 (nm) (± 1 nm)		
6	3 days	AP1	T_6-D_{34}-T_6	220	N/A	91.3	0.359
		AP2	T_8-D_{29}-T_8	1.62	106	0.621	0.569
		AP3	T_{10}-D_{24}-T_{10}	177	N/A	91.3	0.320
		AP4	T_{12}-D_{19}-T_{12}	1.5	106	1.50	0.420
		AP5	T_{14}-D_{15}-T_{14}	177	N/A	24.4	0.527
	1 week	AP1	T_6-D_{34}-T_6	205	N/A	91.3	0.292
		AP2	T_8-D_{29}-T_8	1.5	106	0.621	0.524
		AP3	T_{10}-D_{24}-T_{10}	190	N/A	91.3	0.445
		AP4	T_{12}-D_{19}-T_{12}	122	N/A	58.8	0.418
		AP5	T_{14}-D_{15}-T_{14}	190	N/A	24.4	0.484
	1 month	AP1	T_6-D_{34}-T_6	190	N/A	32.7	0.370
		AP2	T_8-D_{29}-T_8	1.74	142	1.40	0.481
		AP3	T_{10}-D_{24}-T_{10}	205	N/A	91.3	0.335
		AP4	T_{12}-D_{19}-T_{12}	122	N/A	68.1	0.480
		AP5	T_{14}-D_{15}-T_{14}	177	N/A	78.8	0.433

Table 4.4 Summary of DLS results of APs at pH = 7 with different stirring time

pH	Stirring Time	No.	Polymer Structure	Max Peak (by intensity)		Max Peak (nm) (by number) (± 1 nm)	PDI
				Peak 1 (nm) (± 1 nm)	Peak 2 (nm) (± 1 nm)		
7	3 days	AP1	T_6-D_{34}-T_6	98.6	396	68.1	0.714
		AP2	T_8-D_{29}-T_8	255	N/A	91.3	0.381
		AP3	T_{10}-D_{24}-T_{10}	142	N/A	78.8	0.411
		AP4	T_{12}-D_{19}-T_{12}	91.3	459	1.5	0.486
		AP5	T_{14}-D_{15}-T_{14}	275	N/A	142	0.416
	1 week	AP1	T_6-D_{34}-T_6	91.3	1110	78.8	0.707
		AP2	T_8-D_{29}-T_8	255	N/A	43.8	0.348
		AP3	T_{10}-D_{24}-T_{10}	142	N/A	78.8	0.414
		AP4	T_{12}-D_{19}-T_{12}	106	531	1.74	0.571
		AP5	T_{14}-D_{15}-T_{14}	295	N/A	114	0.397
	1 month	AP1	T_6-D_{34}-T_6	106	615	68.1	0.801
		AP2	T_8-D_{29}-T_8	220	N/A	32.7	0.373
		AP3	T_{10}-D_{24}-T_{10}	153	N/A	78.8	0.385
		AP4	T_{12}-D_{19}-T_{12}	91.3	275	1.74	0.498
		AP5	T_{14}-D_{15}-T_{14}	43.8	255	122	0.417

Original pH, dissolved in PBS

In this work, the impact of different fabrication methods (bulk hydration and film rehydration) on vesicle formation is investigated. Bulk hydration is to directly dissolve polymers with PBS, while film rehydration is to dissolve a pre-made polymer thin film. Both methods are solvent free approaches because organic solvent is not involved in the step of forming polymersomes.

The polymer concentration of samples for both methods is 10 mg mL^{-1}.

Bulk hydration

The max peaks (by intensity) and max peaks (by number) are listed in **Table 4.5**. The DLS graphs can be found in **Figure A4.7**, **Appendix**. The column "Peak 1" in max peaks (by intensity) and max peaks (by number) both show a clear decreasing trend along with the decrease of hydrophobicity of the copolymers. In addition, the formation of small micelles has been verified while the formation of large polymersomes seems rare in this method.

Table 4.5 DLS results summary of APs in PBS (bulk hydration)

Stirring Time	No.	Polymer Structure	Max Peaks (nm) (by intensity) (± 1 nm)		Max Peaks (nm) (by number) (± 1 nm)	PDI
			Peak 1	Peak 2		
1 week	AP1	T_6-D_{34}-T_6	106	N/A	58.8	0.316
	AP2	T_8-D_{29}-T_8	24.4	N/A	13.5	0.482
	AP3	T_{10}-D_{24}-T_{10}	24.4	N/A	13.5	0.209
	AP4	T_{12}-D_{19}-T_{12}	21.0	N/A	11.7	0.250
	AP5	T_{14}-D_{15}-T_{14}	15.7	459	3.62	0.432

Film rehydration

Similarly, the DLS results summary is shown in **Table 4.6**. The corresponding DLS

graphs are shown in **Figure A4.8**, **Appendix**. Unlike bulk hydration, film rehydration method does not give a clear trend of size change over hydrophobicity. The max peaks (by intensity) have a significant increase in comparison with bulk hydration, indicating large polymersomes were formed rather than small micelles.

Table 4.6 Summary of DLS results of APs in PBS (film rehydration)

Stirring Time	No.	Polymer Structure	Max Peaks (nm) (by intensity) (± 1 nm)		Max Peaks (nm) (by number) (± 1 nm)	PDI
			Peak 1	Peak 2		
1 week	AP1	T_6-D_{34}-T_6	295	N/A	50.7	0.422
	AP2	T_8-D_{29}-T_8	177	N/A	106	0.301
	AP3	T_{10}-D_{24}-T_{10}	190	N/A	122	0.398
	AP4	T_{12}-D_{19}-T_{12}	164	N/A	91.3	0.291
	AP5	T_{14}-D_{15}-T_{14}	91.3	427.5	58.8	0.456

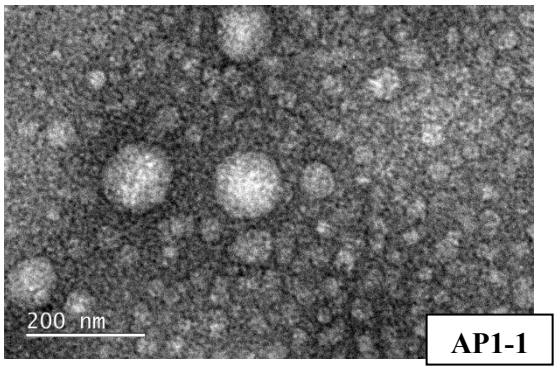
Hence, the increase in max peaks (by intensity) indicates that film rehydration is the preferable method to form polymersomes as it has less micelle formation than bulk hydration. Moreover, AP2, AP3, and AP4 formed polymersomes with diameters less than 200 nm, which is beneficial for this project.

4.3.2 TEM

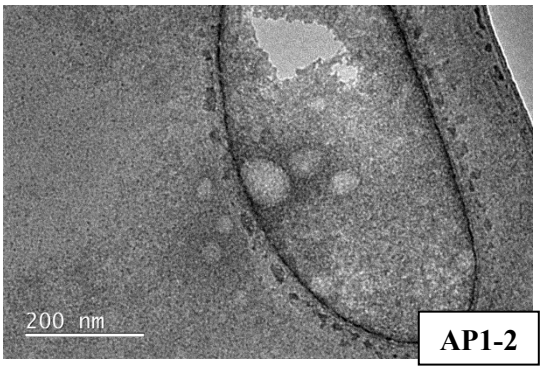
Transmission electron microscopy (TEM) is frequently used for observing the shape, size and size distribution of polymer vesicles and other polymeric structures. It gives the most straight forward understanding of polymeric nano structures. In this work, polymer solutions were dropped on the carbon coated copper grids, and the grids were treated by negative staining technique with uranyl acetate solution in order to increase the contrast of polymeric structures under the microscopy.

4.3.2.1 Polymersome Overview

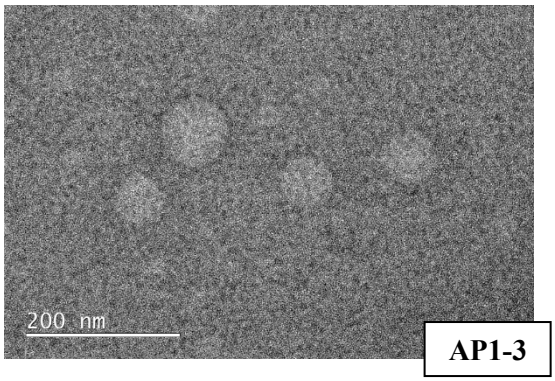
<u>In DI water, pH = 6</u>



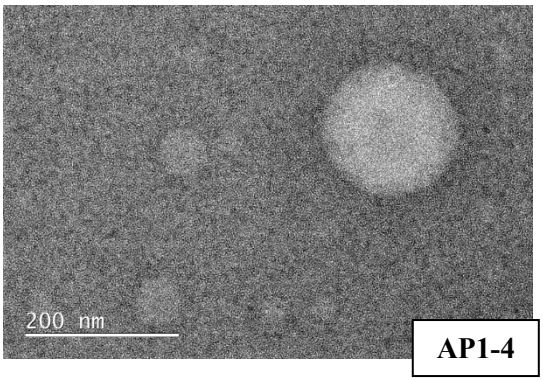
AP1-1



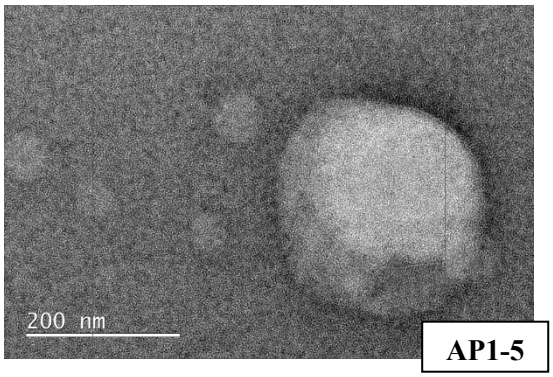
AP1-2



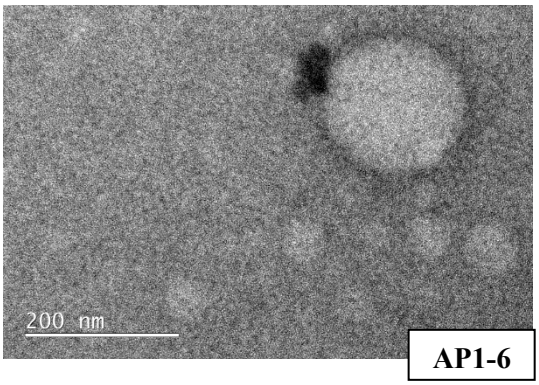
AP1-3



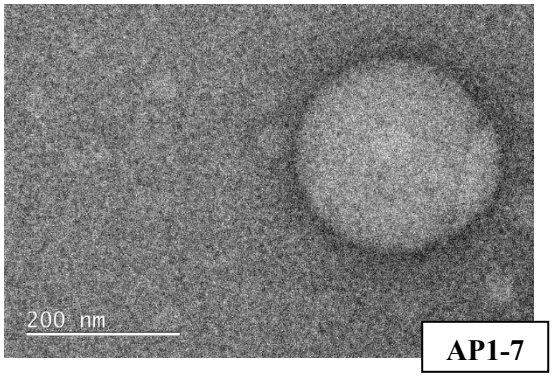
AP1-4



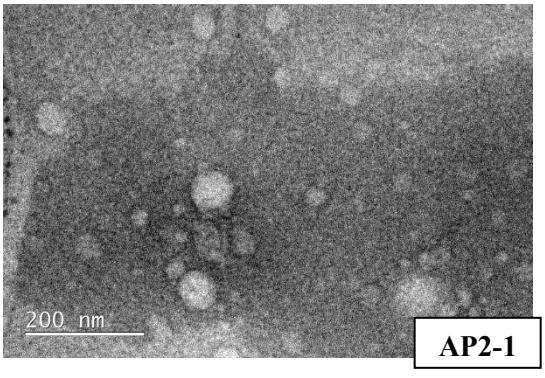
AP1-5



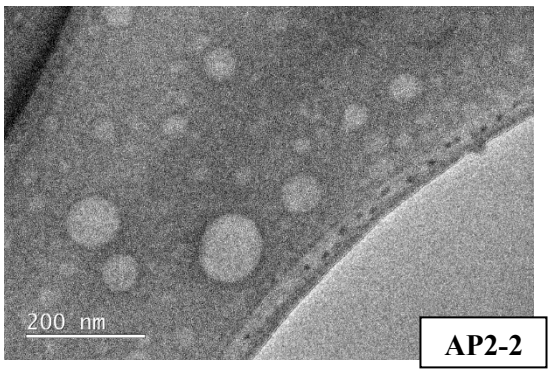
AP1-6



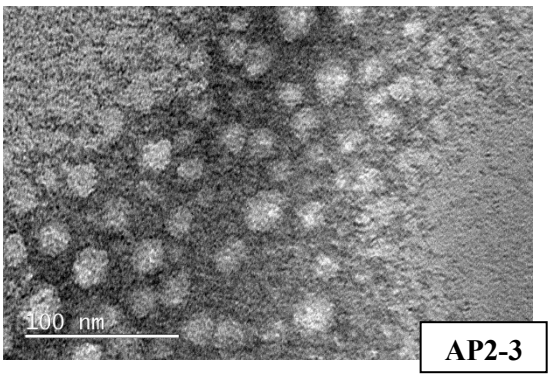
AP1-7



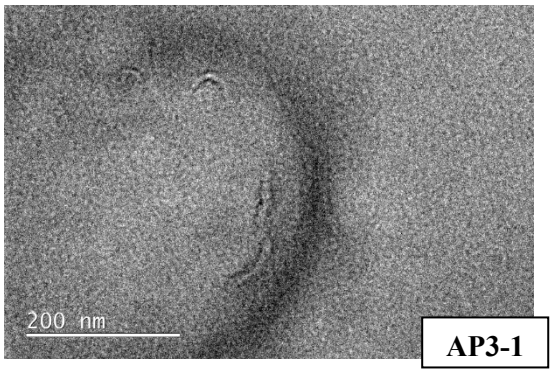
AP2-1



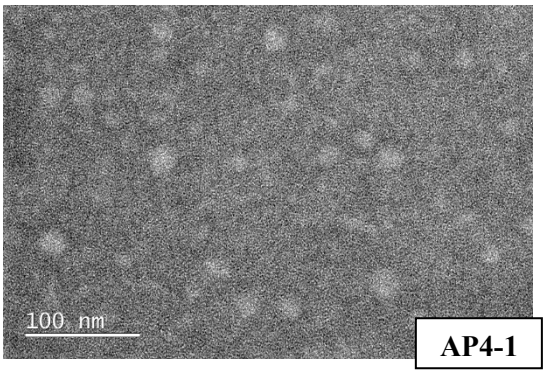
AP2-2



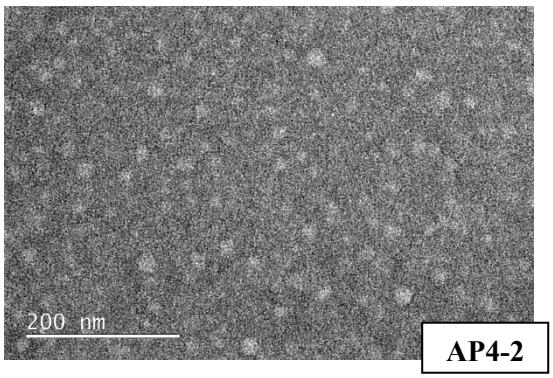
AP2-3



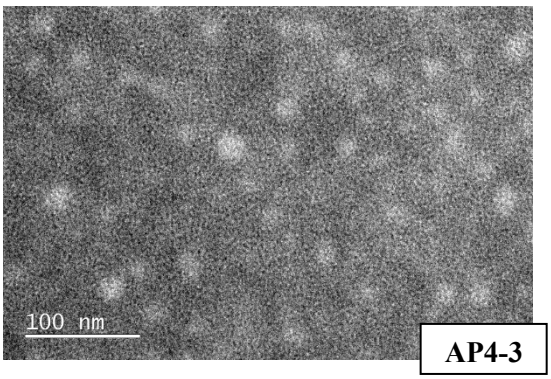
AP3-1



AP4-1



AP4-2



AP4-3

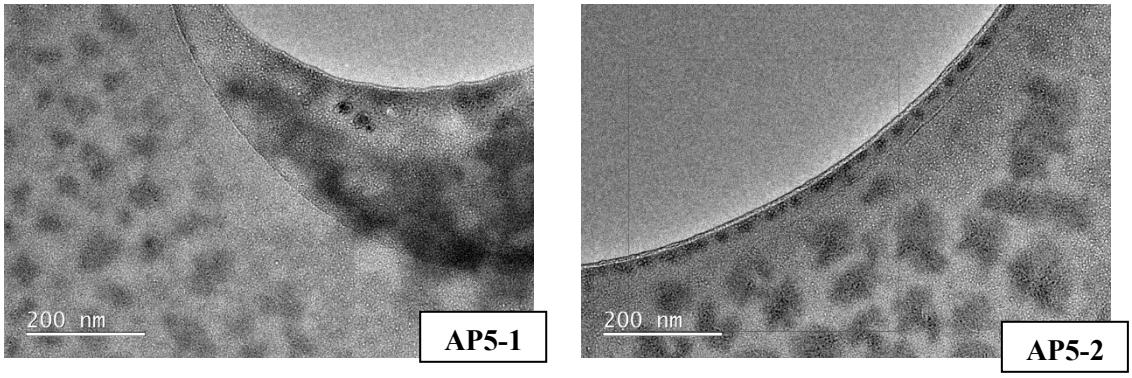
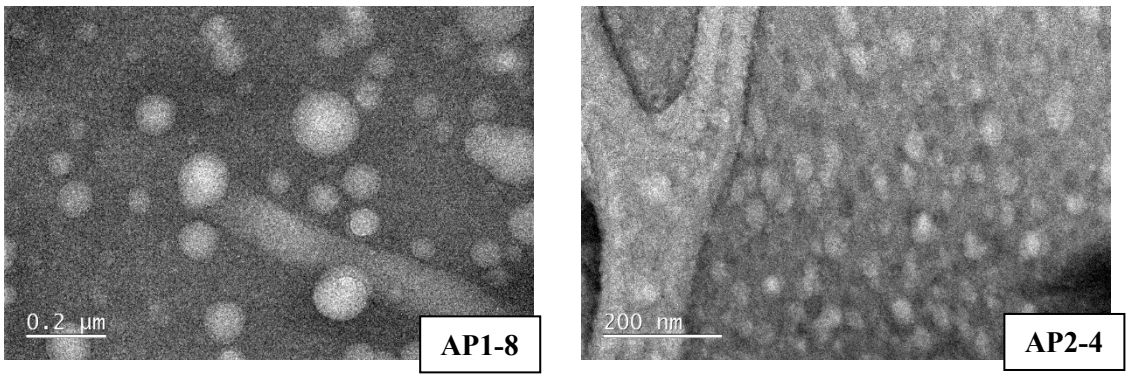
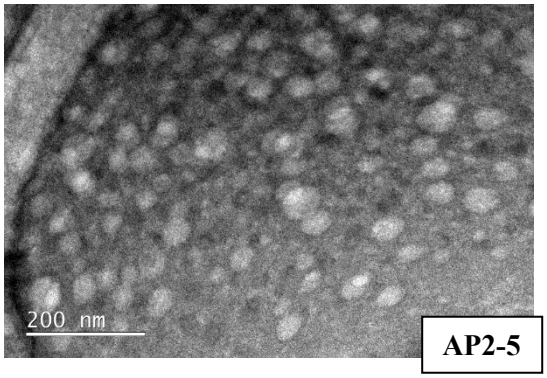


Figure 4.6 TEM images of structures formed by APs. The solutions were prepared via film rehydration in DI water with a polymer concentration of 10 mg mL^{-1}, and the pH of solution was adjusted to 6. Uranyl acetate was used as a negative staining agent.

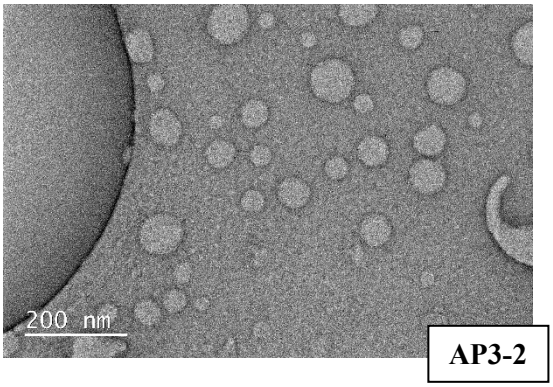
From the above images, for most APs, clear vesicles are shown and their size can be measured via software ImageJ. In fact, AP1 has the largest observable polymersomes with a diameter over 200 nm, while much smaller particles are still present on the images. It is clear that the polymer forms much more small particles than big polymersomes, and this is in agreement with the DLS results (max peaks by number). AP2 forms small particles (micelles) which have diameters from 20 to 100 nm. AP4 forms very small particles and has a narrow size distribution, micelles are formed rather than polymersomes. In addition, AP3 and AP5 show no presence of polymersomes on the TEM images.

In DI water, pH = 7

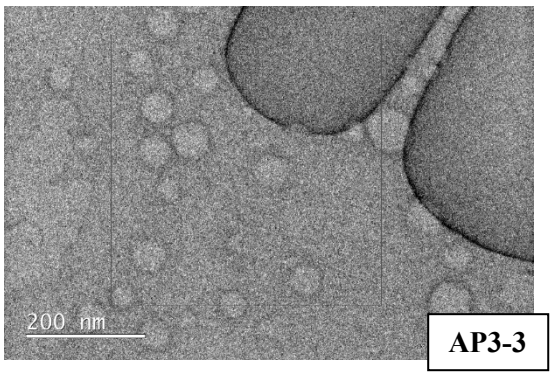




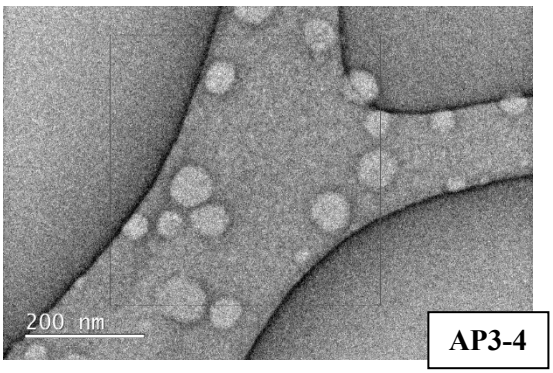
AP2-5



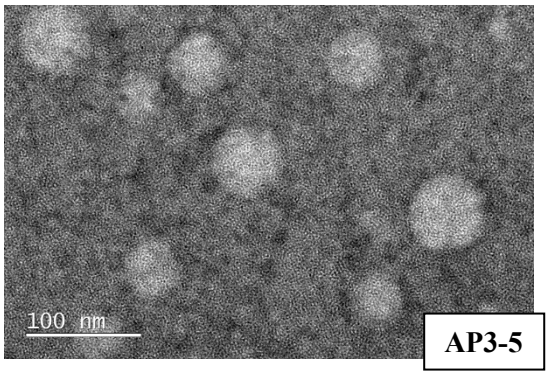
AP3-2



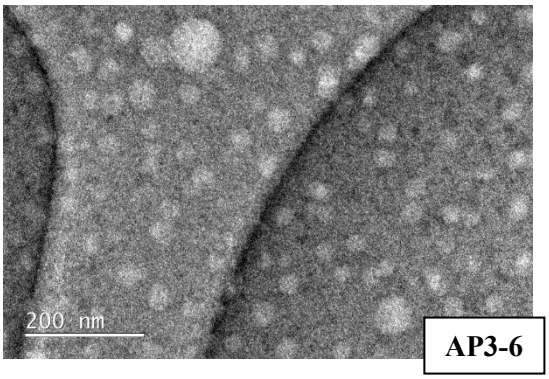
AP3-3



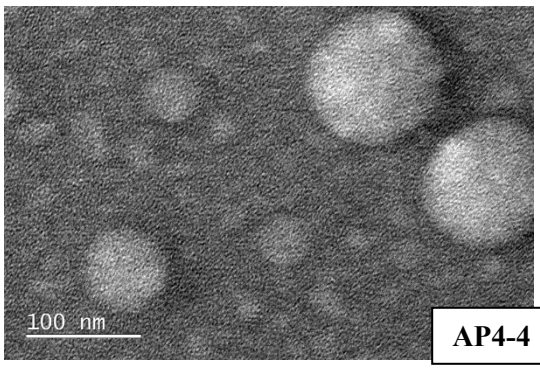
AP3-4



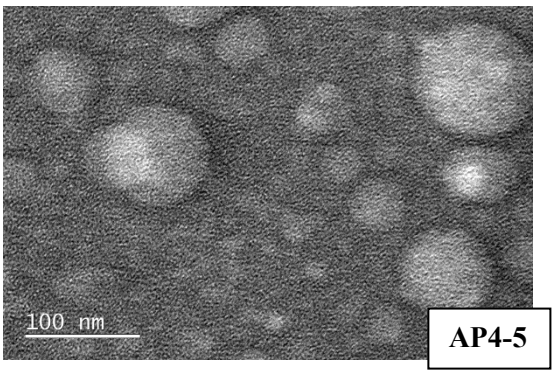
AP3-5



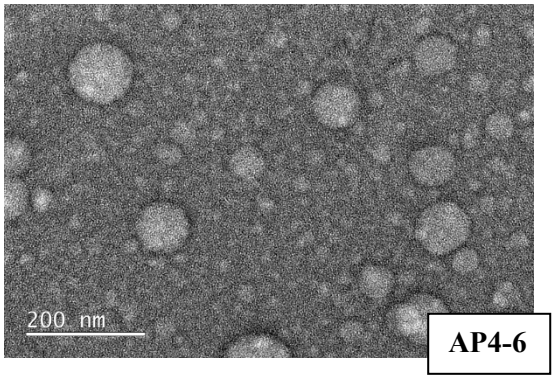
AP3-6



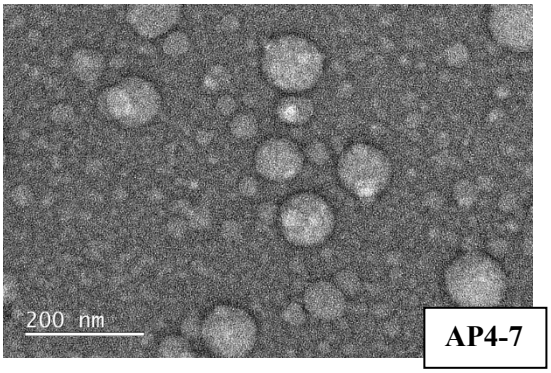
AP4-4



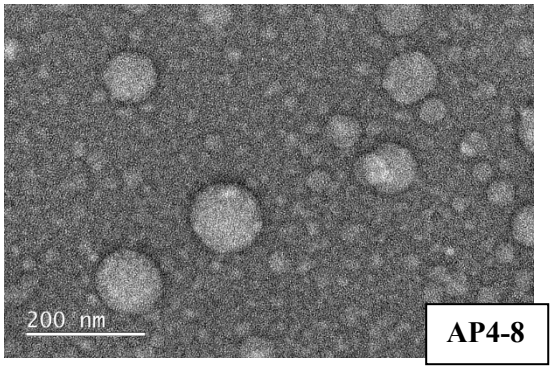
AP4-5



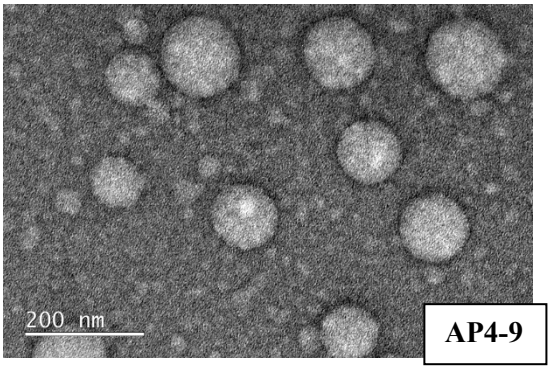
AP4-6



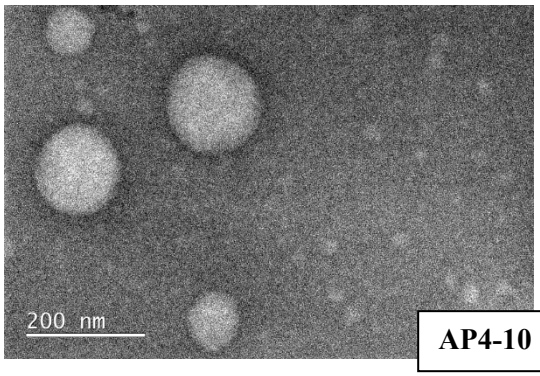
AP4-7



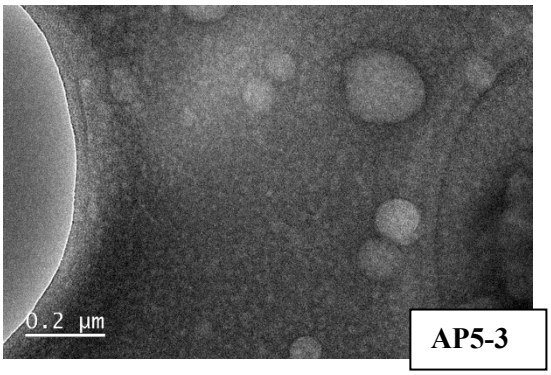
AP4-8



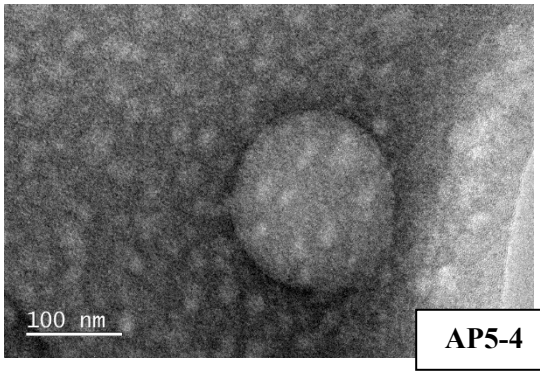
AP4-9



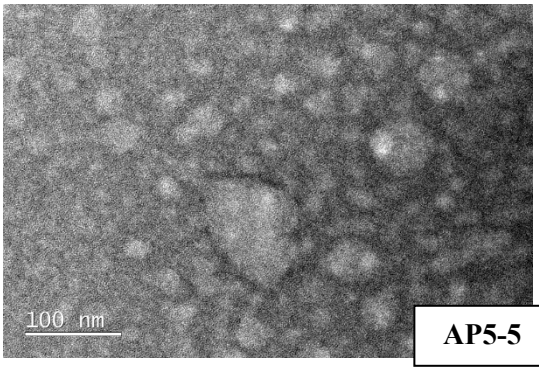
AP4-10



AP5-3



AP5-4



AP5-5

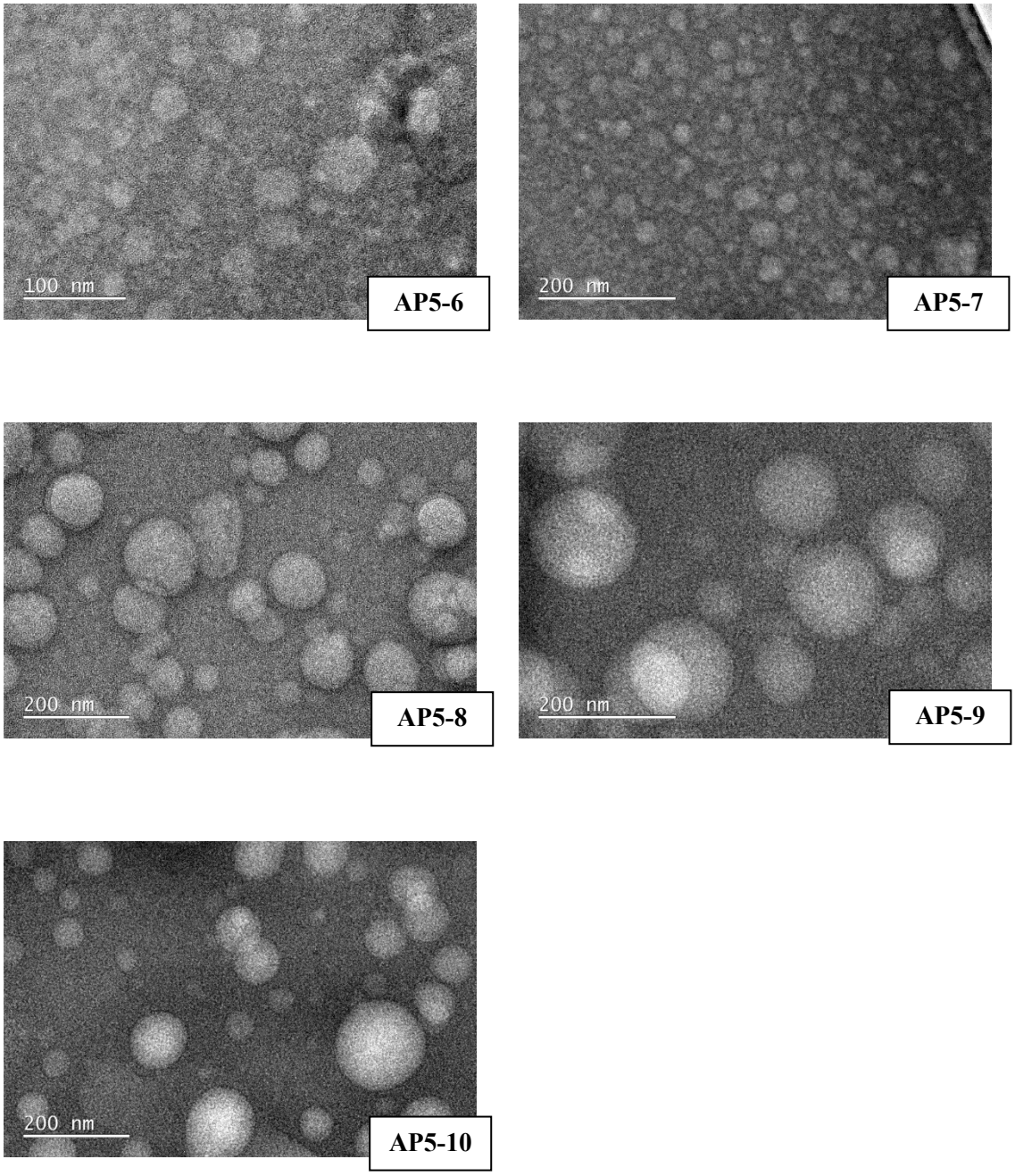


Figure 4.7 TEM images of structures formed by APs. The solutions were prepared via film rehydration in DI water with a polymer concentration of 10 mg mL^{-1}, and the pH of solution was adjusted to 7. Uranyl acetate was used as a negative staining agent.

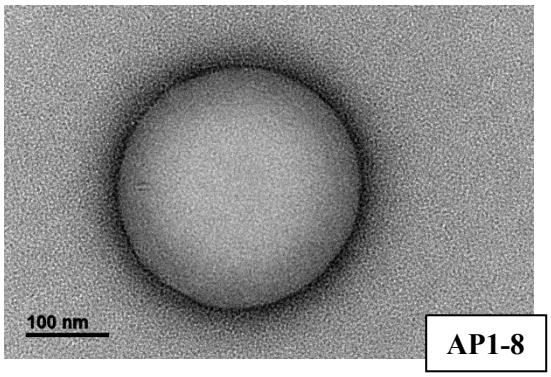
As shown in the images, polymer solutions at pH = 7 give a better formation of large polymersomes in general. This is ascribed to the less protonation of DEAEMA units, resulting in a more preferable hydrophilic/hydrophobic ratio to form large polymersomes.

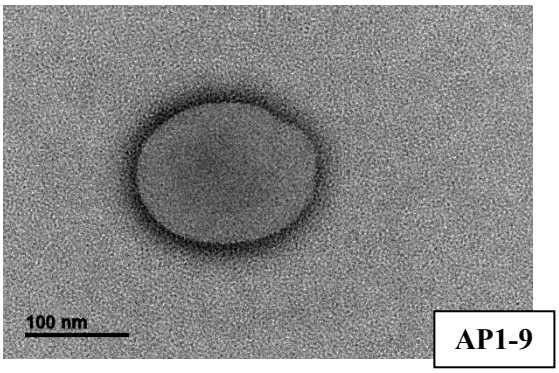
Specifically, for AP1 and AP2, it is verified that at both pH they can form polymersomes, while at pH = 6, larger polymersomes can be seen. For AP3, pH = 7 is the preferable condition as only at this pH the images present scalable, clear polymersomes. For AP4 and AP5, a drastic increase in size can be observed when the pH changes from 6 to 7, and AP5 can form polymersomes with diameters more than 200 nm although there are still a number of small micelles observable.

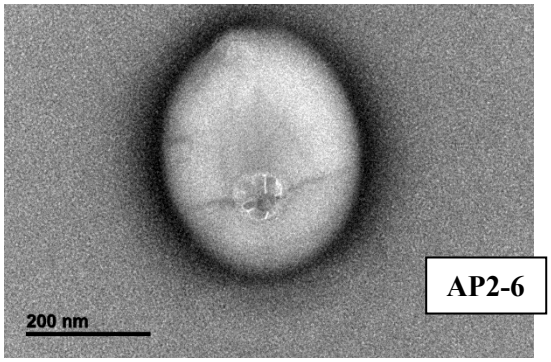
It can be concluded that for more hydrophobic polymers (AP1 and AP2), protonation slightly changes the size and size distribution of the particles; for more hydrophilic polymers (AP3, AP4, AP5) the protonation can lead to no or very few formations of large polymersomes. In summary, pH = 7 in DI water is a preferable condition for APs to form polymersomes than that of pH = 6.

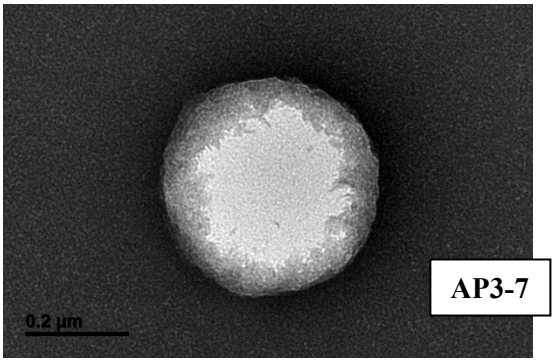
In PBS, Original pH

Note to the readers: *The TEM images in this section were taken with the help of Dr Claudia Contini.*









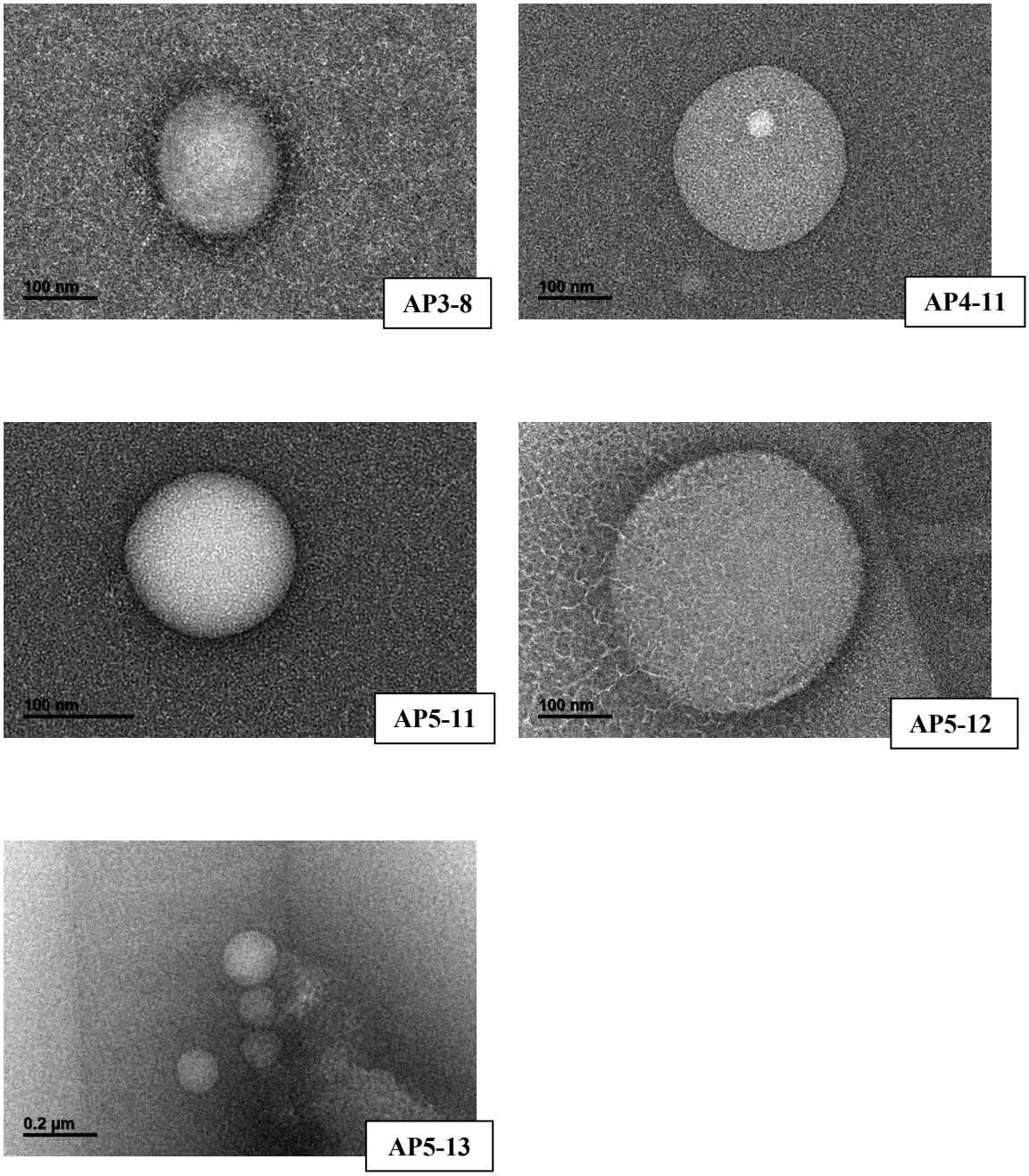


Figure 4.8 TEM images of structures formed by APs. The solutions were prepared via film rehydration in PBS with a polymer concentration of 10 mg mL^{-1}. Uranyl acetate was used as a negative staining agent.

The above images have been taken from the polymer solutions without pH adjustment. The presence of polymersomes with a diameter around 500 nm is confirmed. It is notable that in 3 cases (DI water, pH = 6; DI water, pH = 7; PBS, original pH), polymer solutions in PBS without pH adjustment form the largest polymersomes. The original pH of the polymer solutions is above 7 (due to the nature of amino groups, polymer

solutions are slightly basic), however, it cannot simply be concluded that the higher the pH, the larger the particles, since the difference in solvent can also affect the formation of polymersomes, and the formation of polymersomes is quite different from polymer to polymer.

4.3.2.2 Membrane Thickness

As clear images of polymersomes are taken via TEM, besides discussions on the overall diameter of polymersomes, the hydrophobic membrane thickness of polymersomes is investigated. Theoretically, the more hydrophobic a polymer is, the thicker the membrane should be. Previous works have demonstrated two models for mimicking membrane thickness: fully stretched and random coil,[21] the theoretical values are calculated and presented in **Table 4.7**. Also, the membrane thicknesses obtained from TEM images are listed. From the table it is clear that the actual membrane thickness is between the random coil model and fully stretched model, which means the actual configuration is somewhere in between the two models (more close to the random coil model), the hydrophobic DEAEMA units are neither fully stretched, nor extremely twisted as random coil model.

Table 4.7 Theoretical polymer structures, pK_a values, theoretical and experimental membrane thickness of polymersomes

No.	Theoretical Polymer Structure	pK_a ± 0.1	Theoretical Diameter of hydrophobic membrane (nm)		Membrane thickness from TEM (nm)
			Random Coil[a]	Fully Stretched[b]	±1 (nm)
P1	$TEGMA_6$-*b*-$DEAEMA_{34}$-*b*-$TEGMA_6$	7.2	2.69	13.2	4.3
P2	$TEGMA_8$-*b*-$DEAEMA_{29}$-*b*-$TEGMA_8$	7.2	2.33	9.91	4.2
P3	$TEGMA_{10}$-*b*-$DEAEMA_{24}$-*b*-$TEGMA_{10}$	7.2	2.11	8.13	3.5
P4	$TEGMA_{12}$-*b*-$DEAEMA_{19}$-*b*-$TEGMA_{12}$	7.2	1.97	7.11	2.6
P5	$TEGMA_{14}$-*b*-$DEAEMA_{15}$-*b*-$TEGMA_{14}$	7.2	1.58	4.57	1.4

[a] This was calculated by using the experimentally determined degree of polymerisation (DP) of DMAEMA and using the following equation: $\langle d_g^2 \rangle^{1/2} = 2 \times [2 \times 2.20 \times (DP_A + DP_B + DP_A) / 3]^{1/2} \times 0.154$, where d_g is the theoretical diameter of hydrophobic membrane.

[b] This was calculated assuming the hydrophobic DEAEMA block will be fully stretched. Thus, this the length of the projected DEAEMA block that is the DP × 0.254 nm (that is the projected length of the C-C methacrylate bond on the backbone).

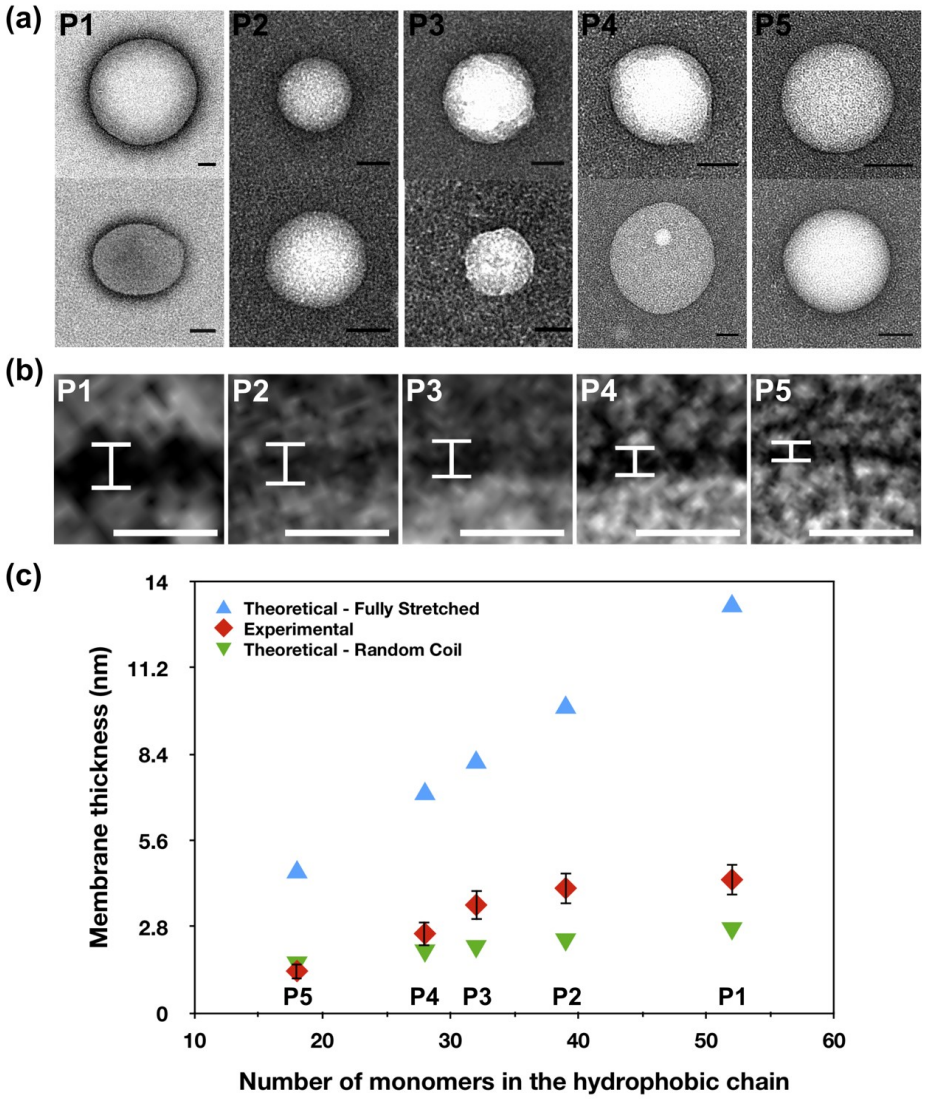


Figure 4.9 (a) TEM images of the TEGMA-*b*-DEAEMA-*b*-TEGMA polymersomes formed by film rehydration and (b) image analysis used to determine the difference in membrane thickness changing from P1 to P5. (c) The measured membrane thickness (blue) is plotted versus the theoretical coil-like conformation (red) of TEGMA-*b*-DEAEMA-*b*-TEGMA copolymers. Scale bars are 50 nm and 10 nm in panel a and b, respectively. The figure has been adapted from "Zhang, Xinmo, et al. "How does the hydrophobic content of methacrylate ABA triblock copolymers affect polymersome formation?." *Journal of Polymer Science* (2021)."

4.4 Encapsulation and Release Study

Encapsulation and release of molecules are the main and most intriguing application of polymersomes. To investigate the composition effect on the encapsulation efficiency

and release rate, several molecules have been tested in this work: curcumin, doxorubicin, calcein and sodium fluorescein. The molecules are dissolved in PBS solution at a certain concentration, and the solution is used to dissolve polymer thin films during film rehydration, resulting in a solution with polymersomes (molecules encapsulated) and dissociative molecules. Dialysis tubes with a MWCO of 3000 g mol^{-1} can retain the polymersomes whilst let the dissociative dye molecules pass through. Three criteria are essential for a good model molecule: 1. The molecules should have good solubility in PBS, 2. The molecules should pass through the dialysis membrane spontaneously and effectively based on the concentration difference between two sides of the membrane, 3. The molecules should not precipitate in the dialysis tube. Based on the criteria, sodium fluorescein is the best option out of the candidates.

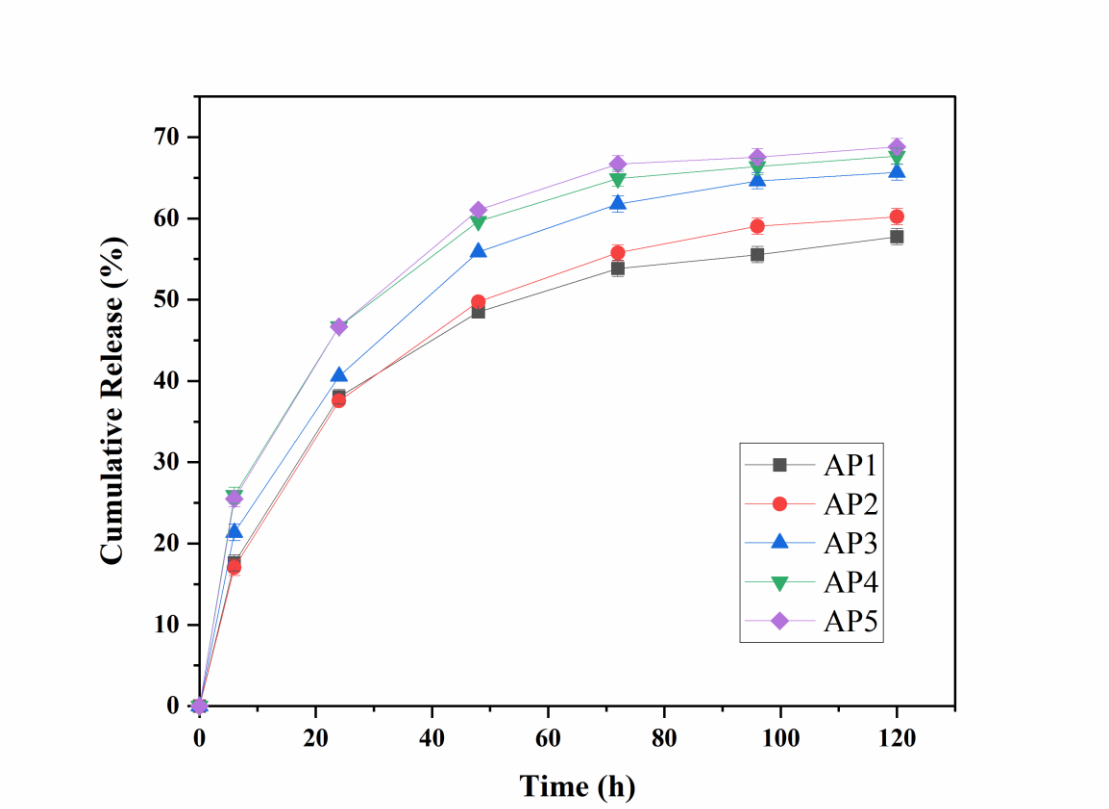


Figure 4.10 Cumulative release of sodium fluorescein versus time by polymersomes. The figure has been adapted from "Zhang, Xinmo, et al. "How does the hydrophobic content of methacrylate ABA triblock copolymers affect polymersome formation?." *Journal of Polymer Science* (2021)."

From **Figure 4.10**, the cumulative release (%) has been increased throughout the time range from 0 to 120 hours, although the speed of release follows a descending trend. At

the end of the first day, polymersomes have released 35% to 50% of encapsulated dye molecules, and the number increased to 50% to 70% at the end of 5 days. The cumulative release percentage reaches maximum at 5 days and without further change afterwards. Overall, it can be concluded that the more hydrophilic a polymer is (more TEGMA units in a polymer), the more dye molecules it releases during the time period studied. Based on the former discussion on membrane thickness, a thicker membrane causes a longer time to diffuse. Thus, this study shows that the release could be tuned by tuning the hydrophilic/hydrophobic ratio of the ABA triblock copolymers.

4.5 Conclusions

In this chapter, five ABA triblock copolymers TEGMA-*b*-DEAEMA-*b*-TEGMA have been successfully synthesised using GTP. The MM of the polymers has been targeted to 9100 g mol^{-1}, whereas the composition varies to investigate the composition effect on polymersome fabrication and properties. Several conclusions have been listed as following:

1. All the triblock copolymers have been successfully synthesised; the MM of which is within the desirable range and $Đ$ is sufficiently close to 1, the compositions of copolymers have been verified by ^{1}H NMR.
2. In aqueous solutions, the pK_a values of polymers have been obtained by titration experiments, which is 7.2 ± 0.1 for all five polymers.
3. Polymers containing DEAEMA units show pH-responsiveness in aqueous solution; the particle size and size distribution change with pH.
4. DLS results have proven that film rehydration is more preferable to fabricate polymersomes in this project rather than bulk hydration, since the latter creates more small size micelles.
5. TEM images have verified that polymersomes with a diameter up to several hundred nm have been fabricated. It can be concluded that for more hydrophobic polymers (AP1 and AP2), protonation slightly changes the size and size distribution of the particles; for more hydrophilic polymers (AP3, AP4, AP5) the protonation can lead to no or very limited formation of large polymersomes.
6. Hydrophobic membrane thickness of polymersomes has been investigated with

TEM. It agrees with the theory that the more hydrophobic units a polymer has, a thicker membrane the fabricated polymersome has. Moreover, the thickness of hydrophobic membrane locates between the theoretical values of two model: fully stretched and random coil, it proves that in actual polymersomes, the way polymer chains collapse is in the middle of the two assumptions.

7. Sodium fluorescein is used as a model drug to test the encapsulation efficiency and release behaviour of the polymersomes. It turns out the cumulative release decreases with the decrease of hydrophilicity; it proves that the composition has an effect on the release of drugs from polymersomes.

REFERENCE

1. Mai, Y., & Eisenberg, A. (2012). Self-assembly of block copolymers. *Chemical Society Reviews*, *41*(18), 5969-5985.

2. Hu, Y., & Qiu, L. (2019). Polymersomes: Preparation and Characterization. In *Pharmaceutical Nanotechnology* (pp. 247-265). Humana, New York, NY.

3. Constantinou, A. P., Zhang, K., Somuncuoğlu, B., Feng, B., & Georgiou, T. K. (2021). PEG-Based Methacrylate Tetrablock Terpolymers: How Does the Architecture Control the Gelation?. *Macromolecules*.

4. Constantinou, A. P., Zhan, B., & Georgiou, T. K. (2021). Tuning the Gelation of Thermoresponsive Gels Based on Triblock Terpolymers. *Macromolecules*, *54*(4), 1943-1960.

5. Constantinou, A. P., & Georgiou, T. K. (2016). Tuning the gelation of thermoresponsive gels. *European Polymer Journal*, *78*, 366-375.

6. Zhang, X., Contini, C., Constantinou, A. P., Doutch, J. J., & Georgiou, T. K. (2021). How does the hydrophobic content of methacrylate ABA triblock copolymers affect polymersome formation?. *Journal of Polymer Science*.

7. Agut, W., Brûlet, A., Schatz, C., Taton, D., & Lecommandoux, S. (2010). pH and temperature responsive polymeric micelles and polymersomes by self-assembly of poly [2-(dimethylamino) ethyl methacrylate]-*b*-poly (glutamic acid) double hydrophilic block copolymers. *Langmuir*, *26*(13), 10546-10554.

8. Zhang, J., Wu, L., Meng, F., Wang, Z., Deng, C., Liu, H., & Zhong, Z. (2012). pH and reduction dual-bioresponsive polymersomes for efficient intracellular protein delivery. *Langmuir*, *28*(4), 2056-2065.

9. Lomas, H., Johnston, A. P., Such, G. K., Zhu, Z., Liang, K., Van Koeverden, M. P., ... & Caruso, F. (2011). Polymersome-loaded capsules for controlled release of DNA. *Small*, *7*(14), 2109-2119.

10. Wang, M. Z., Wang, T., Yuan, K., & Du, J. (2016). Preparation of water dispersible poly (methyl methacrylate)-based vesicles for facile persistent antibacterial applications. *Chinese Journal of Polymer Science*, *34*(1), 44-51.

11. Chen, W., & Du, J. (2013). Ultrasound and pH dually responsive polymer vesicles for anticancer drug delivery. *Scientific reports*, *3*(1), 1-9.

12. Zhang, X., Huang, Q., Wang, F., Sun, H., Xiao, J., Cornel, E. J., ... & Du, J. (2021). Giant Polymer Vesicles with a Latticelike Membrane. *ACS Macro Letters*, *10*(8), 1015-1022.

13. Rakhmatullina, E., & Meier, W. (2008). Solid-supported block copolymer membranes through interfacial adsorption of charged block copolymer vesicles. *Langmuir*, *24*(12), 6254-6261.

14. Ward, M. A., & Georgiou, T. K. (2013). Multicompartment thermoresponsive gels: does the length of the hydrophobic side group matter?. *Polymer Chemistry*, *4*(6), 1893-1902.

15. Ward, M. A., & Georgiou, T. K. (2010). Thermoresponsive terpolymers based on methacrylate monomers: Effect of architecture and composition. *Journal of Polymer Science Part A: Polymer Chemistry*, *48*(4), 775-783.

16. Ward, M. A., & Georgiou, T. K. (2012). Thermoresponsive triblock copolymers based on methacrylate monomers: effect of molecular weight and composition. *Soft Matter*, *8*(9), 2737-2745.

17. Fetsch, C., Gaitzsch, J., Messager, L., Battaglia, G., & Luxenhofer, R. (2016). Self-Assembly of amphiphilic block copolypeptoids–Micelles, worms and polymersomes. *Scientific reports*, *6*(1), 1-13.

18. Discher, D. E., & Ahmed, F. (2006). Polymersomes. *Annu. Rev. Biomed. Eng.*, *8*, 323-341.

19. Constantinou, A. P., Marie-Sainte, U., Peng, L., Carroll, D. R., McGilvery, C. M., Dunlop, I. E., & Georgiou, T. K. (2019). Effect of block copolymer architecture and composition on gold nanoparticle fabrication. *Polymer Chemistry*, *10*(34), 4637-4642.

20. Constantinou, A. P., Lan, T., Carroll, D. R., & Georgiou, T. K. (2020). Tricomponent thermoresponsive polymers based on an amine-containing monomer with tuneable hydrophobicity: Effect of composition. *European Polymer Journal*, *130*, 109655.

21. Constantinou, A. (2019). *Thermoresponsive gels: how do the structural parameters affect the gelation properties?* (PhD). Imperial College London.”.

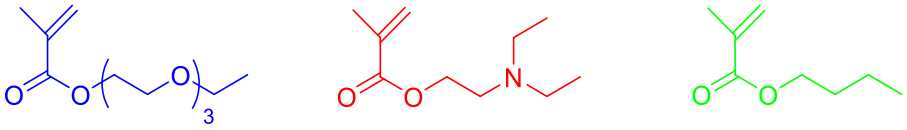
CHAPTER 5 POLYMERSOMES BASED ON TRIBLOCK COPOLYMER TEGEMA-*b*-(DEAEMA-*co*-BUMA)-*b*-TEGEMA

5.1 Chemistry of Block Copolymers

In this chapter, a new series of amphiphilic block copolymers TEGEMA-*b*-(DEAEMA-*co*-BuMA)-*b*-TEGEMA has been synthesised, characterised, and investigated. Distinguishing from **Chapter 4**, this new series has changed the hydrophilic monomer, added one hydrophobic monomer and adjusted the way that constitutes hydrophobic blocks. Firstly, TEGEMA has been chosen to replace TEGMA, and the difference is TEGEMA has an ethyl group at the end of the polymer side chain, instead of a methyl group of TEGMA. Also, the hydrophobic block is statistical mixture of DEAEMA and BuMA, instead of pure DEAEMA. The logic behind this chemistry modification is, the polymer TEGMA-*b*-DEAEMA-*b*-TEGMA has been tested and proved to have rather high cellular toxicity due to the DEAEMA block (shown in **Figure A5.1** and **Figure A5.2**, **Appendix**). To eliminate the toxicity while maintain the pH-responsiveness of the block copolymers, a new hydrophobic monomer BuMA was chosen to co-create the hydrophobic moiety along with DEAEMA, and the two monomers have the same weight ratio which is 50% in the hydrophobic moiety.

Notably, the change in monomer chemistry and the way of constituting hydrophobic moiety may lead to the change of the solubility of the copolymers in aqueous media. Since some of the characterisations of the copolymers and corresponding polymersomes are in aqueous solutions, the change of solubility may have an impact on those aspects. Based on a recent study from our group[1], TEGEMA is more hydrophobic than TEGMA due to the extension of side chains (ethyl ether group is more hydrophobic than methyl ether group). Besides, the hydrophobicity of BuMA is also higher than that of DEAEMA. Hence, TEGEMA-*b*-(DEAEMA-*co*-BuMA)-*b*-TEGEMA polymers are more hydrophobic compared with TEGMA-*b*-DEAEMA-*b*-TEGMA, but with less cellular toxicity.

In **Figure 5.1** the chemical structures, names, abbreviations of the monomers used in this chapter are shown.



Tri(ethylene glycol) ethyl ether methacrylate (TEGEMA) Monomer
Hydrophilic, non-ionic

2-(Diethylamino) ethyl methacrylate (DEAEMA) Monomer,
Hydrophobic, ionic pH- responsive

n-Butyl methacrylate (BuMA, Bu) Monomer,
hydrophobic, non-ionic

Figure 5.1 Chemical structures, names, abbreviations and related properties of the monomers used for the polymerisation of polymer series CP.

Following **Chapter 4**, DEAEMA has been kept as a hydrophobic monomer owing to its high reactivity in polymerisation and pH responsiveness. BuMA has been frequently studied in the research group as a commonly used methacrylate monomer.[1,2,3] All six polymers have the same theoretical MM, which is 9100 g mol^{-1} (including 100 g mol^{-1} of the initiator). **Table 5.1** below shows $MM^{theor.}$, M_n, M_p, $Đ$, theoretical and experimental degree of polymerisation.

The two main aims of this chapter are:

1. Investigate how hydrophilic/hydrophobic ratio of the polymers affect the formation and the properties of polymersomes;

2. Compare the differences in fabrication of polymersomes between polymers TEGEMA-*b*-(DEAEMA-*co*-BuMA)-*b*-TEGEMA and TEGMA-*b*-DEAEMA-*b*-TEGMA**.**

5.1.1 Polymer Synthesis

In this chapter, the series of polymers were named CP and 6 polymers were synthesised via GTP. All six CPs have been prepared via one-pot synthesis. The sequential polymerisation is illustrated in **Figure 5.2**. The catalyst TBABB and solvent THF are firstly added to the reaction flask, the first monomer TEGEMA is injected using a glass syringe to the sealed reaction flask. The polymerisation reaction starts after the addition of initiator MTS. After the completion of chain propagation of TEGEMA monomer,

DEAEMA and BuMA are added at the same time to the reaction flask at the approximately same rate to constitute a statistical block. The second addition of TEGEMA forms the third block, the polymerisation reaction is quenched by addition of methanol at the end.

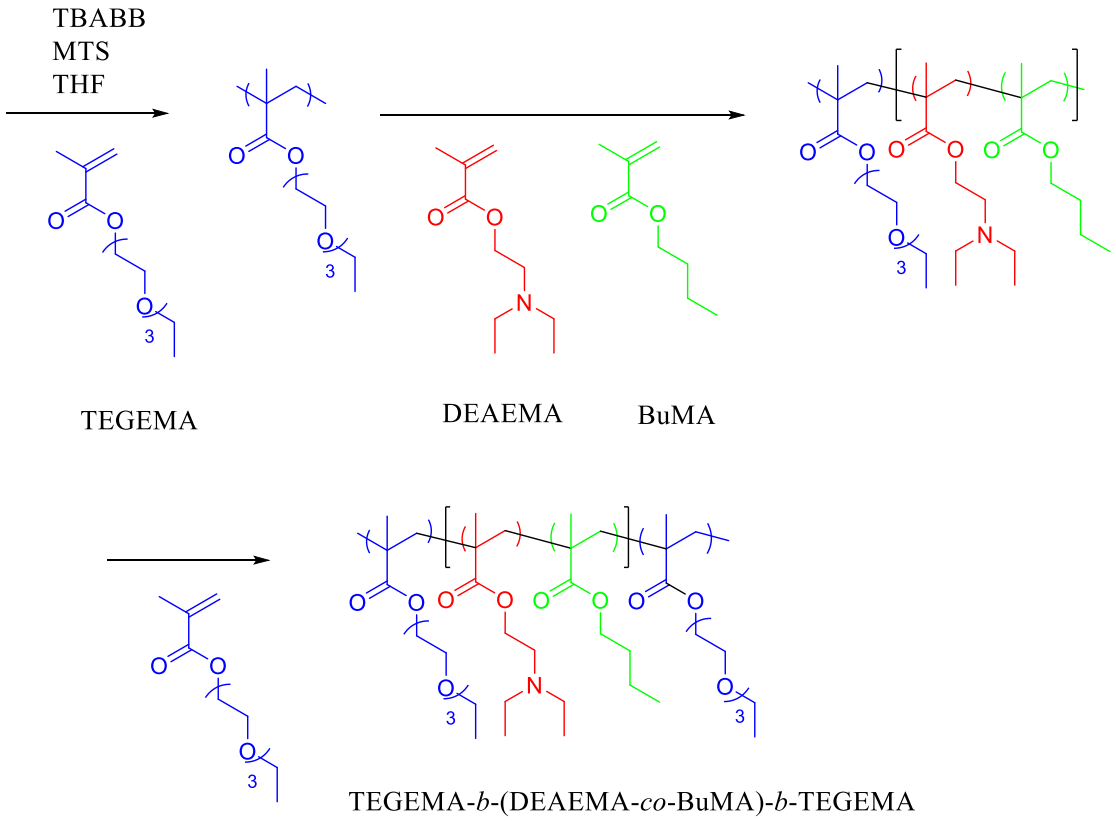


Figure 5.2 Illustration of the sequential GTP reaction for the synthesis of TEGEMA-*b*-(DEAEMA-*co*-BuMA)-*b*-TEGEMA triblock copolymers. TEGEMA, DEAEMA and BuMA are the three monomers; TBABB, MTS, THF are the catalyst, monofunctional initiator and solvent used in the reaction, respectively.

5.1.2 Molar Mass and Composition

Figure 5.3 is a schematic representation of six triblock copolymers investigated in this chapter. The TEGEMA, DEAEMA and BuMA units are represented in blue, red and green coloured circles, respectively. All six polymers belong to the same family and all can be presented as TEGEMA-*b*-(DEAEMA-*co*-BuMA)-*b*-TEGEMA. The $MM^{theor.}$ of all polymers is the same, which is 9100 g mol^{-1} including the average mass of initiator MTS on the polymer chains.

The weight ratios of hydrophilic moieties (TEGEMA units) to the whole polymer mass, from CP1 to CP6, are 80%, 70%, 60%, 50%, 40% and 30%, respectively. Hence, the overall hydrophilicity of polymers decreases in sequence from CP1 to CP6.

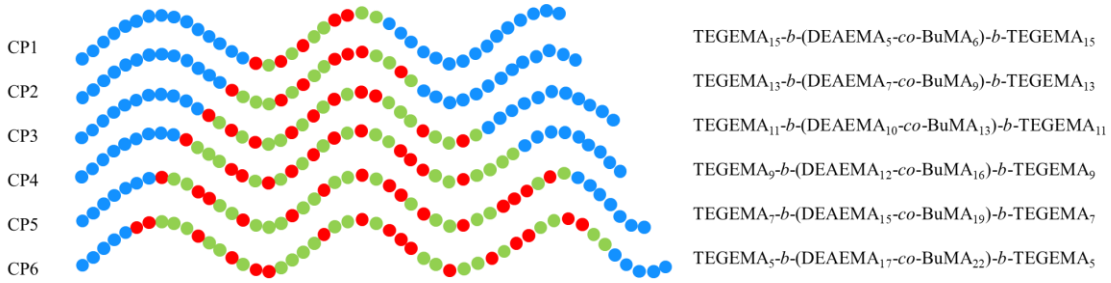


Figure 5.3 Schematic representation of CP triblock copolymers. Blue coloured circles represent hydrophilic TEGEMA units, red and green coloured circles represent hydrophobic DEAEMA and BuMA units, respectively. The theoretical compositions of polymers are listed.

The successful synthesis of 6 polymers has been analysed by GPC in terms of their MM and *Đ*.

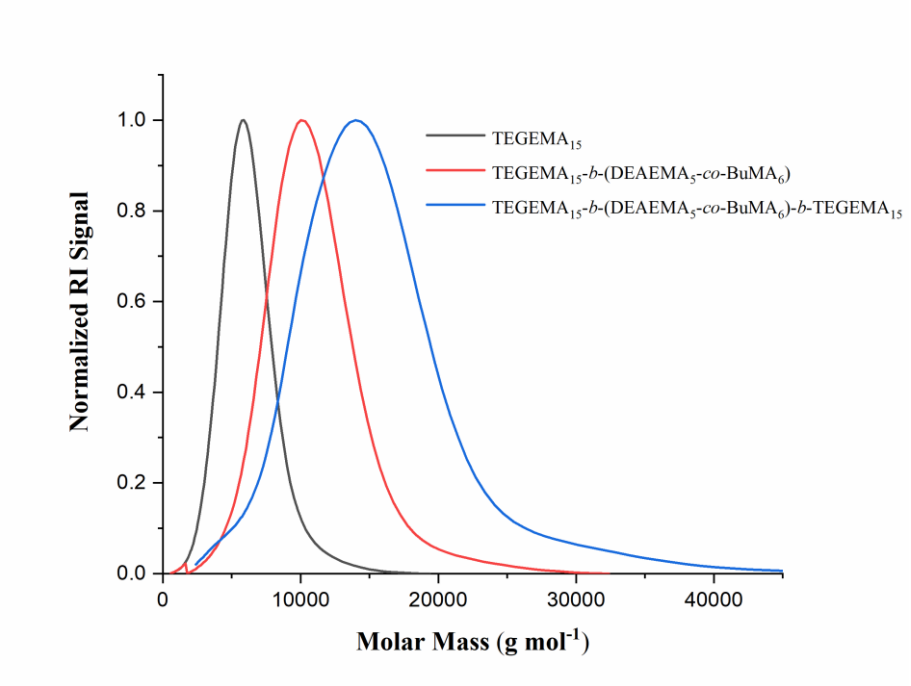


Figure 5.4 GPC chromatograms of ABA triblock polymer $TEGEMA_{15}$-*b*-($DEAEMA_5$-*co*-$BuMA_6$)-*b*-$TEGEMA_{15}$ and its linear precursors: $TEGEMA_{15}$ in black solid line, $TEGEMA_{15}$-*b*-($DEAEMA_5$-*co*-$BuMA_6$) in red solid line and the triblock copolymer $TEGEMA_{15}$-*b*-($DEAEMA_5$-*co*-$BuMA_6$)-*b*-$TEGEMA_{15}$ in blue solid line.

The final triblock copolymers and their linear precursors (homopolymer and diblock copolymer, in this chapter) have been analysed by GPC. In **Figure 5.4**, a GPC chromatogram of CP1 has been shown as an example to illustrate the successful sequential polymerisation. The GPC traces of $TEGEMA_{15}$ are shown in black solid line, the GPC traces of $TEGEMA_{15}$-*b*-($DEAEMA_5$-*co*-$BuMA_6$) are shown in red solid line and GPC traces of the triblock copolymer $TEGEMA_{15}$-*b*-($DEAEMA_5$-*co*-$BuMA_6$)-*b*-$TEGEMA_{15}$ are shown in blue solid line. As shown in the figure, the sequential addition of blocks can be verified since after the addition of a new monomer (or combination of monomers), the MM increases, indicating the monomer (or combination of monomers) has been successfully added to the active chain. The living nature of GTP is confirmed since there is no "shoulder" shown on the chromatogram, because the shoulders indicate the unexhausted usage of monomers and major termination of the active chains. The GPC chromatograms of CP2, CP3, CP4, CP5 and CP6 are similar, hence, the successful polymerisation of the whole series can be confirmed. The rest of the chromatograms can be found in **Figure A1**, **Appendix**.

The theoretical polymer structure, theoretical MM ($MM^{theor.}$), experimental number-average MM (M_n), the MM corresponds to the maximum of the peak (M_p), MM distribution ($Đ$), composition of the polymers and their precursors have been listed in **Table 5.1**. Although the theoretical MM is set at 9100 g mol^{-1}, the experimental MM locates in the range between 10600 g mol^{-1} and 13070 g mol^{-1}, which is slightly higher than the theoretical value. This is due to the minor deactivation of initiator molecules or active polymer chains during polymerisation, and it usually related to the minor leakage of the rubber septa, or residual humidity in the solvent, reaction flasks or glass syringes. The $Đ$ values vary from 1.18 to 1.24, which are efficiently close to 1, indicating the "living" nature of GTP and well control of MM.

The successful synthesis of the polymers has also been proved by ^1H NMR spectroscopy, the experimental compositions of polymers have been obtained by analysing the ^1H NMR spectra. The ^1H NMR spectrum of CP5 is shown in **Figure 5.5** as an example of the analysis. In **Figure 5.5**, from top to bottom, it shows the ^1H NMR spectrum of triblock copolymer $TEGEMA_7$-*b*-($DEAEMA_{15}$-*co*-$BuMA_{19}$)-*b*-$TEGEMA_7$ (theoretical composition, spectrum shown in blue), diblock precursor $TEGEMA_7$-*b*-($DEAEMA_{15}$-*co*-$BuMA_{19}$) (theoretical composition, spectrum shown in green) and homopolymer $TEGEMA_7$ (theoretical composition, spectrum shown in red).

The ^{1}H NMR spectra also confirm the complete consumption of monomers since no peaks of unreacted monomers are observed. From the spectrum at the bottom to the top, the sequential addition of DEAEMA and BuMA has been confirmed since the specific peaks of those units have been added to the homopolymer and the monomer peaks are not observed; the addition of TEGEMA to the diblock precursor has been confirmed since the integration of peaks that correspond to TEGEMA has increased from the diblock precursor to the triblock polymer, while no monomer peaks are observed. Hence, the successful sequential polymerisation has been confirmed.

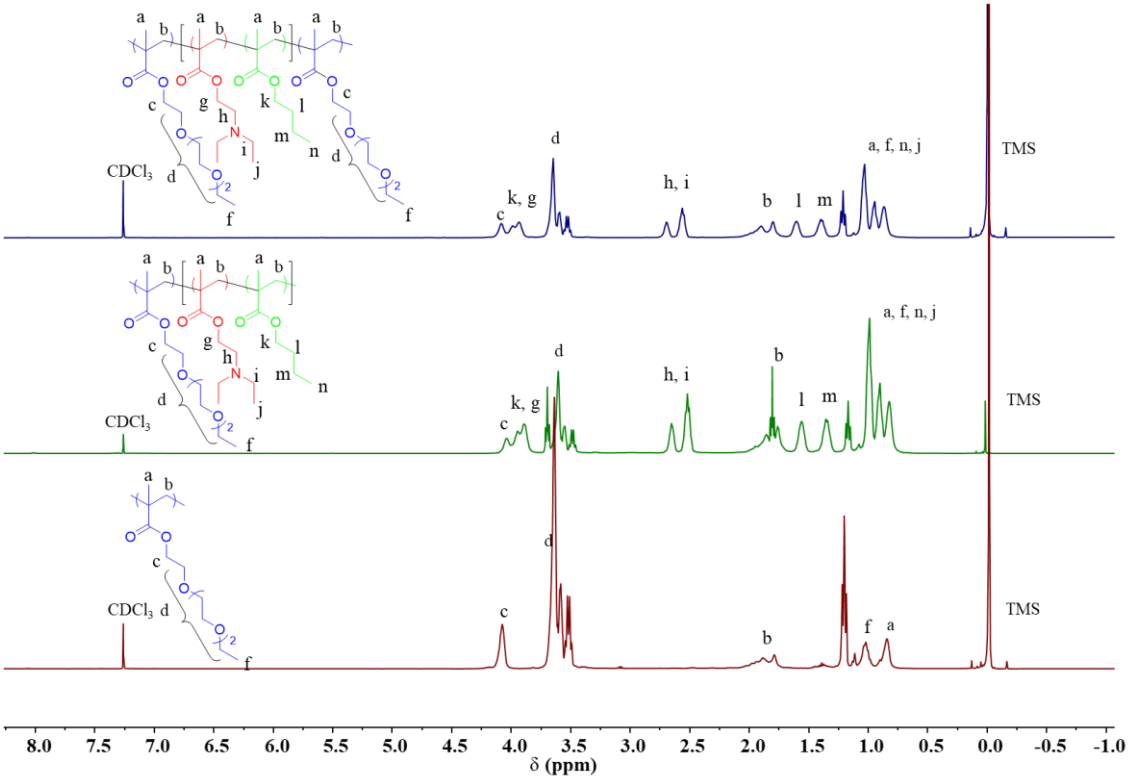


Figure 5.5 The ^{1}H NMR spectra of polymer CP5 and its precursors. From top to bottom: TEGEMA$_{7}$-*b*-(DEAEMA$_{15}$-*co*-BuMA$_{19}$)-*b*-TEGEMA$_{7}$, TEGEMA$_{7}$-*b*-(DEAEMA$_{15}$-*co*-BuMA$_{19}$), and TEGEMA homopolymer. On the left, the chemical structure of TEGEMA units is in light blue, the structure of DEAEMA units is in red and the structure of BuMA units is in green.

Moreover, the ^{1}H NMR spectra give information on the experimental composition and experimental weight percentage of each block of the polymers by comparing the integration of the peaks corresponding to specific units or blocks. The calculated experimental compositions and weight percentage of each block of all 6 polymers are listed in **Table 5.1**. All the other ^{1}H NMR spectra of polymers are available and listed

in **Appendix**.

Table 5.1 Theoretical polymer structure, theoretical molar mass ($MM^{theor.}$), experimental number-average MM (M_n), the MM that corresponds to the maximum of the peak (M_p), MM distribution ($Đ$), experimental weight percentage of each block of the polymers and their precursors of CPs.

No.	Theoretical Polymer Structure [a]	$MM^{theor.}$ [b] (g mol^{-1})	M_n [c] (g mol^{-1})	M_p [c] (g mol^{-1})	$Đ$ [c]	TEGEMA-*b*-(DEAEMA-*co*-BuMA)-*b*-TEGEMA (w/w%)	
						Theoretical	Experimental
CP1	$TEGEMA_{15}$	3700	4860	5750	1.16	100-(0-0)-0	100-(0-0)-0
	$TEGEMA_{15}$-*b*-($DEAEMA_5$-*co*-$BuMA_6$)	5500	8780	10000	1.14	66-(17-17)-0	66-(17-17)-0
	$TEGEMA_{15}$-*b*-($DEAEMA_5$-*co*-$BuMA_6$)-*b*-$TEGEMA_{15}$	9100	10600	14000	1.24	40-(10-10)-40	40-(10-10)-40
CP2	$TEGEMA_{13}$	3250	4400	5230	1.14	100-(0-0)-0	100-(0-0)-0
	$TEGEMA_{13}$-*b*-($DEAEMA_7$-*co*-$BuMA_9$)	5950	7740	9150	1.15	54-(23-23)-0	56-(22-22)-0
	$TEGEMA_{13}$-*b*-($DEAEMA_7$-*co*-$BuMA_9$)-*b*-$TEGEMA_{13}$	9100	10700	14200	1.24	35-(15-15)-35	36-(14-14)-36
CP3	$TEGEMA_{11}$	2800	3580	4100	1.16	100-(0-0)-0	100-(0-0)-0
	$TEGEMA_{11}$-*b*-($DEAEMA_{10}$-*co*-$BuMA_{13}$)	6400	7890	9500	1.17	42-(29-29)-0	46-(27-27)-0
	$TEGEMA_{11}$-*b*-($DEAEMA_{10}$-*co*-$BuMA_{13}$)-*b*-$TEGEMA_{11}$	9100	10900	13500	1.20	30-(20-20)-30	33-(19-19)-29
CP4	$TEGEMA_9$	2350	3590	4070	1.13	100-(0-0)-0	100-(0-0)-0
	$TEGEMA_9$-*b*-($DEAEMA_{12}$-*co*-$BuMA_{16}$)	6850	10200	12400	1.19	34-(33-33)-0	37-(31-31)-0
	$TEGEMA_9$-*b*-($DEAEMA_{12}$-*co*-$BuMA_{16}$)-*b*-$TEGEMA_9$	9100	12700	16100	1.23	25-(25-25)-25	26-(22-22)-30
CP5	$TEGEMA_7$	1900	3000	3310	1.14	100-(0-0)-0	100-(0-0)-0
	$TEGEMA_7$-*b*-($DEAEMA_{15}$-*co*-$BuMA_{19}$)	7300	10600	12100	1.14	25-(37-38)-0	31-(35-34)-0
	$TEGEMA_7$-*b*-($DEAEMA_{15}$-*co*-$BuMA_{19}$)-*b*-$TEGEMA_7$	9100	12300	14900	1.18	20-(30-30)-20	23-(26-26)-24
CP6	$TEGEMA_5$	1450	2420	2640	1.13	100-(0-0)-0	100-(0-0)-0
	$TEGEMA_5$-*b*-($DEAEMA_{17}$-*co*-$BuMA_{22}$)	7750	12100	14000	1.16	18-(41-41)-0	25-(38-38)-0
	$TEGEMA_5$-*b*-($DEAEMA_{17}$-*co*-$BuMA_{22}$)-*b*-$TEGEMA_5$	9100	13070	15600	1.20	15-(35-35)-15	21-(32-32)-15

[a] TEGEMA, DEAEMA and BuMA stand for tri(ethylene glycol) ethyl ether methacrylate, 2-(diethylamino) ethyl methacrylate, n-Butyl methacrylate, respectively.

[b] The theoretical MM values have been calculated by adding the product of the molar mass of each repeated unit by the degree of polymerisation. 100 g mol^{-1} corresponds to the part of the

initiator that stays on the polymer chain after the completion of the polymerisation, thus it is added to the result.

c The values of the number-average molar mass (M_n), the molar mass that corresponds to the maximum of the peak (M_p), and the dispersity indices ($Đ$) are based on a linear calibration using well-defined poly(methyl methacrylate) standard samples of molar mass equal to 2000, 4000, 8000, 20000, 50000, 100000 g mol^{-1}.

5.2 Properties in Aqueous Solution

Polymer CPs were dissolved in DI water for further characterisation, however, as introduced in **5.1**, polymers synthesised in this chapter has an increased hydrophobicity compared to the polymers in **Chapter 4**, they are not all soluble in aqueous media. For instance, CP5 and CP6 can not dissolved in water even after constant stirring for 1 week. Hence, three types of solvent mixtures of water/ethanol with different compositions were used to dissolve the CPs and the polymers are characterised in the three solvents instead of DI water or PBS.

Table 5.2 Solubility of CPs in 3 solvents at 25°C by visual observation, polymer concentration is 10 mg mL^{-1}. Partially dissolved means polymer pieces are present in the solution, dissolved means the solution is transparent, with no polymers visible.

No.	Theoretical Polymer Structure	Solvents		
		water/ethanol = 70/30 (vol%)	water/ethanol = 50/50 (vol%)	water/ethanol = 30/70 (vol%)
CP1	$TEGEMA_{15}$-*b*-($DEAEMA_5$-*co*-$BuMA_6$)-*b*-$TEGEMA_{15}$	Partially dissolved	dissolved	dissolved
CP2	$TEGEMA_{13}$-*b*-($DEAEMA_7$-*co*-$BuMA_9$)-*b*-$TEGEMA_{13}$	Partially dissolved	dissolved	dissolved
CP3	$TEGEMA_{11}$-*b*-($DEAEMA_{10}$-*co*-$BuMA_{13}$)-*b*-$TEGEMA_{11}$	Partially dissolved	dissolved	dissolved
CP4	$TEGEMA_9$-*b*-($DEAEMA_{12}$-*co*-$BuMA_{16}$)-*b*-$TEGEMA_9$	Partially dissolved	dissolved	dissolved
CP5	$TEGEMA_7$-*b*-($DEAEMA_{15}$-*co*-$BuMA_{19}$)-*b*-$TEGEMA_7$	Partially dissolved	dissolved	dissolved

CP6	TEGEMA$_5$-*b*-(DEAEMA$_{17}$-*co*-BuMA$_{22}$)-*b*-TEGEMA$_5$	Partially dissolved	Partially dissolved	dissolved

Cloud point measurements

CP solutions in three solvents have been prepared at a polymer concentration of 10 mg mL^{-1}. It is notable that in this chapter, all cloud points were obtained by visual tests following the procedure that our group has reported before.[4,5] The results are summarised as below:

1. For CP solutions in water/ethanol = 70/30 (vol%), from 20°C to 80°C, the solutions are all clear, no cloud point has shown.
2. For CP solutions in water/ethanol = 50/50 (vol%), solutions of CP1, CP2 and CP3 are all clear from 20°C to 80°C; solution of CP4 has a cloud point of 71°C, solution of CP5 has a cloud point of 29°C, solution of CP6 is cloudy at room temperature (25°C). These observations show that the cloud point of polymer solutions decreases with the increase of hydrophobicity of polymers, and this agrees with previous findings in our research group although the solvent used was water/ethanol = 50/50 (vol%), not pure water.[6]
3. For CP solutions in water/ethanol = 30/70 (vol%), solutions are all cloudy, the cloudiness increases from DP1 to DP6 due to the increase of hydrophobicity.

5.3 Size Distribution in Polymer Solutions

Similar with **Chapter 4**, two methods have been used to fabricate polymersomes: bulk hydration and film rehydration. Since the polymers are not soluble in DI water, PBS or solution of water/ethanol = 70/30 (vol%), the other two solutions were prepared to dissolve polymers, which are water/ethanol = 50/50 (vol%) and water/ethanol = 30/70 (vol%). The polymer concentration is 10 mg mL^{-1}. The size distribution of particles in the polymer solutions has been investigated by DLS and TEM.

5.3.1 DLS

DLS measurements were carried out with polymer solutions in two solvents. In addition,

two fabrication methods of polymersomes, bulk hydration and film rehydration were tested in this work to compare the particles size.

Comparison between two polymersomes fabrication methods

The experimental hydrodynamic diameters of polymer solutions are listed in **Table 5.3**. The solvent used to dissolve polymers was water/ethanol = 50/50 (vol%), the concentration of polymers is 10 mg mL^{-1}. From the table, it is clearly shown that polymer solutions prepared from bulk hydration have formed smaller particles, in both dimensions (by intensity and by number). In bulk hydration, only the solution of CP1 has a diameter of 100 nm, all the rest polymer solutions seem to have particles around 10 to 20 nm in diameter. According to **Equation 4.1**, all the calculated hydrodynamic diameter (d_h) is listed in **Table 5.3**. Interestingly, the experimental hydrodynamic diameter of particles is sufficiently close to the theoretical micelle diameter, indicating the particles formed by bulk hydration are mostly micelles. CP6 is an exception: the obtained hydrodynamic diameters by both intensity and number show much bigger values, which are over 500 nm. This can be explained by the fact that the solution of CP6 was very cloudy, showing that CP6 was only partially dissolved in the solution. The cloudiness of the solution has a great impact on the sensitivity of DLS measurements, hence, the results of CP6 were not accurate, and that was the reason that the CP6 solution prepared by film rehydration was not tested.

For the solutions of CP1, CP2 and CP3, it is obviously shown that larger particles have been formed by film rehydration rather than bulk hydration. For solutions of CP4 and CP5, the results show that two methods produce particles in similar sizes. Overall, bulk hydration method seems to produce more small micelles rather than larger vesicles, film rehydration is preferable in this project.

Table 5.3 Polymer structures, theoretical and experimental hydrodynamic diameters, polydispersity indices (PDI) of polymer solutions between two fabrication methods.

No.	Polymer Structure	Theoretical Micelle Diameter (d_h) (nm)	Bulk Hydration			Film Rehydration		
			Max Peaks (nm) (by Intensity) (± 1 nm)	Max Peaks (nm) (by number) (± 1 nm)	PDI	Max Peaks (nm) (by Intensity) (± 1 nm)	Max Peaks (nm) (by number) (± 1 nm)	PDI
CP1	T_{15}-(D_5-*co*-B_6)-T_{15}	10.4	100	8	0.223	300	8	0.203
CP2	T_{13}-(D_7-*co*-B_9) - T_{13}	10.7	10	9	0.365	300	8	0.356
CP3	T_{11}- (D_{10}-*co*-B_{13})-T_{11}	11.4	20	9	0.291	400	9	0.322
CP4	T_9-(D_{12}-*co*-B_{16})-T_9	11.7	30	10	0.329	20	10	0.393
CP5	T_7- (D_{15}-*co*-B_{19})-T_7	12.2	40	20	0.335	40	25	0.388
CP6	T_5-(D_{17}-*co*-B_{22})-T_5	12.4	600	500	1	N/A		

Comparison between two solvents that dissolve the polymers

Two solvents were used to dissolve the polymers and investigate the size of the particles. The results of the theoretical micelle diameter and experimental hydrodynamic diameter are listed in **Table 5.4**. For solutions with solvent of water/ethanol = 30/70 (vol%), it is clear that the hydrodynamic diameter measured by intensity and by number are close to each other, and the PDI is sufficiently low. In addition, the experimental

hydrodynamic diameters are 8 to 10 times the theoretical micelle diameter. Hence, it can be speculated that the particles in water/ethanol = 30/70 (vol%) solution are quite homogeneous, the particles are 8 to 10 times larger than micelles (in diameter). Moreover, from CP1 to CP6, an increasing trend of hydrodynamic diameters can be observed.

Table 5.4 Polymer structures, theoretical and experimental hydrodynamic diameters, polydispersity indices (PDI) of polymer solutions between two solutions.

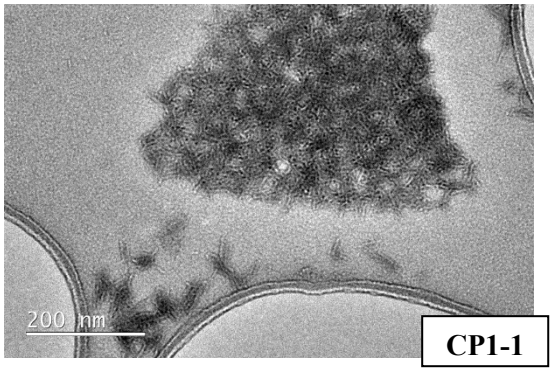
No.	Polymer Structure	Theoretical Micelle Diameter (d_h) (nm)	Solvent					
			water/ethanol = 30/70 (vol%)			water/ethanol = 50/50 (vol%)		
			Max Peaks (nm) (by Intensity) (± 1 nm)	Max Peaks (nm) (by number) (± 1 nm)	PDI	Max Peaks (nm) (by Intensity) (± 1 nm)	Max Peaks (nm) (by number) (± 1 nm)	PDI
CP1	T_{15}-(D_5-*co*-B_6)-T_{15}	10.4	80	80	0.109	300	8	0.203
CP2	T_{13}-(D_7-*co*-B_9) - T_{13}	10.7	100	80	0.137	300	8	0.356
CP3	T_{11}- (D_{10}-*co*-B_{13})-T_{11}	11.4	100	80	0.233	400	9	0.322
CP4	T_9-(D_{12}-*co*-B_{16})-T_9	11.7	100	90	0.145	20	10	0.393
CP5	T_7- (D_{15}-*co*-B_{19})-T_7	12.2	100	90	0.208	40	25	0.388
CP6	T_5-(D_{17}-*co*-B_{22})-T_5	12.4	110	90	0.223	N/A		

When compare the results from the two solvents, for CP1, CP2 and CP3, the particles in water/ethanol = 50/50 (vol%) have very small values by number and large values by intensity whereas CP4 and CP5 have similar values by both intensity and number. The values by number are sufficiently close to the theoretical micelle diameters but the structures need to be further verified by TEM.

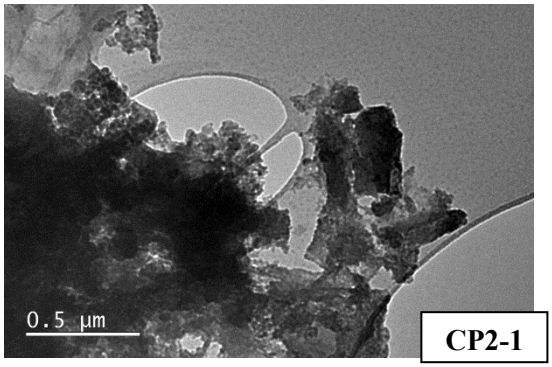
In summary, the same polymers have formed different particles in size, when dissolved in different solutions. This is due to the change of solubility of the blocks. The former discussions on hydrophilic and hydrophobic blocks of polymers are based on aqueous media, when the aqueous media mixed with organic solvents, the hydrophilicity, or to be more precise, the solubility of the blocks is not the same case. The series of polymers have severe solubility issues in aqueous media, and this is the reason that the results are differently analysed compared with **Chapter 4**.

5.3.2 TEM

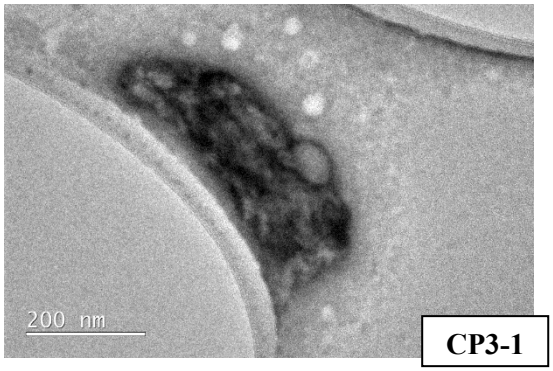
Film rehydration in solvent water/ethanol = 50/50% (vol%)



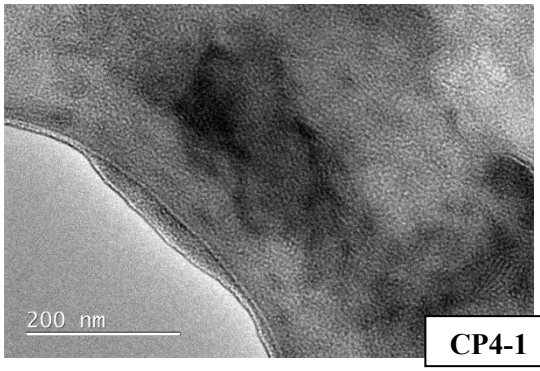
CP1-1



CP2-1



CP3-1



CP4-1

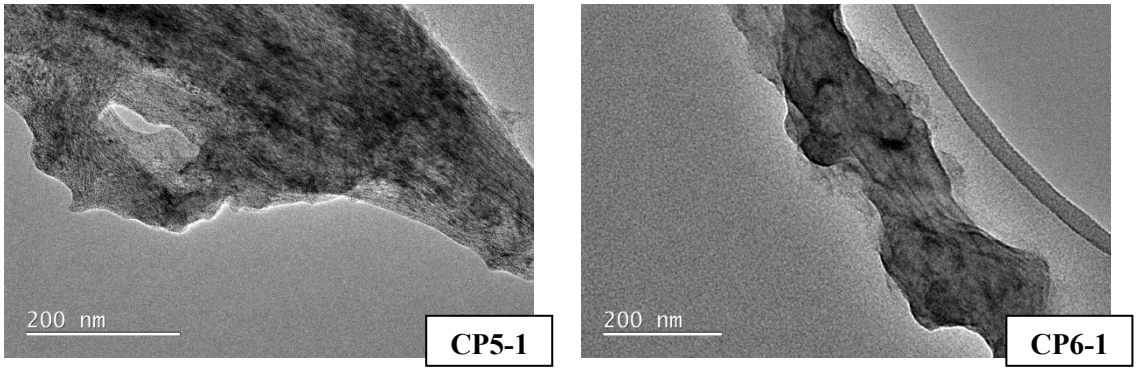
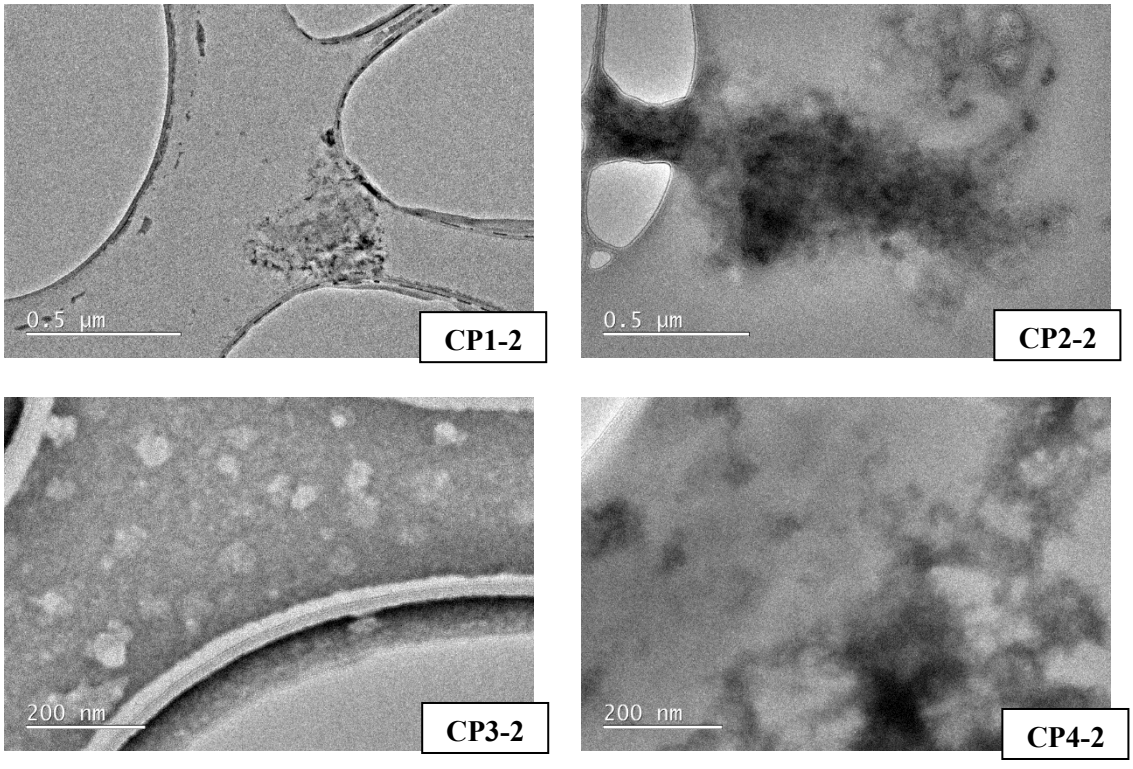


Figure 5.6 TEM images of structures formed by CPs. The solutions were prepared via film rehydration in water/ethanol = 50/50 (vol%) with a polymer concentration of 10 mg mL^{-1}. Uranyl acetate was used as a negative staining agent.

TEM images were taken for the solutions of CP1 to CP6 and the images are shown above, respectively. Polymers have shown amorphous structures in those samples and no clear images of polymersomes have been observed. In the images, clumps of polymers and the excess uranyl acetate are present rather than polymer vesicles.

Film rehydration in solvent water/ethanol = 30/70% (vol%)



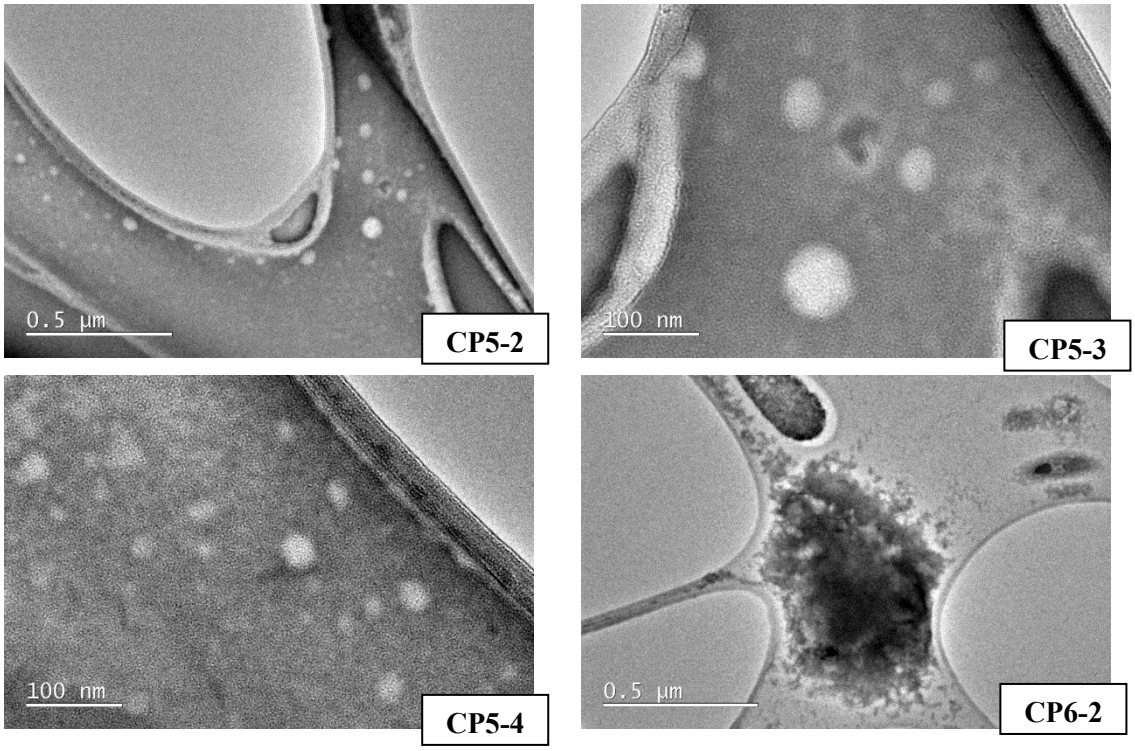


Figure 5.7 TEM images of structures formed by CPs. The solutions were prepared via film rehydration in water/ethanol = 30/70 (vol%) with a polymer concentration of 10 mg mL^{-1}. Uranyl acetate was used as a negative staining agent.

Similarly, TEM images were taken for polymer solutions in the solvent of water/ethanol = 30/70 (vol%). Polymer vesicles have been observed from the solution of CP5, while other solutions mostly show amorphous polymers and the staining agent. The diameter of the particles from the CP5 images agree with the hydrodynamic diameter obtained from DLS measurements.

5.4 Conclusions

In this study, six ABA triblock copolymers based on TEGEMA (A unit), DEAEMA and BuMA (B unit) have been successfully synthesised using GTP. The MM of all the polymers has been targeted to 9100 g mol^{-1}, whereas the composition of the polymers has been varied to investigate its effect on the polymersomes fabrication and the properties of polymersomes. Several conclusions regarding the synthesis and the aqueous characterisation are listed below:

1. All the triblock copolymers have been successfully synthesised; the MM is

within the desirable range and $Đ$ is sufficiently low.

2. The increased hydrophobicity of monomers results in the increase hydrophobicity of polymers; thus, the polymers are not soluble at RT in aqueous media.
3. Three solvents were prepared to dissolve the polymers by mixing DI water and ethanol: water/ethanol = 70/30 (vol%), water/ethanol = 50/50 (vol%) and water/ethanol = 30/70 (vol%). The introduction of organic solvent (ethanol) changes the solubility of polymers, and, polymers can be fully dissolved in water/ethanol = 30/70 (vol%) and water/ethanol = 50/50 (vol%) (apart from CP6). However, polymers cannot be appropriately dissolved in water/ethanol = 70/30 (vol%).
4. CP4 and CP5 have cloud point in solution water/ethanol = 50/50 (vol%), and CP4 has a higher cloud point than CP5, which means as the hydrophobicity increases, cloud point reduces.
5. DLS measurements have investigated the particle size between bulk hydration and film rehydration method, film rehydration in general produces larger particles; also, the solvent effect on particle size has been studied, polymers in solution water/ethanol = 30/70 (vol%) have more homogenous particles in size.
6. TEM images have been taken for polymers in solution water/ethanol = 50/50 (vol%) and water/ethanol = 30/70 (vol%); only CP5 in solution water/ethanol = 30/70 (vol%) has shown clear vesicles, the other images only contain amorphous polymers and attaining agents.
7. Overall, the fabrication of polymersomes using these polymers was not very successful, so adjustments were made to increase the hydrophilicity and water solubility as it will be discussed in the next chapter.

REFERENCE

1. Li, Q., Constantinou, A. P., & Georgiou, T. K. (2021). A library of thermoresponsive PEG-based methacrylate homopolymers: How do the molar mass and number of ethylene glycol groups affect the cloud point?. *Journal of Polymer Science*, *59*(3), 230-239.

2. Constantinou, A. P., Sam-Soon, N. F., Carroll, D. R., & Georgiou, T. K. (2018). Thermoresponsive Tetrablock Terpolymers: Effect of Architecture and Composition on Gelling Behavior. *Macromolecules*, *51*(18), 7019-7031.

3. Constantinou, A. P., & Georgiou, T. K. (2016). Tuning the gelation of thermoresponsive gels. *European Polymer Journal*, *78*, 366-375.

4. Constantinou, A. P., & Georgiou, T. K. (2016). Thermoresponsive gels based on ABC triblock copolymers: effect of the length of the PEG side group. *Polymer Chemistry*, *7*(11), 2045-2056.

5. Constantinou, A. P., Zhao, H., McGilvery, C. M., Porter, A. E., & Georgiou, T. K. (2017). A comprehensive systematic study on thermoresponsive gels: beyond the common architectures of linear terpolymers. *Polymers*, *9*(1), 31.

6. Constantinou, A. P., Marie-Sainte, U., Peng, L., Carroll, D. R., McGilvery, C. M., Dunlop, I. E., & Georgiou, T. K. (2019). Effect of block copolymer architecture and composition on gold nanoparticle fabrication. *Polymer Chemistry*, *10*(34), 4637-4642.

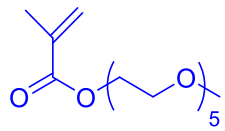
CHAPTER 6 POLYMERSOMES BASED ON TRIBLOCK COPOLYMER PEGMA-*b*-(DEAEMA-*co*-BUMA)-*b*-PEGMA

6.1 Chemistry of Block Copolymers

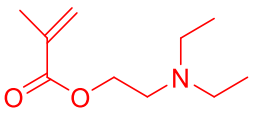
In this chapter, a series of ABA triblock copolymers have been synthesised, characterised and the fabricated polymersomes have been investigated.

PEG-based methacrylate polymers have drawn great attention for their thermoresponsiveness,[1-7] since PEG is a hydrophilic, biocompatible FDA approved polymer.[1,5] Previous study in our group reveals the EG groups on the side chain of the methacrylate unit have an impact on the hydrophilicity of a copolymer,[8] proven that PEGMA has better solubility than TEGMA or TEGEMA, and it helps to minimize the solubility issue of the copolymers in aqueous solutions. Hence, the main problem in **Chapter 5** can be solved due to the change of hydrophilic monomer.

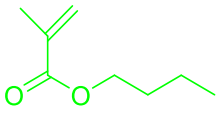
The monomers selected in this chapter are PEGMA, DEAEMA and BuMA, for the synthesis of triblock copolymers PEGMA-*b*-(DEAEMA-*co*-BuMA)-*b*-PEGMA, where DEAEMA and BuMA are statistically mixed, constituting the hydrophobic block of the polymer, whereas PEGMA constitutes the hydrophilic. Chemical structures, names, abbreviations and related properties of the monomers are shown in **Figure 6.1**.



Penta(ethylene glycol) methyl ether methacrylate (PEGMA, PEG) Monomer
Hydrophilic, non-ionic



2-(Diethylamino) ethyl methacrylate (DEAEMA) Monomer,
Hydrophobic, ionic pH- responsive



n-Butyl methacrylate (BuMA, Bu) Monomer,
hydrophobic, non-ionic

Figure 6.1 Chemical structures, names, abbreviations and related properties of the monomers used for the polymerisation of polymer series DP.

DEAEMA has been proven to be effective as a hydrophobic monomer and it shows pH-responsiveness in **Chapter 4**. BuMA has also been used in **Chapter 5**. In **Chapter 4**, the TEGMA-*b*-DEAEMA-*b*-TEGMA copolymers have been run through a test *in vivo*, the results indicate the polymers have rather high cellular toxicity due to the amino groups in DEAEMA. To minimise this side effect, meanwhile keeping the pH-responsiveness of the copolymers, DEAEMA-*co*-BuMA is designed as the hydrophobic block of the copolymers. During polymerisation, DEAEMA and BuMA monomers have been injected to the reaction flask dropwise at the same time and same rate, the weight ratios of two monomers are 50% to 50%.

Identically, the MM of copolymers in this chapter is designed to be 9100 g/mol (including 100 g mol^{-1} of the initiator MTS). The series of polymers are named "DP". Six polymers have been synthesised, so they have been recognised as DP1, DP2, DP3, DP4, DP5 and DP6, respectively. All DPs have a common structure of $PEGMA_x$-*b*-($DEAEMA_y$-*co*-$BuMA_z$)-*b*-$PEGMA_x$, the only variation is the value of x, y and z (DP of the blocks). In other words, DPs have different hydrophilic/hydrophobic ratio while their overall MMs have been designed the same, although in practical, the MMs have minor differences.

The two main aims of this chapter are:

1. Investigate how hydrophilic/hydrophobic ratio of the polymers affect the formation and properties of polymersomes;
2. Compare the differences in fabrication of polymersomes and the properties of the formed polymersomes between PEGMA-*b*-(DEAEMA-*co*-BuMA)-*b*-PEGMA copolymers and the other copolymers formed in **Chapter 4** and **Chapter 5**.

6.1.1 Polymer Synthesis

GTP has also been used to synthesise DPs. Regardless of the composition, all DPs have been prepared via one-pot synthesis. The synthetic routes of all six polymers are identical, except for the amount of chemicals added. The sequential GTP reaction is illustrated in **Figure 6.2**. The catalyst TBABB and solvent THF have been firstly added to the reaction flask, followed by the addition of initiator MTS. PEGMA has

been diluted by THF due to its high viscosity, and it has been added dropwise to the flask. DEAEMA and BuMA have been added dropwise to the flask at the same time to make a statistical hydrophobic block, followed by a second addition of PEGMA. In the end, methanol was injected to the reaction flask to quench the reaction. The final polymer products (after purification) are sticky, transparent solids.

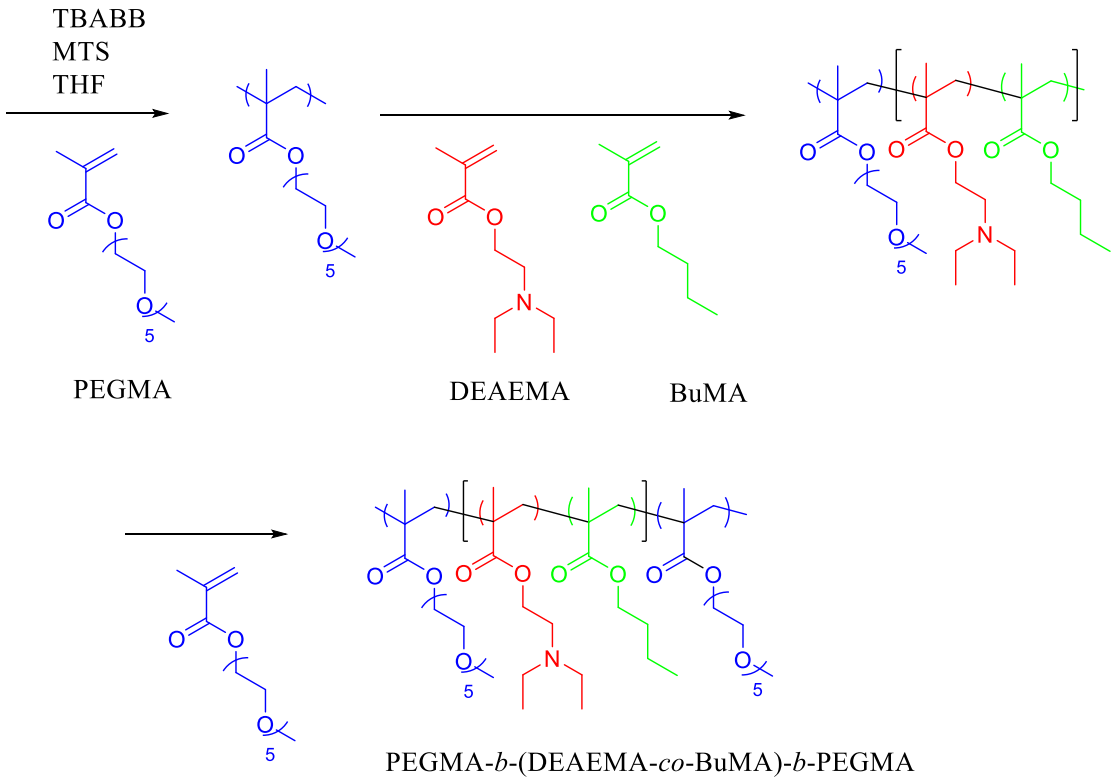


Figure 6.2 Illustration of the sequential GTP reaction for the synthesis of PEGMA-*b*-(DEAEMA-*co*-BuMA)-*b*-PEGMA triblock copolymers. PEGMA, DEAEMA and BuMA are the three monomers; TBABB, MTS, THF are the catalyst, monofunctional initiator and solvent used in this reaction.

6.1.2 Molar Mass and Composition

Figure 6.3 is a schematic representation of the six triblock copolymers synthesised in this chapter. The blue, red and green circles represent PEGMA, DEAEMA and BuMA units, respectively. The number of the circles indicates the degree of polymerisation. One notable fact in **Figure 6.3** is, although from DP1 to DP6, the presented total length of polymer chain increases, the experimental MM for 6 polymers is designed to be

identical.

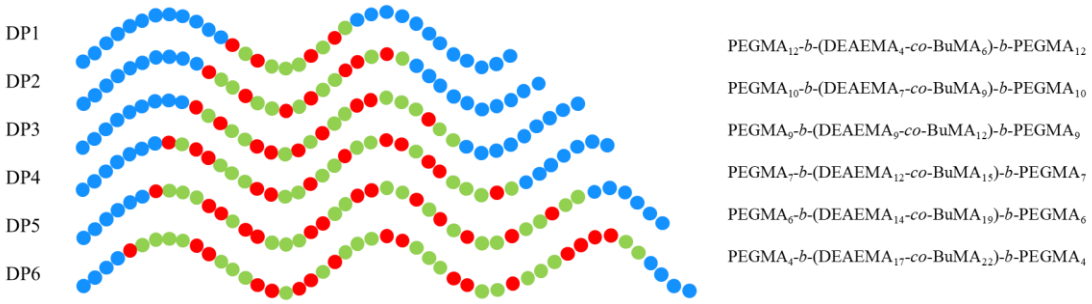


Figure 6.3 A schematic representation of DP triblock copolymers. Blue coloured circles represent hydrophilic PEGMA units, red circles represent hydrophobic DEAEMA units, green circles represent hydrophobic BuMA units, respectively, and the theoretical composition of the polymers are listed.

The hydrophobicity increases gradually from DP1 to DP6 as the ratio of red and green circles increases gradually from DP1 to DP6. The chemical structures of polymers are shown on the right in **Figure 6.3**, the weight ratios of hydrophobic units, from DP1 to DP6, are 20, 30, 40, 50, 60, 70%, respectively. Interestingly, the softness of the polymers increases along with the hydrophilicity, the most hydrophilic polymer DP1 has the softest texture.

The MM and composition of the polymers have been verified by GPC and ^{1}H NMR. Since the polymers have been synthesised by a sequential polymerisation, the product of each step has been collected and confirmed. **Figure 6.4** presents the GPC chromatograms of DP2 and its linear precursors. The 3 samples have been taken from the same reaction flask at different times. The peaks move to higher MM values from the homopolymer PEGMA$_{10}$, to the diblock precursor PEGMA$_{10}$-*b*-(DEAEMA$_{7}$-*co*-BuMA$_{9}$), and to the final triblock copolymer PEGMA$_{10}$-*b*-(DEAEMA$_{7}$-*co*-BuMA$_{9}$)-*b*-PEGMA$_{10}$. The GPC chromatograms confirm the successful sequential polymerisation (chain extended upon addition of the next monomer). The peaks corresponding to monomers have not been seen in the figure, indicating the complete consumption of the monomers. The GPC chromatograms of other polymers in the series can be found in **Figure A1**, **Appendix**.

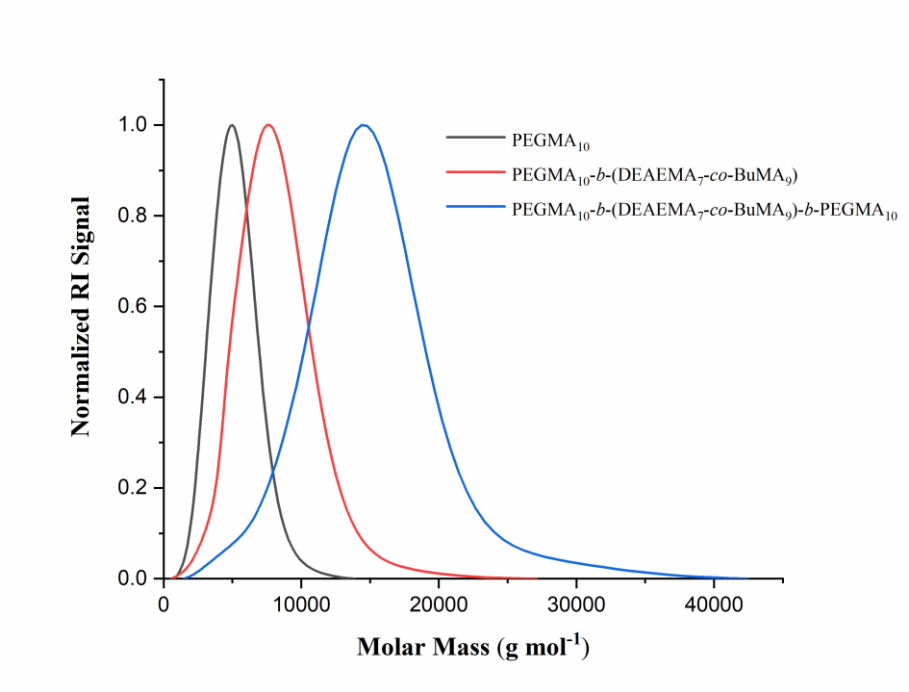


Figure 6.4 GPC chromatograms of ABA triblock polymer $PEGMA_{10}$-*b*-($DEAEMA_7$-*co*-$BuMA_9$)-*b*-$PEGMA_{10}$ and its linear precursors. $PEGMA_{10}$ in black solid line, $PEGMA_{10}$-*b*-($DEAEMA_7$-*co*-$BuMA_9$) in red solid line and the polymer in blue solid line.

Moreover, some GPC chromatograms of polymers have a low intensity shoulder at low MM, it is ascribed to the minor deactivation happened during the polymerisation. This deactivation is also observed in other GTP studies containing PEG based methacrylate monomers,[9,10] however, the shoulders are very small and negligible. Hence, the synthesis of all six polymers is considered successful.

Theoretical polymer structures, theoretical and experimental MMs, *Đ* and polymer compositions are listed in **Table 6.1**. All six polymers have the same theoretical MM, which is 9100 g mol^{-1}, whereas their experimental number-average MMs vary in a range from 11200 to 12600 g mol^{-1}. Those values are slightly higher than the theoretical MM, due to the partial deactivation of the initiator or the reactive polymer chains, but they are still in an acceptable range for this project. *Đ* of the polymers locate in the range from 1.18 to 1.23, attributes to the "living" nature of GTP,[9,10] and the values are satisfactorily close to the theoretical value (1).

Table 6.1 Theoretical polymer structure, molar mass ($MM^{theoretical}$), experimental number-average MM (M_n), the MM that corresponds to the maximum of the peak (M_p), MM distribution ($Đ$), composition of the polymers and their precursors of DPs.

No.	Theoretical Polymer Structure [a]	$MM^{theor.}$ [b] (g mol^{-1})	M_n [c] (g mol^{-1})	M_p [c] (g mol^{-1})	$Đ$ [c]	PEGMA-*b*-(DEAEMA-*co*-BuMA)-*b*-PEGMA (w/w%)	
						Theoretical	Experimental
DP1	$PEGMA_{12}$	3700	5510	6480	1.14	100-(0-0)-0	100-(0-0)-0
	$PEGMA_{12}$-*b*-($DEAEMA_4$-*co*-$BuMA_6$)	5500	7930	9080	1.12	67-(17-16)-0	66-(17-17)-0
	$PEGMA_{12}$-*b*-($DEAEMA_4$-*co*-$BuMA_6$)-*b*-$PEGMA_{12}$	9100	11200	15600	1.23	40-(10-10)-40	38-(10-10)-42
DP2	$PEGMA_{10}$	3250	4010	5010	1.16	100-(0-0)-0	100-(0-0)-0
	$PEGMA_{10}$-*b*-($DEAEMA_7$-*co*-$BuMA_9$)	5950	6040	7520	1.20	54-(23-23)-0	55-(22-23)-0
	$PEGMA_{10}$-*b*-($DEAEMA_7$-*co*-$BuMA_9$)-*b*-$PEGMA_{10}$	9100	11200	14400	1.20	35-(15-15)-35	34-(14-15)-35
DP3	$PEGMA_9$	2800	3700	4590	1.16	100-(0-0)-0	100-(0-0)-0
	$PEGMA_9$-*b*-($DEAEMA_9$-*co*-$BuMA_{12}$)	6400	7860	9790	1.20	43-(29-28)-0	44-(27-29)-0
	$PEGMA_9$-*b*-($DEAEMA_9$-*co*-$BuMA_{12}$)-*b*-$PEGMA_9$	9100	12100	16000	1.21	30-(20-20)-30	29-(18-19)-34
DP4	$PEGMA_7$	2350	3600	4420	1.16	100-(0-0)-0	100-(0-0)-0
	$PEGMA_7$-*b*-($DEAEMA_{12}$-*co*-$BuMA_{15}$)	6850	8730	10700	1.17	33-(34-33)-0	39-(32-29)-0
	$PEGMA_7$-*b*-($DEAEMA_{12}$-*co*-$BuMA_{15}$)-*b*-$PEGMA_7$	9100	12000	14900	1.19	25-(25-25)-25	31-(26-23)-20
DP5	$PEGMA_6$	1900	2980	3460	1.16	100-(0-0)-0	100-(0-0)-0
	$PEGMA_6$-*b*-($DEAEMA_{14}$-*co*-$BuMA_{19}$)	7300	11000	12600	1.14	25-(38-37)-0	27-(37-36)-0
	$PEGMA_6$-*b*-($DEAEMA_{14}$-*co*-$BuMA_{19}$)-*b*-$PEGMA_6$	9100	12600	15600	1.21	20-(30-30)-20	22-(30-30)-18
DP6	$PEGMA_4$	1450	2400	2800	1.15	100-(0-0)-0	100-(0-0)-0
	$PEGMA_4$-*b*-($DEAEMA_{17}$-*co*-$BuMA_{22}$)	7750	10000	11300	1.14	18-(41-41)-0	20-(40-40)-0
	$PEGMA_4$-*b*-($DEAEMA_{17}$-*co*-$BuMA_{22}$)-*b*-$PEGMA_4$	9100	12600	14900	1.18	15-(35-35)-15	17-(34-34)-15

[a] PEGMA, DEAEMA and BuMA stand for penta(ethylene glycol)methyl ether methacrylate, 2-(diethylamino) ethyl methacrylate, n-Butyl methacrylate, respectively.

[b] The theoretical MM values have been calculated by adding the product of the molar mass of each repeated unit by the degree of polymerisation. 100 g mol^{-1} corresponds to the part of the initiator that stays on the polymer chain after the completion of the polymerisation, thus it is added to the result.

c The values of the number-average molar mass (M_n), the molar mass that corresponds to the

maximum of the peak (M_p), and the dispersity indices ($Đ$) are based on a linear calibration using well-defined poly(methyl methacrylate) standard samples of molar mass equal to 2000, 4000, 8000, 20000, 50000, 100000 g mol^{-1}.

The compositions of polymers are listed in **Table 6.1**, to determine whether they are close enough to the theoretical values. As can be seen from the table, the experimental compositions obtained from ^{1}H NMR are reasonably close to the theoretical values. These values have been calculated from the ^{1}H NMR spectra. **Figure 6.5** is the stacked ^{1}H NMR spectra of DP5 and its two precursors as an example to illustrate the determination of the polymer composition.

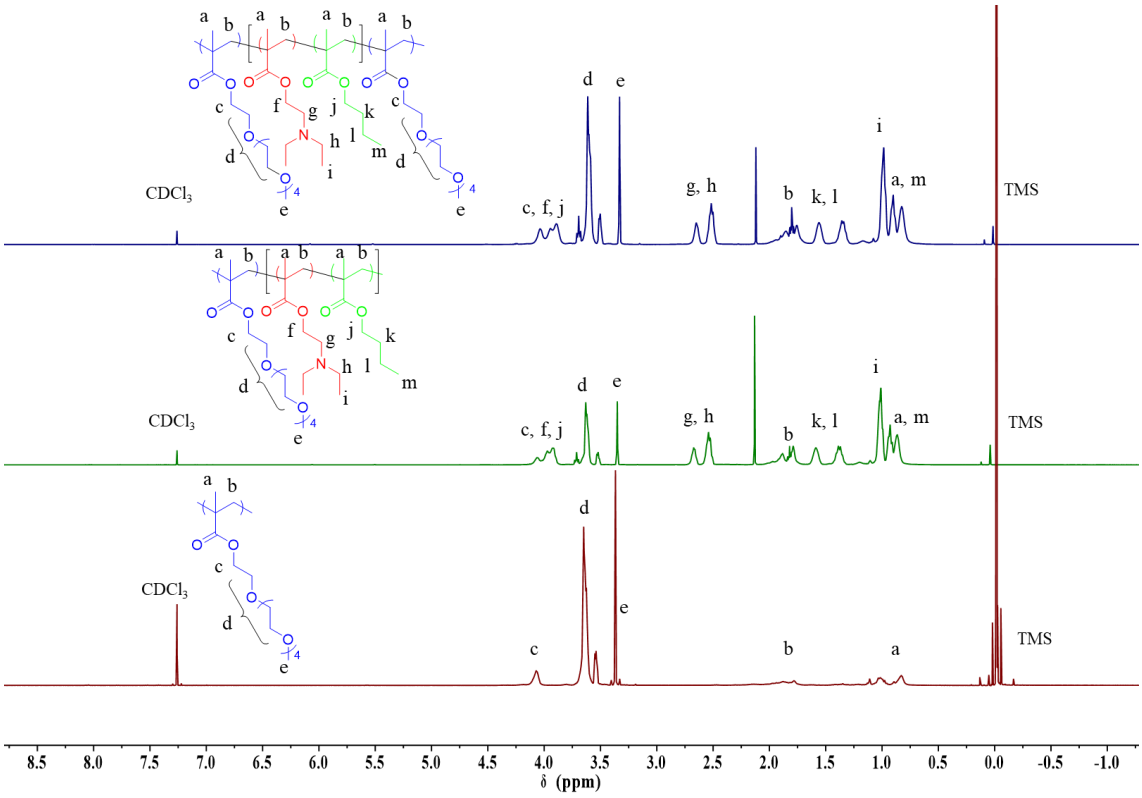


Figure 6.5 The ^{1}H NMR spectra of Polymer DP5 and its precursors. From top to bottom shows triblock copolymer $PEGMA_6$-*b*-($DEAEMA_{14}$-*co*-$BuMA_{19}$)-*b*-$PEGMA_6$, diblock precursor $PEGMA_6$-*b*-($DEAEMA_{14}$-*co*-$BuMA_{19}$), and PEGMA homopolymer. On the left, the chemical structure of PEGMA units is in light blue, the structure of DEAEMA units is in red and the structure of BuMA units is in green.

Overall, **Table 6.1** and **Figure 6.5** confirm, based on the MM, $Đ$, and composition, the listed polymers are satisfactory to be further investigated.

6.2 Properties in Aqueous Solution

6.2.1 Effective pK_as

In an aqueous solution, pK_a is frequently used to indicate the acidity, it is the negative log of the acid dissociation constant (K_a). The lower the pK_a value, the stronger the acid.

In this work, pK_as have been determined by potentiometric titrations. The pK_a values of all six polymer solutions have been calculated and the final results have been plotted over the hydrophilic weight ratio of polymers. The results are presented in **Figure 6.6**. In general, the pK_a values increase along with the increase of the hydrophilic weight ratio of copolymers (decrease of DEAEMA units in copolymers). This trend has been observed previously, and it is due to the increased dielectric constant by increasing hydrophilicity.[11,12,13,14] However, the pK_a of DP4 is slightly higher than that of DP3. When considering the error of the titration experiments, the trend can still be valid. Overall, the pK_as of the six copolymers locate in the range of 5.8 to 6.8, and the values increase along with the increase of the hydrophilicity of polymers.

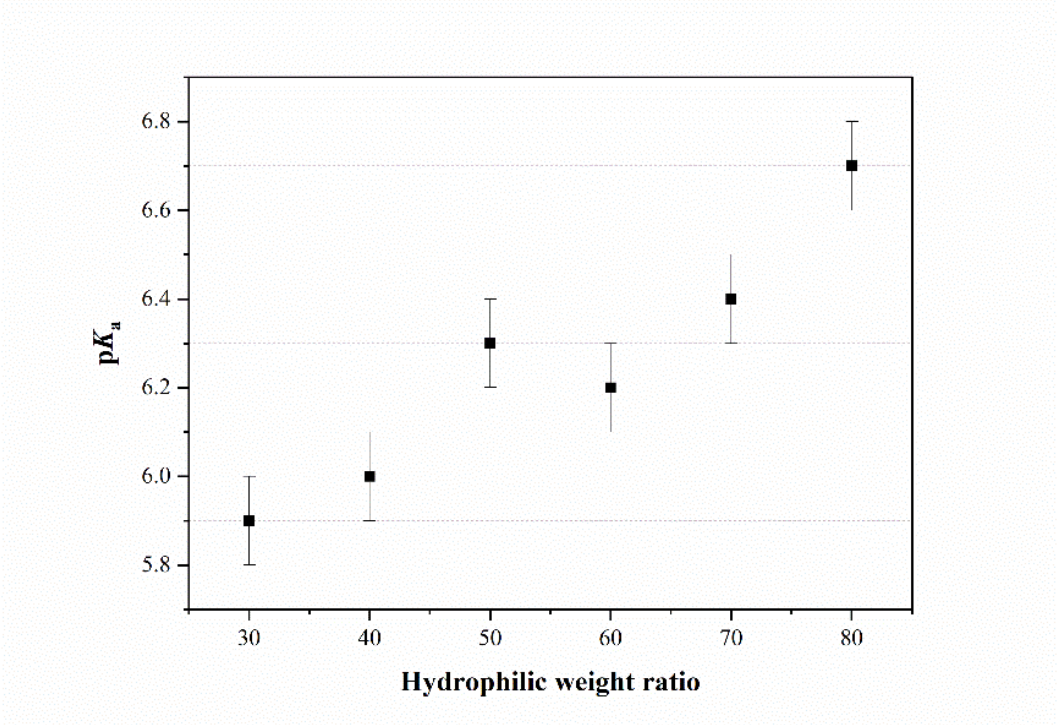


Figure 6.6 Effective pK_as of the six copolymers. Data points from right to left represent DP1, DP2, DP3, DP4, DP5 and DP6, respectively.

6.2.2 Cloud Point

Similarly, six copolymers in this chapter have been dissolved in DI water to determine their cloud point to investigate their thermoresponsiveness. Cloud point is the temperature beyond which the transparent polymer solution turns cloudy due to phase transition. In this work, two methods have been applied to determine the cloud point: Ultraviolet−Visible (UV−Vis) Spectroscopy and the visual tests. All six polymers have been dissolved in DI water at a concentration of 10 mg mL^{-1}.

The results of cloud point are listed in **Table 5.2**. In the table, cloud point by visual test and by UV-Vis measurements are both presented, along with the precipitation temperature of the polymers.

Table 6.2 Theoretical polymer structures, cloud point and precipitation temperature of DPs.

Polymer	Theoretical Polymer Structure	Cloud Point by Visual Test ± 2°C	Cloud Point by UV-Vis Spectroscopy ± 2°C	Precipitation Temperature ± 2°C
DP1	$PEGMA_{12}$-*b*-($DEAEMA_4$-*co*-$BuMA_6$)-*b*-$PEGMA_{12}$	62	63	Above 80
DP2	$PEGMA_{10}$-*b*-($DEAEMA_7$-*co*-$BuMA_9$)-*b*-$PEGMA_{10}$	61	61	70
DP3	$PEGMA_9$-*b*-($DEAEMA_9$-*co*-$BuMA_{12}$)-*b*-$PEGMA_9$	58	59	60
DP4	$PEGMA_7$-*b*-($DEAEMA_{12}$-*co*-$BuMA_{15}$)-*b*-$PEGMA_7$	56	56	60
DP5	$PEGMA_6$-*b*-($DEAEMA_{14}$-*co*-$BuMA_{19}$)-*b*-$PEGMA_6$	Cloudy at RT	Cloudy at RT	55
DP6	$PEGMA_4$-*b*-($DEAEMA_{17}$-*co*-$BuMA_{22}$)-*b*-$PEGMA_4$	Cloudy at RT	Cloudy at RT	55

The cloud point data obtained by visual test and UV−Vis Spectroscopy are sufficiently close to each other, and they both follow a descending trend from DP1 to DP4, thus, it can be summarised that the cloud point decreases with the decrease of hydrophilicity. This phenomenon has also been observed and reported before.[9,11,12,15]

For the most hydrophobic polymers DP5 and DP6, the solutions are already cloudy at RT. Moreover, the six polymers have been heated up from RT to 80 °C, in this temperature range only DP1 has been transparent at all times, other polymers all have a precipitation temperature and the data has been listed in **Table 6.2**. The precipitation temperature of polymer solutions also decreases with the decrease of hydrophilicity of polymers. For DP2 to DP6, beyond precipitation temperature, the polymer solutions have phase separation, white polymer pieces have precipitated at the bottom of the vials while the upper solution maintains transparent.

6.3 Size Distribution in Polymer Solutions

When dissolved in aqueous solutions, polymers tend to self-assemble into various nano structures. Polymersomes are the structures this work focuses on while other structures are also often observed. DLS and TEM are two main tools to investigate the size and size distribution of self-assembled structures in aqueous media.

6.3.1 DLS

6.3.1.1 Three Variables of Experiments

DLS gives a numerical understanding of the polymer self-assembly behaviour in aqueous solutions by measuring the hydrodynamic diameter of particles in solution. In this chapter, to get a comprehensive study of the polymer behaviour, three variables have been considered:

Polymersome fabrication method According to **Chapter 1**, in solvent free approach, bulk hydration and film rehydration are the easiest and most common methods. Although in **Chapter 4**, film rehydration method has been proven preferable to fabricate polymersomes, it is still worthy to compare the hydrodynamic diameter between the two methods since the polymers are different.

Solvent DI water has been used to dissolve polymers for the determination of pK_a and cloud point, however, PBS is commonly used in biological research, it helps to maintain a constant pH, the osmolarity and ion concentrations of the solutions match those of the human body (isotonic). Thus, the polymers have also been dissolved in PBS and the

results are compared with those in DI water.

Stirring time The polymer solutions have been stirred by a stir bar on a stir plate at a constant rate since dissolution, it is important to investigate if the size and size distribution of the polymeric structures are affected by stirring time. To get a comprehensive understanding, samples of polymer solutions have been taken daily from the first week of dissolution. Moreover, samples stirred for 1 month time have also been run through DLS test. The corresponding results have been summarised and listed in **Table 6.3**, **Table 6.4** and **Table 6.5**.

6.3.1.2 Results and Discussion

All DLS graphs corresponding to the data listed in **Table 6.3**, **Table 6.4** and **Table 6.5** can be found in **Figure A4.9** – **A4.13**, **Appendix**.

In **Table 6.3**, the results of hydrodynamic diameters obtained from DLS are listed and compared between bulk hydration method and film rehydration method. The max peaks by intensity indicate the diameters which have the strongest signal intensity detected by the machine. On the other hand, different particles in solution may have the same diameter, the diameters that the most particles have are the max peaks by number. In the table, it is clearly observed that in bulk hydration method, DP1 to DP4 all have only one peak by both intensity and number, the values are around 8 to 16 nm, which means only small micelles have been formed for DP1 to DP4 via bulk hydration method. On contrast, two peaks have been observed for DP1 to DP4 via film rehydration method and the large peaks show correspondence to the diameters of polymersomes. As for DP5 and DP6, the polymers have two peaks by intensity, and the values are drastically higher than the other polymers, which means the more hydrophobic one polymer is, the larger vesicles it forms rather than small micelles. Another notable fact is, DP5 and DP6 have cloudy solutions at RT, which can affect the accuracy of the DLS measurements.

In **Table 6.4**, the size of nanoparticles formed in different solvent has been compared. Polymers tend to have two max peaks by intensity while only one max peak is observed by number. Water and PBS do not have a huge difference on the size of the nano particles by intensity, however, water has a better quality of result in terms of the PDI.

As for the data by number, it seems that the polymers form slightly larger particles in the solvent of PBS.

Table 6.5 presents the comparison of DLS results based on time difference. Polymers were dissolved in PBS at a concentration of 10 mg mL^{-1}, and have been kept stirring from day 1 to 1 month time. In this time period, DLS measurements had been taken every day at approximately same time from day 1 to day 7, and finally at the end of the first month. The purpose of the set of experiments is to optimise the most preferable condition to form polymersomes with desirable size (ideally less than 200 nm for intracellular drug delivery). By analysing the table, conclusions are listed as following:

1. DP1, DP2, DP3 and DP4 are very stable, the size distribution by intensity and number have not changed much from day 1 to day 7, while at 1 month only DP3 has a smaller average size by intensity. DP1 and DP2 have very similar results to each other, the composition effect has not been clear between these two polymers. DP3 has a drastic increase in both hydrodynamic diameters by intensity and by number than DP1 and DP2. Moreover, all of the polymers have at least two peaks by intensity, but for DP3, the two peaks have a huge difference in intensity so the smaller peak can be neglected. It means that DP3 is an excellent candidate for forming large particles. Surprisingly, DP4 does not have further increment in hydrodynamic diameters, on contrary, the value is smaller than DP3, whereas still bigger than DP1 and DP2.

2. DP5 and DP6 have rather random results because of the cloudiness of those two solutions. Due to the high hydrophobicity, DP5 tend to precipitate in the cuvettes, and it strongly affects the accuracy of DLS results. The peaks by intensity show values more than 1000 nm for DP5 and DP6, those values are not usually considered to be polymersomes. For the hydrodynamic diameters by number, DP5 and DP6 also have much larger numbers than DP1 to DP4. It means that DP5 and DP6 tend to form large polymersomes rather than small micelles. In fact, the size distribution of polymers (especially DP5 and DP6) needs to be further confirmed by TEM and SANS.

Table 6.3 Summary of DLS results of DPs with different fabrication methods (bulk hydration and film rehydration). Polymers are dissolved in DI water (10 mg mL^{-1}).

Stirring Time	No.	Polymer Chemical Structure	Bulk Hydration					Film Rehydration				
			Max Peaks (nm) (by intensity) (± 1 nm)		Max Peaks (nm) (by number) (± 1 nm)		PDI	Max Peaks (nm) (by intensity) (± 1 nm)		Max Peaks (nm) (by number) (± 1 nm)		PDI
			Peak 1	Peak 2	Peak 1	Peak 2		Peak 1	Peak 2	Peak 1	Peak 2	
1 week	DP1	P_{12}-*b*-(D_4-*co*-B_6)-*b*-T_{12}	13.5	N/A	8.72	N/A	0.106	15.7	295	3.62	10.1	0.528
	DP2	P_{10}-*b*-(D_7-*co*-B_9)-*b*-T_{10}	15.7	N/A	8.72	N/A	0.248	11.7	531	3.12	N/A	0.443
	DP3	P_9-*b*-(D_9-*co*-B_{12})-*b*-T_9	15.7	N/A	8.72	N/A	0.244	15.7	396	8.72	N/A	0.372
	DP4	P_7-*b*-(D_{12}-*co*-B_{15})-*b*-T_7	15.7	N/A	8.72	N/A	0.18	15.7	615	10.1	N/A	0.272
	DP5	P_6-*b*-(D_{14}-*co*-B_{19})-*b*-T_6	106	615	24.4	N/A	0.863	68.1	2550	21	N/A	0.974
	DP6	P_4-*b*-(D_{17}-*co*-B_{22})-*b*-T_4	190	1480	164	N/A	0.342	190	1480	91.3	N/A	0.558

Table 6.4 Summary of DLS results of DPs in different solvents (DI water and PBS). The polymer concentration is 10 mg mL^{-1}.

Stirring Time	No.	Polymer Chemical Structure	Solvent									
			DI water					PBS				
			Max Peaks (nm) (by intensity) (± 1 nm)		Max Peaks (nm) (by number) (± 1 nm)		PDI	Max Peaks (nm) (by intensity) (± 1 nm)		Max Peaks (nm) (by number) (± 1 nm)		PDI
			Peak 1	Peak 2	Peak 1	Peak 2		Peak 1	Peak 2	Peak 1	Peak 2	
1 week	DP1	P_{12}-*b*-(D_4-*co*-B_6)-*b*-T_{12}	15.7	295	3.62	10.1	0.528	15.7	220	11.7	N/A	1
	DP2	P_{10}-*b*-(D_7-*co*-B_9)-*b*-T_{10}	11.7	531	3.12	N/A	0.443	15.7	220	11.7	N/A	0.624
	DP3	P_9-*b*-(D_9-*co*-B_{12})-*b*-T_9	15.7	396	8.72	N/A	0.372	N/A	531	15.7	N/A	0.599
	DP4	P_7-*b*-(D_{12}-*co*-B_{15})-*b*-T_7	15.7	615	10.1	N/A	0.272	21	295	11.7	N/A	0.439
	DP5	P_6-*b*-(D_{14}-*co*-B_{19})-*b*-T_6	68.1	255	21	N/A	0.974	58.8	2550	50.7	N/A	1
	DP6	P_4-*b*-(D_{17}-*co*-B_{22})-*b*-T_4	190	1480	91.3	N/A	0.558	190	1280	106	N/A	0.533

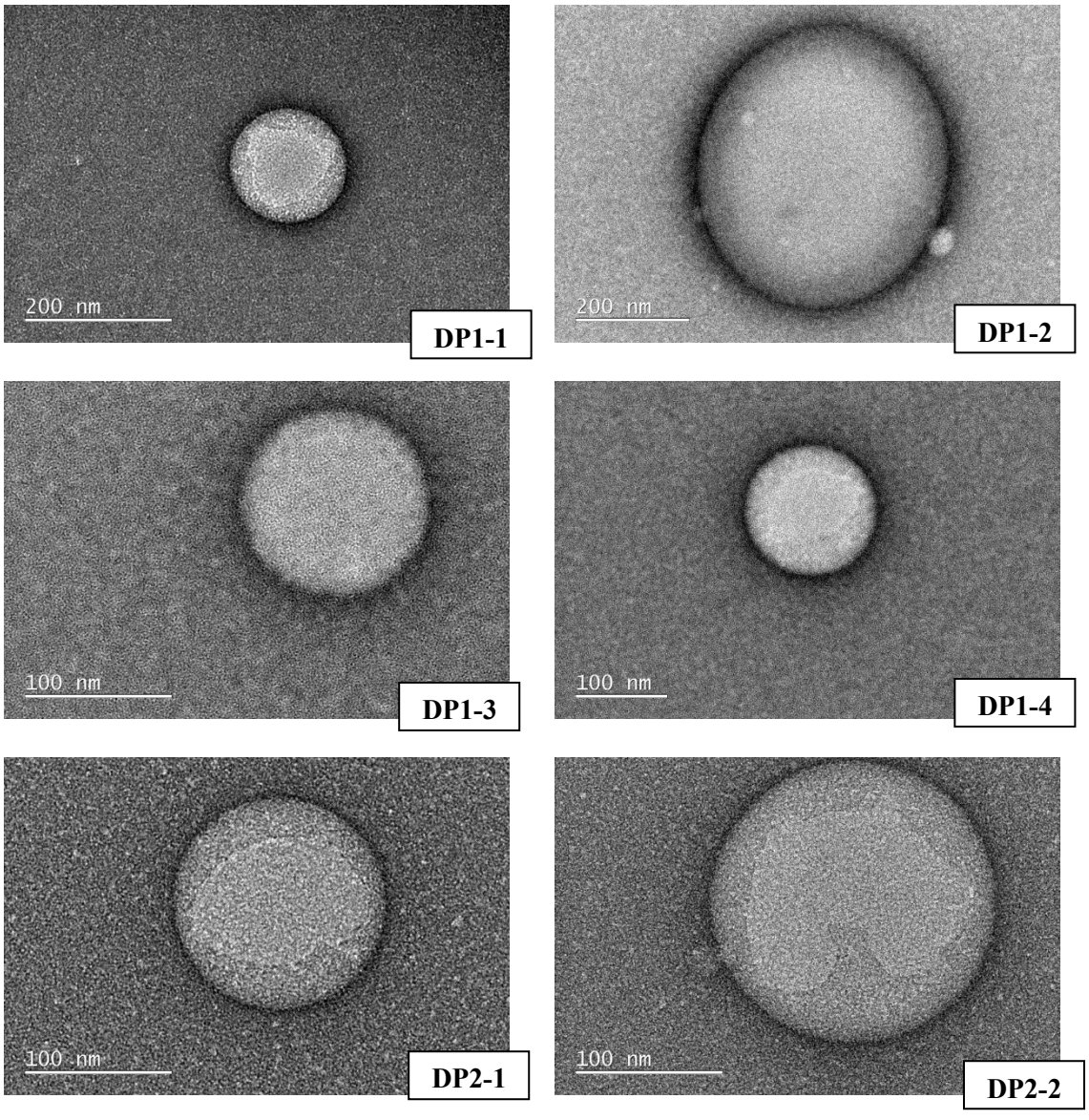
Table 6.5 Summary of DLS results of DPs in different stirring time (from 1 day to 1 week, and at 1 month), the polymers were dissolved in PBS, the concentration is 10 mg mL^{-1}.

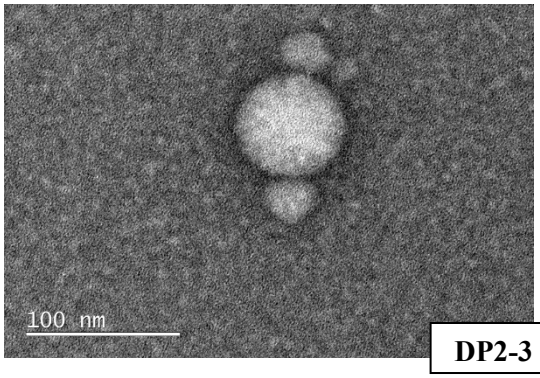
No.	Polymer Chemical Structure	Stirring Time															
		Day 1				Day 2				Day 3				Day 4			
		Max Peaks (nm) (by intensity) (± 1 nm)		Max Peaks (nm) (by number) (± 1 nm)	PDI	Max Peaks (nm) (by intensity) (± 1 nm)		Max Diameter (nm) (by number) (± 1 nm)	PDI	Max Peaks (nm) (by intensity) (± 1 nm)		Max Peaks (nm) (by number) (± 1 nm)	PDI	Max Peaks (nm) (by intensity) (± 1 nm)		Max Peaks (nm) (by number) (± 1 nm)	PDI
		Peak 1	Peak 2	Peak 1		Peak 1	Peak 2	Peak 1		Peak 1	Peak 2	Peak 1		Peak 1	Peak 2	Peak 1	
DP1	P_{12}-*b*-(D_4-*co*-B_6)-*b*-T_{12}	15.7	255	13.5	0.607	15.7	255	11.7	0.682	15.7	255	11.7	0.668	15.7	255	11.7	1
DP2	P_{10}-*b*-(D_7-*co*-B_9)-*b*-T_{10}	15.7	255	11.7	0.642	15.7	255	11.7	0.676	15.7	255	13.5	0.669	15.7	255	13.5	0.650
DP3	P_9-*b*-(D_9-*co*-B_{12})-*b*-T_9	21.0	531	18.2	0.651	21.0	531	18.2	0.608	21.0	531	18.2	0.659	21.0	615	18.2	0.637
DP4	P_7-*b*-(D_{12}-*co*-B_{15})-*b*-T_7	21.0	295	15.7	0.669	21.0	255	13.5	0.520	21.0	255	13.5	0.604	21.0	255	13.5	0.475
DP5	P_6-*b*-(D_{14}-*co*-B_{19})-*b*-T_6	58.8	396	50.7	0.856	68.1	396	50.7	0.651	91.3	531	68.1	0.794	37.8	58.8	0.965	0.652
DP6	P_4-*b*-(D_{17}-*co*-B_{22})-*b*-T_4	142	955	106	0.550	122	955	91.3	0.578	122	825	78.8	0.507	N/A	1110	68.1	0.504

No.	Polymer Chemical Structure	Stirring Time															
		Day 5				Day 6				Day 7				1 month			
		Max Peaks (nm) (by intensity) (± 1 nm)		Max Peaks (nm) (by number) (± 1 nm)	PDI	Max Peaks (nm) (by intensity) (± 1 nm)		Max Peaks (nm) (by number) (± 1 nm)	PDI	Max Peaks (nm) (by intensity) (± 1 nm)		Max Peaks (nm) (by number) (± 1 nm)	PDI	Max Peaks (nm) (by intensity) (± 1 nm)		Max Peaks (nm) (by number) (± 1 nm)	PDI
		Peak 1	Peak 2	Peak 1		Peak 1	Peak 2	Peak 1		Peak 1	Peak 2	Peak 1		Peak 1	Peak 2	Peak 1	
DP1	P_{12}-*b*-(D_4-*co*-B_6)-*b*-T_{12}	15.7	255	11.7	0.960	15.7	220	11.7	1	15.7	220	11.7	1	15.7	220	11.7	1
DP2	P_{10}-*b*-(D_7-*co*-B_9)-*b*-T_{10}	15.7	220	13.5	0.629	15.7	220	11.7	0.621	15.7	220	11.7	0.624	18.2	205	13.5	0.776
DP3	P_9-*b*-(D_9-*co*-B_{12})-*b*-T_9	N/A	531	15.7	0.571	N/A	615	15.7	0.637	N/A	531	15.7	0.599	18.2	342	13.5	0.990
DP4	P_7-*b*-(D_{12}-*co*-B_{15})-*b*-T_7	21	255	13.5	0.460	21	295	13.5	0.453	21	295	11.7	0.439	21	235	11.7	0.426
DP5	P_6-*b*-(D_{14}-*co*-B_{19})-*b*-T_6	106	3580	58.8	1	220	5560	24.4	1	58.8	2550	50.7	1	24.4	2550	18.2	0.863
DP6	P_4-*b*-(D_{17}-*co*-B_{22})-*b*-T_4	220	1280	58.8	0.572	142	1110	91.3	0.559	190	1280	106	0.533	142	1110	106	1

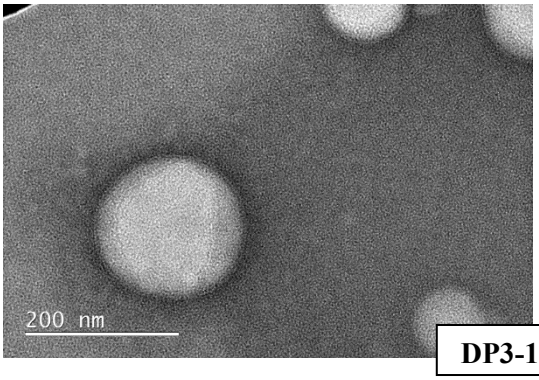
6.3.2 TEM

The shape, size and size distribution of the nanoparticles formed in aqueous solution by dissolution of polymers can be easily observed by TEM. Polymer solutions have been kept stirring for 1 week before loading onto the carbon-coated copper grids, and negative staining is applied to increase the contrast between polymeric particles and the carbon films. The TEM images of DP1 to DP6 are listed as following:

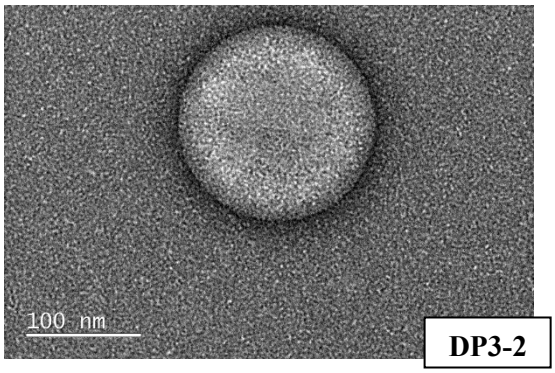




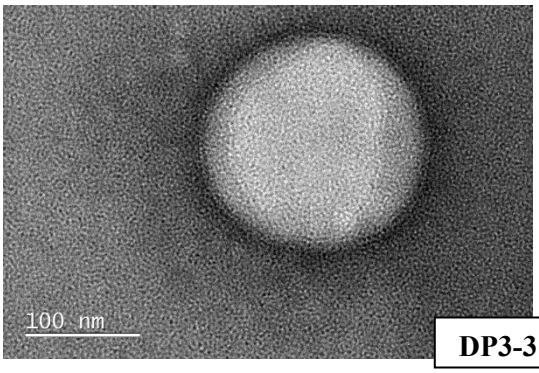
DP2-3



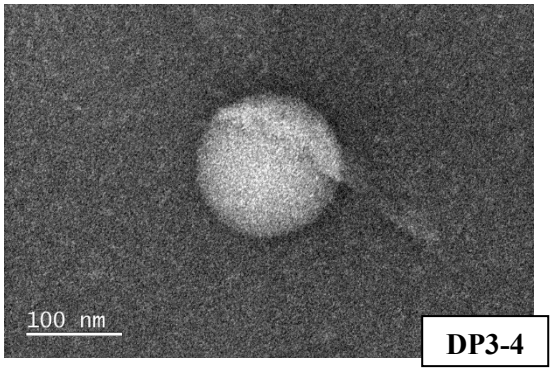
DP3-1



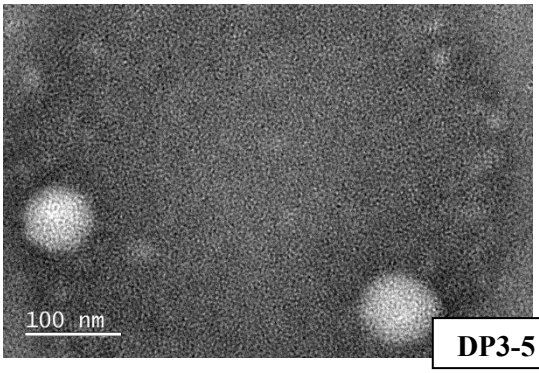
DP3-2



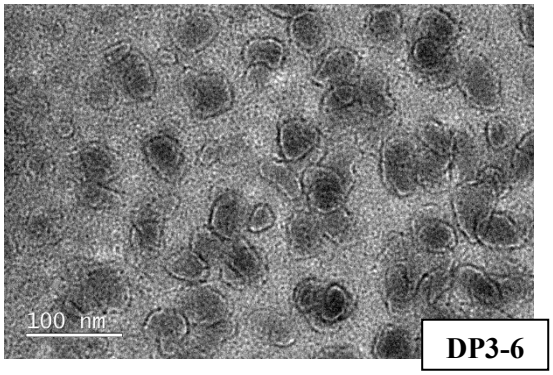
DP3-3



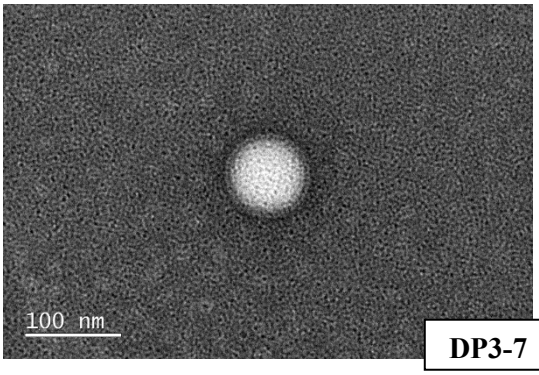
DP3-4



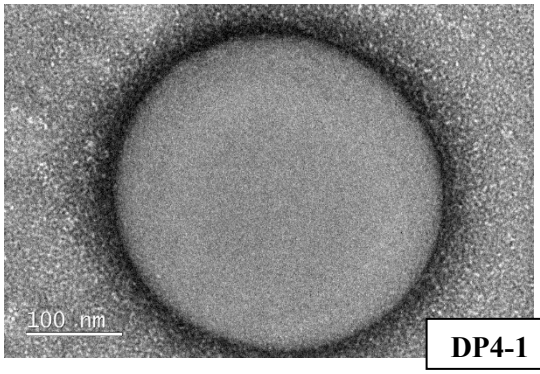
DP3-5



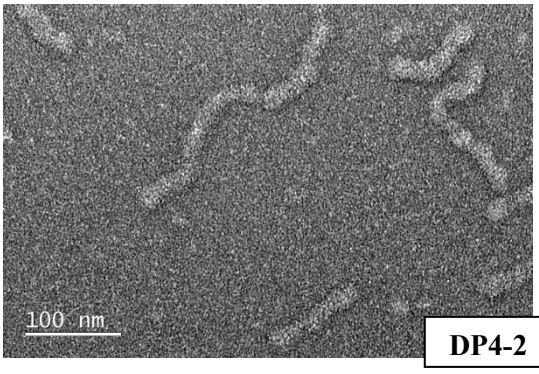
DP3-6



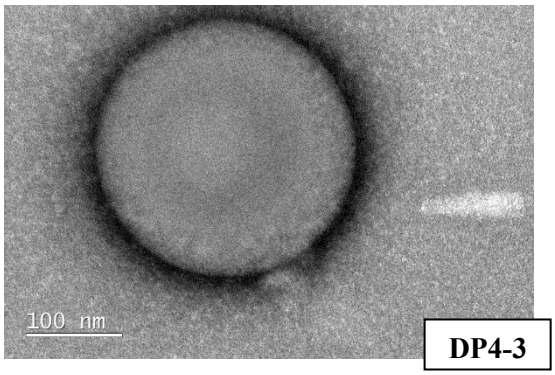
DP3-7



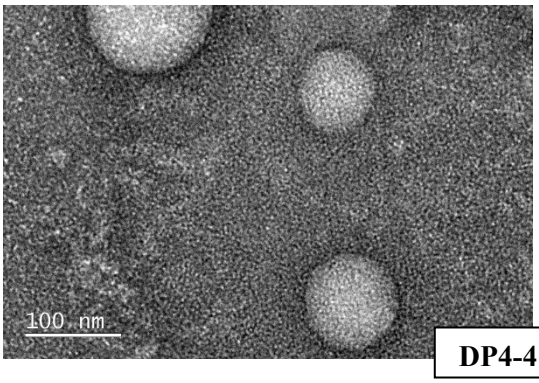
DP4-1



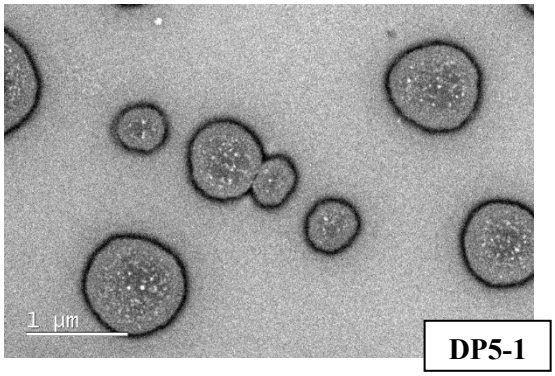
DP4-2



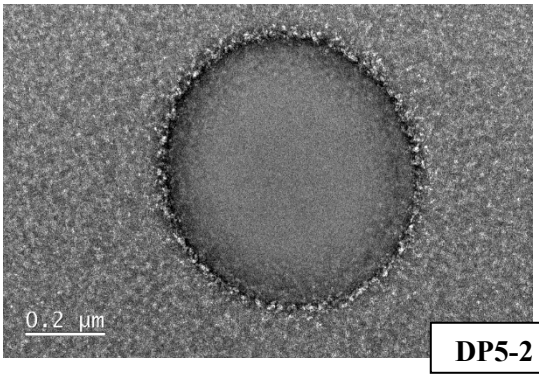
DP4-3



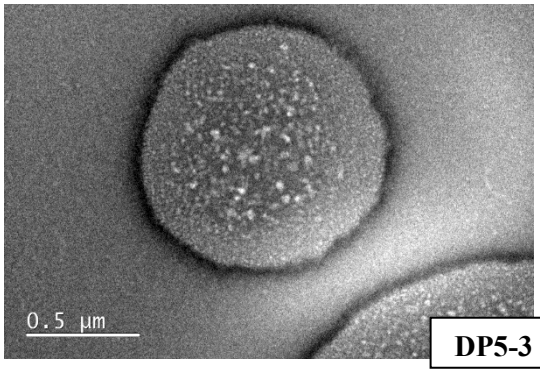
DP4-4



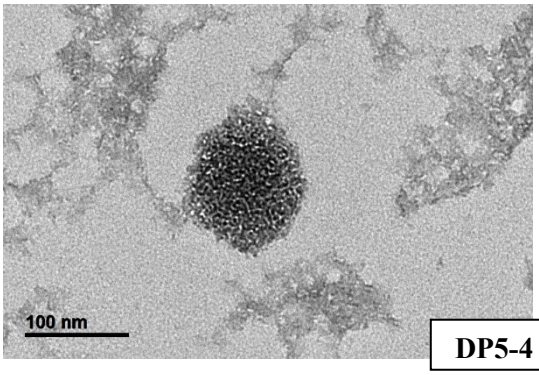
DP5-1



DP5-2



DP5-3



DP5-4

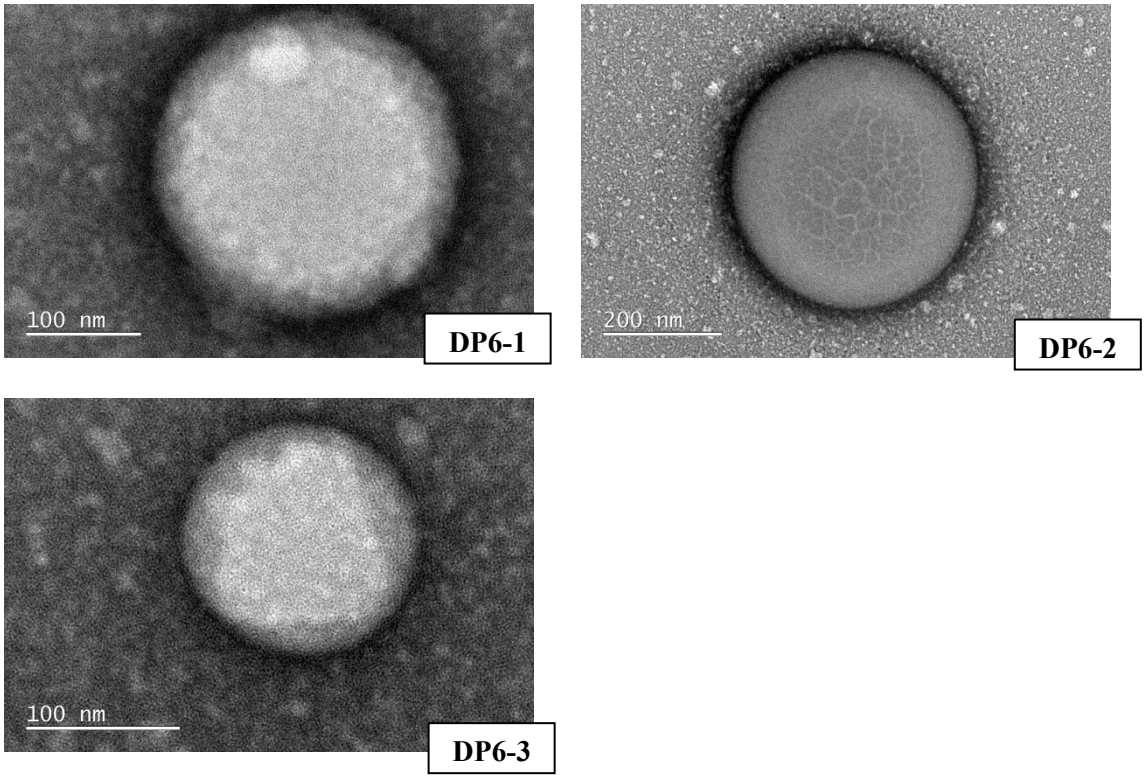


Figure 6.7 TEM images of structures formed by DPs. The solutions were prepared via film rehydration in PBS with a polymer concentration of 10 mg mL^{-1}. Uranyl acetate was used as a negative staining agent.

The above images exemplify most polymers have formed polymersomes while other structures are also observed. Some of the polymers form small micelles, DP4 even has worm-like micelles. It is notable that DP5 forms different structures than others, as spherical coacervates are observed rather than polymersomes, and the sizes of which are a few times larger than polymersomes formed by other polymers. Interestingly, the particles observed in TEM for DP5 explains the precipitation during DLS measurements.

Although large particles are easier to distinguish and observe, small structures should still not be neglected, and this is in agreement with the hydrodynamic diameters obtained by DLS (by number). A rough estimation of the size of the polymersomes has been assisted by ImageJ to analyse the TEM images. The results are listed in the following **Table 6.6**. These results have been obtained by measuring the contour length of the polymersomes, however, the number of vesicles analysed have been subject to

the images taken. From DP1 to DP6, the hydrophobicity of copolymers increases, the average vesicle size has an increasing trend (apart from DP5 since it forms coacervates). From the table, it is clearly shown that the average sizes of the polymersomes observed are located in the range of 90 to 300 nm while the maximum diameters are in 190 to 509 nm.

Table 6.6 Diameters of large vesicles measured by ImageJ.

Polymer	Theoretical Polymer Structure	Average Vesicle Diameter (±1 nm)	Max Vesicle Diameter (±1 nm)
DP1	$PEGMA_{12}$-*b*-($DEAEMA_4$-*co*-$BuMA_6$)-*b*-$PEGMA_{12}$	100	509
DP2	$PEGMA_{10}$-*b*-($DEAEMA_7$-*co*-$BuMA_9$)-*b*-$PEGMA_{10}$	92	191
DP3	$PEGMA_9$-*b*-($DEAEMA_9$-*co*-$BuMA_{12}$)-*b*-$PEGMA_9$	135	190
DP4	$PEGMA_7$-*b*-($DEAEMA_{12}$-*co*-$BuMA_{15}$)-*b*-$PEGMA_7$	186	341
DP5	$PEGMA_6$-*b*-($DEAEMA_{14}$-*co*-$BuMA_{19}$)-*b*-$PEGMA_6$	715	1022
DP6	$PEGMA_4$-*b*-($DEAEMA_{17}$-*co*-$BuMA_{22}$)-*b*-$PEGMA_4$	291	445

6.4 Encapsulation and Release of Dyes

According to **Chapter 1**, drug delivery is the most common application of polymersomes in biomedical fields. To mimic the encapsulation and release behaviour of drugs *in vivo*, dye molecules are chosen to be the candidates to represent drugs since their fluorescence can be easily detected and traced. Several dye candidates have been tried in this work:

Curcumin displays green fluorescence under UV light, it has been applied to previous study on drug release of polymer vesicles.[16] Curcumin has been mixed with Tween 80

(a detergent that helps curcumin to dissolve in PBS) and dissolved in PBS. However, it has been proved that curcumin molecules cannot efficiently pass through the membrane of the dialysis tube. In this way, dissociative curcumin molecules cannot be excluded from the encapsulated molecules, thus, curcumin is not preferable in this experiment. The same reason stands valid for rhodamine B and calcein. The two chemicals are more soluble in aqueous solutions, and they have often been used as fluorescent dyes in biomedical fields. However, the poor permeability through the dialysis tube limits their applications in this experiment.

Doxorubicin is a chemotherapy medication used to treat cancer.[17,18] DOX·HCl is the hydrochloride salt of doxorubicin, it is more soluble in aqueous solution than the original form. Doxorubicin is known to be fluorescent, although its fluorescence can be affected by various factors such as the pH of the environment, solvent dielectric constant. In the experiment of dialysis, it is exciting to find that doxorubicin can penetrate the dialysis membrane efficiently. However, the low solubility in PBS becomes the decisive reason of giving up this chemical: without constant stirring, the dissolved doxorubicin molecules tend to precipitate inside the dialysis tube, the precipitation cannot go through the membrane, leading to incorrect results. If decrease the concentration of doxorubicin to avoid precipitation, the fluorescence will be too low to detect.

Sodium fluorescein has been widely used as a fluorescent tracer, especially in microscopy. When dissolved in water, sodium fluorescein gives a strong signal in fluorometer even at a low concentration. Moreover, sodium fluorescein molecules can easily penetrate the dialysis membrane in a short time. These two features make sodium fluorescein an excellent chemical for the encapsulation and release assays.

In conclusion, among all these five chemicals, sodium fluorescein is the only candidate that fulfils the experimental requirements.

The experiments to discover the encapsulation and release of sodium fluorescein have been conducted. Referring to a calibration curve of sodium fluorescein in PBS, the cumulative release of the dye can be studied, and the curve of final results is presented in **Figure 6.8**.

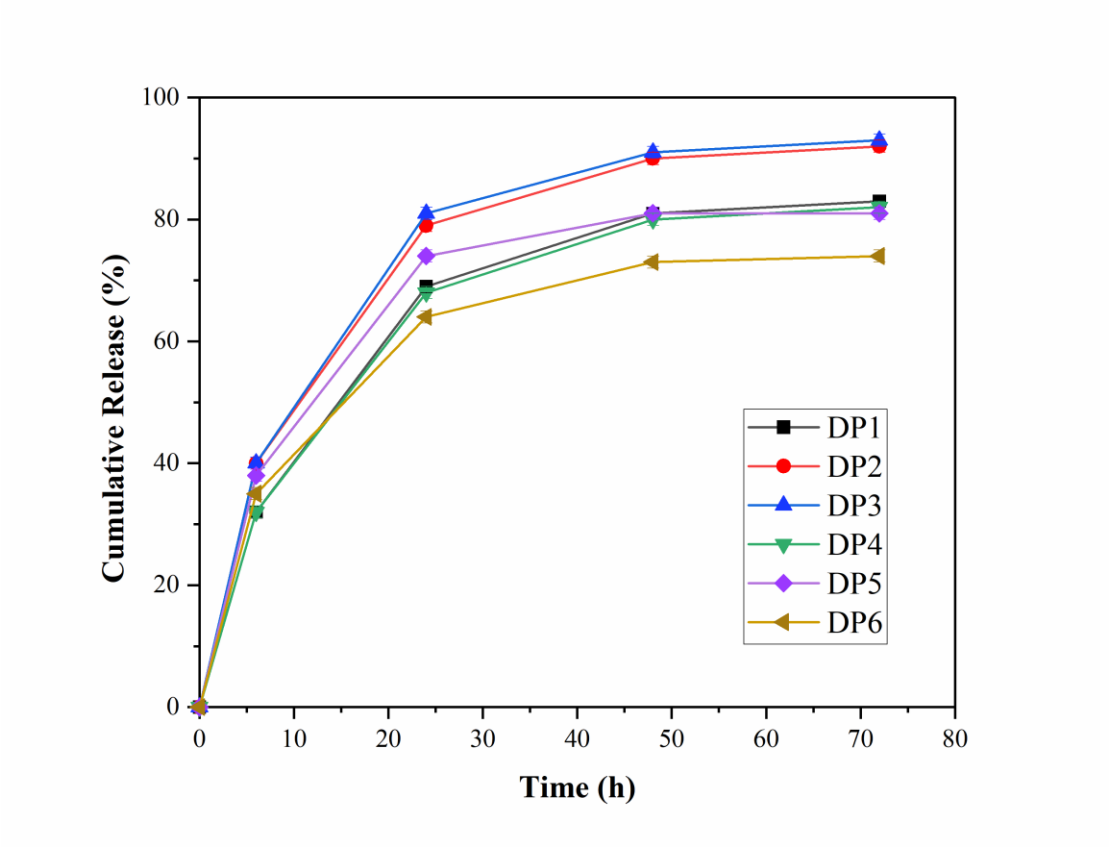


Figure 6.8 Time dependent cumulative release of sodium fluorescein by polymersomes.

Figure 6.8 illustrates the time dependent cumulative release of sodium fluorescein by polymers DP1 to DP6. The highest release exceeds 90% while the lowest gets around 70%. The shape of the curves epitomises that the release rates of all polymers decrease with time. After 6 h of stirring, all polymers have released 30 to 40% of molecules while at the end of the first day, polymers have released 60 to 81%. Between the first day and the second day, polymers only have a slight increase in release, and the curves are almost flat between the second day and the third day.

The release behaviour varies among the six polymers. DP3 and DP2 are the two polymers that release the most sodium fluorescein, while DP6 is the polymer that encapsulated the most molecules in the end. Unlike the other series of polymers, DPs do not have a linear trend between the hydrophilicity of polymers and the cumulative release of polymersomes. However, if have a closer look, except for DP1, the rest of the polymers still roughly follow a rule that the more hydrophilic the polymer is, the more sodium fluorescein it releases during the same time period (DP2 releases less

sodium fluorescein than DP3, but the results are close to each other and within the error range). Also, the hydrophilic ratios of DP2 to DP6 correspond to those of AP5 to AP1, respectively. Thus, the conclusions from **Chapter 4** are still applicable for the polymer series in this chapter,[19] but only for the polymers that have a hydrophilic block weight ratio of 30 to 70% (DP2 to DP6).

DP1 has a very high hydrophilic block weight ratio, which is 80%. It is not common to have that hydrophilic copolymer in the formation of polymersomes. However, DLS and TEM both verify the presence of polymersomes. In TEM, the sizes of polymersomes formed by DP1 are exceptionally larger than those of DP2, DP3 and DP4, which is also surprising.

If compare the TEM and release results, it is also notable that the sizes of polymersomes have a relationship with the release of sodium fluorescein, DP6 forms the largest polymersomes among all polymers, whereas it has the least release of molecules.

6.5 SANS

SANS experiments have been applied to polymer solutions of DPs. Based on the results from DLS, large polymersomes and small micelles were both detected in the solution; thus, the SANS results were analysed via software SasView by the combination of two models: Sphere and Vesicle. Sphere model corresponds to micelles formed in solution whereas vesicle model refers to polymersomes.

The fitting graphs of this technique can be found in **Figure A4.1 – A4.6**, **Appendix**, and results are listed in **Table 6.7**. Apparently, according to the aim of the thesis in **Chapter 2**, DP5 and DP6 are not preferable since they form particles (polymersomes or aggregates) close to 1000 nm in diameter, which is considered too big for biomedical applications. This finding is in agreement with DLS and TEM results.

On contrary, DP1, DP2, DP3 and DP4 all have polymersomes whose average sizes are below 200 nm, and these polymers are promising to form polymersomes in desirable size range. Moreover, SANS experiments confirmed the presence of hollow spherical structures in the solutions as it also gave membrane thickness data.

Table 6.7 Summary of SANS results. The concentration of the polymer solutions is 10 mg mL^{-1} and the polymers were dissolved in PBS.

No.	Size of Micelles in Diameter (nm)	Size of Polymersomes in Diameter (nm)	Thickness of Polymersome Membrane (nm)
DP1	10.8	200.0	0.26
DP2	10.4	42.6	12.8
DP3	13.6	187.4	7.1
DP4	14.4	74.4	14.8
DP5	18.4	801.2	10.7
DP6	14.2	981.2	10.2

6.6 Conclusions

In this chapter, six ABA triblock copolymers PEGMA-*b*-(DEAEMA-*co*-BuMA)-*b*-PEGMA have been synthesised successfully using GTP. The MM of the copolymers has been targeted to 9100 g mol^{-1}, and the composition of the copolymers was varied to investigate the composition effect on fabrication of polymersomes and the properties of polymersomes. Several conclusions of this chapter are listed as following:

1. All six triblock copolymers have been synthesised successfully; the MMs of the polymersomes are in desirable range and $Đ$ is sufficiently close to 1. The compositions of copolymers have been verified by ^{1}H NMR.

2. pK_a and cloud point of polymers are affected by polymer composition: they both increase with the increase of hydrophilic weight ratio of copolymers; this trend is in agreement with previously reported work in our research group.

3. Film rehydration method has been proven to form larger vesicles than bulk hydration method. DI water and PBS as different solvents do not have a huge difference in the size of formed particles. DP1 to DP4 form particles with similar sizes from 1 day stirring to 1 month stirring, whereas DP5 and DP6 are affected by stirring time.

4. TEM images have been taken for solutions of DPs. The images prove that in

polymer solutions, various structures can be formed, including small micelles, polymersomes, worm-like structures and spherical coacervates. DP5 forms large spherical coacervates rather than polymersomes and the sizes of coacervates are obviously larger than any other structures. This finding is in agreement with DLS results of DP5.

5. The cumulative release of model drug sodium fluorescein has been studied. The composition of the polymers has an impact on the release of drugs, the most hydrophobic polymer DP6 has the least release of sodium fluorescein.
6. SANS results have proven the presence of micelles and polymersomes (and larger particles) in polymer solutions of DPs.
7. It can be concluded that DP1, DP2, DP3 and DP4 are all good candidates for forming polymersomes; however, DP5 and DP6 form particles that are too large for biomedical applications.

REFERENCE

1. Lutz, J. F., Akdemir, Ö., & Hoth, A. (2006). Point by point comparison of two thermosensitive polymers exhibiting a similar LCST: is the age of poly (NIPAM) over?. *Journal of the American Chemical Society*, *128*(40), 13046-13047.

2. Lutz, J. F., Weichenhan, K., Akdemir, Ö., & Hoth, A. (2007). About the phase transitions in aqueous solutions of thermoresponsive copolymers and hydrogels based on 2-(2-methoxyethoxy) ethyl methacrylate and oligo (ethylene glycol) methacrylate. *Macromolecules*, *40*(7), 2503-2508.

3. Sefcik, L. S., Kaminski, A., Ling, K., Laschewsky, A., Lutz, J. F., & Wischerhoff, E. (2013). Effects of PEG-based thermoresponsive polymer brushes on fibroblast spreading and gene expression. *Cellular and Molecular Bioengineering*, *6*(3), 287-298.

4. Badi, N., & Lutz, J. F. (2009). PEG-based thermogels: applicability in physiological media. *Journal of Controlled Release*, *140*(3), 224-229.

5. Lutz, J. F., & Hoth, A. (2006). Preparation of ideal PEG analogues with a tunable thermosensitivity by controlled radical copolymerization of 2-(2-methoxyethoxy) ethyl methacrylate and oligo (ethylene glycol) methacrylate. *Macromolecules*, *39*(2), 893-896.

6. Fechler, N., Badi, N., Schade, K., Pfeifer, S., & Lutz, J. F. (2009). Thermogelation of PEG-based macromolecules of controlled architecture. *Macromolecules*, *42*(1), 33-36.

7. Buller, J., Laschewsky, A., Lutz, J. F., & Wischerhoff, E. (2011). Tuning the lower critical solution temperature of thermoresponsive polymers by biospecific recognition. *Polymer Chemistry*, *2*(7), 1486-1489.

8. Constantinou, A. P.; Georgiou, T. K. Thermoresponsive gels based on ABC triblock copolymers: effect of the length of the PEG side group. Polym. Chem. 2016, 7, 2045-2056.

9. Ward, M. A., & Georgiou, T. K. (2010). Thermoresponsive terpolymers based on methacrylate monomers: Effect of architecture and composition. *Journal of Polymer Science Part A: Polymer Chemistry*, *48*(4), 775-783.

10. Ward, M. A., & Georgiou, T. K. (2013). Multicompartment thermoresponsive gels: does the length of the hydrophobic side group matter?. *Polymer Chemistry*, *4*(6), 1893-1902.

11. Constantinou, A. P., Marie-Sainte, U., Peng, L., Carroll, D. R., McGilvery, C. M., Dunlop, I. E., & Georgiou, T. K. (2019). Effect of block copolymer architecture and composition on gold nanoparticle fabrication. *Polymer Chemistry*, *10*(34), 4637-4642.

12. Ward, M. A., & Georgiou, T. K. (2012). Thermoresponsive triblock copolymers based on methacrylate monomers: effect of molecular weight and composition. *Soft Matter*, *8*(9), 2737-2745.

13. Georgiou, T. K., Patrickios, C. S., Groh, P. W., & Iván, B. (2007). Amphiphilic model conetworks of polyisobutylene methacrylate and 2-(dimethylamino) ethyl methacrylate prepared by the combination of quasiliving carbocationic and group

transfer polymerizations. *Macromolecules*, *40*(7), 2335-2343.

14. Philippova, O. E., Hourdet, D., Audebert, R., & Khokhlov, A. R. (1997). pH-responsive gels of hydrophobically modified poly (acrylic acid). *Macromolecules*, *30*(26), 8278-8285.

15. Triftaridou, A. I., Hadjiyannakou, S. C., Vamvakaki, M., & Patrickios, C. S. (2002). Synthesis, characterization, and modeling of cationic amphiphilic model hydrogels: Effects of polymer composition and architecture. *Macromolecules*, *35*(7), 2506-2513.

16. Banerjee, S. L., Samanta, S., Sarkar, S., & Singha, N. K. (2020). A self-healable and antifouling hydrogel based on PDMS centered ABA tri-block copolymer polymersomes: a potential material for therapeutic contact lenses. *Journal of Materials Chemistry B*, *8*(2), 226-243.

17. Du, Y., Chen, W., Zheng, M., Meng, F., & Zhong, Z. (2012). pH-sensitive degradable chimaeric polymersomes for the intracellular release of doxorubicin hydrochloride. *Biomaterials*, *33*(29), 7291-7299.

18. Alibolandi, M., Ramezani, M., Abnous, K., Sadeghi, F., & Hadizadeh, F. (2015). Comparative evaluation of polymersome versus micelle structures as vehicles for the controlled release of drugs. *Journal of Nanoparticle Research*, *17*(2), 1-16.

19. Zhang, X., Contini, C., Constantinou, A. P., Doutch, J. J., & Georgiou, T. K. (2021). How does the hydrophobic content of methacrylate ABA triblock copolymers affect polymersome formation?. *Journal of Polymer Science*.

CHAPTER 7 CONCLUSIONS AND FUTURE WORK

7.1 Conclusions

In this thesis, three studies on polymersomes based on ABA (hydrophilic-hydrophobic-hydrophilic) triblock methacrylate copolymers have been performed. To be specific, three families of ABA amphiphilic block copolymers, which are TEGMA-*b*-DEAEMA-*b*-TEGMA, TEGEMA-*b*-(DEAEMA-*co*-BuMA)-*b*-TEGEMA and PEGMA-*b*-(DEAEMA-*co*-BuMA)-*b*-PEGMA have been synthesised and their MM, *Đ*, and their properties in aqueous solution have been determined. Furthermore, polymer structures, mainly polymersomes, have been fabricated via film rehydration method, and the morphologies of particles and particle size distribution have been studied by DLS and TEM, and verified by SANS (in **Chapter 6**). The main findings of this thesis have been listed as following:

1. In total, seventeen copolymers have been synthesised using GTP, and their MM, *Đ*, compositions have been confirmed by GPC and ^{1}H NMR, indicating they are all satisfactory for the purpose of this study.

2. The methacrylate-based copolymers in this thesis have never been synthesised before and they have been proven efficient in fabrication of polymersomes. Moreover, their thermoresponsiveness and pH responsiveness have been confirmed.

3. Polymer composition has an impact on the softness, pK_a, cloud point of the polymers; it also affects the polymersome formation, for instance, polymers with high hydrophilicity cannot form polymersomes at low pH (6) although they can form polymersomes normally at higher pH (7) and the original pH of polymer solutions. Moreover, composition can affect the size and size distribution of particles in polymer solutions. Polymers with similar MM but different compositions have distinct results in terms of particle size and size distribution, and this has been verified by DLS and TEM. In addition, polymer compositions can also affect the drug release of polymersomes. The most hydrophobic polymers tend to have lowest cumulative release of the model drug (sodium fluorescein).

4. Polymers that have high hydrophilic weight ratio (70% to 80%) have been proven to form polymersomes by DLS, TEM and SANS. Very few previous works reported polymersomes formed by polymers with high hydrophilicity and it can supplement the current theory on polymersome formation.

5. Various polymer structures have been observed by TEM including polymersomes, spherical micelles, worm-like micelles, spherical coacervates, indicating that in aqueous solutions different configuration of polymers chains are present at the same time.

6. Film rehydration method has been proven preferable to produce polymersomes rather than bulk hydration method.

7. For polymersomes formed by copolymers TEGMA-*b*-DEAEMA-*b*-TEGMA (**Chapter 4**), the membrane thickness is related to polymer composition. Polymers with more hydrophobic blocks (DEAEMA) form thicker membranes.

8. For copolymers TEGEMA-*b*-(DEAEMA-*co*-BuMA)-*b*-TEGEMA (**Chapter 5**), their hydrophobicity causes trouble in studying their properties in aqueous media. Whereas copolymers PEGMA-*b*-(DEAEMA-*co*-BuMA)-*b*-PEGMA can dissolve much better in aqueous solutions.

To summarise, self-assembly of ABA triblock methacrylate copolymers have been investigated and methacrylate-based polymersomes have the potential to be used in biomedical applications.

7.2 Future Work

1. DEAEMA has been used as (or one of) the hydrophobic monomer(s) in this thesis. However, it has shown cell toxicity in a cellular test with APs (**Figure A5.1** and **A5.2**, **Appendix**). To reduce the cell toxicity, CPs and DPs have been synthesised but more cellular tests are needed to prove if they can fulfil the requirements of biocompatibility for polymersomes. Options for other ionic hydrophobic monomers may be considered to thoroughly solve the problem.

2. Sodium fluorescein has been used as a model drug in the study of drug release of the polymersomes and it has been proven successful. Further experiments on

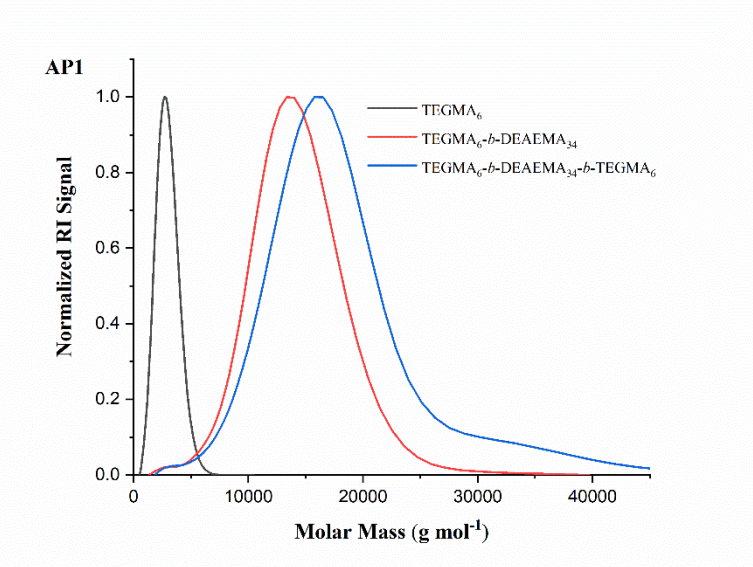
the encapsulation and release of anticancer drugs need to be conducted.

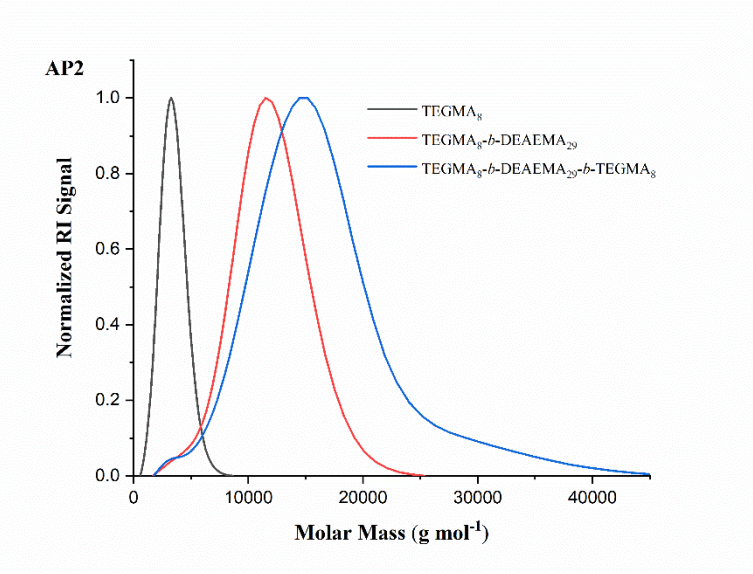
3. This thesis studies the pH-responsiveness of polymersomes, but mainly on size and size distribution. It is also interesting to study the pH-responsiveness of polymersomes on drug encapsulation and release. To be specific, it would be beneficial to prove that polymersomes tend to release encapsulated drugs in lower pH (around 5), as tumour, inflammatory tissues and intracellular compartments such as endosomes and lysosomes of cells all have mildly acidic pH. This pH-triggered release is desirable in intracellular drug delivery.

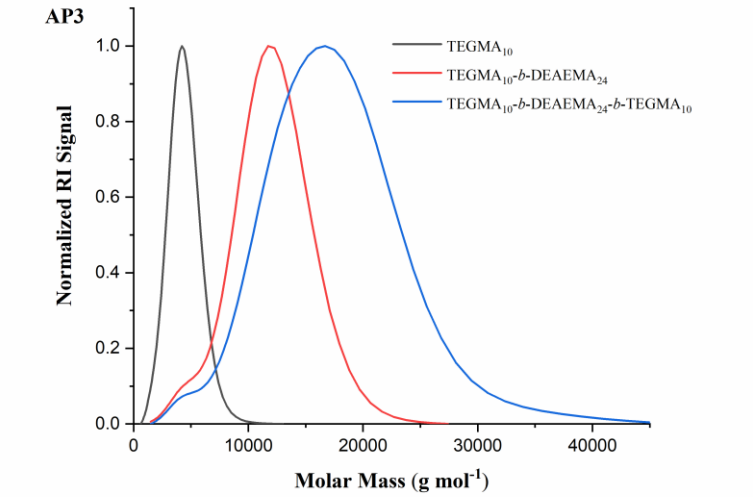
APPENDIX

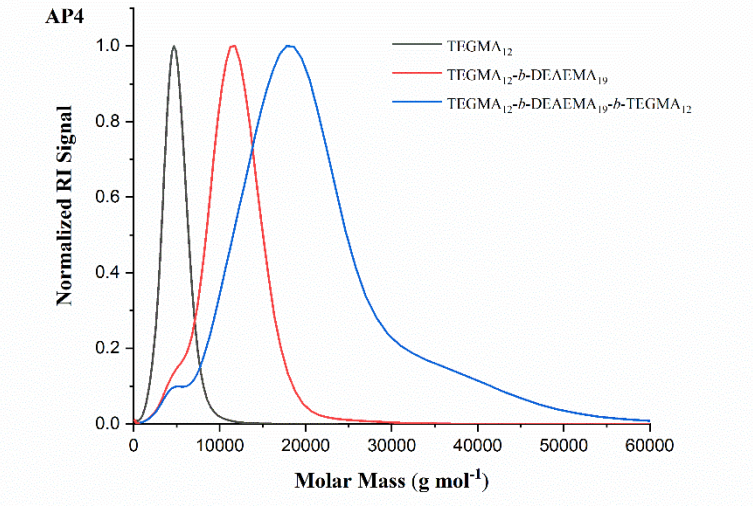
Table A1. Abbreviations, densities, MMs used for the polymerisations.

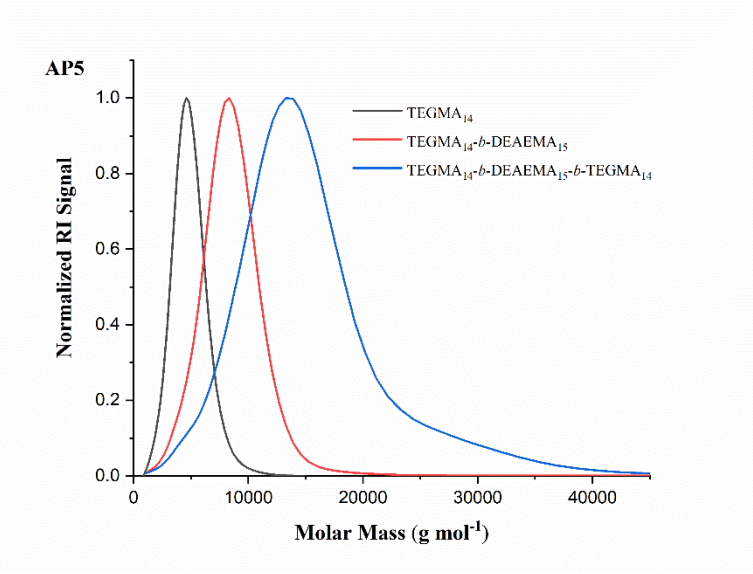
Abbreviation	Role	Density (g mL^{-1})	Molar Mass (g mL^{-1})
MTS	Initiator	0.858	174.31
TEGMA	Monomer	1.027	232.27
DEAEMA	Monomer	0.92	185.27
TEGEMA	Monomer	N/A	246.30
BuMA	Monomer	0.894	142.20
PEGMA	Monomer	1.05	300

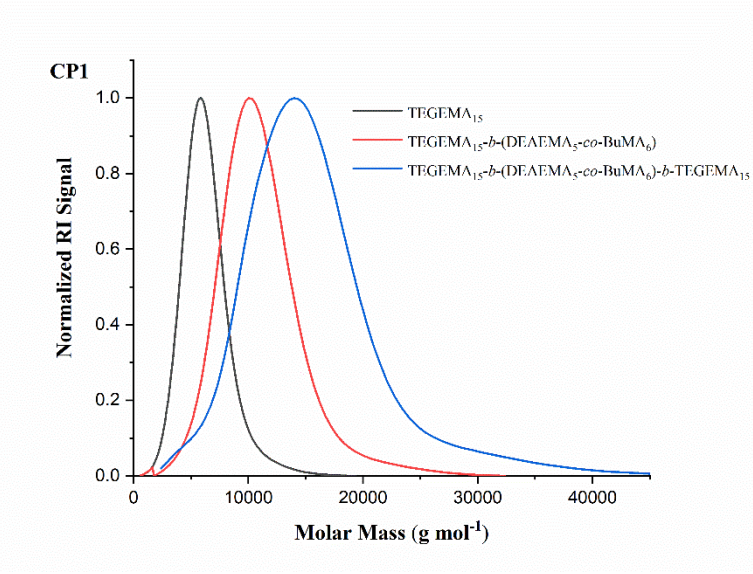


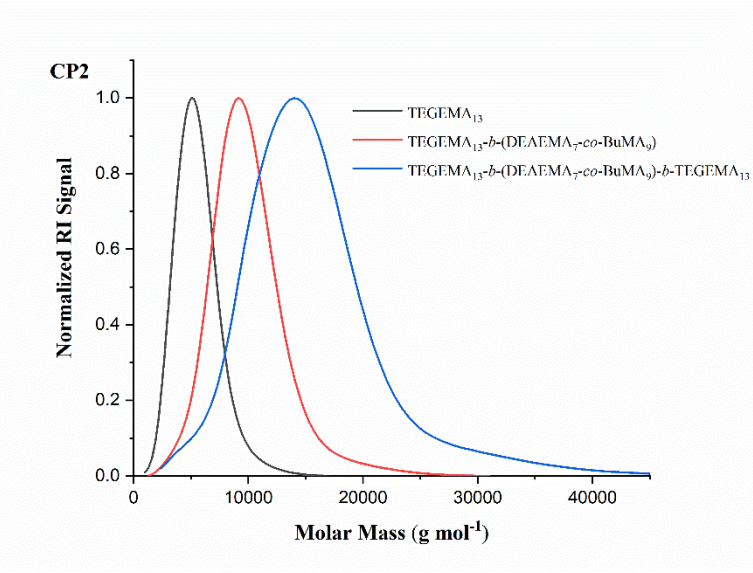

AP2
Normalized RI Signal
Molar Mass (g mol-1)
TEGMA8
TEGMA8-b-DEAEMA29
TEGMA8-b-DEAEMA29-b-TEGMA8

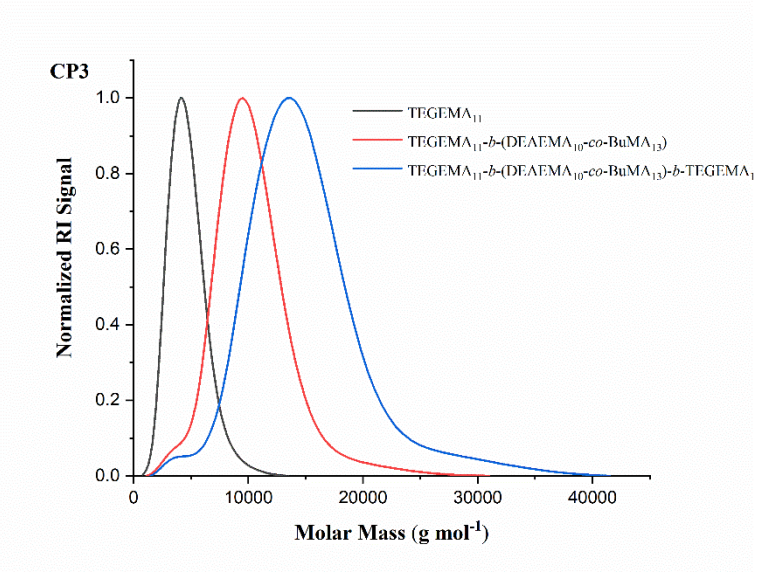

AP3
Normalized RI Signal
Molar Mass (g mol-1)
TEGMA10
TEGMA10-b-DEAEMA24
TEGMA10-b-DEAEMA24-b-TEGMA10

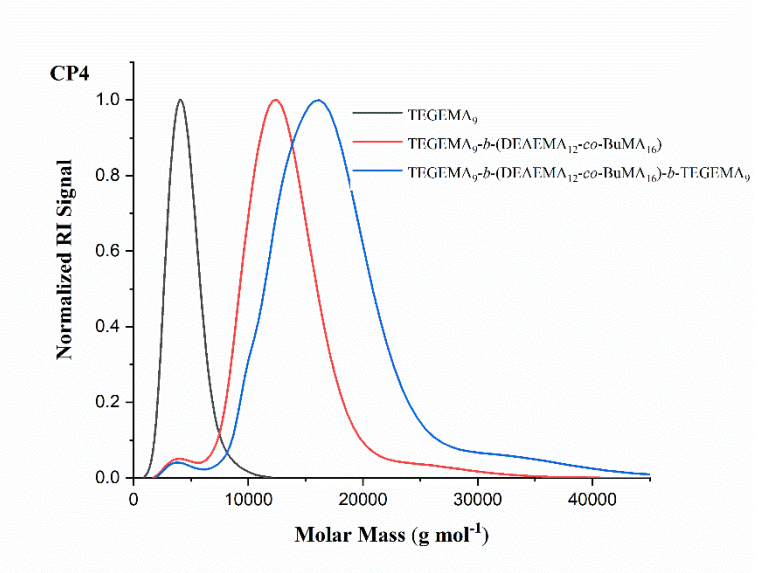

AP4
Normalized RI Signal
Molar Mass (g mol-1)
TEGMA12
TEGMA12-b-DEAEMA19
TEGMA12-b-DEAEMA19-b-TEGMA12

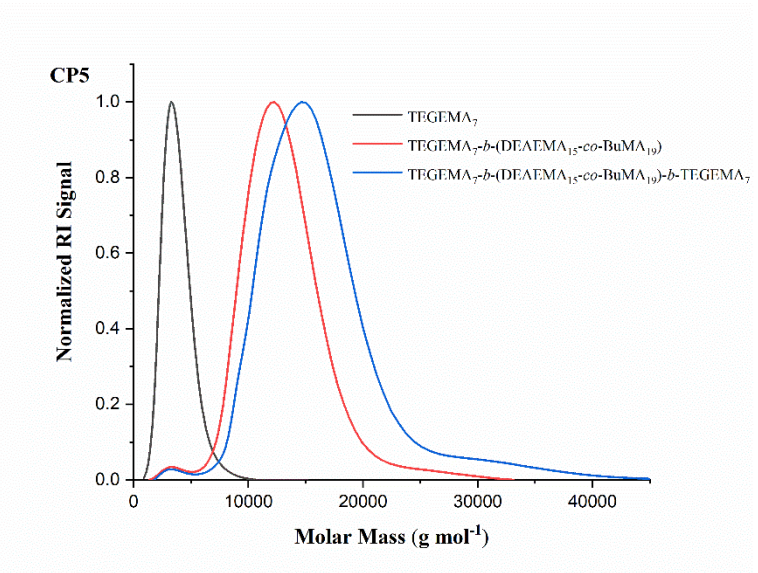

AP5
Normalized RI Signal
Molar Mass (g mol-1)
TEGMA14
TEGMA14-b-DEAEMA15
TEGMA14-b-DEAEMA15-b-TEGMA14

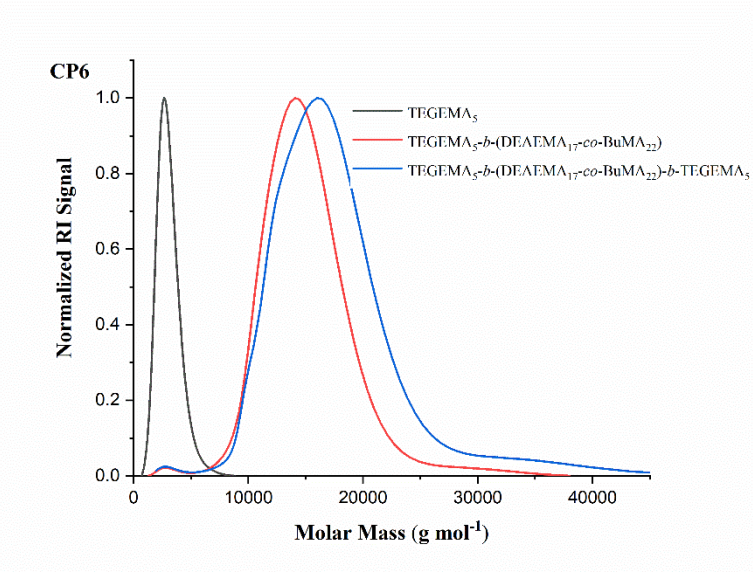

CP1
Normalized RI Signal
Molar Mass (g mol-1)
TEGEMA15
TEGEMA15-b-(DEAEMA5-co-BuMA6)
TEGEMA15-b-(DEAEMA5-co-BuMA6)-b-TEGEMA15

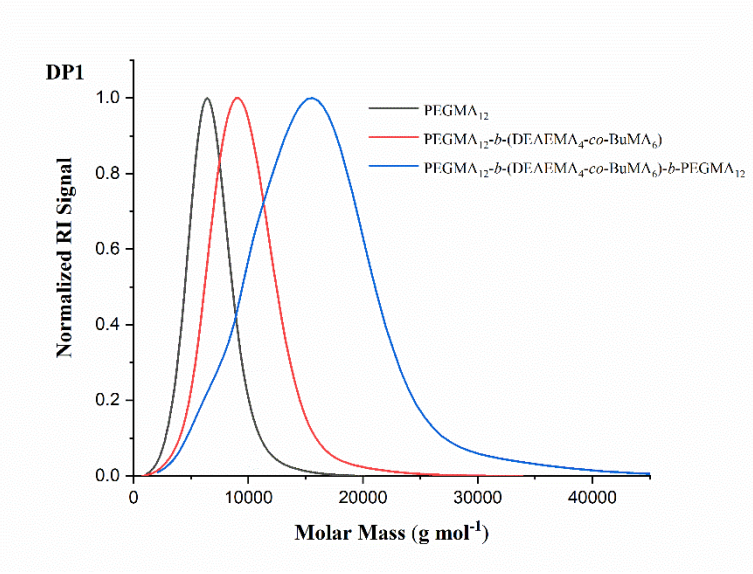

CP2
Normalized RI Signal
Molar Mass (g mol-1)
TEGEMA13
TEGEMA13-b-(DEAEMA7-co-BuMA9)
TEGEMA13-b-(DEAEMA7-co-BuMA9)-b-TEGEMA13

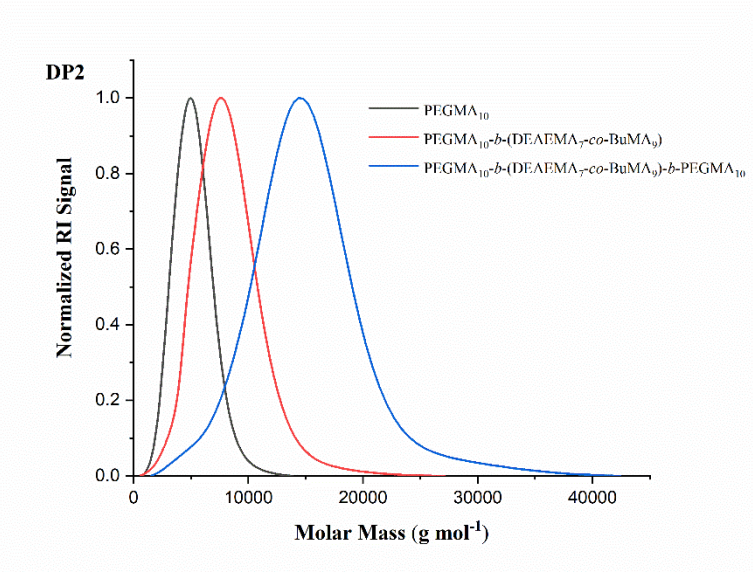

CP3
Normalized RI Signal
Molar Mass (g mol-1)
TEGEMA11
TEGEMA11-b-(DEAEMA10-co-BuMA13)
TEGEMA11-b-(DEAEMA10-co-BuMA13)-b-TEGEMA1

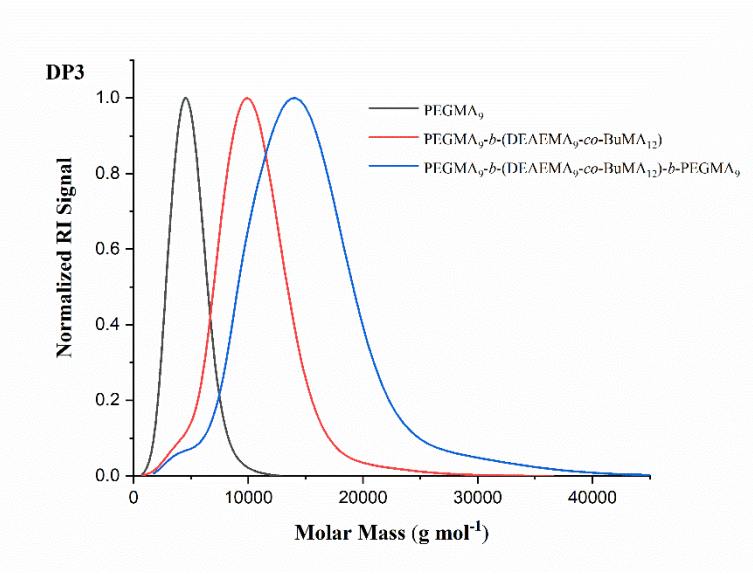

CP4
Normalized RI Signal
Molar Mass (g mol-1)
TEGEMA9
TEGEMA9-b-(DEAEMA12-co-BuMA16)
TEGEMA9-b-(DEAEMA12-co-BuMA16)-b-TEGEMA9

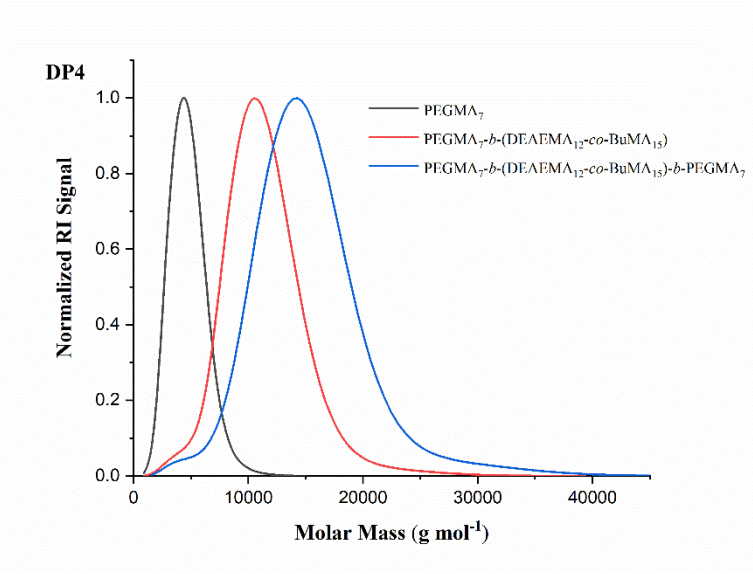

CP5
Normalized RI Signal
Molar Mass (g mol-1)
TEGEMA7
TEGEMA7-b-(DEAEMA15-co-BuMA19)
TEGEMA7-b-(DEAEMA15-co-BuMA19)-b-TEGEMA7

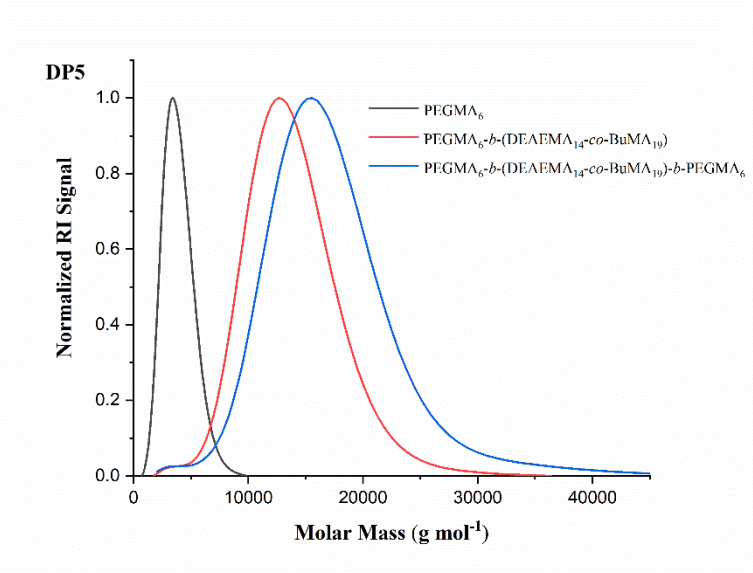

CP6
Normalized RI Signal
Molar Mass (g mol-1)
TEGEMA5
TEGEMA5-b-(DEAEMA17-co-BuMA22)
TEGEMA5-b-(DEAEMA17-co-BuMA22)-b-TEGEMA5


DP1
Normalized RI Signal
Molar Mass (g mol-1)
PEGMA12
PEGMA12-b-(DEAEMA4-co-BuMA6)
PEGMA12-b-(DEAEMA4-co-BuMA6)-b-PEGMA12


DP2
Normalized RI Signal
Molar Mass (g mol-1)
PEGMA10
PEGMA10-b-(DEAEMA7-co-BuMA9)
PEGMA10-b-(DEAEMA7-co-BuMA9)-b-PEGMA10


DP3
Normalized RI Signal
Molar Mass (g mol-1)
PEGMA9
PEGMA9-b-(DEAEMA9-co-BuMA12)
PEGMA9-b-(DEAEMA9-co-BuMA12)-b-PEGMA9


DP4
Normalized RI Signal
Molar Mass (g mol-1)
PEGMA7
PEGMA7-b-(DEAEMA12-co-BuMA15)
PEGMA7-b-(DEAEMA12-co-BuMA15)-b-PEGMA7


DP5
Normalized RI Signal
Molar Mass (g mol-1)
PEGMA6
PEGMA6-b-(DEAEMA14-co-BuMA19)
PEGMA6-b-(DEAEMA14-co-BuMA19)-b-PEGMA6

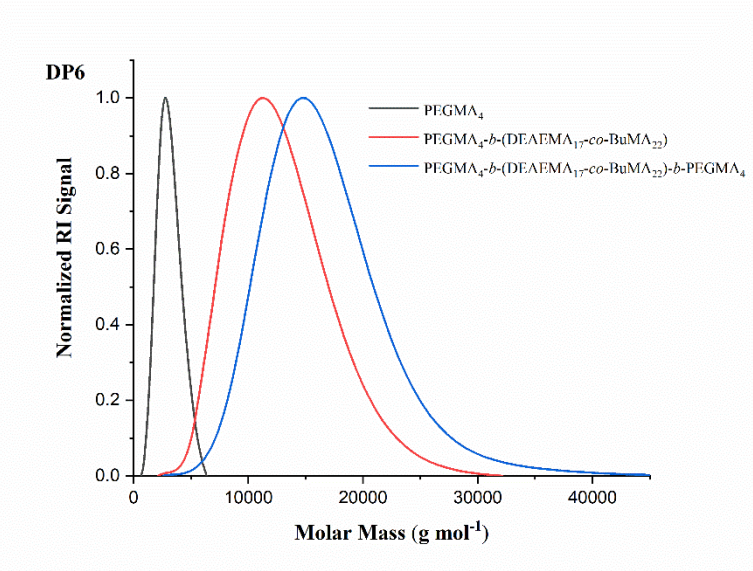


Figure A1. GPC chromatograms of AP, CP and DP polymers and their precursors.

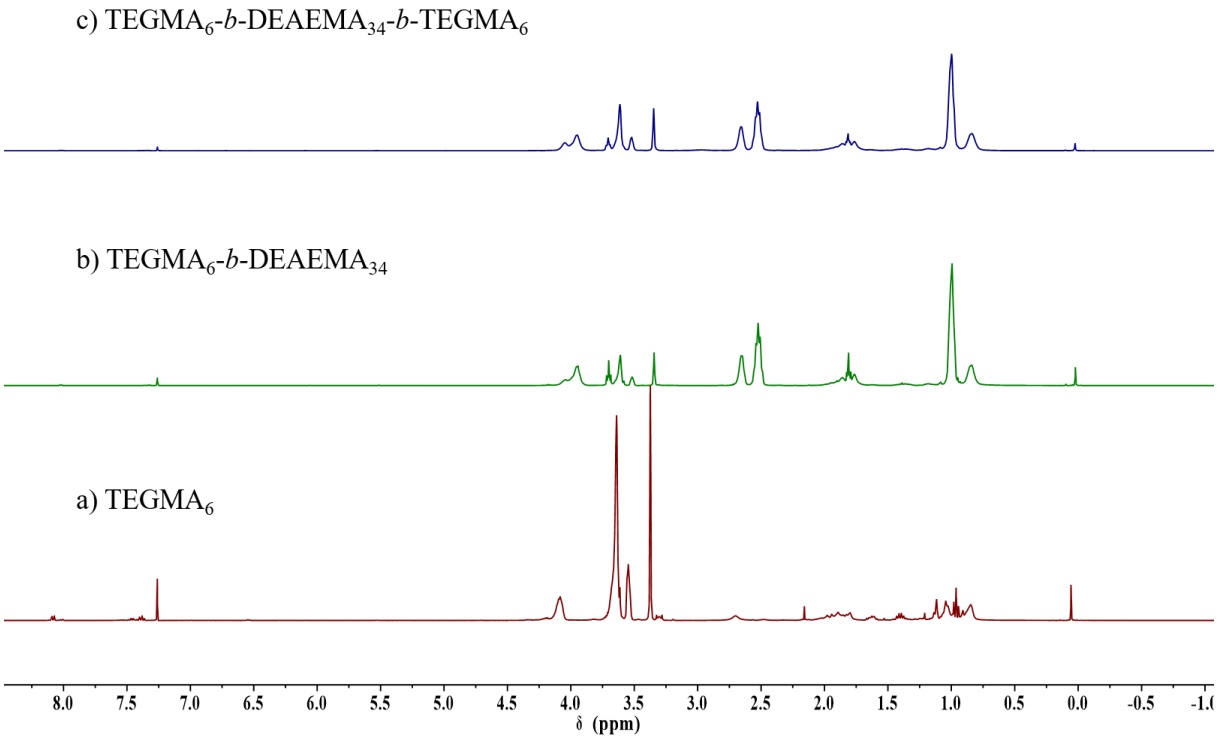


Figure A2.1: ^{1}H NMR spectra of a) $TEGMA_6$ homopolymer in red, b) $TEGMA_6$-*b*-$DEAEMA_{34}$ diblock precursor in green and c) $TEGMA_6$-*b*-$DEAEMA_{34}$-*b*-$TEGMA_6$ triblock copolymer in blue. The polymer is AP1.

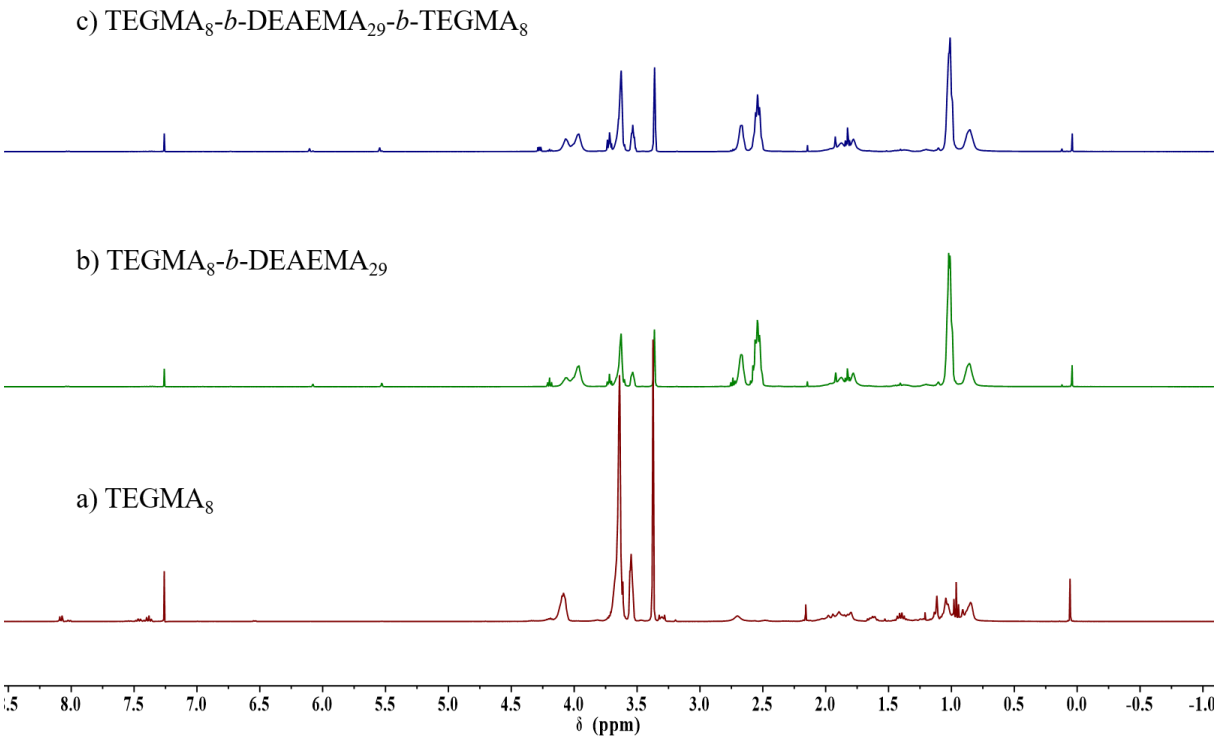


Figure A2.2: ^{1}H NMR spectra of a) $TEGMA_8$ homopolymer in red, b) $TEGMA_8$-*b*-$DEAEMA_{29}$ diblock precursor in green and c) $TEGMA_8$-*b*-$DEAEMA_{29}$-*b*-$TEGMA_8$ triblock copolymer in blue. The polymer is AP2.

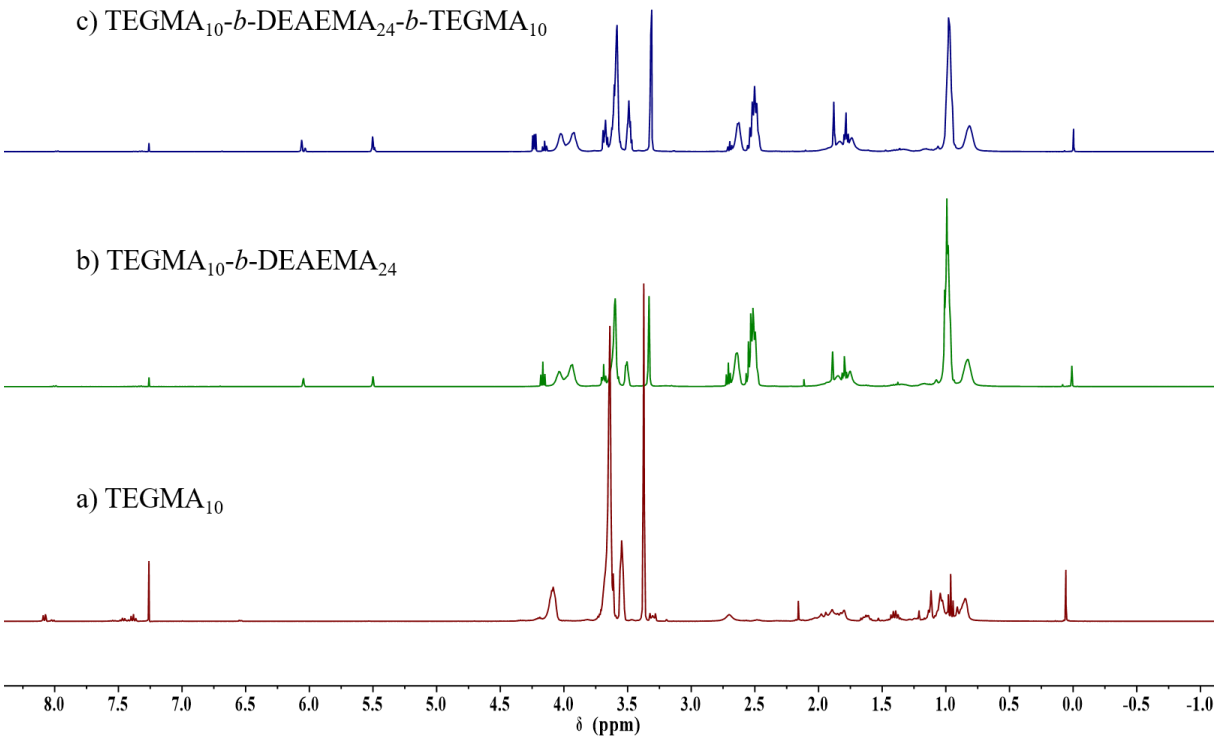


Figure A2.3: ^{1}H NMR spectra of a) $TEGMA_{10}$ homopolymer in red, b) $TEGMA_{10}$-*b*-$DEAEMA_{24}$ diblock precursor in green and c) $TEGMA_{10}$-*b*-$DEAEMA_{24}$-*b*-$TEGMA_{10}$ triblock copolymer in blue. The polymer is AP3.

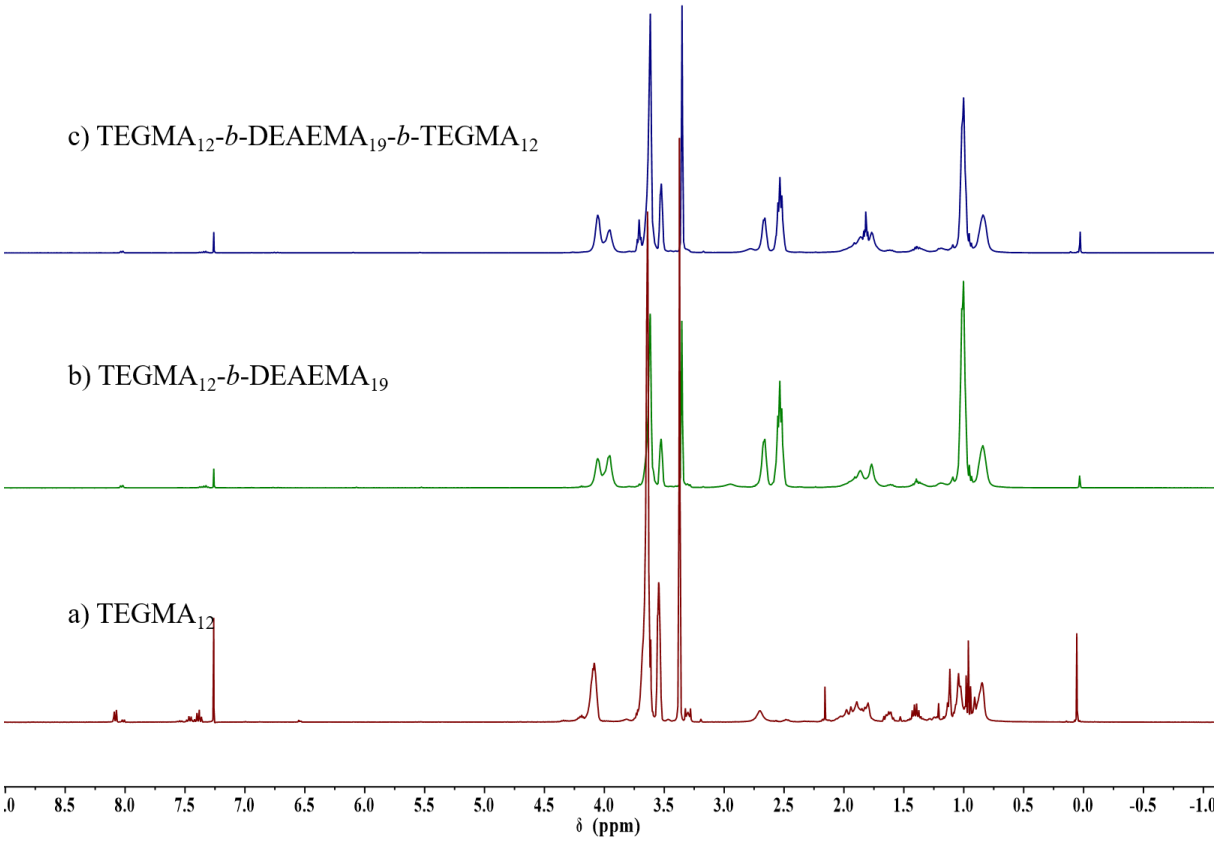


Figure A2.4: ^{1}H NMR spectra of a) $TEGMA_{12}$ homopolymer in red, b) $TEGMA_{12}$-*b*-$DEAEMA_{19}$ diblock precursor in green and c) $TEGMA_{12}$-*b*-$DEAEMA_{19}$-*b*-$TEGMA_{12}$ triblock copolymer in blue. The polymer is AP4.

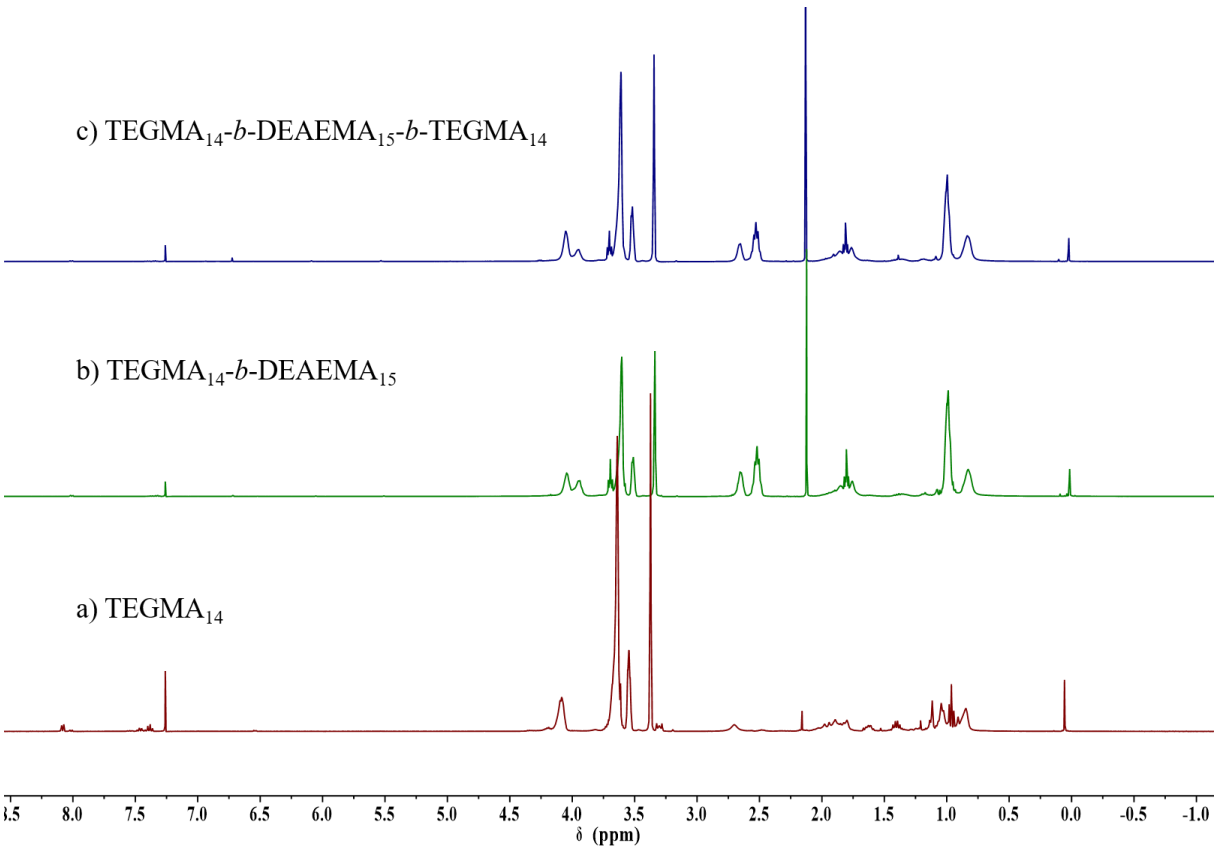


Figure A2.5: ^{1}H NMR spectra of a) $TEGMA_{14}$ homopolymer in red, b) $TEGMA_{14}$-*b*-$DEAEMA_{15}$ diblock precursor in green and c) $TEGMA_{14}$-*b*-$DEAEMA_{15}$-*b*-$TEGMA_{14}$ triblock copolymer in blue. The polymer is AP5.

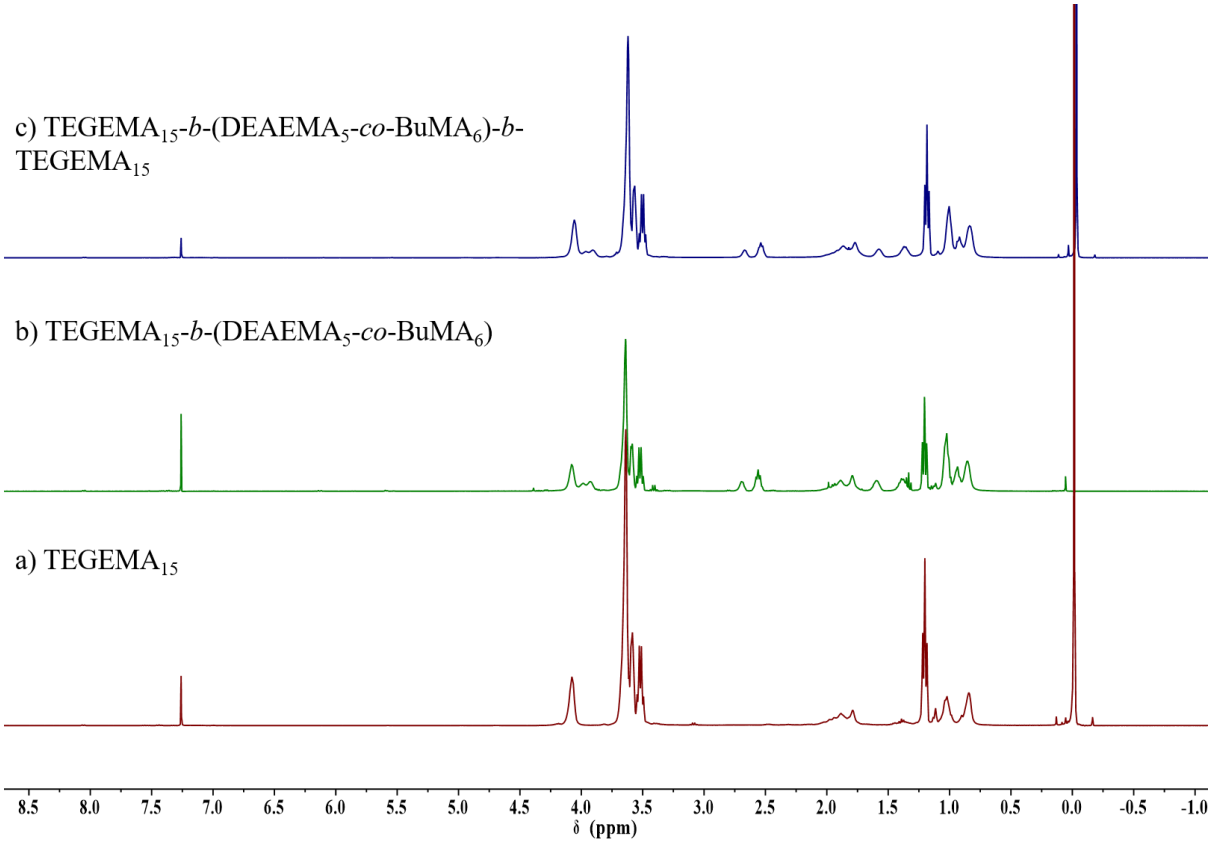


Figure A2.6: ^{1}H NMR spectra of a) $TEGEMA_{15}$ homopolymer in red, b) $TEGEMA_{15}$-*b*-($DEAEMA_5$-*co*-$BuMA_6$) diblock precursor in green and c) $TEGEMA_{15}$-*b*-($DEAEMA_5$-*co*-$BuMA_6$)-*b*-$TEGEMA_{15}$ triblock copolymer in blue. The polymer is CP1.

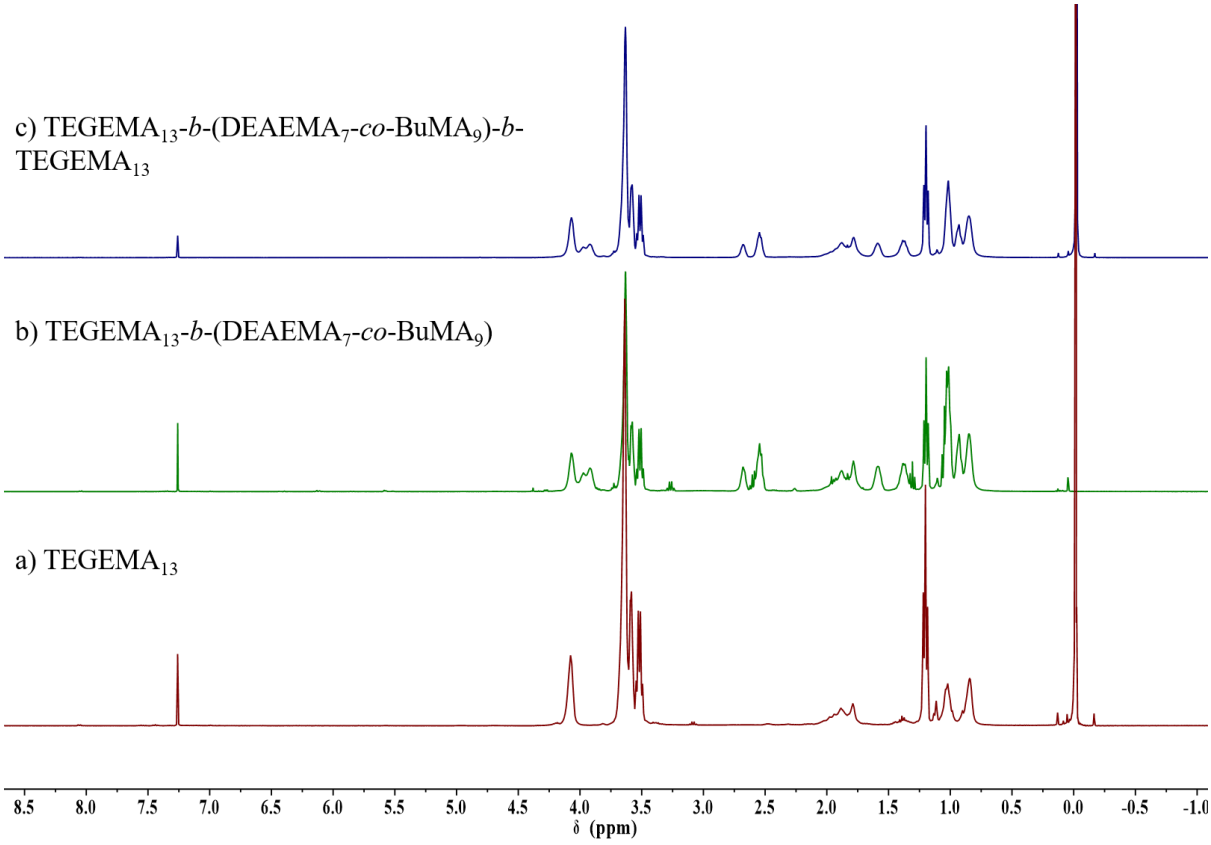


Figure A2.7: ^{1}H NMR spectra of a) $TEGEMA_{13}$ homopolymer in red, b) $TEGEMA_{13}$-*b*-($DEAEMA_{7}$-*co*-$BuMA_{9}$) diblock precursor in green and c) $TEGEMA_{13}$-*b*-($DEAEMA_{7}$-*co*-$BuMA_{9}$)-*b*-$TEGEMA_{13}$ triblock copolymer in blue. The polymer is CP2.

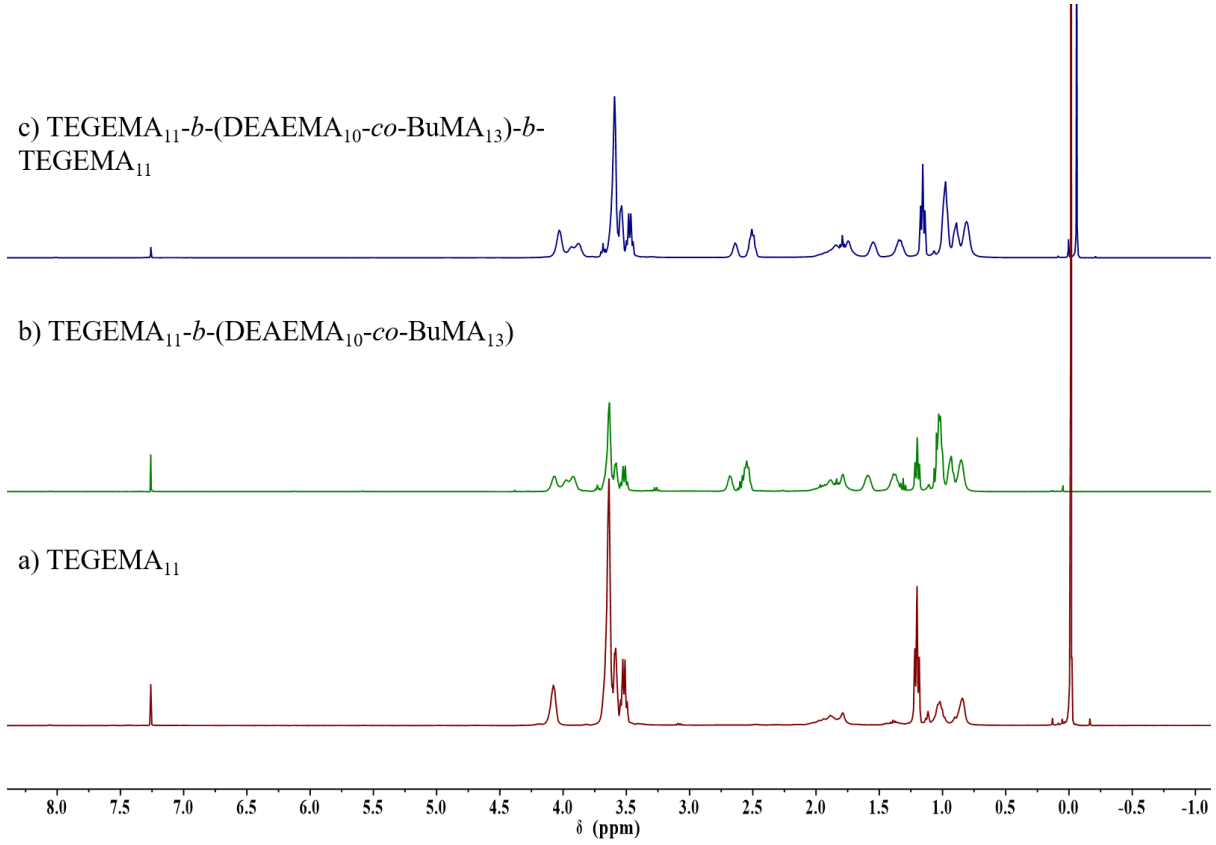


Figure A2.8: ^{1}H NMR spectra of a) $TEGEMA_{11}$ homopolymer in red, b) $TEGEMA_{11}$-*b*-($DEAEMA_{10}$-*co*-$BuMA_{13}$) diblock precursor in green and c) $TEGEMA_{11}$-*b*-($DEAEMA_{10}$-*co*-$BuMA_{13}$)-*b*-$TEGEMA_{11}$ triblock copolymer in blue. The polymer is CP3.

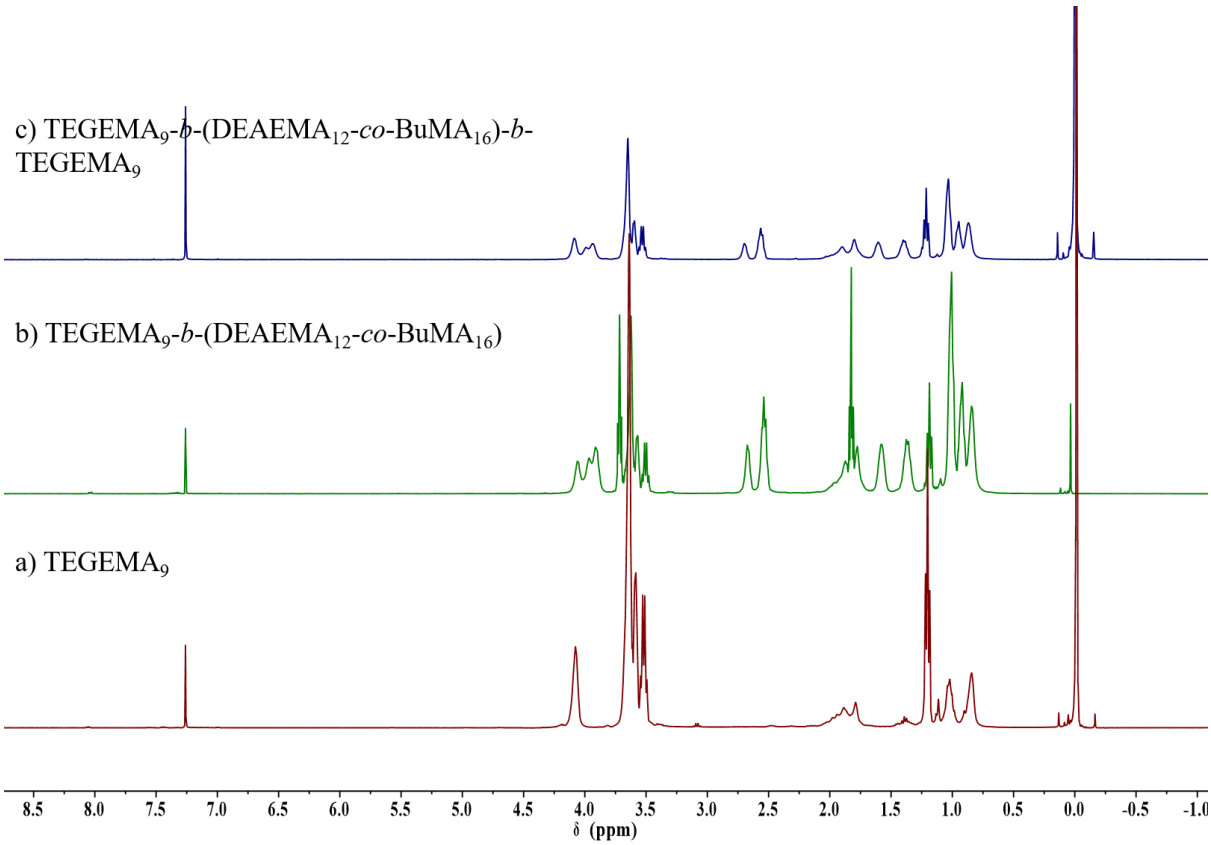


Figure A2.9: ^{1}H NMR spectra of a) TEGEMA$_9$ homopolymer in red, b) TEGEMA$_9$-*b*-(DEAEMA$_{12}$-*co*-BuMA$_{16}$) diblock precursor in green and c) TEGEMA$_9$-*b*-(DEAEMA$_{12}$-*co*-BuMA$_{16}$)-*b*-TEGEMA$_9$ triblock copolymer in blue. The polymer is CP4.

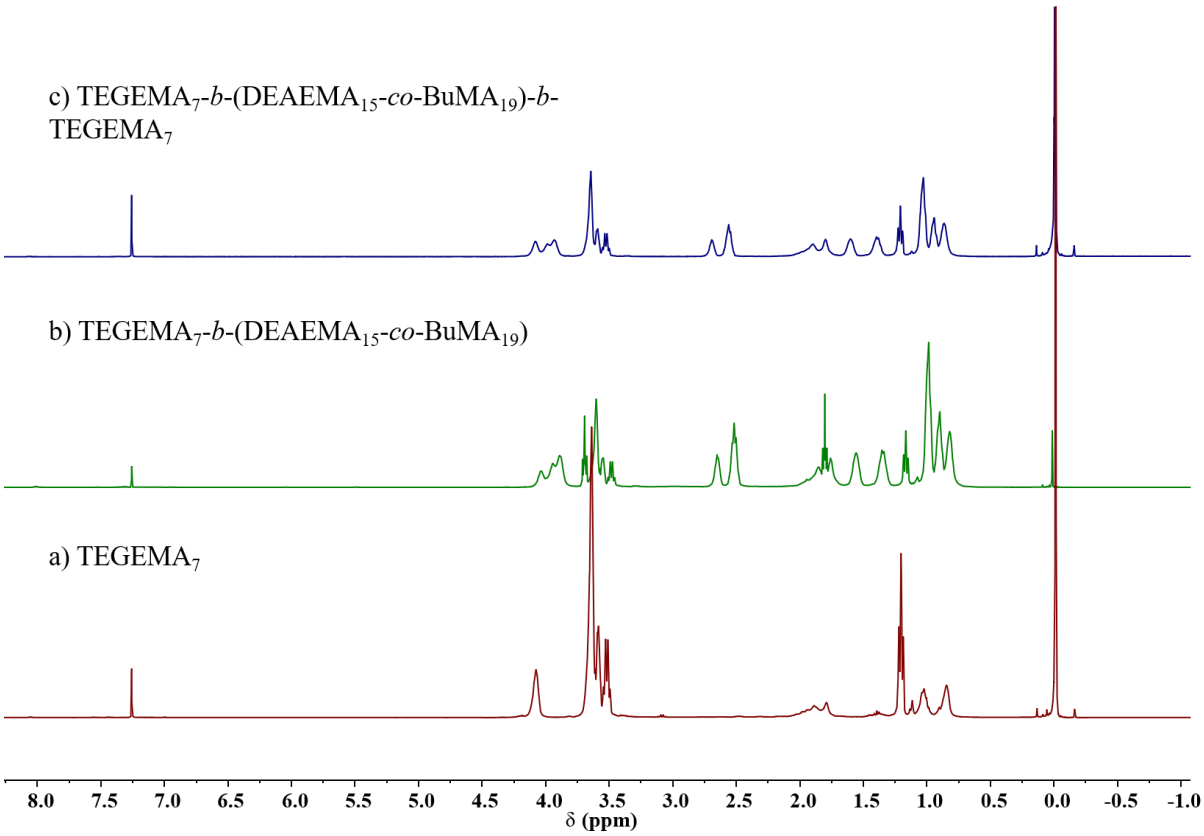


Figure A2.10: ^{1}H NMR spectra of a) TEGEMA$_7$ homopolymer in red, b) TEGEMA$_7$-*b*-(DEAEMA$_{15}$-*co*-BuMA$_{19}$) diblock precursor in green and c) TEGEMA$_7$-*b*-(DEAEMA$_{15}$-*co*-BuMA$_{19}$)-*b*-TEGEMA$_7$ triblock copolymer in blue. The polymer is CP5.

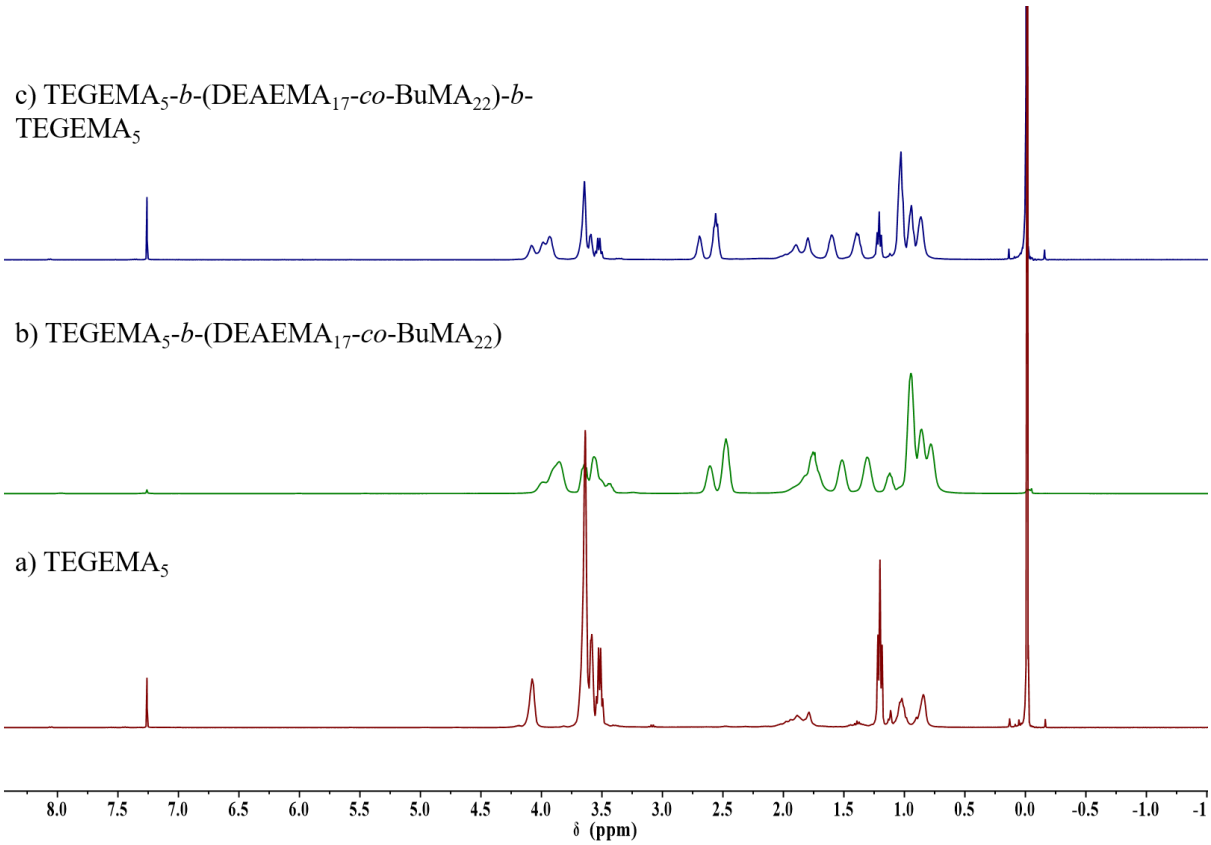


Figure A2.11: ^{1}H NMR spectra of a) $TEGEMA_5$ homopolymer in red, b) $TEGEMA_5$-*b*-($DEAEMA_{17}$-*co*-$BuMA_{22}$) diblock precursor in green and c) $TEGEMA_5$-*b*-($DEAEMA_{17}$-*co*-$BuMA_{22}$)-*b*-$TEGEMA_5$ triblock copolymer in blue. The polymer is CP6.

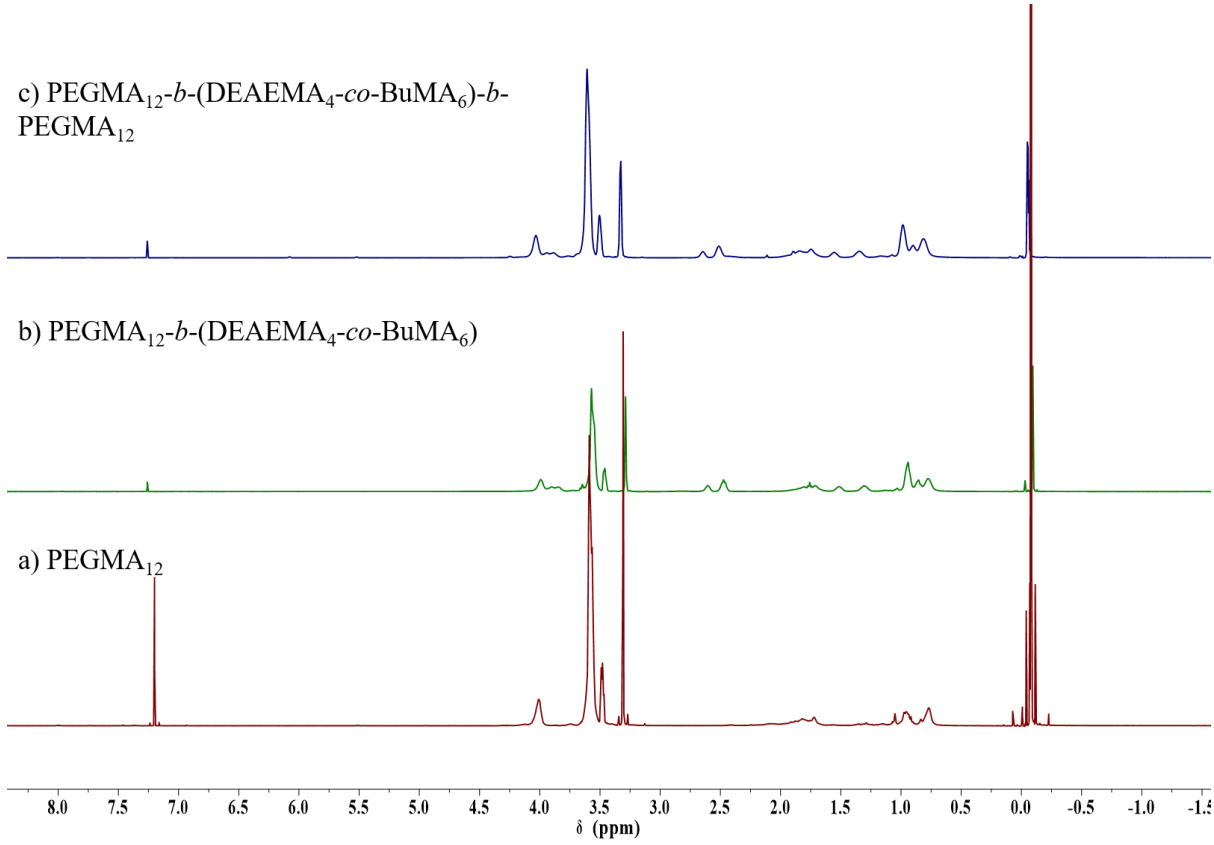


Figure A2.12: ^{1}H NMR spectra of a) $PEGMA_{12}$ homopolymer in red, b) $PEGMA_{12}$-*b*-($DEAEMA_4$-*co*-$BuMA_6$) diblock precursor in green and c) $PEGMA_{12}$-*b*-($DEAEMA_4$-*co*-$BuMA_6$)-*b*-$PEGMA_{12}$ triblock copolymer in blue. The polymer is DP1.

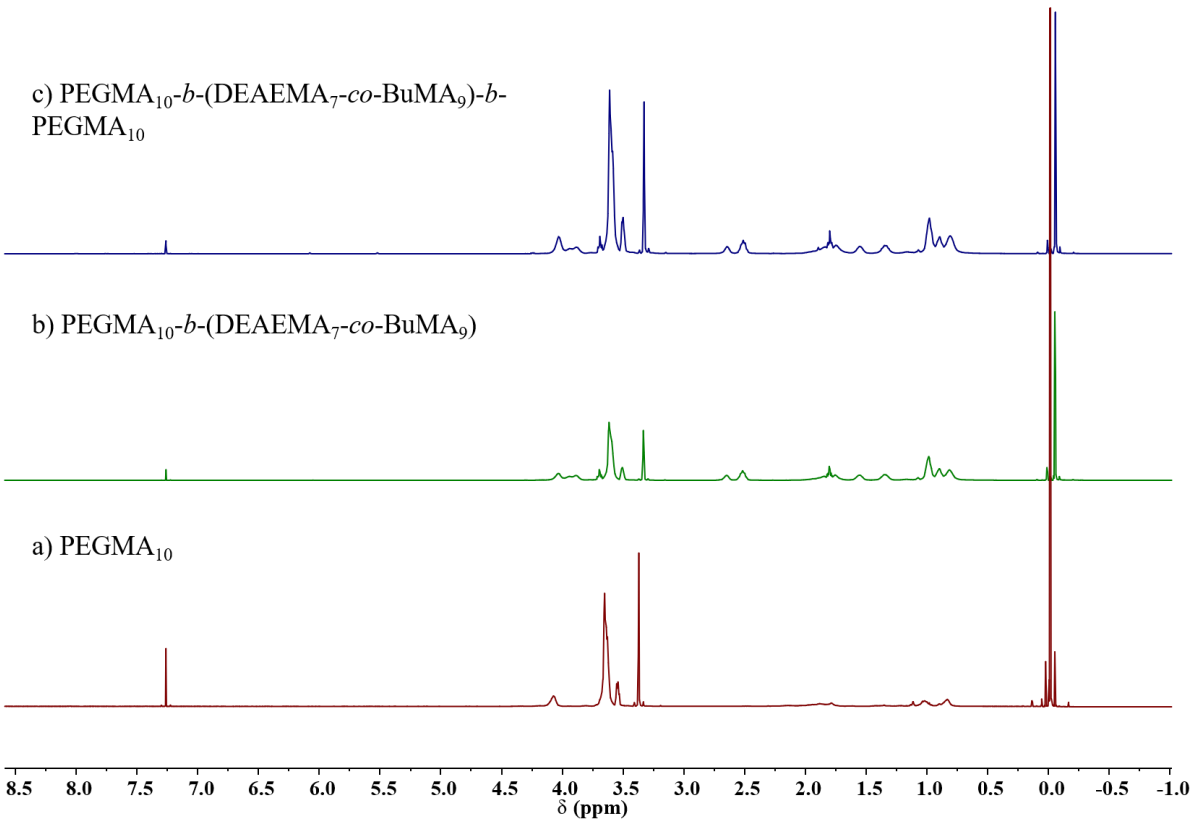


Figure A2.13: ^{1}H NMR spectra of a) $PEGMA_{10}$ homopolymer in red, b) $PEGMA_{10}$-*b*-($DEAEMA_{7}$-*co*-$BuMA_{9}$) diblock precursor in green and c) $PEGMA_{10}$-*b*-($DEAEMA_{7}$-*co*-$BuMA_{9}$)-*b*-$PEGMA_{10}$ triblock copolymer in blue. The polymer is DP2.

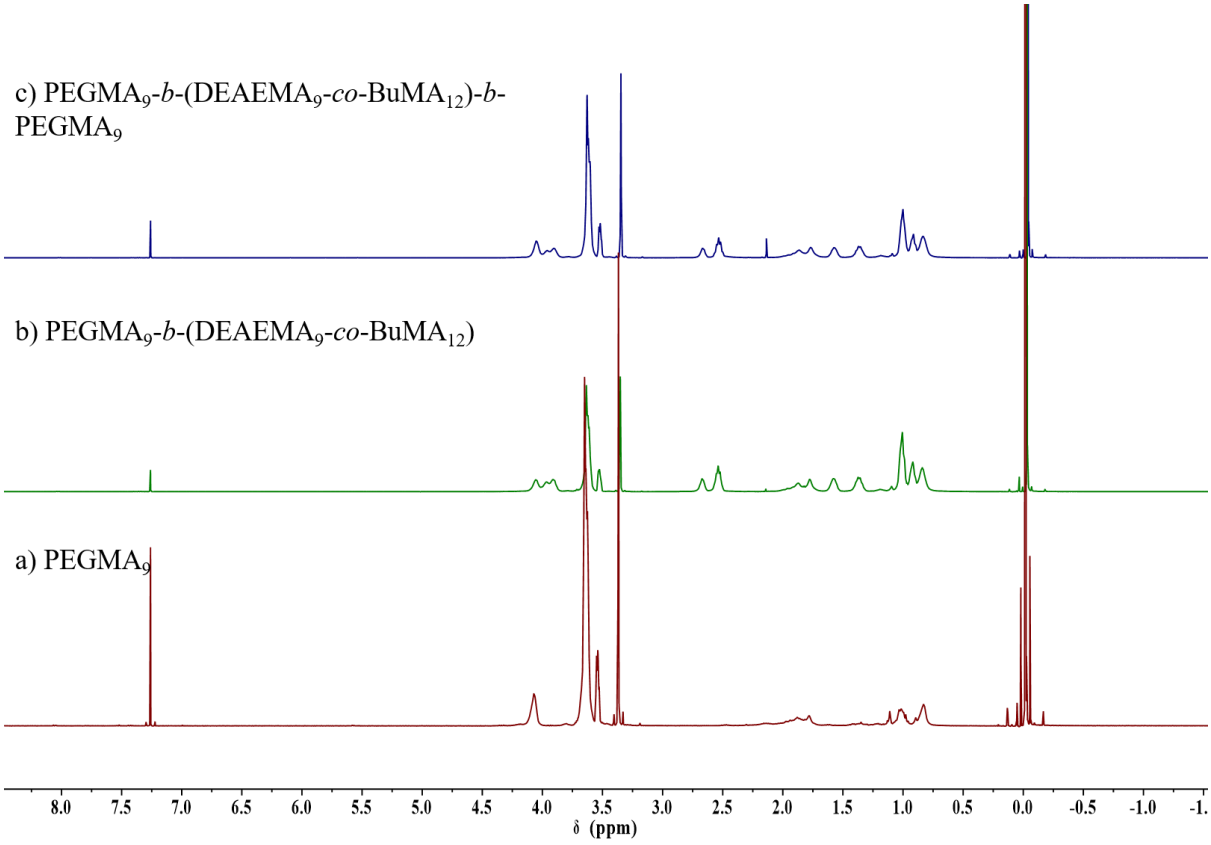


Figure A2.14: ^{1}H NMR spectra of a) PEGMA$_9$ homopolymer in red, b) PEGMA$_9$-*b*-(DEAEMA$_9$-*co*-BuMA$_{12}$) diblock precursor in green and c) PEGMA$_9$-*b*-(DEAEMA$_9$-*co*-BuMA$_{12}$)-*b*-PEGMA$_9$ triblock copolymer in blue. The polymer is DP3.

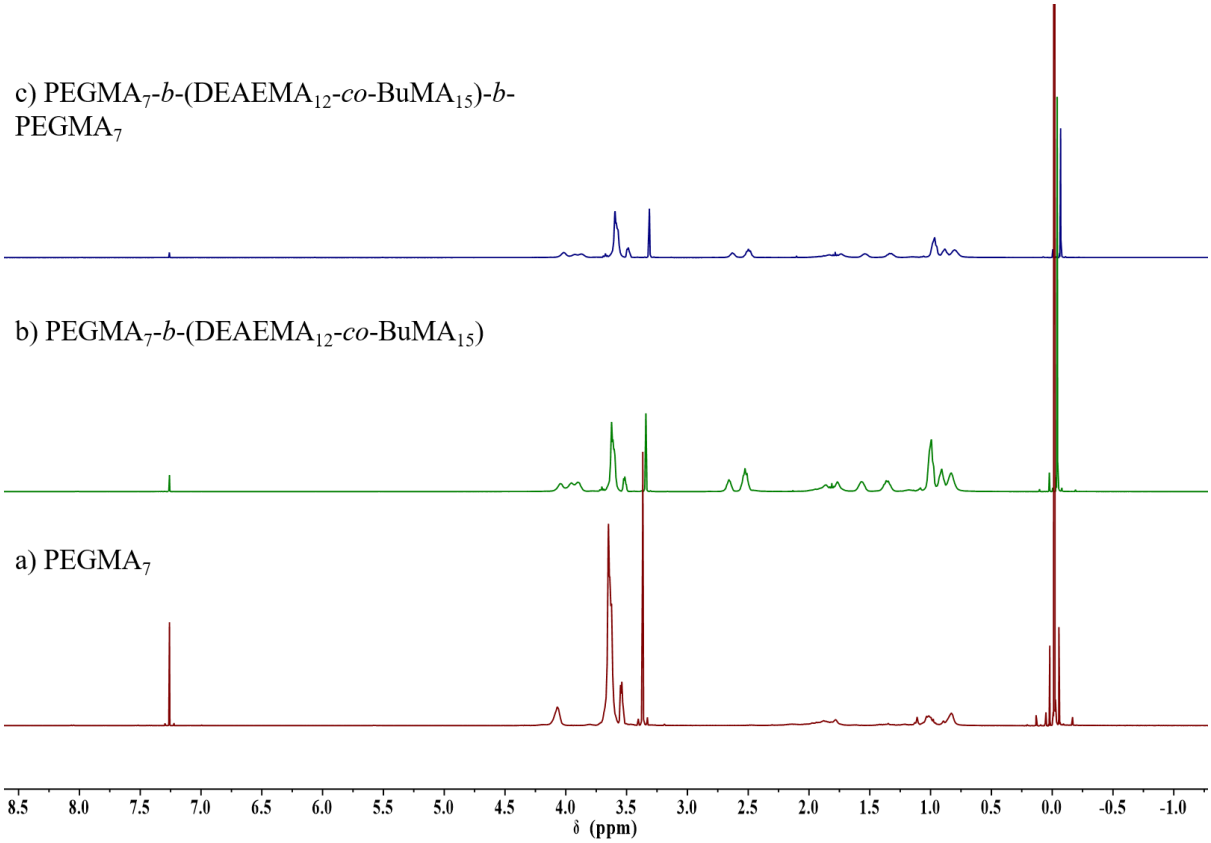


Figure A2.15: ^{1}H NMR spectra of a) PEGMA$_7$ homopolymer in red, b) PEGMA$_7$-*b*-(DEAEMA$_{12}$-*co*-BuMA$_{15}$) diblock precursor in green and c) PEGMA$_7$-*b*-(DEAEMA$_{12}$-*co*-BuMA$_{15}$)-*b*-PEGMA$_7$ triblock copolymer in blue. The polymer is DP4.

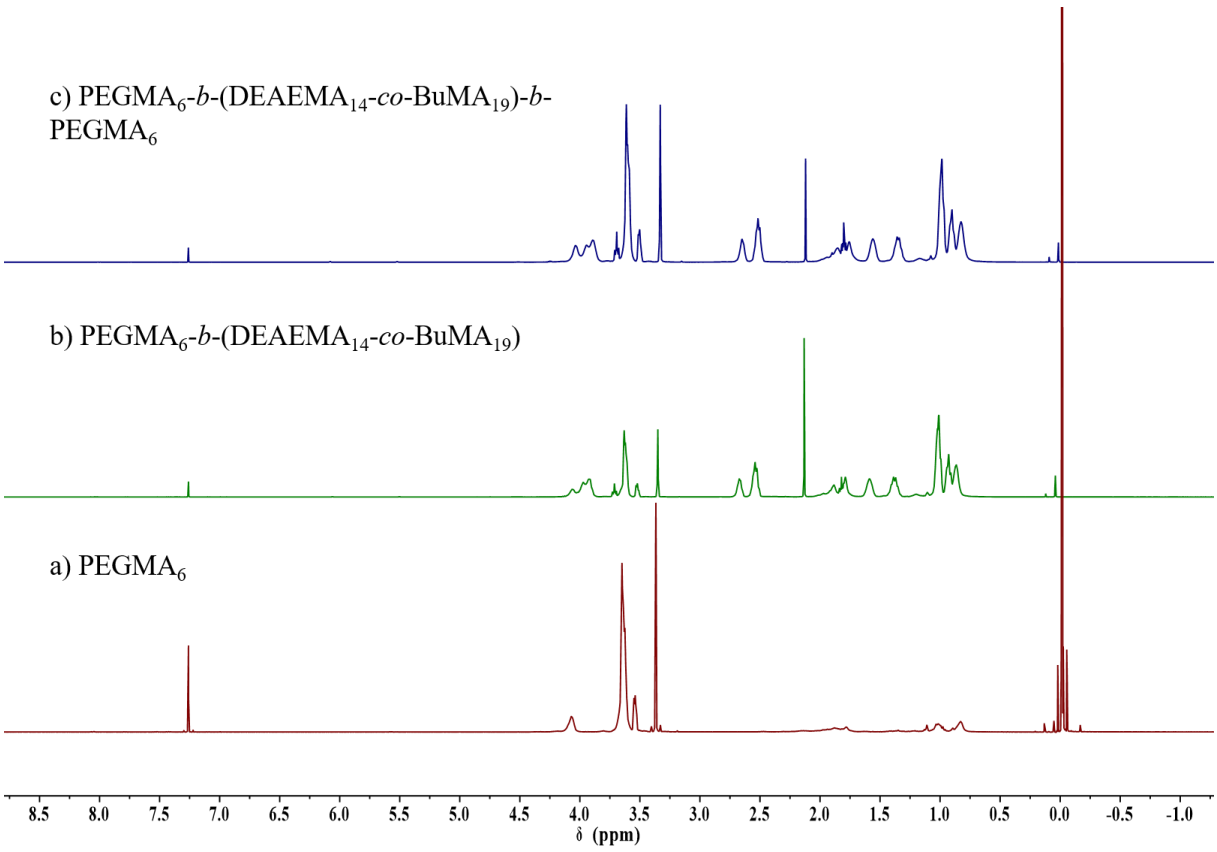


Figure A2.16: ^{1}H NMR spectra of a) $PEGMA_6$ homopolymer in red, b) $PEGMA_6$-*b*-($DEAEMA_{14}$-*co*-$BuMA_{19}$) diblock precursor in green and c) $PEGMA_6$-*b*-($DEAEMA_{14}$-*co*-$BuMA_{19}$)-*b*-$PEGMA_6$ triblock copolymer in blue. The polymer is DP5.

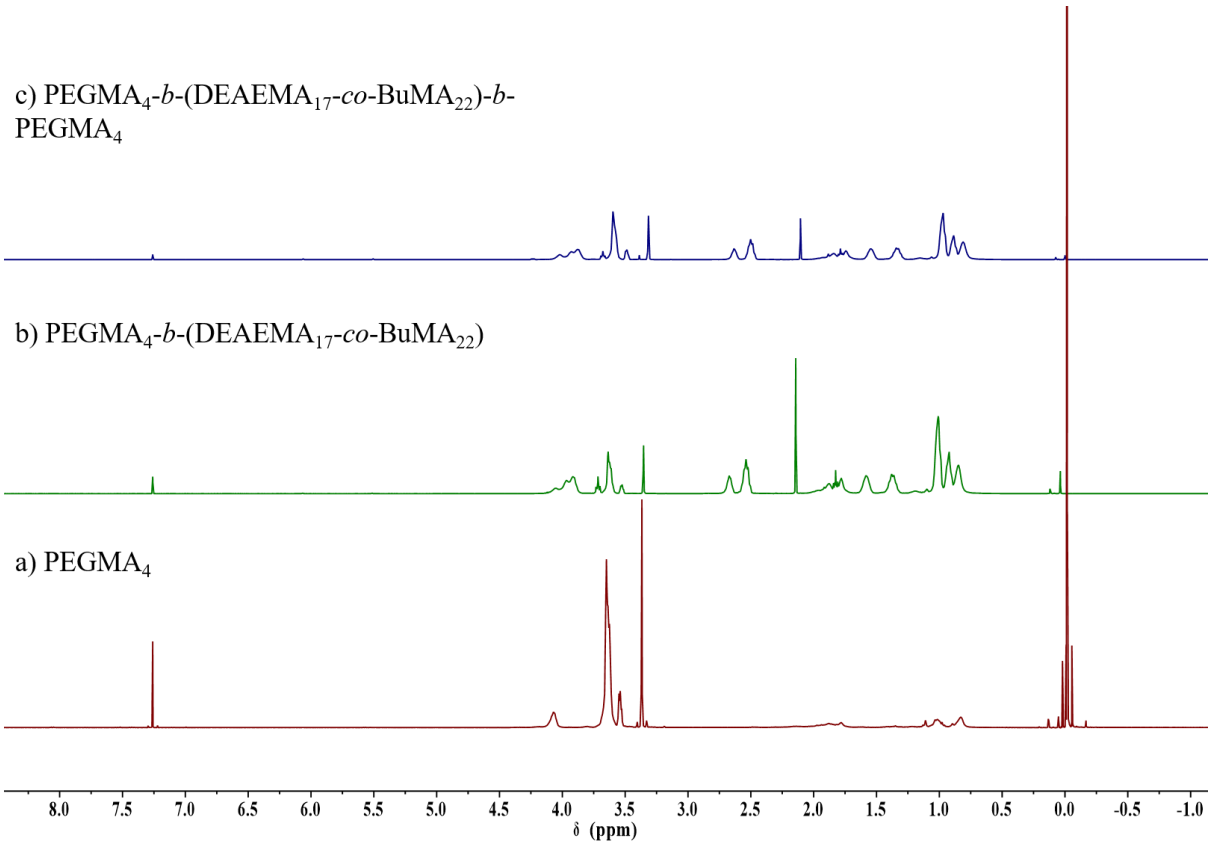


Figure A2.17: ^{1}H NMR spectra of a) $PEGMA_4$ homopolymer in red, b) $PEGMA_4$-*b*-($DEAEMA_{17}$-*co*-$BuMA_{22}$) diblock precursor in green and c) $PEGMA_4$-*b*-($DEAEMA_{17}$-*co*-$BuMA_{22}$)-*b*-$PEGMA_4$ triblock copolymer in blue. The polymer is DP6.

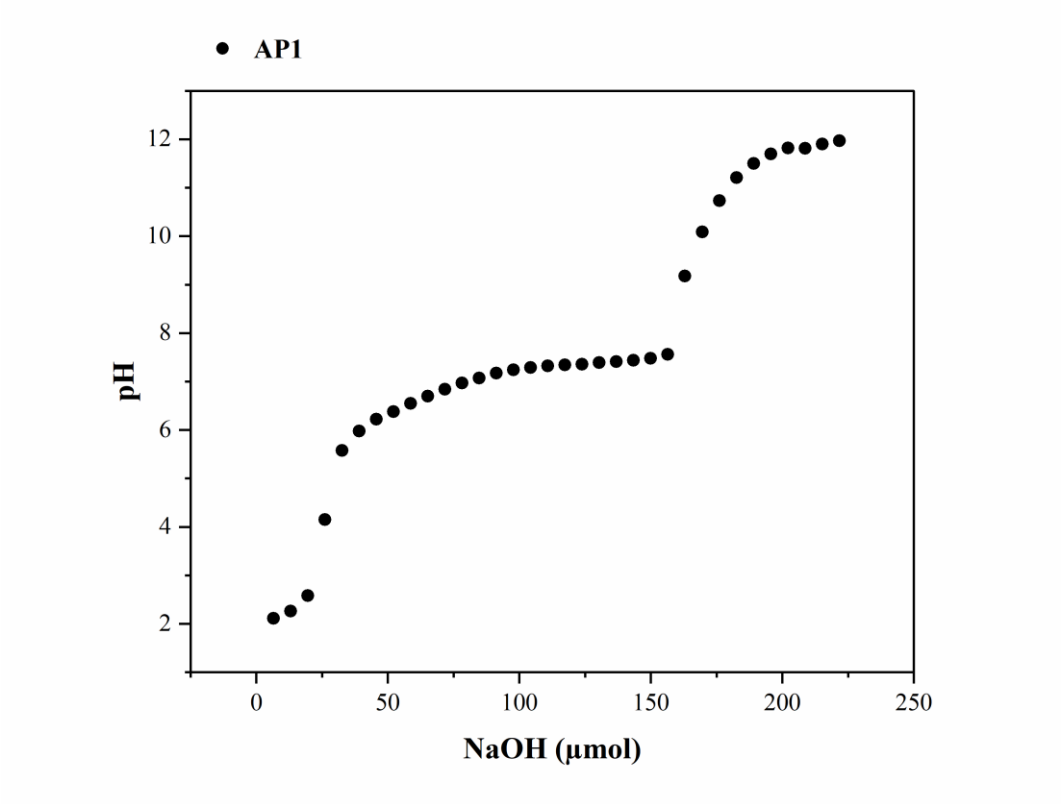


Figure A3.1: Potentiometric titration curve of AP1 solution.

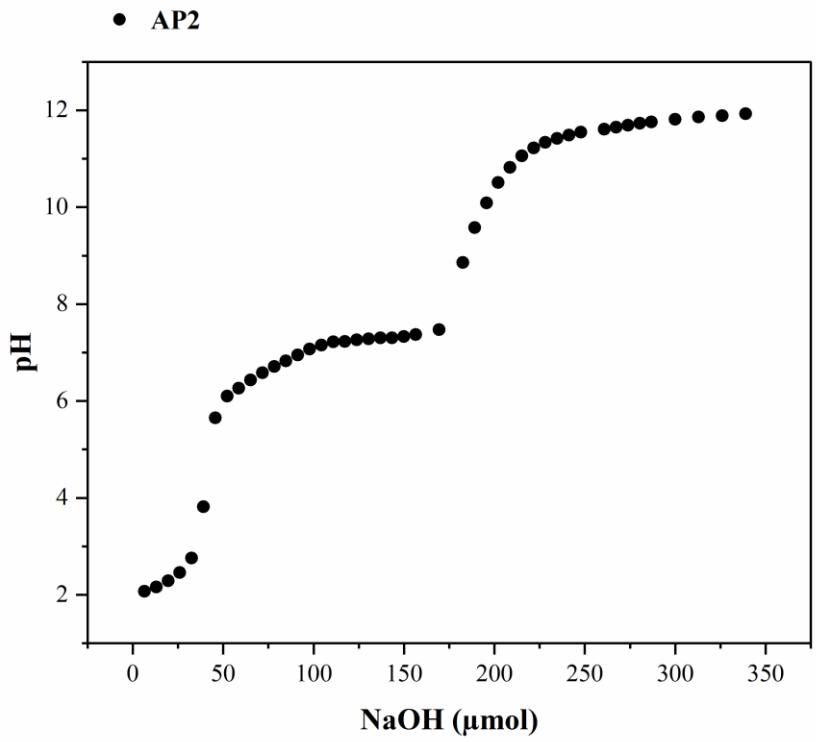


Figure A3.2: Potentiometric titration curve of AP2 solution.

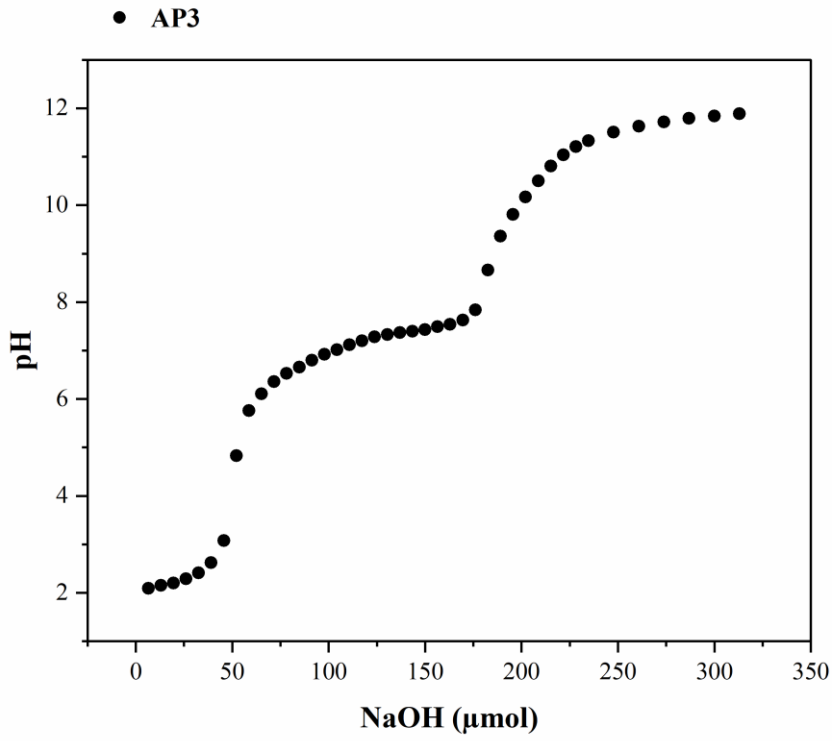


Figure A3.3: Potentiometric titration curve of AP3 solution.

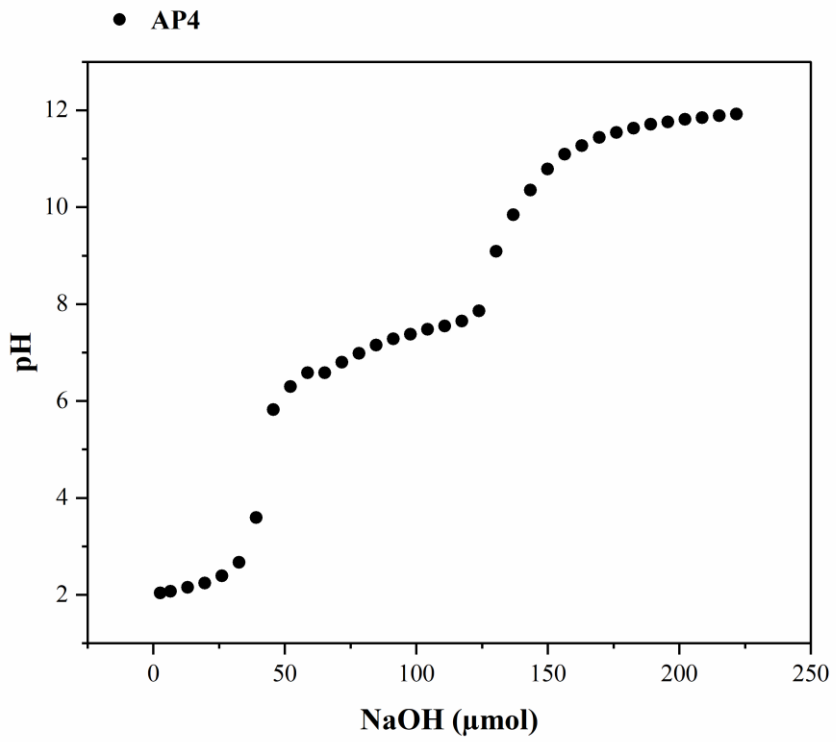


Figure A3.4: Potentiometric titration curve of AP4 solution.

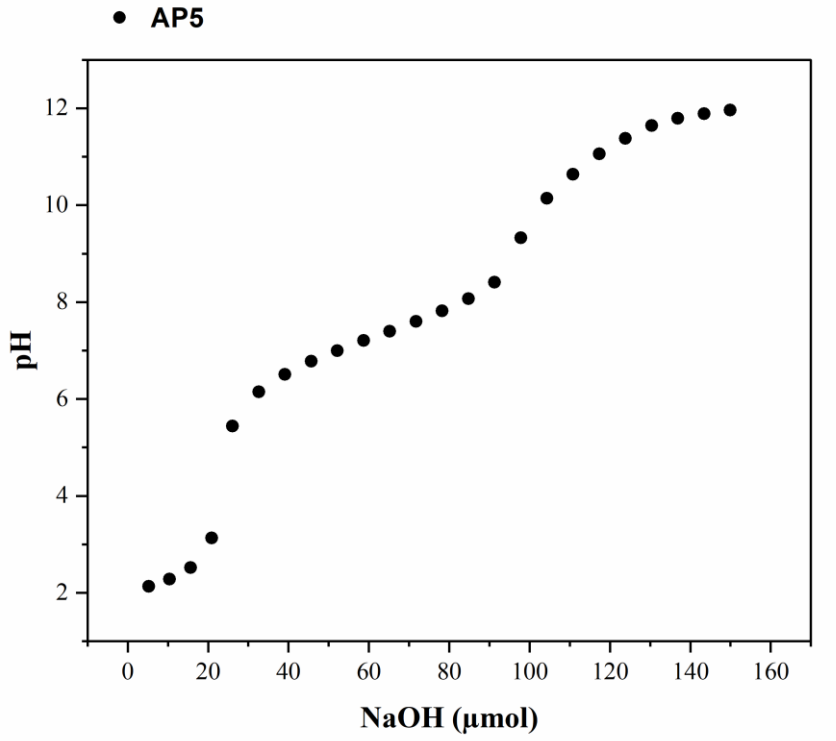


Figure A3.5: Potentiometric titration curve of AP5 solution.

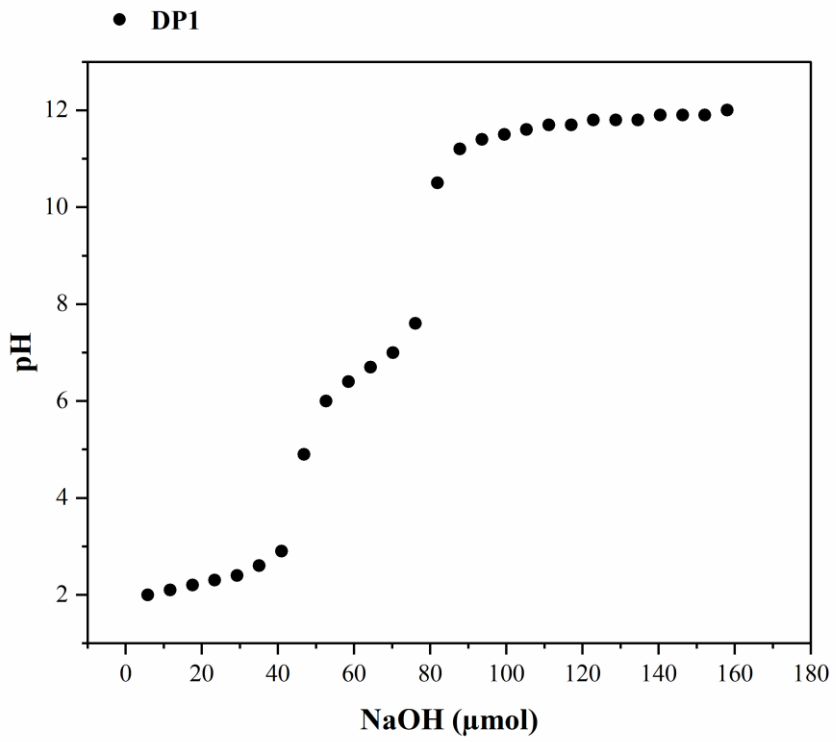


Figure A3.6: Potentiometric titration curve of DP1 solution.

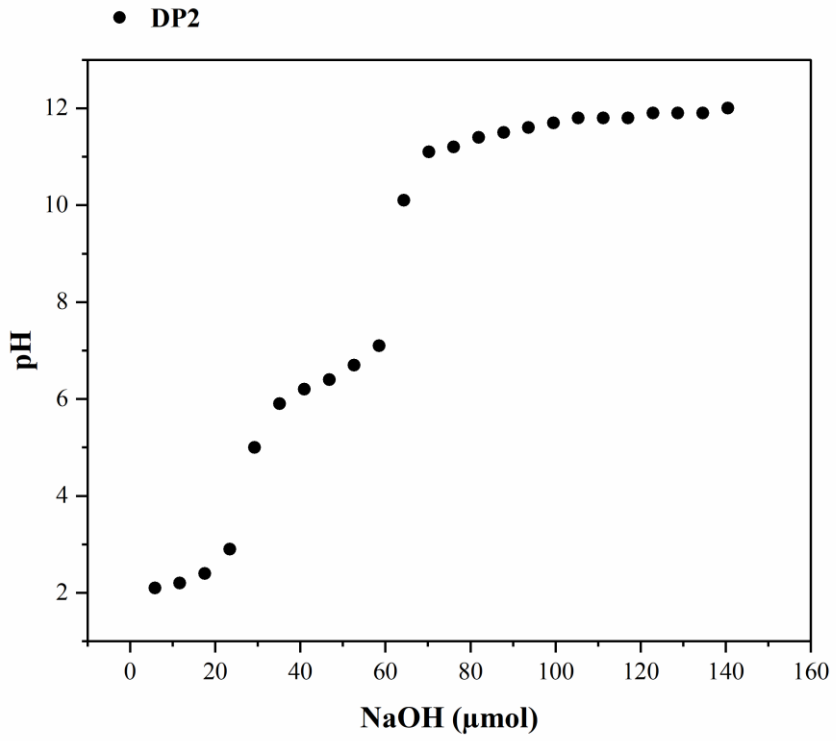


Figure A3.7: Potentiometric titration curve of DP2 solution.

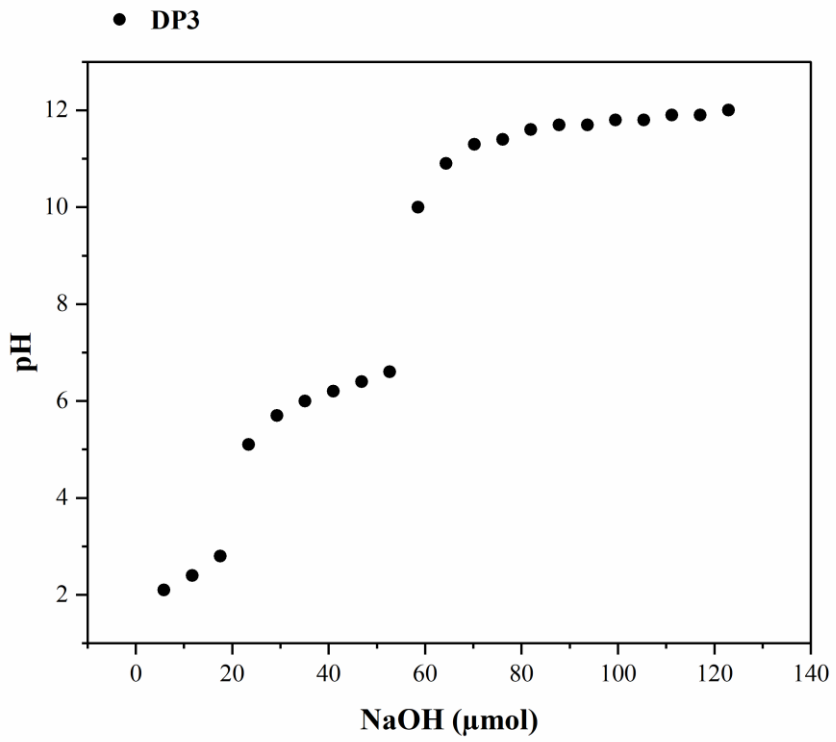


Figure A3.8: Potentiometric titration curve of DP3 solution.

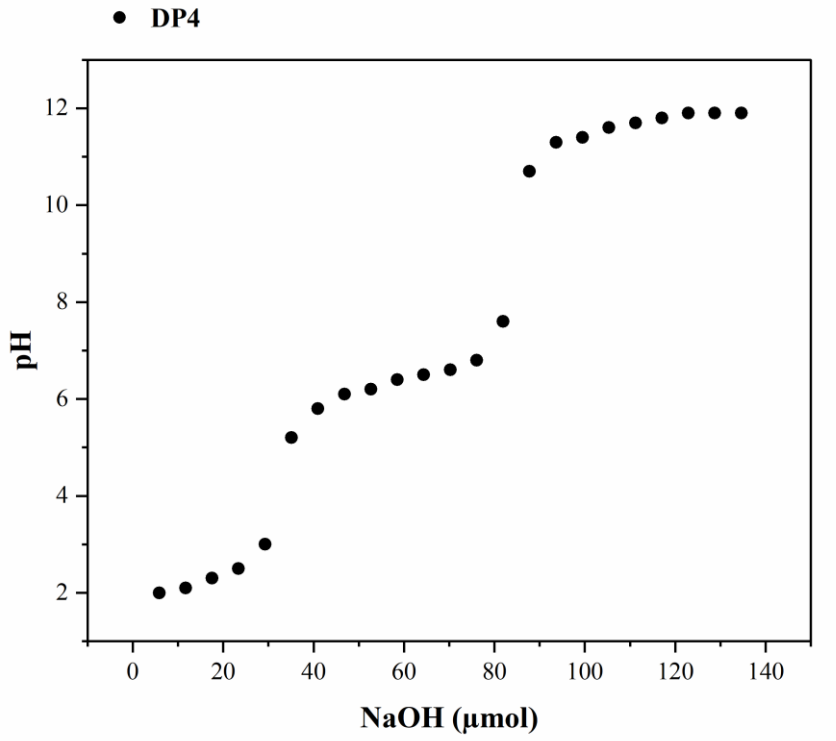


Figure A3.9: Potentiometric titration curve of DP4 solution.

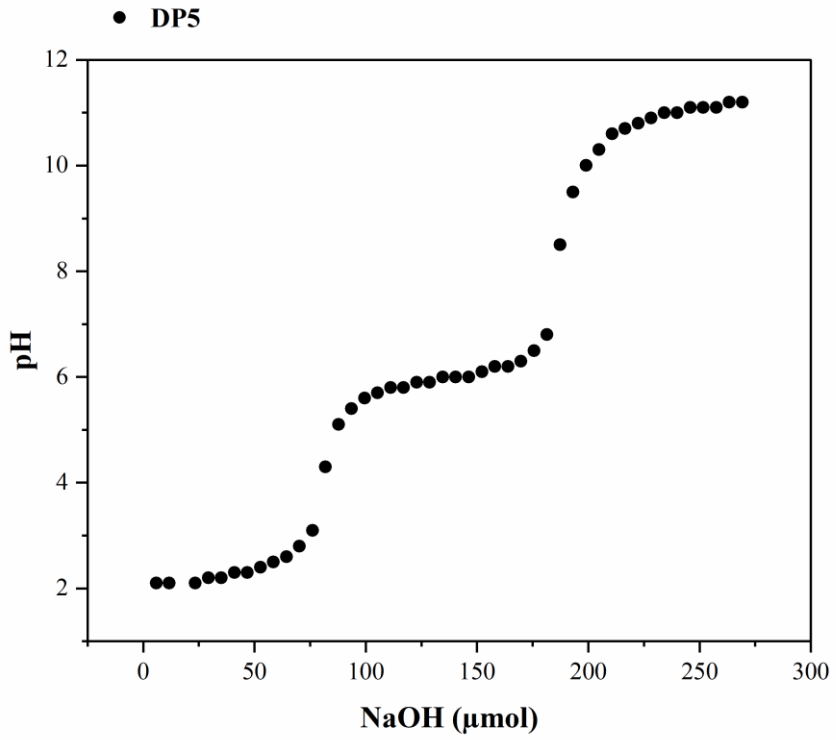


Figure A3.10: Potentiometric titration curve of DP5 solution.

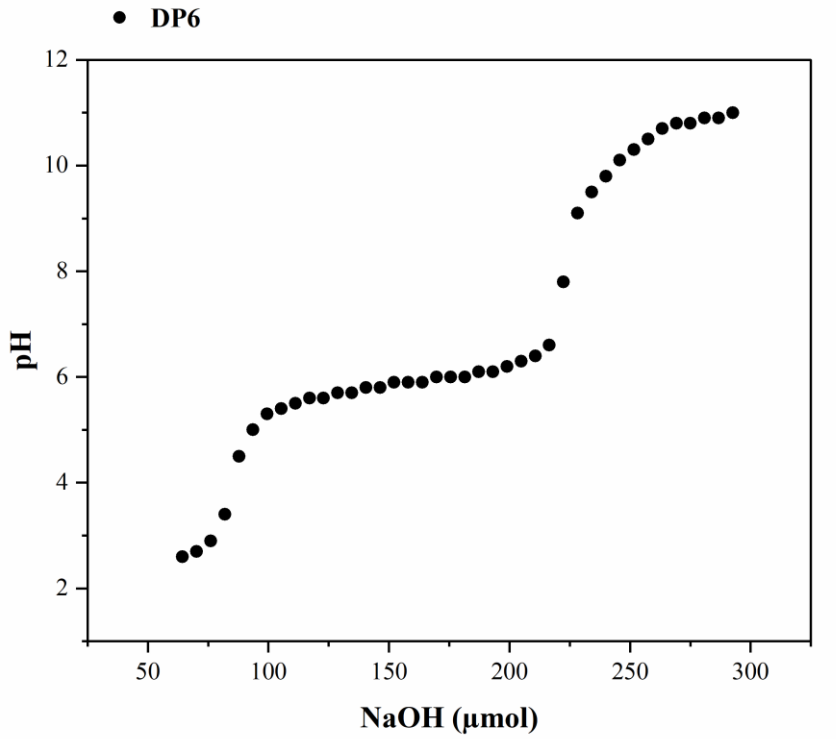


Figure A3.11: Potentiometric titration curve of DP6 solution

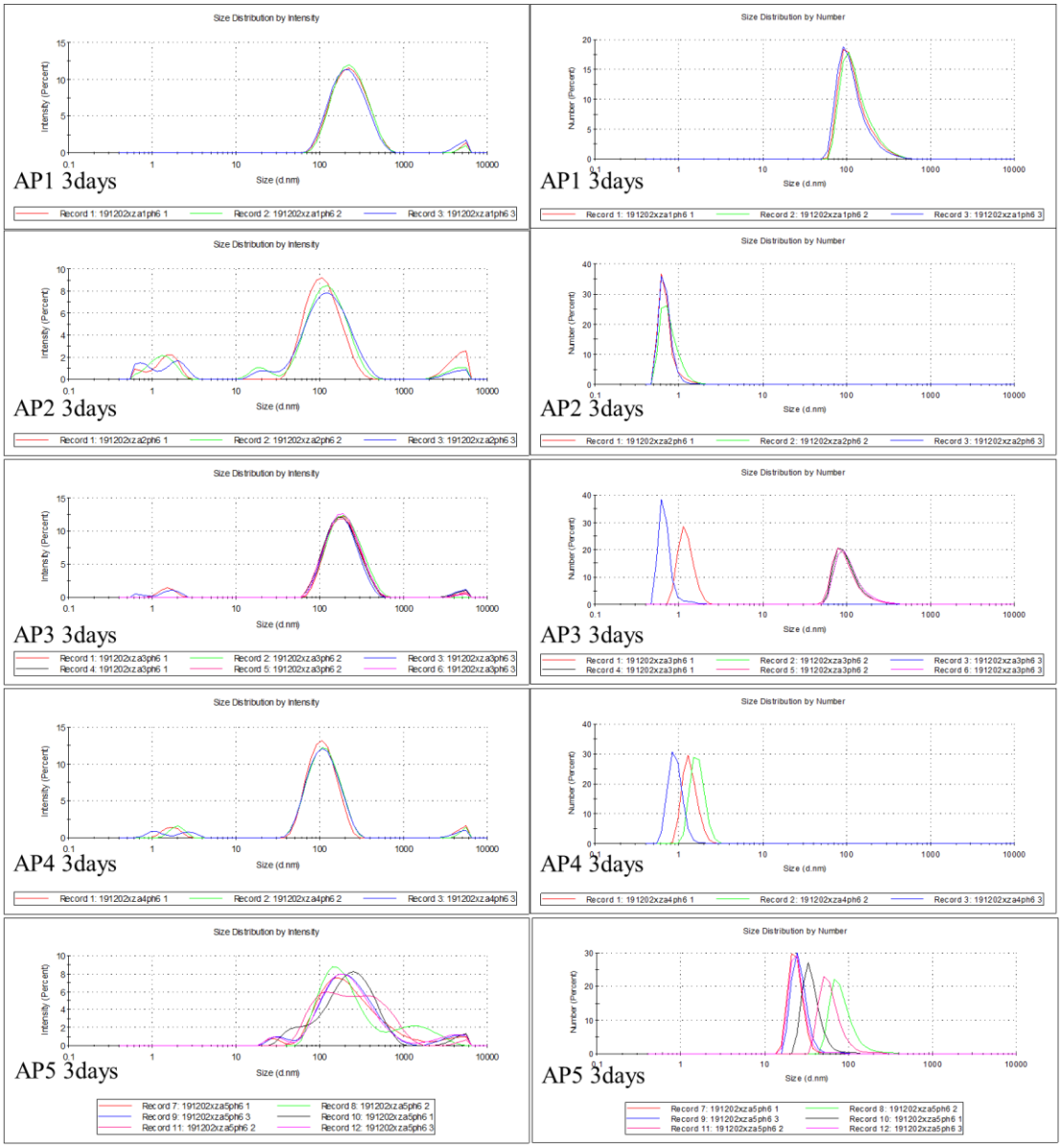


Figure A4.1: DLS graphs of APs in **Table 4.3** (3 days, pH = 6, 10 mg mL^{-1} in DI water).

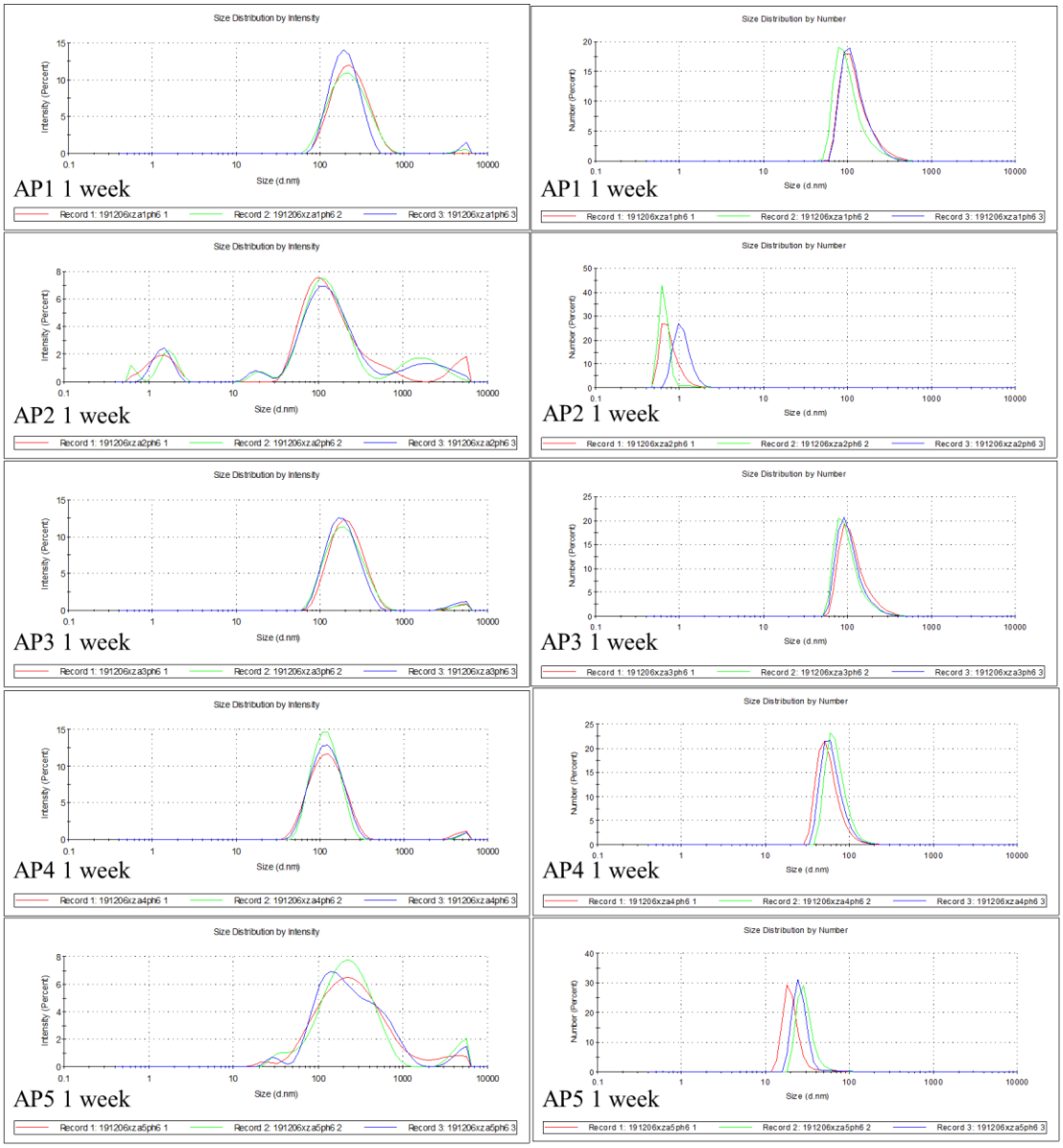


Figure A4.2: DLS graphs of APs in **Table 4.3** (1 week, pH = 6, 10 mg mL^{-1} in DI water).

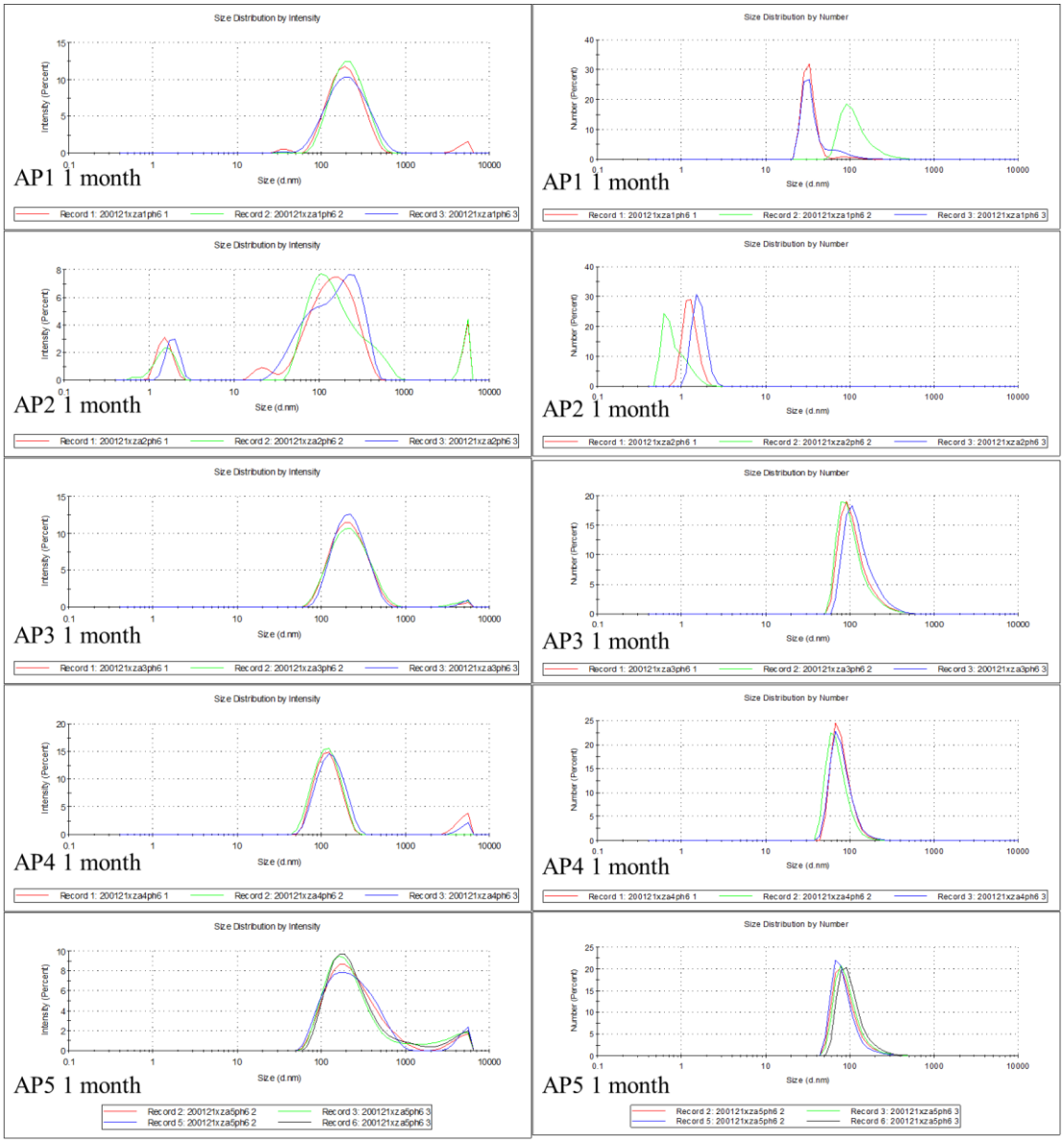


Figure A4.3: DLS graphs of APs in **Table 4.3** (1 month, pH = 6, 10 mg mL^{-1} in DI water).

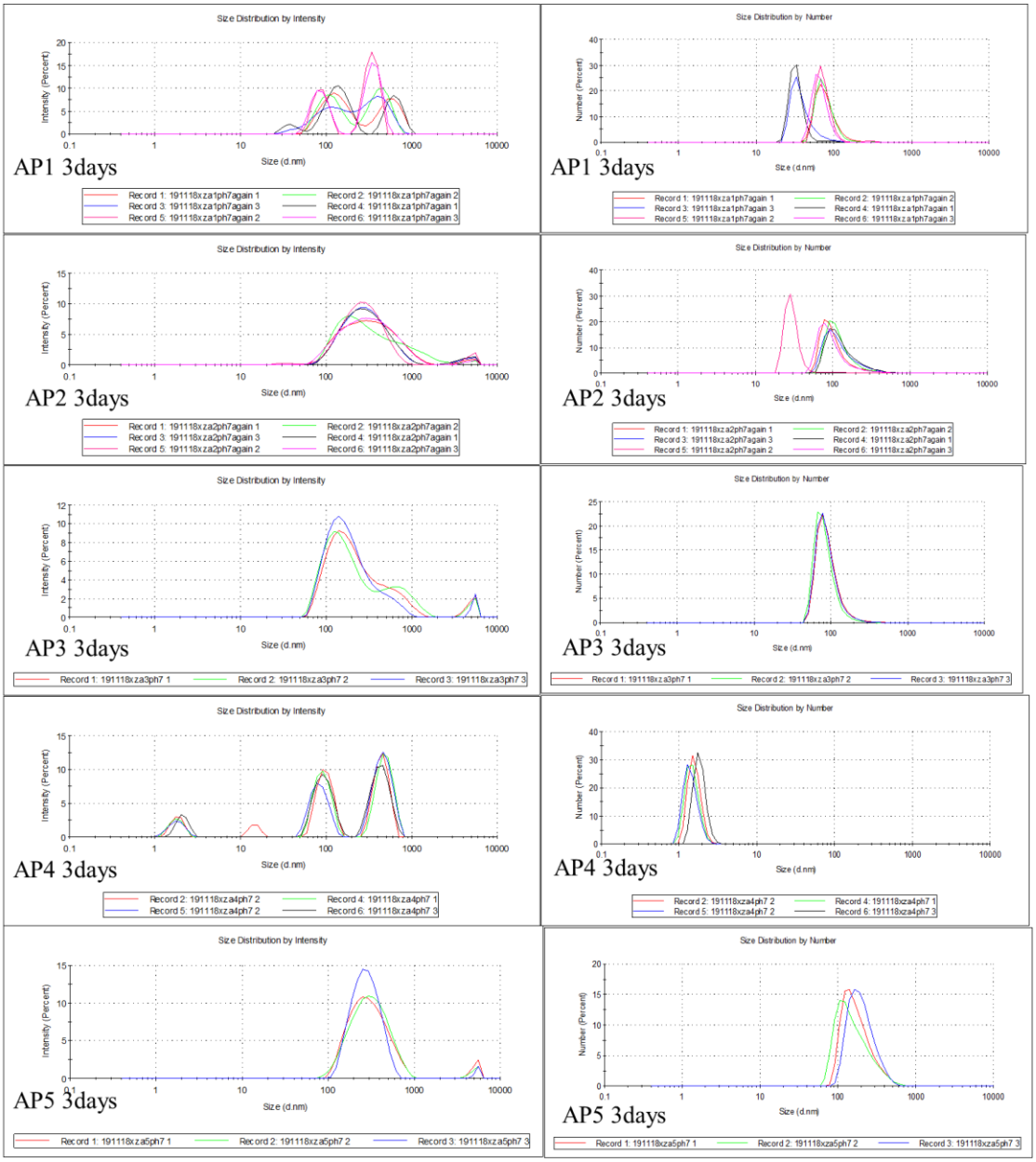


Figure A4.4: DLS graphs of APs in **Table 4.4** (3 days, pH = 7, 10 mg mL^{-1} in DI water).

.

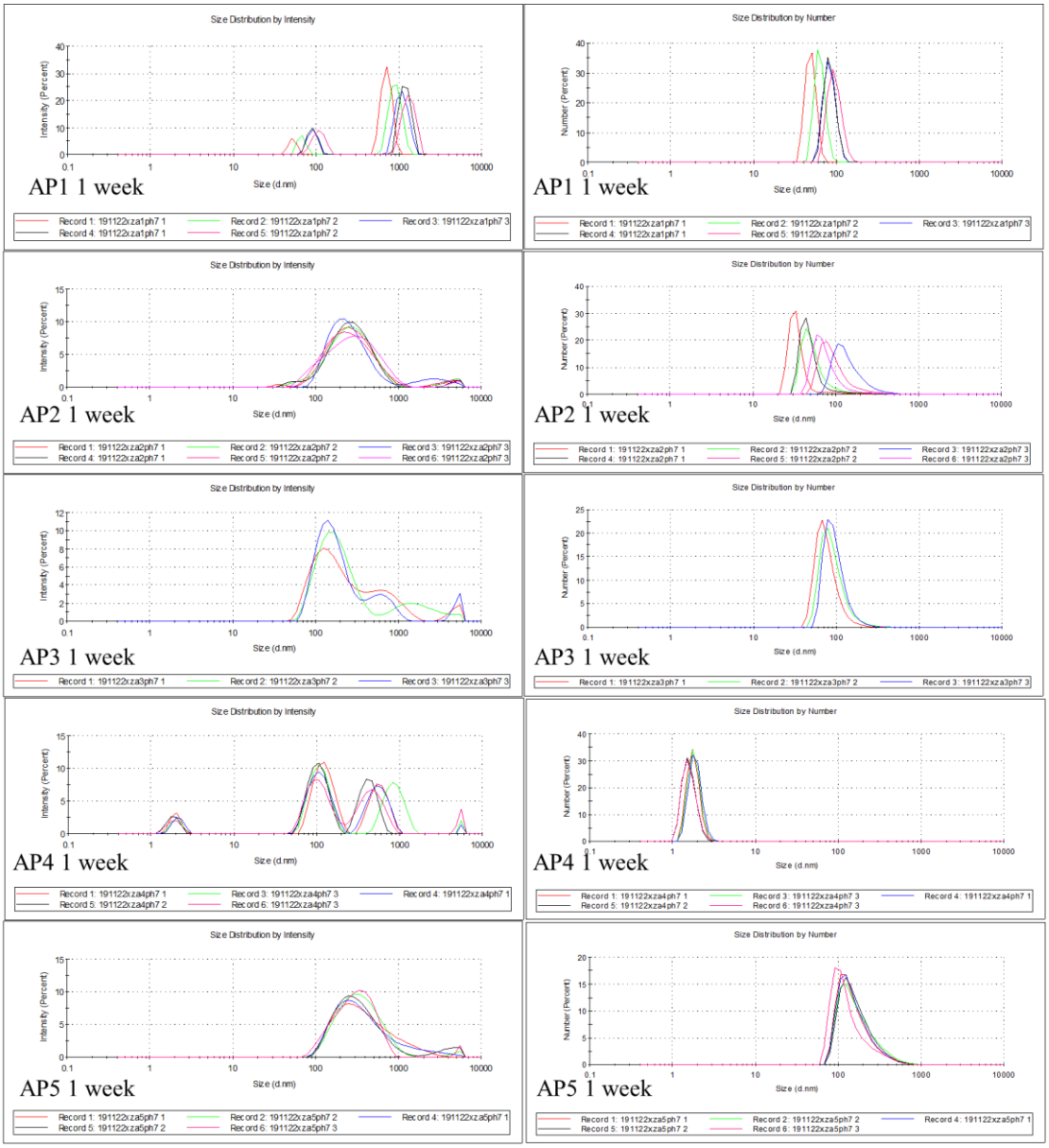


Figure A4.5: DLS graphs of APs in **Table 4.4** (1 week, pH = 7, 10 mg mL^{-1} in DI water).

.

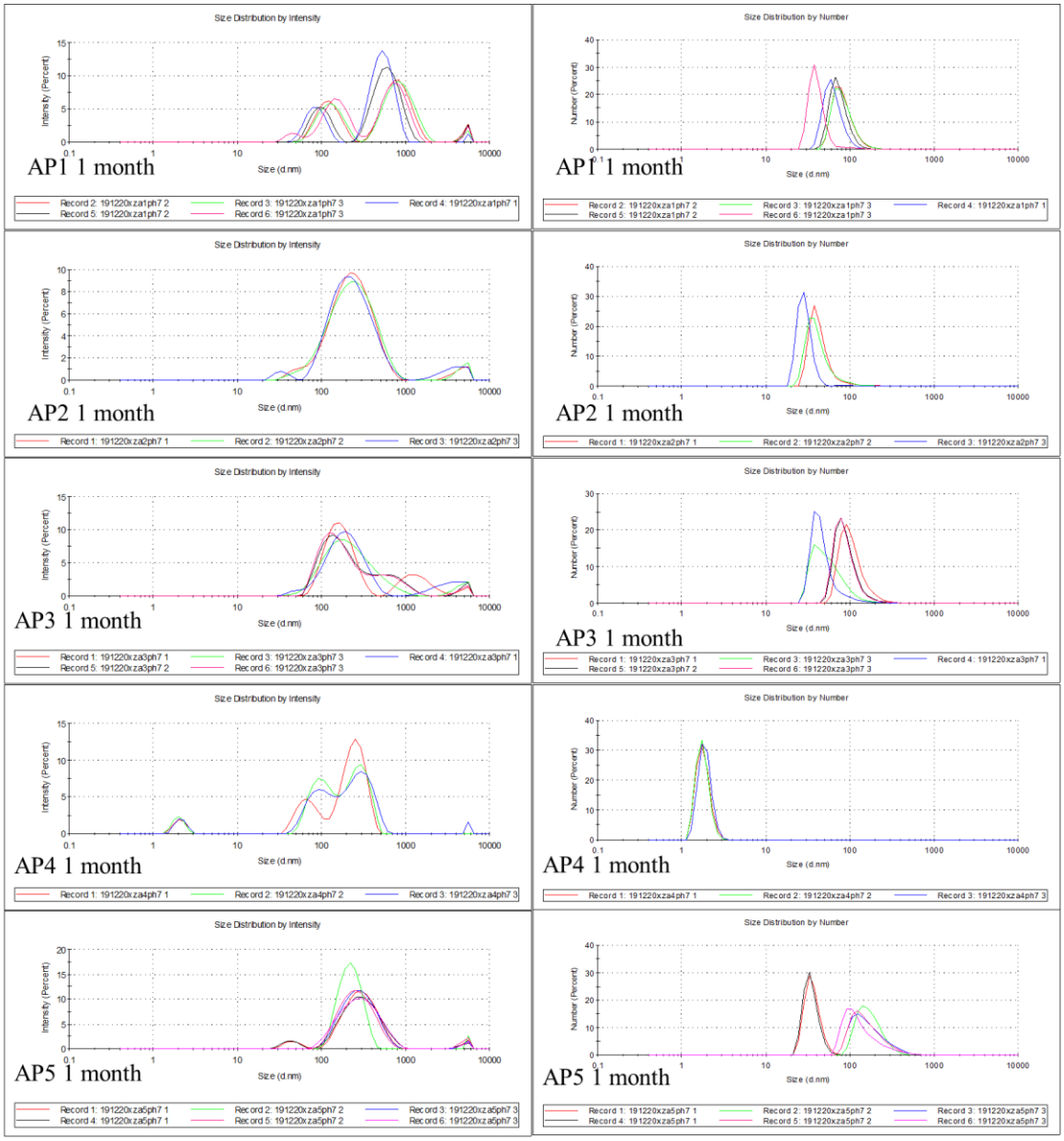


Figure A4.6: DLS graphs of APs in **Table 4.4** (1 month, pH = 7, 10 mg mL^{-1} in DI water).

.

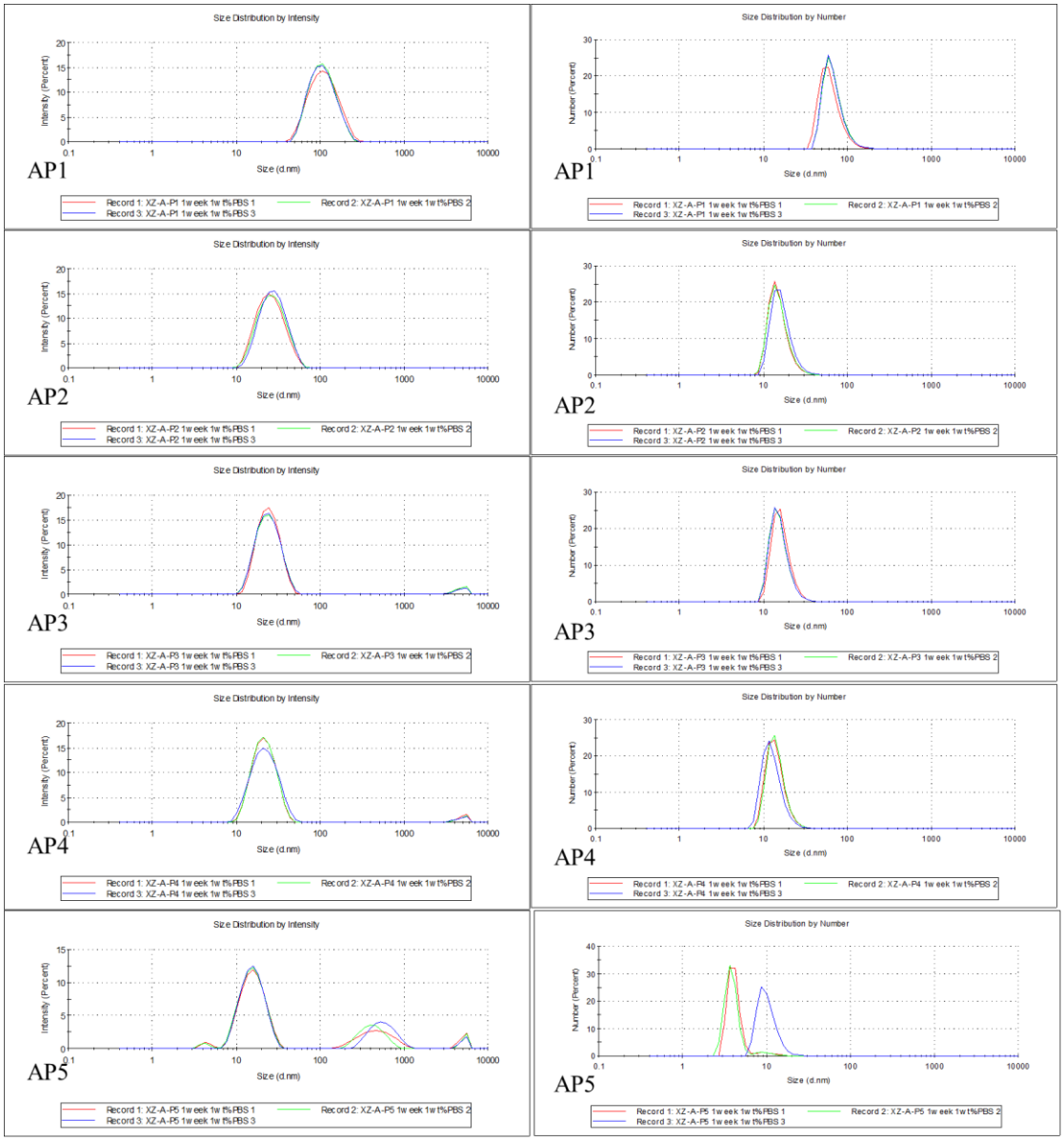


Figure A4.7: DLS graphs of APs in **Table 4.5** (1 week, original pH, 10 mg mL^{-1} in PBS).

.

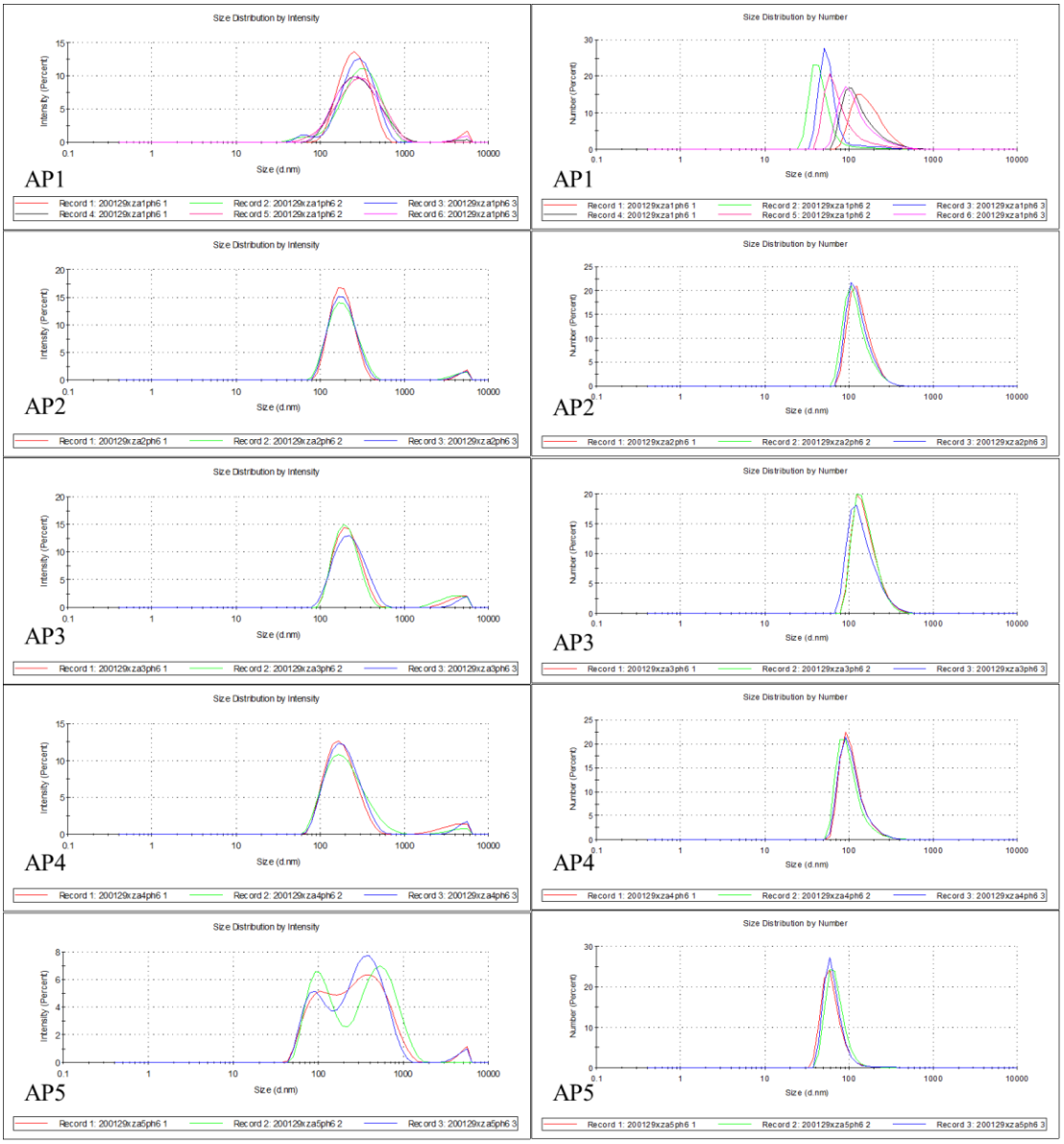


Figure A4.8: DLS graphs of APs in **Table 4.6** (1 week, original pH, 10 mg mL^{-1} in PBS).

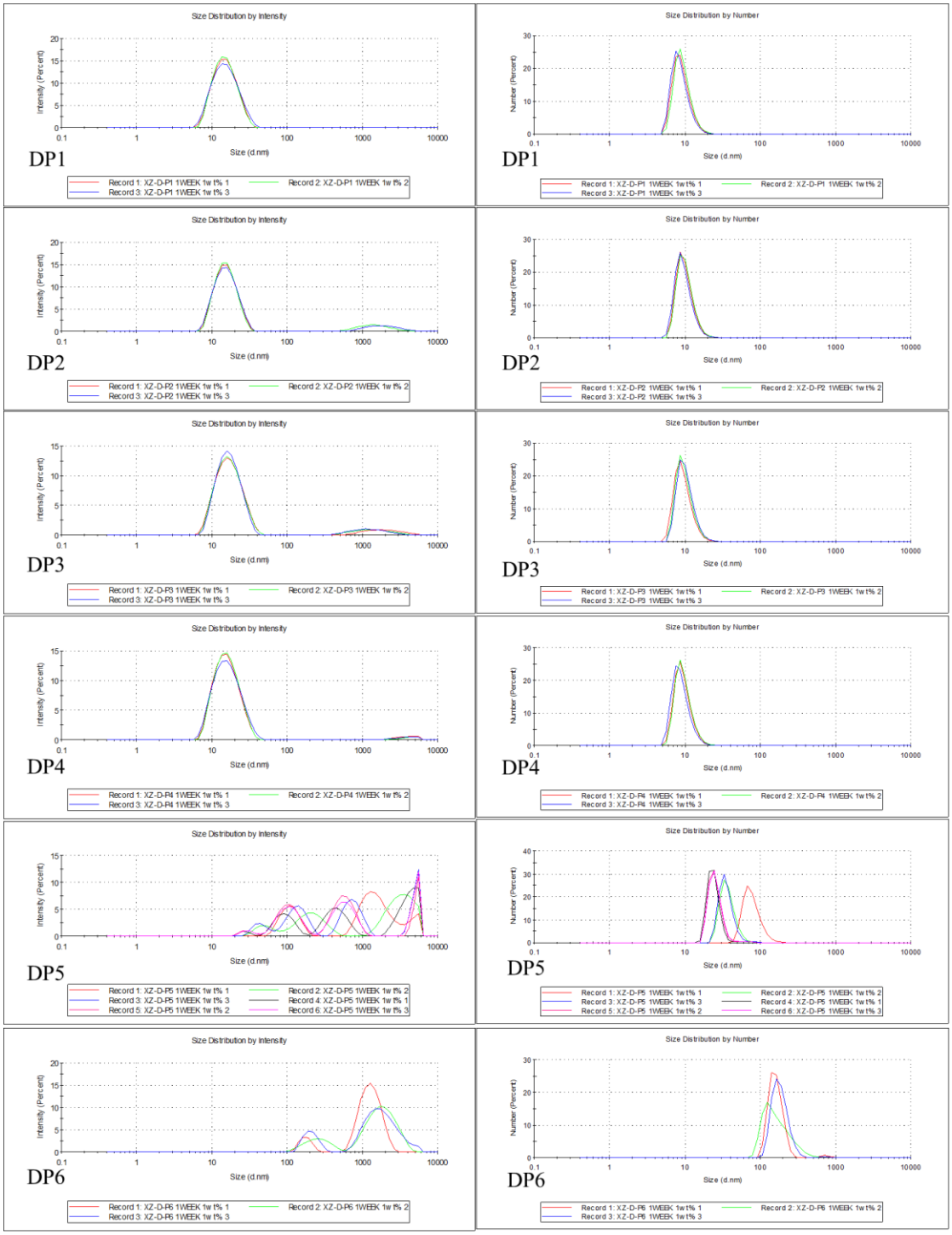


Figure A4.9: DLS graphs of DPs in **Table 6.3** (bulk hydration, 1 week, original pH, 10 mg mL^{-1} in DI water).



Figure A4.10: DLS graphs of DPs in **Table 6.3** (film rehydration, 1 week, original pH, 10 mg mL^{-1} in DI water).

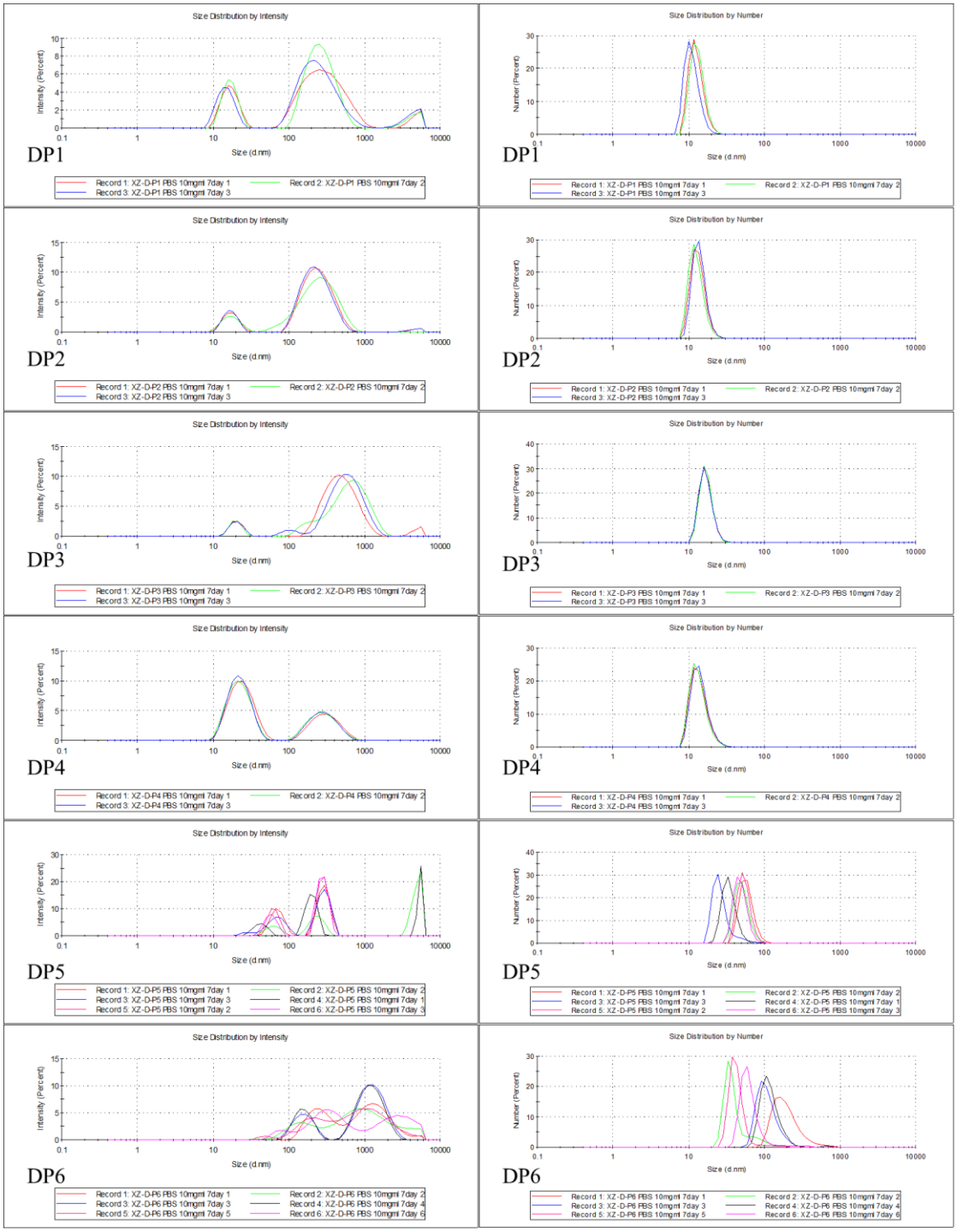


Figure A4.11: DLS graphs of DPs in **Table 6.4** (1 week, original pH, 10 mg mL^{-1} in PBS).

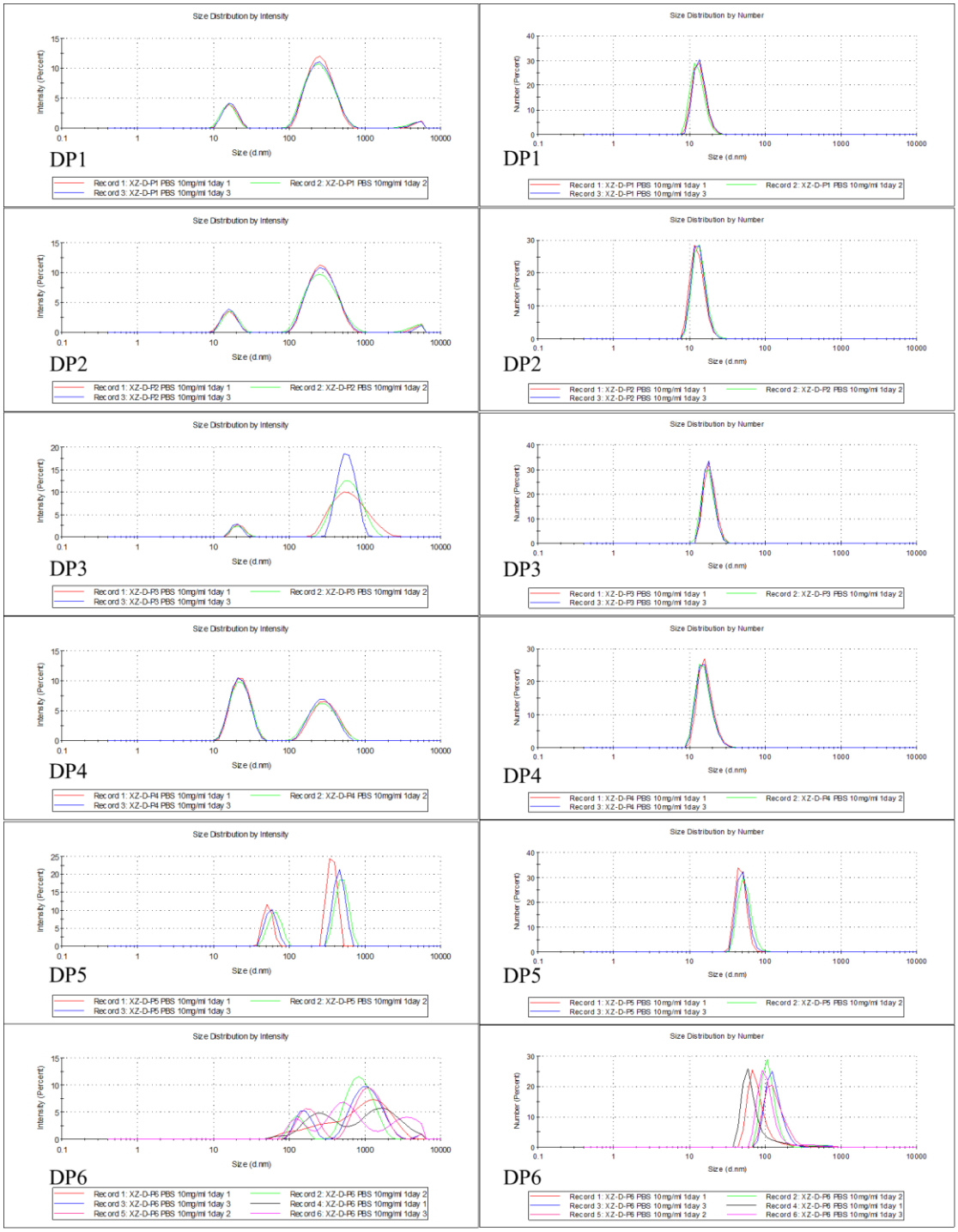


Figure A4.12: DLS graphs of DPs in **Table 6.5** (1 day, original pH, 10 mg mL^{-1} in PBS).

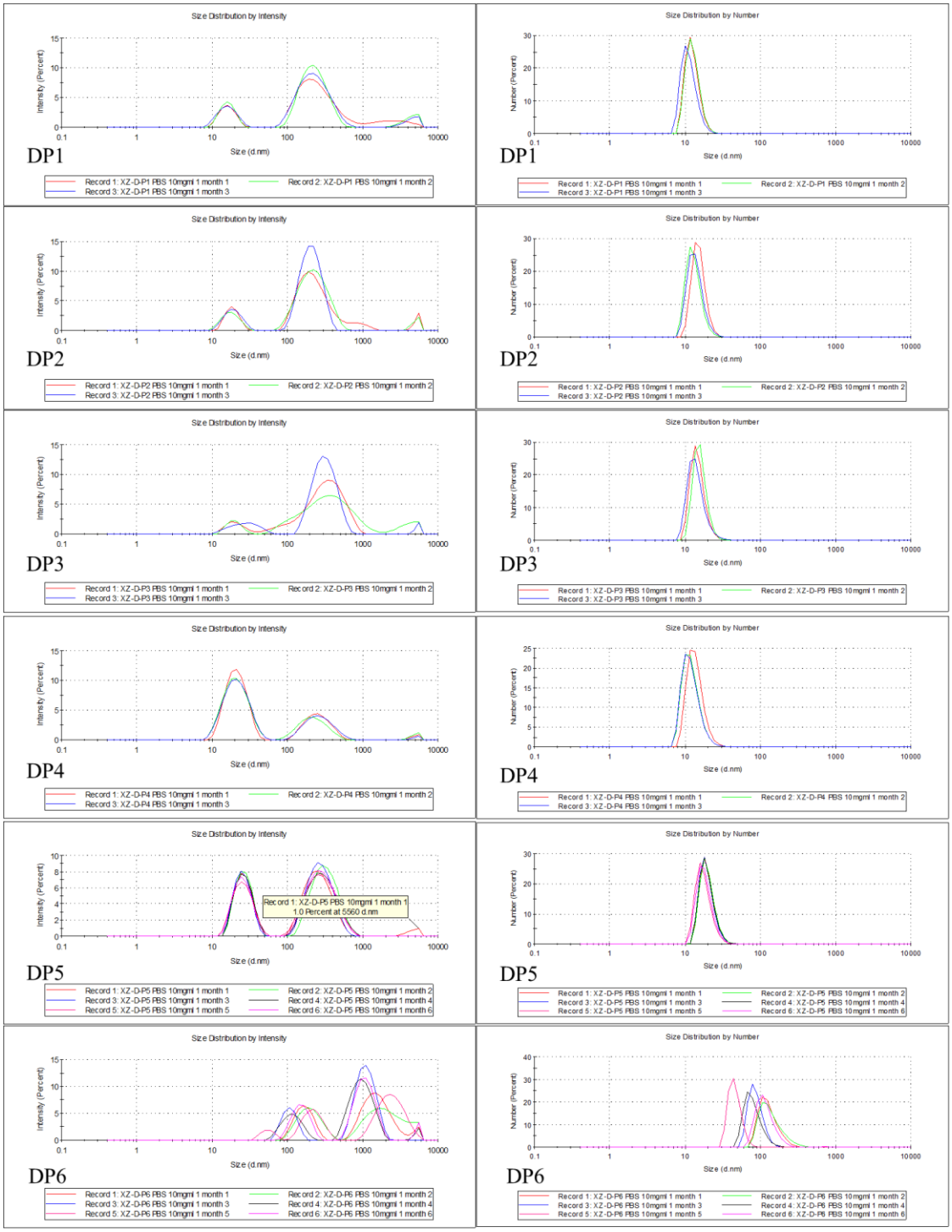


Figure A4.13: DLS graphs of DPs in **Table 6.5** (1 month, original pH, 10 mg mL^{-1} in PBS).

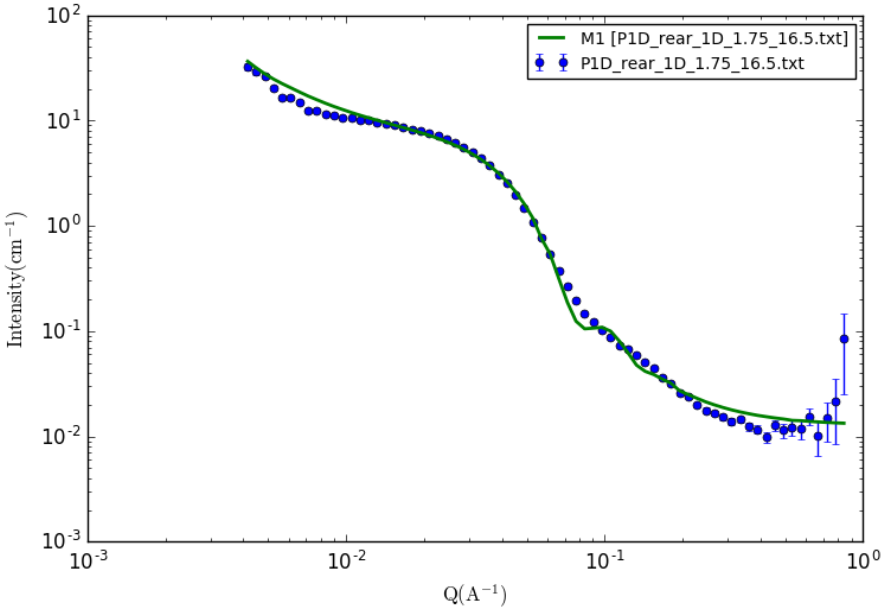


Figure A5.1: SANS results for DP1. The fitting took into account the presence of both micelles (sphere model) and the presence of polymersomes (vesicles model).

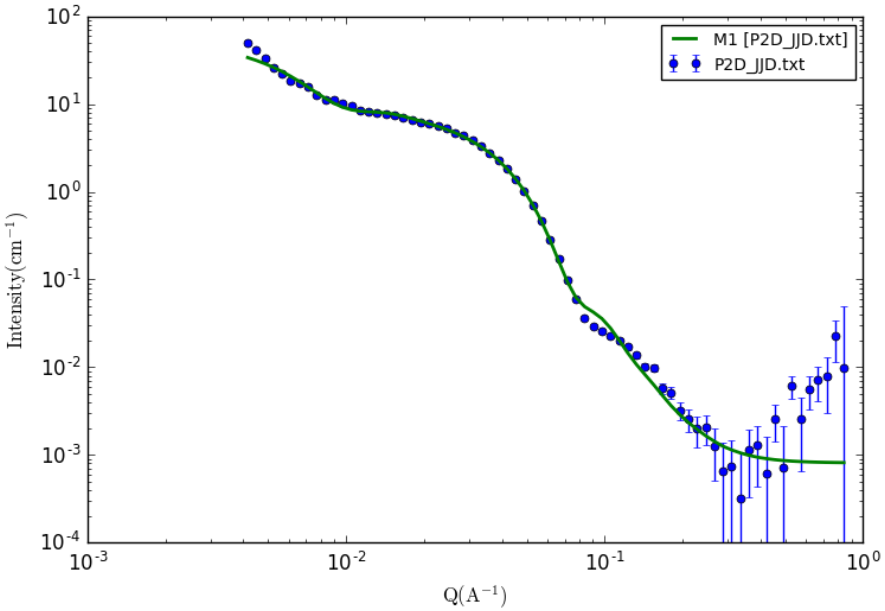


Figure A5.2: SANS results for DP2. The fitting took into account the presence of both micelles (sphere model) and the presence of polymersomes (vesicles model).

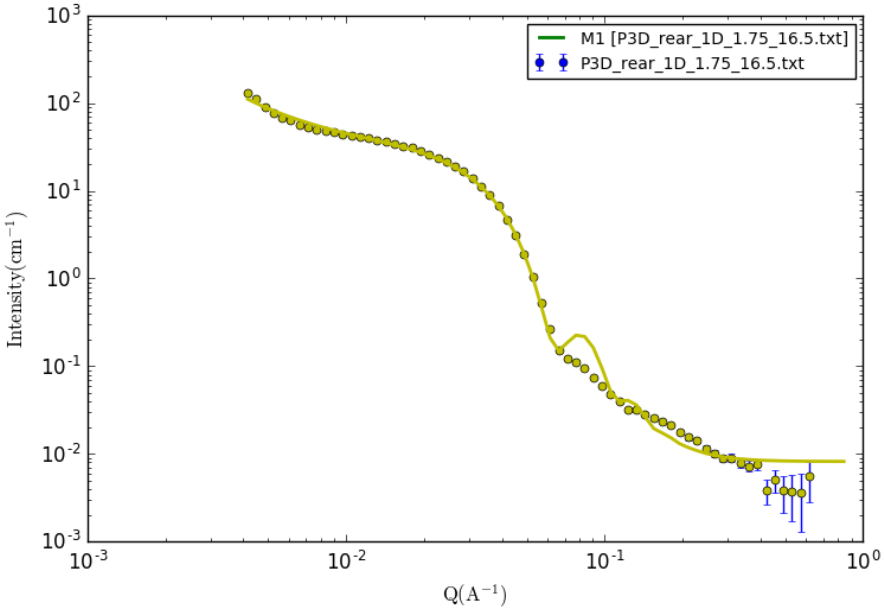


Figure A5.3: SANS results for DP3. The fitting took into account the presence of both micelles (sphere model) and the presence of polymersomes (vesicles model).

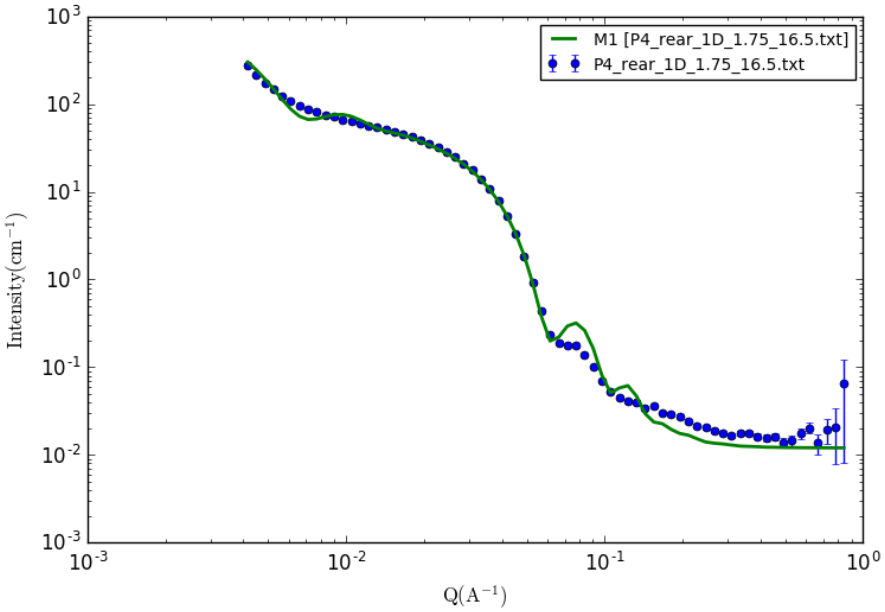


Figure A5.4: SANS results for DP4. The fitting took into account the presence of both micelles (sphere model) and the presence of polymersomes (vesicles model).

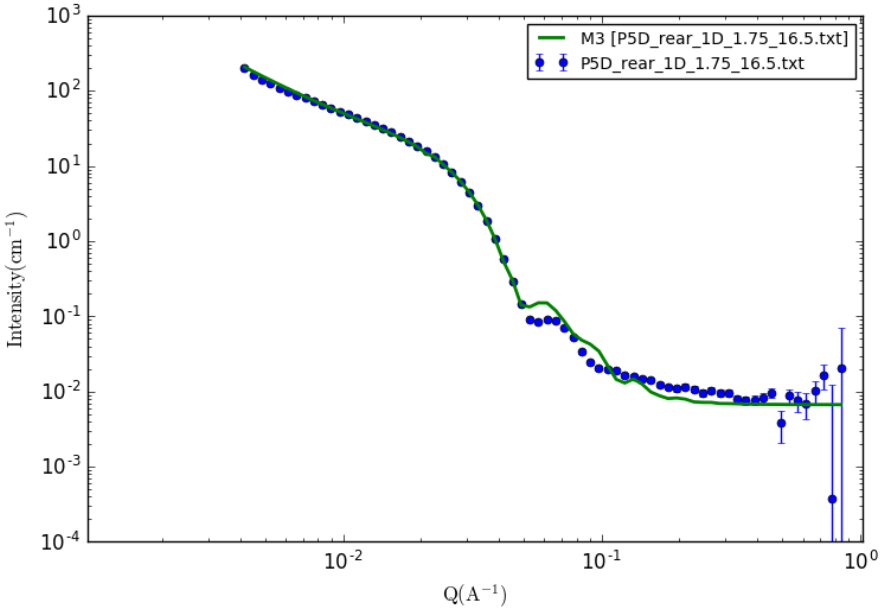


Figure A5.5: SANS results for DP5. The fitting took into account the presence of both micelles (sphere model) and the presence of polymersomes (vesicles model).

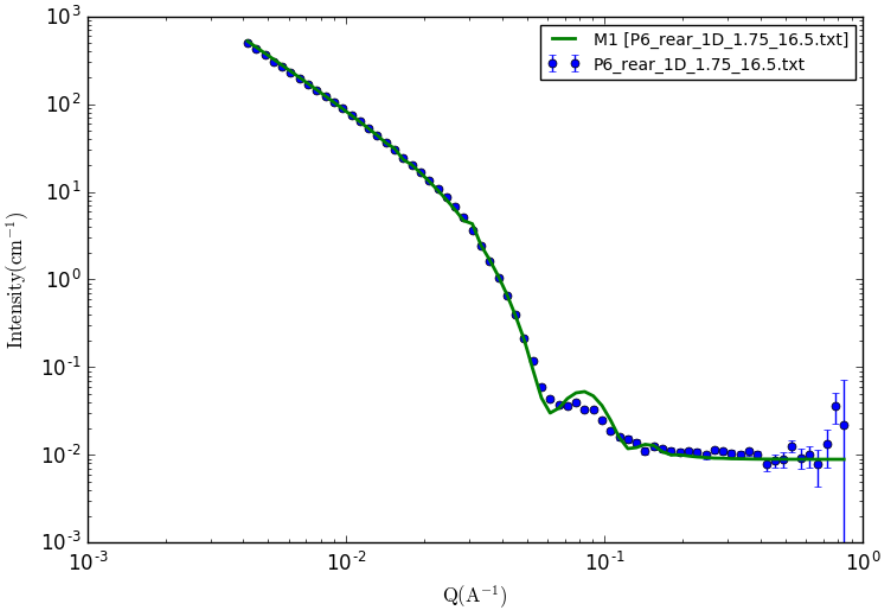


Figure A4.6: SANS results for DP6. The fitting took into account the presence of both micelles (sphere model) and the presence of polymersomes (vesicles model).

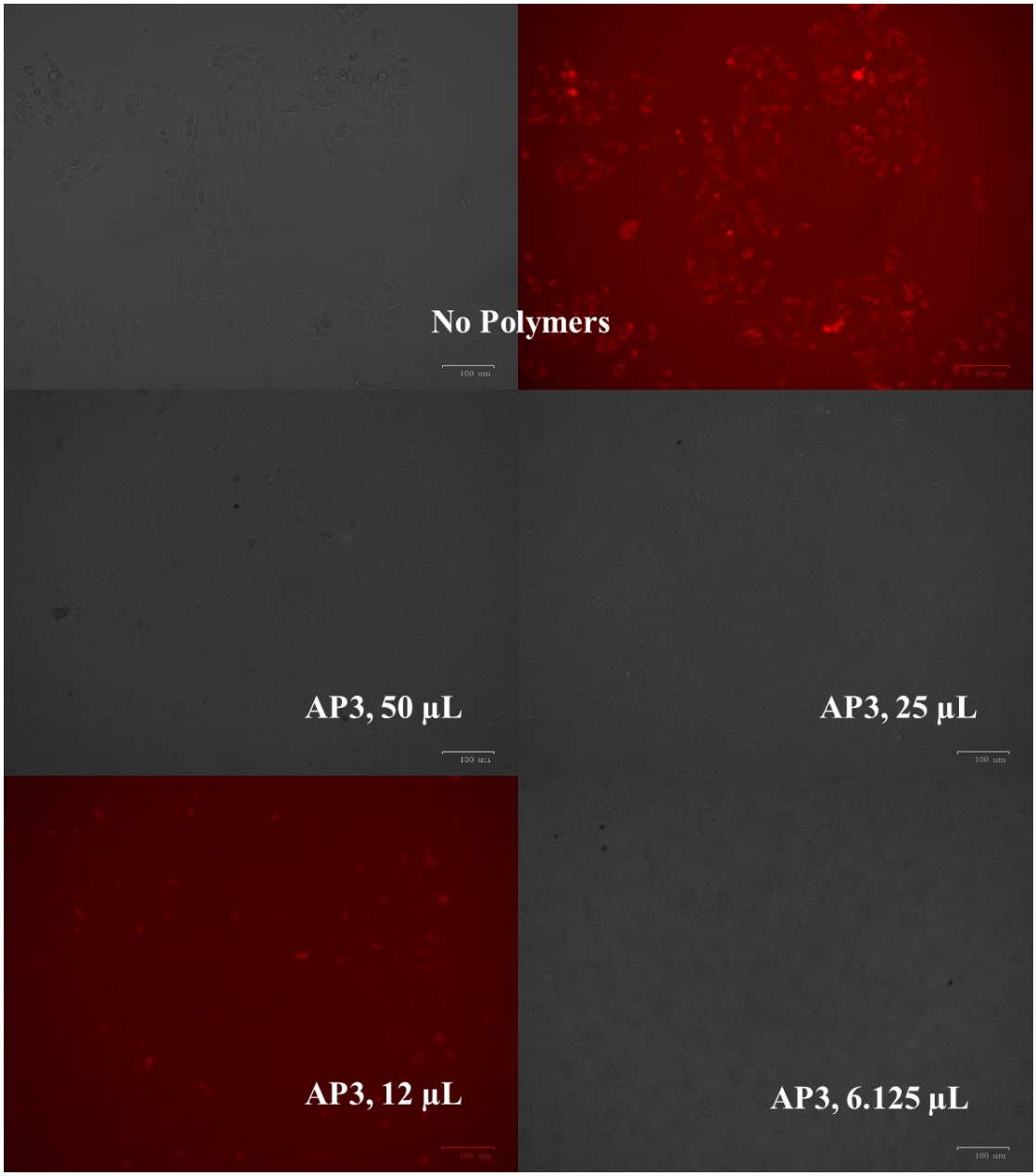


Figure A5.1 Cell toxicity study on polymer solution AP3. The concentration of the solution is 10 mg mL^{-1} (in PBS). GBM31 cells were plated at 2000 cells per well and next day gels were added at different doses with Mito tracker. Pictures taken after 5 days.

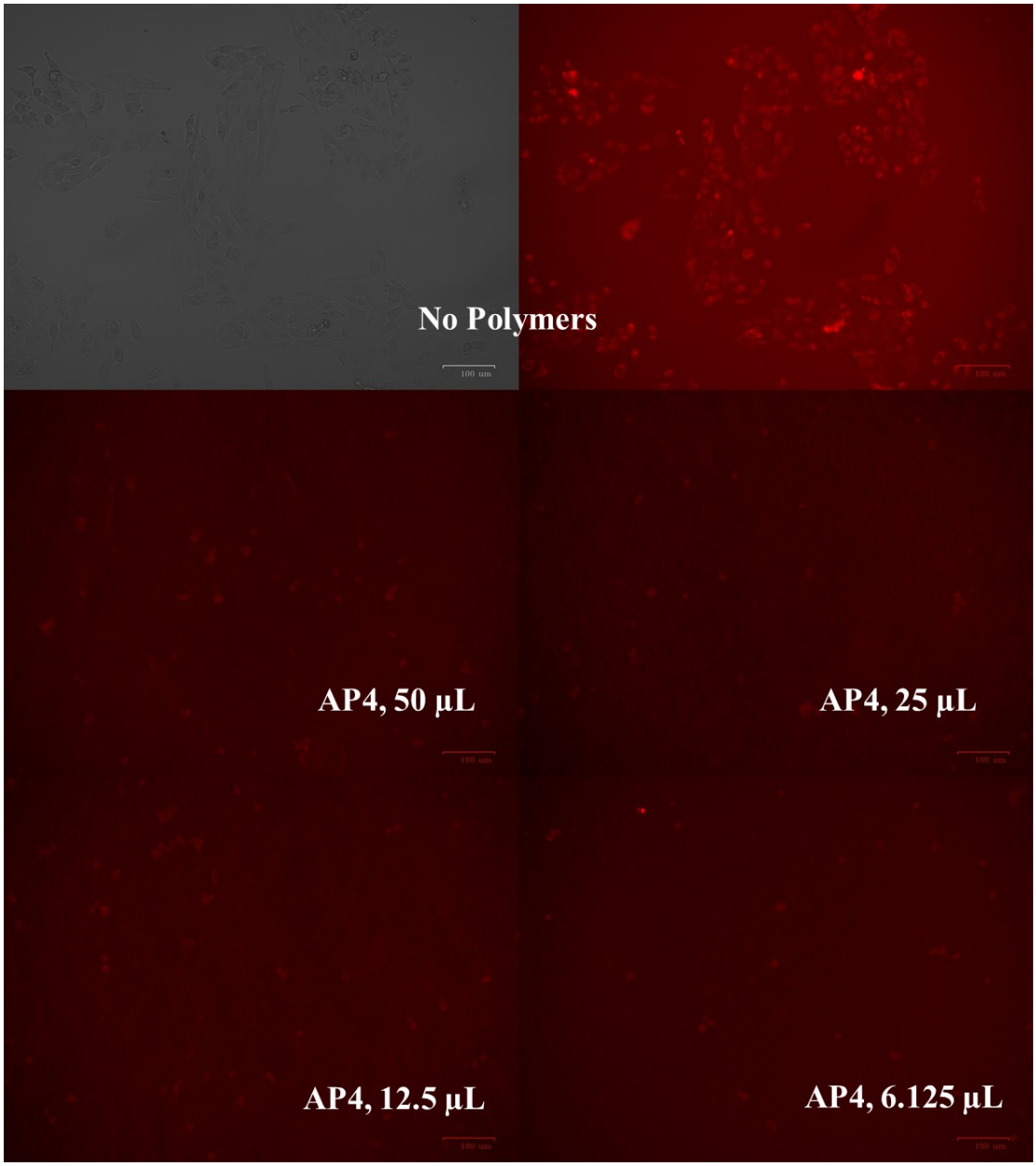


Figure A5.2 Cell toxicity study on polymer solution AP4. The concentration of the solution is 10 mg mL^{-1} (in PBS). GBM31 cells were plated at 2000 cells per well and next day gels were added at different doses with Mito tracker. Pictures taken after 5 days.